Isolation and characterization of *Arabidopsis* mutants with altered homologous recombination levels; a new function for an INO80 SWI/SNF ATPase

Inauguraldissertation

zur

Erlangung der Würde eines Doktors der Philosophie

vorgelegt der

Philosophisch-Naturwissenschaftlichen Fakultät

der Universität Basel

von

Olivier Fritsch

aus Frankreich

Basel, Juni 2004

Genehmigt von der Philosophisch-Naturwissenschaftlichen fakultät

Auf Antrag von

Prof Dr Barbara Hohn

Dr Jean Masson

Prof Dr Jerzy Paszkowski

Prof Dr Frederick Meins (chairman)

Basel, den 18.06.2004

Dekanin/Dekan

Ich erkläre, dass ich diese Dissertation “Isolation and characterization of *Arabidopsis* mutants with altered homologous recombination levels; a new function for an INO80 SWI/SNF ATPase” nur mit der darin angegebenen Hilfe verfasst und bei keiner anderen Fakultät eingereicht habe.

Olivier Fritsch

Basel, 25. Mai 2004

Table of Contents

Summary

Homologous recombination (HR) in eukaryotic organisms serves a dual role in providing genetic flexibility by creating novel sequence assortments upon meiosis and in maintaining genome integrity through DNA repair in somatic tissues. HR represents an alternative pathway to non-homologous end-joining (NHEJ) for the repair of double-strand breaks (DSB). The repair by NHEJ may not preserve the integrity of the genetic information whereas the HR pathway is more faithful. The choice of a pathway to repair DSBs is thus crucial for genome integrity and evolution, especially in plants where the germline is only determined late during development. Very little is known on what influences the choice of the pathway taken, but chromatin structure at the site of a lesion likely will play a major role in the recruitment of repair enzymes and thereby the choice of repair pathway. As a consequence, various proteins that are not part of the core of the recombination machinery may directly participate in the regulation of HR. At the time this work was initiated, no plant gene involved in the HR pathway or its regulation was characterized yet. As plants are powerful genetic tools especially for screening, we decided on designing and conducting a genetic screen to identify plant genes involved in HR.

Here I describe a genetic screen in *Arabidopsis thaliana* for mutants with altered somatic recombination levels and the characterization of the resulting mutant candidates. For the screen, I used a stably integrated luciferase based intrachromosomal HR substrate and a T-DNA construct designed for activation tagging as a mutagenic agent. Out of 19520 individual transformants tested, 37 exhibited an altered HR phenotype. Nine of them were sterile and/or exhibited important developmental or growth phenotypes that precluded the formation of progeny seeds, which is more than the average number of sterile plants expected. However, in most cases the altered recombination phenotype was lost in the offspring. To characterize the mutations, I cloned all the T-DNA insertion sites by plasmid rescue and determined the potential target genes. I discuss the genes likely to be responsible of the observed phenotype.

Here I report the thorough analysis of a mutant in the *Arabidopsis INO80* ortholog of the SWI/SNF ATPase family, which shows a reduced frequency of HR. In contrast, sensitivity to genotoxic agents and efficiency of T-DNA integration remain unaffected. This suggests that INO80 is a positive regulator of HR, while not affecting other repair pathways. Further, transcriptionaly silent TSI loci are not reactivated in absence of INO80, suggesting that *Arabidopsis* INO80 function is independent of transcriptional silencing. Using whole genome expression studies by microarray profiling I show evidence that INO80 regulates a small subset of *Arabidopsis* genes, suggesting a dual role for INO80 in transcription and repair by HR. Moreover, the recombination-promoting function of INO80 is not likely to involve general transcriptional regulation, and the transcriptional regulation of repair related genes is unaffected in the mutant. This is the first report of INO80 function in a higher eukaryote. Mononucleosome binding studies support the suggestion that INO80 positively regulates HR through modification of chromatin structure at sites of DNA repair by HR. Finally, I provide evidence for the existence and/or connectivity of INO80 with other INO80 complex partners in *Arabidopsis*.

A. General Introduction

1) Pecularities of the plant life style

Compared to animals, plants have a very special relation to the environment. This is mainly due to the fact that they live in a fixed position in their surrounding most of their life. The surrounding influences to a great extent the development, and final shape of plants. Trees, for instance, develop into very different final shapes when they grow in the forest or in an isolated place, and this is independent of seed variation. Similar differences can be found for most plant species. Because of their fixed life style, plants evolved specific strategies to recover from damage caused by the environment.

This all means that the environment of plants has dramatic consequences on the organism at various levels. This has to be considered together with another fundamental difference that exists in the life cycle of plants and animals. Unlike animals, plants lack a predetermined germline, and it is only late in development that germline cells are differentiated. In other words, the germline is determined after the plant developed and adapted to a specific environment, i.e. it carries marks of the individual plant history. Often, multiple germline(s) are differentiated on each flowering shoot, and at different times of the plant life. Therefore, somatic modifications representing new genetic information accumulated in different cells of the organism, may be selected and may contribute to genetic evolution (Walbot, 1996; Walbot and Evans, 2003).

2) Genotoxic stress, causes and consequences

Although tightly packaged in the nucleus of the cell and being a rather stable molecule, the DNA is constantly facing damages. A single change or deletion in the genomic sequence can have dramatic deleterious effects for the cell ultimately resulting in cell death or uncontrolled cell proliferation leading to cancer in mammals. Thus, a tight control of genome integrity is crucial and important for cell viability. Long after the initial discovery of the DNA double helix structure, the issue of genetic maintenance and DNA damage repair became an issue (Friedberg, 2003). What was actually underestimated was the complexity of the genome repair and maintenance machinery. The increasing amount of data in the field of DNA repair sheds light on our understanding of the maintenance and control of changes in the genome, providing a

complex picture composed of numerous interconnected pathways with a tight multilevel regulation.

Various stresses may cause DNA damage, either directly by altering the DNA molecule, or indirectly by producing reactive molecular species. In the latter case, other molecules of the cell may also be affected by the stress. Depending on their origin, genotoxic stresses can be grouped in three categories. First are the various stresses that are provided by the environment of the cell; these can be of abiotic or biotic origin. The former can be genotoxic molecules arising from nutrients, oxidative chemical species and radiations like γ-rays, UV-C and UV-B (Fig. 1). Some of these radiations such as γ-rays have a direct and rather specific effect on the DNA, others such as UV-B are less specific and affect the DNA mainly through the reactive oxygen species they produce in the cell (Frohnmeyer and Staiger, 2003). Biotic stresses such as pathogens may also result in DNA injury, mainly through the effect of reactive oxygen species produced by the pathogen or associated with the plant response to the pathogen. A second source of stress to the DNA is associated with genetic changes. These can result from, for example, intraspecific or interspecific crosses. Also comprised in this category are chromosomal set changes, i.e. changes in the number or representation of the chromosomes. The third class of genotoxic stress encompasses all the internal stresses, which are usually produced by the cell metabolism, by the spontaneous degradation of various molecules and the metabolism of DNA. These damages are mediated by oxidative species, various small reactive intracellular molecules such as *S*-adenosylmethionine and also directly by the DNA metabolism (replication, cell division), and last but not least, by the frequency of spontaneous hydrolysis of nucleotide residues that is not negligible at the temperature of living cells.

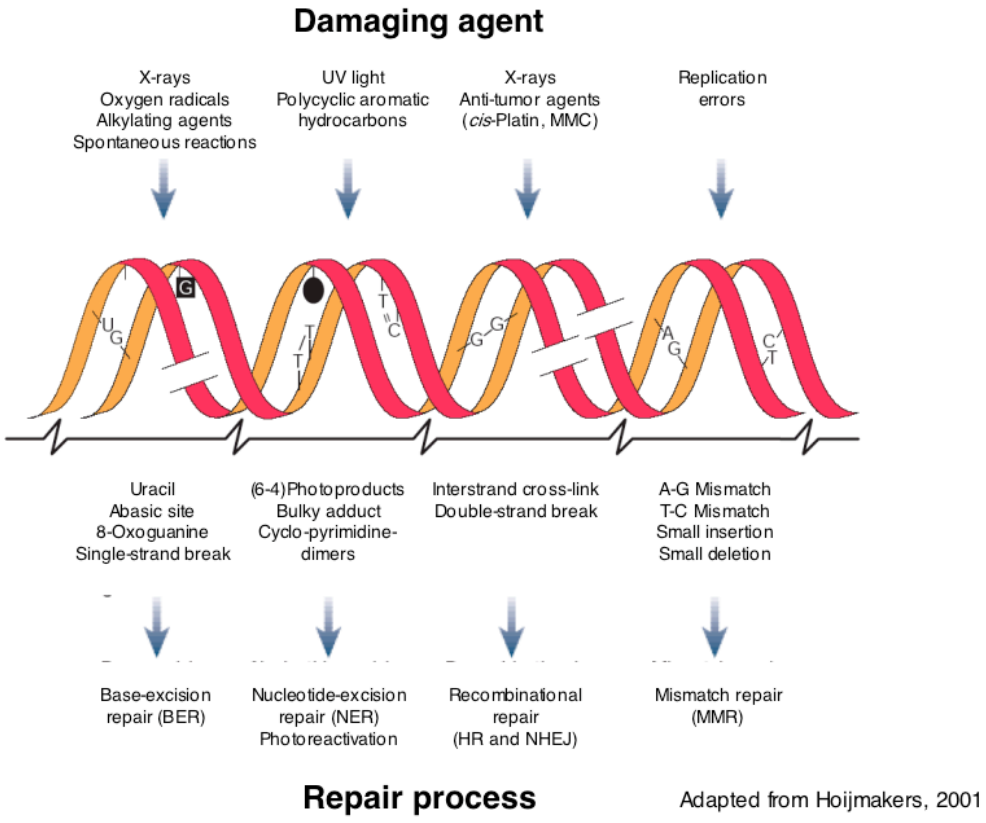

Figure 1. Genotoxic stresses and DNA repair pathways

DNA injuries have very diverse molecular consequences and, accordingly, their implications for the cell and the organism differ to a great extent (Fig. 1). The injury can lead to alteration of the nucleotide residues like simple base modification by addition, change or removal of chemical functions (O^6-methylguanine, uracil…), or alteration of the sugar part. More deleterious are intra- or interstrand crosslinks between nucleotides. The problem with the latter is that the resulting DNA injury cannot be repaired using the other strand, since both strands are affected. This is also true for clustered sites of DNA damage, that may result from water hydrolysis or ionizing radiation (Lindahl and Wood, 1999). Single-strand breaks can also be produced and together with other important lesions may result in double-strand breaks (DSBs).

3) DNA damage repair pathways

All types of damage must be repaired in order to maintain the genome integrity, although the consequences of DNA damage for the cell or the organism depend on the type of lesion and the specific part of genetic material affected, i.e in or outside genes, in non essential intergenic region or encoding an important protein. For example, change of base

or even a deletion may remain silent if the genetic information affected is not essential. To the contrary, a single unrepaired DSB in yeast may result in cell-death even in a dispensable genetic material (Bennett et al., 1996). In fact, perhaps due to the large diversity of DNA lesion types, a complex interwoven network of repair factors has evolved and is constantly at work to maintain the integrity of the genetic material.

A few DNA lesions, actually the more common ones, can be repaired directly in a one step reaction by a single protein without cleaving the sugar-base or the phospho-diester bound (Lindahl and Wood, 1999). This is the case for the photoreactivation that involves photolyases. However, in most circumstances, the repair of DNA damage involves a complex set of proteins and the interaction of specific repair pathways. This is the situation with damages that only affect one strand of the DNA but require removal of whole nucleotides. The injury is first removed, with or without flanking sequences, and replaced using the complementary strand as template. Damages repaired by these pathways include uracil, abasic-sites (that may result from altered DNA bases processed by glycosylases), 8-Oxoguanine and single-strand breaks (Fig. 1). In mammals, after the removal of the base, this pathway, called base excision repair (BER), continues with cleavage on the 5' side of the abasic site and recruitment of DNA-polymerase-β (POL-β) that changes the abasic site for the correct nucleotide. Finally, a complex like Ligase3-XRCC1 in mammals is recruited by POL-β to seal the nick. Although this is a representative example for BER, some variation in this scheme exists together with alternative BER routes (Lindahl and Wood, 1999). BER mostly operates on endogenous lesions across the genome. In addition, because some of these lesions block transcription, BER can also be linked to transcription in a transcription coupled repair (TCR) pathway.

Other lesions that are more severe in terms of helix distortion, like cyclobutane pyrimidine dimmers, 6-4 photoproducts and bulky adducts are rather repaired via nucleotide excision repair (NER) (Fig. 1). The NER pathway involves numerous proteins, and the first recognition step is largely diversified to accommodate to the various lesions this pathway deals with. NER comprises the global genome NER and a TCR sub-pathway, that differ in terms of damage recognition, regulation, and protein machinery in the first steps. An important difference to the BER is the removal of a whole stretch of nucleotides in a region comprising about 30 nucleotides around the lesion upon opening of the DNA helical structure (Hoeijmakers, 2001).

Mismatch repair MMR, is another important repair pathway mainly correcting post-replication or post-transcription errors (Fig. 1). MMR deals with mismatches, small

insertions and deletions, and involves a step to differentiate the strand containing the sequence variation from the correct template strand to be used for repair. MMR involves a heterodimer, like MSH2-MSH6 in mammals, which plays a central role in the recruitment of factors and in the interaction with the replication machinery (Hoeijmakers, 2001). These heterodimer-forming MSH proteins, that are the eukaryotic homologs of the bacterial MutS protein, were also reported in plants and have different specificities for the mismatched DNA (Culligan and Hays, 1997, 2000).

Another class of DNA injury affects both strands of the DNA molecule. These are interstrand-crosslinks, or tight clusters of lesions on both strands of the DNA that are usually repaired via a DSB intermediate, or DSBs themselves (Fig. 1). Also, residual single-strand breaks entering into the replication machinery can lead to DSBs (Hoeijmakers, 2001). If directly repaired by ligation, such damages may lead to loss of genetic information. This can be avoided by the use for the repair of a DNA template homologous to the damaged molecule. The homologous template can be the sister chromatid, or the homologous chromosome, or any piece of DNA that has enough sequence identity. This conservative repair can be achieved by the use of the homologous recombination (HR) pathway.

4) DSB repair

4.1) Early events in the processing of DSBs

DSBs are generally accepted to be the biologically most significant lesions by which ionizing radiation causes cancer and hereditary disease in mammals and major loss of genetic information in other organisms. As mentioned, there are two alternatives for the repair of DSBs. First, the direct ligation by the non-homologous end-joining (NHEJ) pathway with or without preservation of the sequence integrity, and second, the conservative HR pathway (Fig. 2). The choice of DSB repair pathway is thus crucial for genome integrity and evolution. Until recently, very little was known about the events leading to the processing of DSBs and the choice of pathway. The response of eukaryotic cells to genomic DSBs seem to include the sequestration of many factors into nuclear foci close to or at the break site. The coordinated action and presence of these many factors may reflect the complexity of the mechanism that determines the pathway to use. A few years ago, the discovery of a precocious chromatin event at DNA breaks started to shed light on the molecular basis of this mechanism. Upon DNA damage, a member of the

histone H2A family, H2AX, becomes extensively and rapidly (1–3 minutes) phosphorylated and forms foci at break sites. Recent studies show that this phosphorylation event is an evolutionarily conserved cellular response to DSB (Modesti and Kanaar, 2001). H2AX is actually required for the accumulation into foci of various essential repair proteins like the repair factors RAD50 and RAD51 or the tumor suppressor gene product BRCA1 (Fig. 2). In a coordinated fashion, protein kinases of the phosphoinositide (PI)-3 family are suggested to mediate the cellular response to DSBs (Paull et al., 2000). These giant kinases include ATM (ataxia telangiectasia mutated) that is involved in ionizing radiation response in mammalian cells. The ATM *Arabidopsis* counterpart has also been implicated in DNA damage response (Garcia et al., 2000; Garcia et al., 2003). Recent studies shed light on the molecular mechanism underlying ATM activation; ATM dimers undergo intermolecular autophosphorylation and dimer dissociation (Bakkenist and Kastan, 2003). These early steps involving ATM and p53 finally affect the cell-cycle machinery leading to cell-cycle arrest or retardation and help to recruit repair factors either through direct interaction or by providing the right conformation of the breaks (Khanna and Jackson, 2001) (Fig. 2). This may also explain why DSB in dispensable artificial yeast chromosome lead to cell-death when left unrepaired for a long time (Bennett et al., 1996).

The extremities of the DNA at the break site are also directly subjected to processing leading to the resection of the ends into single-stranded DNA (ssDNA) that is then coated with proteins like the RPA complex in yeast and mammals (Fig. 2). This step has dramatic consequences since it can be associated with deletion of nucleotide at either of the ends that can then be precisely repaired only through HR. During this precocious step of DSB processing, some repair factors like the trimeric RAD50-MRE11-XRS2/NBS1 complex are mobilized and bind to the DNA ends, perhaps helping to protect them from degradation and also participating into the recruitment of further repair factors.

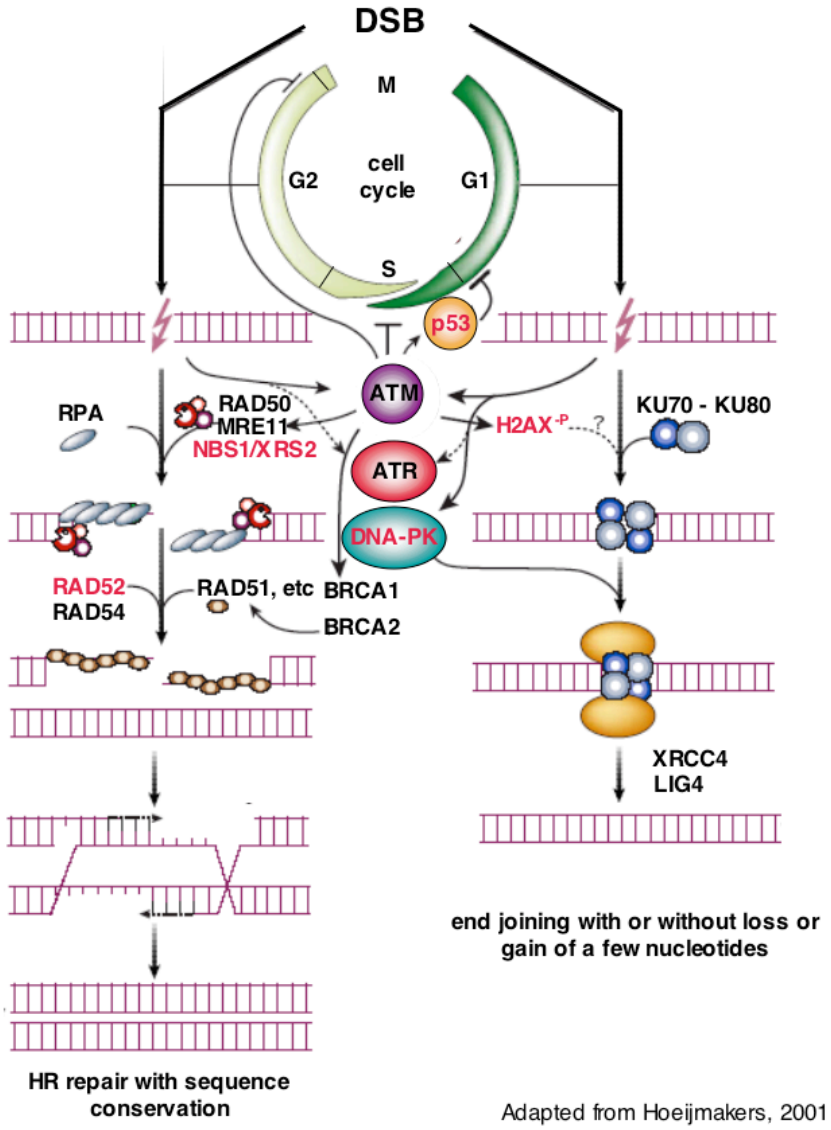

Figure 2. DSB repair pathways. The conservative HR pathway and the end-joining pathway are the alternative for DSB repair. The choice between HR and end-joining involves a complex interplay of factors and correlates with cell-cycle. Of the major factors depicted on the scheme, some were not reported in the *Arabidopsis* genome so far (red letters).

4.2) Illegitimate recombinational repair of DSBs

As already mentioned, the major pathway of DSB repair in higher eukaryotes – excluding post-replicative repair – is the NHEJ repair. The use of the NHEJ pathway leads to direct ligation of the DNA ends regardless of genetic changes (Fig. 2). For instance, the processing of the break ends may result in deletions and/or insertions. In addition, illegitimate ends may be ligated since no mechanism ensures the proper ends are used for

repair. NHEJ is initiated by the recruitment of the KU70/KU80 complex at both processed ends, and involves the DNA-PK protein kinase in mammals (the counterpart was not found yet in *Arabidopsis*). This is followed by ligation by the XRCC4-Ligase4 complex (LIF1-DNL4 in yeast) (Fig. 2).

4.3) HR repair of DSBs and choice of repair pathway

Apart from its use during meiosis – meiotic recombination, which also involves DSBs in the initial steps – HR is mainly involved in the repair of damages resulting in or processed to DSBs. Therefore the classical model for HR, as an alternative pathway to NHEJ, represent the involvement of HR in DSB repair, where the two pathways act in a competitive way. Generally, HR was found to be prominent over NHEJ for the repair of DSBs in *Saccharomyces cerevisiae* (Paques and Haber, 1999), whereas in plants and mammals NHEJ is the preferred repair pathway. In mammals and yeast, the decision towards HR mostly relies on the recruitment of the RAD52 protein to the RAD51-MRE11-XRS2 protected ends. In *S. cerevisiae*, when RAD52 is not available, the KU70-KU80 dimer binds the ends, promoting NHEJ through DNA-PK recruitment (Clikeman et al., 2001). It is not known to which extent these initial steps and the following ones in the specific pathways are reversible. But it is possible that such reversibility may provide an additional level of regulation for the choice of pathway in addition to and together with the availability of factors in general and of the homologous template for HR.

The paradigm of the respective prevalence of NHEJ versus HR for the repair of DSBs is much too simplistic, as revealed by some studies in mammalian cells showing that, indeed, homology directed repair is a major pathway of DSB repair. In one study an endonuclease-generated DSB was introduced into one of two direct repeats, and homologous repair was found to account for one third to half of the observed repair events (Liang et al., 1998). There, HR seems to be associated with gene conversion without reciprocal exchange, which represents a bias against crossing-over in mitotic cells, perhaps to reduce genome alterations (Johnson and Jasin, 2000). This may also reflect the fact that the choice of pathway depends on the particular phase of the cell-cycle in which repair has to take place, due to template availability but also other levels of regulation (Fig. 2). After replication, when the homologous sister chromatid is present, HR repair plays an important role up to early mitosis. In G1 however, NHEJ is preferred over HR in mammals and plants (Khanna and Jackson, 2001).

This means that, depending on the HR factors present and the cell-cycle progression, the exchange of information between the template and the damaged molecule during HR may result in gene conversion either associated or not associated with crossing-over. As already mentioned, the conservative mode provided by HR repair is important for repair after replication, when the sister chromatid can be used as homologous template. However, cells in G1 have only the homologous chromosome for HR repair that may be difficult to find. In addition, it may be risky to use it as a template since it can provide homozygocity for potentially harmful recessive mutations. Moreover, because of the many duplicated sequences present in higher eukaryotic genomes, HR repair may also result in mixing different genes and regions of the genome. This may explain why HR in general is the minor DSB repair pathway in mammals and plants, whereas HR is a major pathway for post-replication sister-chromatid repair. However, HR is still an important pathway for the repair of DNA lesions in plants (Puchta and Hohn, 1996).

5) The homologous recombination pathway

The mechanism of HR is best understood in prokaryotes, and to a lesser extent in *Saccharomyces cerevisiae* (Paques and Haber, 1999). However, information on specific steps, can be transferred to higher eukaryotes, although some differences were unraveled in the protein sets used at some steps of the pathway. For the proteins responsible for defined activities, the end products of HR and the prevalence of variant-pathways, major differences have been found between organisms (Johnson and Jasin, 2000; Constantinou et al., 2001; Hays, 2002; Symington, 2002). As a consequence, a profusion of models for HR were proposed to explain the observations in specific organisms and conditions.

The use of the HR pathway may or may not depend on replication, and this determines – together with the phase of the cell-cycle – the homologous template that can be used. This template can be a homologous chromosome or the sister-chromatid. A special case has to be made for the newly synthesized sister chromatid upon DNA replication, as in this situation the sequence to be repaired and the homologous template are located close by. Such configuration, seems to be responsible for most recombinational repair, which is consistent with models in which recombination is intimately coupled with replication (Paques and Haber, 1999; Johnson and Jasin, 2000). In fact, several pathways have been implicated in the repair of DNA damage during

replication, and most of them employ sister-chromatids for recombinational repair, to restart replication following double-strand break formation or even as a potential template for replication-bypass processes (Kadyk and Hartwell, 1992; Malkova et al., 1996; Paques and Haber, 1999).

The synthesis-dependent strand annealing (SDSA) pathway of HR constitutes an alternative pathway of HR in which the free DNA ends invade either different templates or the same template at a different time (Fig. 3.7 & 3.8). After synthesis the ends separate from the template and anneal to each other (Nassif et al., 1994; Ray and Langer, 2002) (Fig. 3.9). As a consequence, repair by the SDSA pathway leaves the template unchanged (Fig. 3.10). In plants, SDSA seem to be prevalent over the classical recombinational repair of breaks (Salomon and Puchta, 1998; Ray and Langer, 2002), which could explain the difficulties to achieve homology directed gene targeting.

The classical model for HR – the DSB repair model – starts with or involves a DSB in the DNA, and the presence of a homologous template. In a first step that is shared with NHEJ, the ends of the DNA at the break are thought to be processed into ssDNA, protected by various proteins and coated with RPA (see above and Fig. 3.1). After this, HR can be divided into a few major steps: strand invasion, synthesis of complementary DNA, Holliday-junction formation, migration and resolution. Within the steps, slight variations exist depending on the model considered.

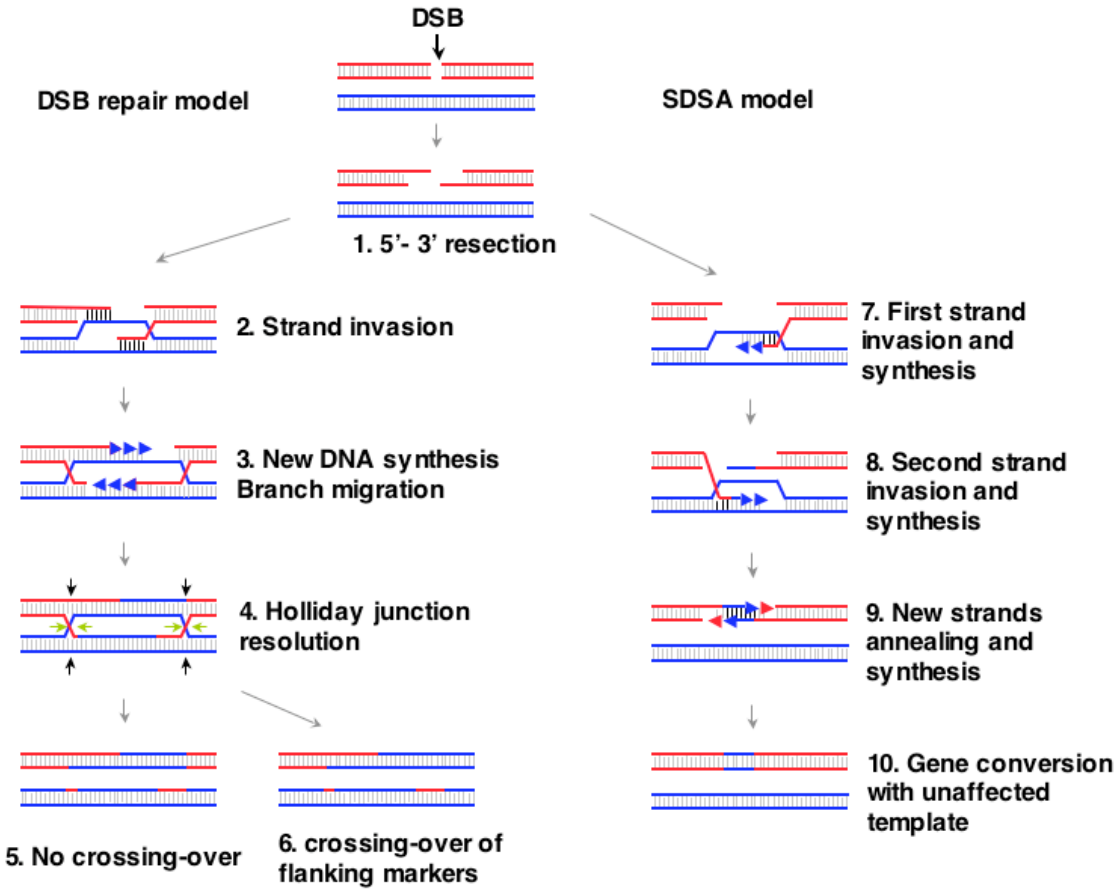

Figure 3. The DSB repair and SDSA model of HR. (1) to (6) DSB repair model for HR. (1) Initially the DSB is 5'-to-3' resected, producing 3' single-stranded DNA ends. (2) The 3' ends invade a homologous DNA duplex forming a DNA crossover or Holliday junction and providing a primer to initiate new DNA synthesis. (3) Branch migration of the Holliday junction extends the region of heteroduplex from the initial crossover site. (4) Holliday junctions are resolved by cleavage of either the crossed strands (green arrows) or the non crossed strands (black arrows) of the junction. A mixed resolution of the two Holliday junctions results in the exchange of the flanking markers (6), while resolution in the same orientation does not affect the flanking markers (5). **(7) to (10)** The SDSA model for HR. (7) One of the 3' single-stranded tails invades the homologous duplex, priming DNA synthesis. (8) The other 3' single-stranded tail may also subsequently invade the homologous duplex and prime synthesis. After displacement from the donor duplex, (9) the nascent strand pairs with the other 3' single-stranded tail and DNA synthesis completes repair (10).

In the early steps of HR, involving homologous pairing and strand exchange (Fig. 3.2), the RecA/RAD51 family of recombinases plays an important role. These conserved proteins, stimulated by the RAD52 protein, bind to the ssDNA formed upon resection of the DNA ends at the break, and this is most probably achieved by replacing RPA on the ssDNA (Fig. 2). Then, the RAD54 ATPase, a member of the SWI/SNF family, stimulates the following step in which the ssDNA invades the homologous duplex DNA molecule (Fig.3.2). However, the exact *in vivo* role of RAD54 is not known. The invasion of the

second ssDNA extremity is more enigmatic and involves either the same RAD51 mediated mechanism or uses solely the RAD52 ssDNA annealing activity (West, 2003). Surprisingly, some studies suggest a direct role for some of the MMR pathway MSH proteins in these first steps of HR (Evans and Alani, 2000). Most likely, MMR plays a role in the interaction of the recombining molecules by helping in the removal of non-homologous ends (Paques and Haber, 1999). This is actually one example out of many for the interconnection between different repair pathways.

After strand invasion, the next step involves recruitment of a DNA-polymerase complex and DNA synthesis utilizing the homologous template. In the SDSA model, this synthesis step provides another possibility for the second ssDNA end invasion, namely the displacement of the first newly synthesized DNA strand before the second strand invasion and synthesis (see above and Fig. 3) (Paques and Haber, 1999). This alternative way is consistent with many observations in plants and mammals (Nassif et al., 1994; Ray and Langer, 2002). Strand exchange and DNA synthesis result in the formation of two Holliday-junctions, which are branched four-stranded cruciform structures (Fig. 3.3 & 3.4).

To continue in the pathway, branch migration must occur, followed by resolution of the junctions, i.e. separation of the complex structure in two recombined molecules. The position and direction the resolution happens will determine the actual recombination products, that is, the extent of exchange of the genetic material. Although most recombination events occur within a one kb region from the initial DNA break, there is also evidence that it can occur as far as tens of kbs away from the break (Smith, 2001). These events are not well understood, but may be explained by long distance migration of the Holliday-junction or the creation of break-induced replication forks. Such re-combination events can give rise to extensive gene conversion events (more than 30 kb), and might participate in the repair of telomeres (Paques and Haber, 1999; Smith, 2001).

In prokaryotes, Holliday-junction migration and resolution are carried out by the RuvABC proteins. RuvB act as a hexameric ring structure (Yamada et al., 2001) and its helicase activity and DNA binding affinity are enhanced by interaction with RuvA (Shinagawa and Iwasaki, 1996; West, 1997). These two factors form a large motor protein complex to promote branch migration of the Holliday junctions in a concerted manner before the RuvC endonuclease resolves the junctions. Despite many efforts to unravel the eukaryotic counterpart of RuvABC, its nature remains elusive. However, the corresponding activities have been purified from yeast and mammals where concerted

branch-migration and resolution activities similar to that catalyzed by RuvABC were found, (Constantinou et al., 2001). Recent studies have identified the Mus81-Mms4 heterodimer as a resolvase in *Schizosaccharamyces pombe*, but the data in *S. cerevisiae* suggest the existence of another class of resolvase in eukaryotes (Constantinou et al., 2002; Symington, 2002). Indeed, the *Drosophila* XPF (that shows some homology with Mus81p) possesses such a resolvase activity and the human RAD51C variant was recently shown to be required for Holliday-junction resolution (Heyer et al., 2003; Liu et al., 2004). This may represent a further possibility for junctions other than the classical Holliday junctions to contribute to crossovers (Heyer et al., 2003). In mammals also the BLM and WRN RecQ like DNA helicases stimulate the migration of Holliday-junctions (Yang et al., 2002). The WRN protein possesses helicase and exonuclease activities and interacts with the NHEJ repair complex KU70/KU80. Mutations in the *WRN* gene have been associated with the inherited Werner syndrome disease in humans that is characterized by genomic instability and premature aging. The fact that BLM and WRN promote branch migration suggests that these proteins may be involved in Holliday-junction resolution and may contribute to the cleavage, perhaps in a topological way in combination with topoisomerase III (Heyer et al., 2003).

The resolution of Holliday-junctions leads to gene conversion that is associated or not with crossing-over of the flanking DNA, depending on which strands of the Holliday-junction were cut (Fig. 3.4). If the resolvase cleaves both Holliday-junctions the same way, gene conversion will not be associated with crossing-over (Fig. 3.5), whereas if the cross-over strands of one Holliday-junction and the non-cross-over strands of the other are cleaved, there will be crossing-over and exchange of the flanking markers (Fig. 3.6). As an important consequence, one of the molecules might remain unchanged after the process, which is also true when the SDSA pathway is employed. Because of this, and also because HR associated with crossing-over can be used to achieve homology dependent gene targeting (i.e. site-specific modification of the genomic sequence), most studies look at gene conversion associated with crossing-over, which may have biased our general knowledge on HR (more details and complexity of HR are reviewed in Paques and Haber, 1999; Smith, 2001; Symington, 2002).

6) Monitoring somatic homologous recombination, the tools

6.1) Natural systems

It is relatively easy to monitor meiotic recombination; the recombination frequency between two genetic or visible markers on the chromosomes can be calculated by recording the segregation of these traits after a cross. For somatic HR it is much more complicated since most events are not transmitted to the next generation. In plants, a few natural systems exist that allow the visualization of somatic HR events on whole plants.

In the first system, recombination at the endogenous *Sulphur (Su)* gene is visualized on the leaves of *Nicotiana tabacum* plants. The *Sulphur* gene controls chlorophyll pigmentation in Tobacco. The *sulphur* mutation is semi-dominant and leads to pale green heterozygous (*Su/su*) plants, and white non-viable homozygous (*su/su*) seedlings. In the pale green *sulphur* (*Su/su*) heterozygous plants, somatic recombination events at the *Sulphur* locus are revealed by dark green (wild-type) or white (*Sulphur* defficient) sectors on the leaves (Burk and Menser, 1964; Shalev et al., 1999). Another system exists in *Tradescantia hirsuticaulis* were recombination in stamen hair cells results in changed pigmentation of hairs (Christianson, 1975). Although these systems provide a way to monitor somatic HR at endogenous loci, they have as disadvantage that the molecular nature of the visualized recombination events is not well established.

6.2) Transgenic approach

In order to measure somatic HR frequency in different contexts in plants, specific constructs containing a HR reporter marker were designed. The reporter consists in a disrupted marker gene, which can be either an antibiotic resistance gene (neomycin or hygromycin phosphotransferase gene for kanamycin and hygromycin resistance, respectively), a visible marker like the β-glucuronidase gene (GUS) and the firefly luciferase gene, or a viral sequence (Offringa et al., 1990; Bilang et al., 1992; Swoboda et al., 1993; Gorbunova et al., 2000). In such constructs, HR must happen in order to restore the screenable functional version of the disrupted reporter gene. The classical intrachromosomal HR GUS based system consists of two partially overlapping parts of the β-glucuronidase gene interrupted by a marker gene for the selection of the construct (Fig. 4) (Swoboda et al., 1994). The repeats can be either in direct or indirect orientation that may enable the visualization of the use of slightly different recombination pathways (Fig. 4) (Gherbi et al., 2001). Although they can be used in transient experiments to assay

extra-chromosomal HR, the constructs are usually integrated in the plant genome making achievable the detection of intrachromosomal HR events (Lucht et al., 2002). Depending on the respective orientation and position of the repeats, intermolecular HR events can be monitored as well (Molinier et al., 2004a). The detection by histochemical GUS staining allows for the localization of the recombination events and a quantitative assay on whole plants. Although the HR frequency observed using this system varies according to the genomic location of the reporter, the HR events at the reporter locus happen at an overall frequency of about one per 10^6 cells (Swoboda et al., 1993; Swoboda et al., 1994; Puchta and Hohn, 1996). This system was originally developed in tobacco and in the C24 ecotype of *Arabidopsis*, (Swoboda et al., 1994; Puchta et al., 1995b) and more recently for the Columbia ecotype of *Arabidopsis* (Gherbi et al., 2001; Lucht et al., 2002). A similar system, based on the Firefly luciferase gene was established for tobacco (Gorbunova et al., 2000) and *Arabidopsis* (J. Molinier, O. Fritsch, D. Schuermann, G. Ries, J. Lucht and B. Hohn in prep.). In this latter case HR events can be visualized in living plants and can be followed over time.

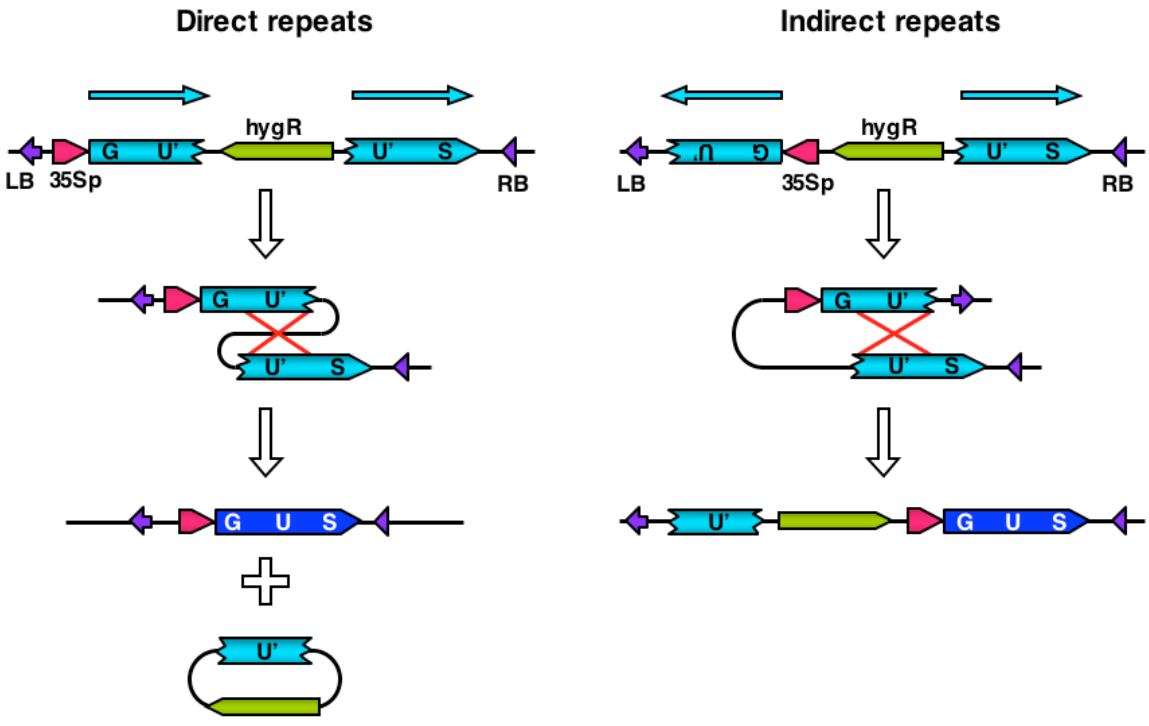

Figure 4. Intrachromosomal HR reporter constructs with direct and indirect repeats. With both types of constructs, intramolecular HR events restore a functional GUS gene but with different molecular products. The direct repeat configuration (GU'-U'S) gives rise to the deletion of sequence comprised between the two repeats, in the form of a short life non-replicative circular molecule. The indirect repeat orientation (U'G-U'S) results in the inversion and conservation of the central sequence. RB and LB, right and left borders of the T-DNA; 35Sp, CaMV viral promoter driving GUS expression; HygR hygromycin resistance gene.

7) The regulation of homologous recombination

As mentioned above, HR must be tightly regulated in order to preserve genome integrity while providing sufficient flexibility for evolution. In an oversimplified view, three major types of regulation are expected to influence HR. First are the factors directly involved in the process, like proteins of the HR machinery and the concerned DNA molecules; this aspect was already discussed in chapter 6. Then, various factors from the environment might also contribute to the regulation of HR, either directly or indirectly through the reactions they provoke in the cell. This aspect is discussed below, with much information originating from plant systems. A third possibility for HR regulation by the cell is provided by (i) recently discovered molecular factors that control HR but are not directly involved in the HR machinery (some of them are mentioned at the end of this chapter), (ii) the possible contribution of the chromatin structure both as a physical barrier and as a potential active dynamic regulator of HR, (this will be addressed in the next chapter), and (iii) the relative importance of the various DSB repair pathways (mainly the different forms of HR and NHEJ) that are commonly considered to compete with each other for the repair of the DSB. It is well possible that plants have evolved subtle mechanisms to regulate HR at this level, due to the particular importance that it has for genome stability and evolution (see below and Ray and Langer, 2002).

Many studies have shown that meiotic recombination frequency varies along the length of chromosomes in *Arabidopsis* and maize (Lichten and Goldman, 1995; Puchta and Hohn, 1996), as well as in mammalian cells or yeast (Nachman, 2002). As a consequence, “hot”- and “cold”-spots for recombination exist in the genome, which seem to coincide with transcriptionaly active and inactive regions. Many factors were described to influence the frequency of meiotic recombination. In plants, these include various genetic factors: sequence diversity like the heterogeneity of the sequences assembled during interspecific crosses (Ganal and Tanksley, 1996), direction of crossing (Wang et al., 1995), as well as environmental factors (Baker et al., 1976b; Baker et al., 1976a). In contrast, the factors regulating recombination at the somatic level in plants and animals remained much less understood until recently. But the development over the last ten years of reporters to visualize and measure the frequency of HR events especially in plants (see above), allowed for the study of factors influencing HR frequency.

The effect of genotoxic factors such as DNA-damaging chemicals was investigated. Both methyl methanesulfonate (MMS), which is a methylating agent that primarily methylates purine bases and Mitomycin-C (MMC), a DNA cross-linking agent, were found to induce somatic HR (Lebel et al., 1993; Puchta et al., 1995a). Abiotic stress factors like heat and high salinity seem to stimulate HR as well (Lebel et al., 1993; Puchta et al., 1995a). The UV-B radiations that pass the UV-screening ozone layer and that inevitably accompany photosynthetic radiations are, for plants, an important component of natural genotoxic stresses. UV-B has a broad range of direct and indirect effects on plants, including deleterious influences on the photosynthetic apparatus and on membranes, induction of various pathways and production of free-radicals that affect proteins and induce the formation of cyclobutan-pyrimidine dimers (CPDs) and (6-4)photoproducts on the DNA (Jansen, 1998). At natural as well as at higher doses, UV-B irradiation was found to stimulate HR, (Ries et al., 2000a). Also, γ-irradiation, such as the nuclear pollution caused by the Chernobyl accident was found to stimulate HR (Kovalchuk et al., 1998). In fact, the change in recombination frequency could be seen at very low radioactivity levels, rendering these systems suitable for the detection of radioactive pollution but also of chemical mutagens (Fritsch et al., 2000; Kovalchuk et al., 2001a; Kovalchuk et al., 2001b). In addition to being more sensitive than most other assays, this system has the advantage to visualize the impact of such pollution directly on living organisms (Kovalchuk et al., 2001b).

In two recent studies the effect of stress due to pathogens was assessed. Attack by the oomycete pathogen *Peronospora parasitica* was shown to increase HR frequency in *Arabidopsis*, and the same effect on recombination was observed when plant defense mechanisms were triggered by chemicals or a plant defense mutant (Lucht et al., 2002). The second study reports an increased HR frequency in treated but also untreated leaves of tobacco plants infected with different viruses (Kovalchuk et al., 2003). Together with the previous studies, these latest results suggest that increased somatic recombination is a general stress response in plants, and that this response may act systemically. What remains unclear, however, is whether the general stress response affects HR through a specific signaling pathway or if the general stress signaling indirectly affects HR regulation. To answer this question, the isolation of mutants affected in the control of HR will be a useful tool.

The general stimulating effect of environmental stresses on HR can be significant for the plant, as it increases genome flexibility and therefore may allow new resistance

genes to evolve, as suggested earlier (Parniske et al., 1997; Richter and Ronald, 2000). A large number of disease resistance-like genes are present in clusters in plants genomes, and would be a good substrate for such recombination events (Ellis et al., 2000; Young, 2000). The intriguing point there is that this creation of genetic diversity in the resistance genes may result from a global change of the recombination at the genome level or alternatively from a specific increase of recombination at these gene clusters. In addition, besides the basic interest on the regulation of HR and its application to gene delivery methods, such studies unraveled the dramatic impact that small changes in our life environment can have on genome stability and evolution.

The data discussed above suggest that stress signaling leads to HR regulation and that the general control of HR by the cellular machinery evolved various mechanisms to control HR. Some of the molecular regulators of HR must provide a link to the actual recombination process. During the time of this work, a number of studies unraveled such new molecular regulators of HR. As an example, the yeast SRS2 helicase protein was found to be a negative regulator of HR, acting by disrupting the RAD51 nucleofilaments at early steps of HR (Ira et al., 2003; Krejci et al., 2003; Van Komen et al., 2003; Veaute et al., 2003). The local frequencies of HR along the chromosome may also be linked with transcriptional activity. For instance, transcriptional activity and DSBs were found to have a similar stimulating effect on recombination (Gonzalez-Barrera et al., 2002), although a more recent study suggests that the HR promoting effect of transcription comes primarily from an increased accessibility to DNA damaging agents (Garcia-Rubio et al., 2003).

8) The chromatin

The DNA of eukaryotes is compacted, together with proteins, into a highly organized and dense structure called chromatin. This complex structure is built of basic bricks, the nucleosome units, which are arranged in a repetitive array along the chromosome. The nucleosomes have to be seen as rather stable structural components for the compaction of the DNA, as well as a support for molecular modifications mediating chromatin function. About 145 bp of DNA are wrapped around the histone protein octamer formed by two copies each of H2A, H2B, H3 and H4, the so-called core histones. Whereas the core of the octamer is very stable and for its major part hidden by the DNA, the molecular tails of the individual histones (N-terminal part for all histones but H2A, which has a C-terminal

tail) representing about 25% of the histone mass, protrude from the surface of the nucleosome (Wolffe and Hayes, 1999). These tails can mediate many interactions with other proteins and are the substrates for chemical modifications. Through this, histone tails play an important role in determining higher structural levels, i.e. in regulating chromatin accessibility and in controlling the diverse chromatin functions (reviewed in Iizuka and Smith, 2003; Khorasanizadeh, 2004; Loidl, 2004).

The incorporation of non-nucleosomal linker histones into chromatin facilitates the folding of nucleosomal arrays into higher order structures while restricting the mobility of the individual nucleosomes with respect to the DNA. Linker histones like H1 have C- and N-terminal tails that bind the DNA within the nucleosomal core and between nucleosomes (Wolffe and Hayes, 1999). Whereas core-histones are essential for chromatin assembly, the linker histones are not, and their weak interaction with the DNA – compared to the nucleosome core-histones – may provide an easy way to alter both local and higher order chromatin structure. In addition, a variety of non-histone proteins and divalent metal ions are also involved in the higher order chromatin folding (Luger, 2003). Besides the *bona fide* core histones, a large diversity of histone variants for H3 and H2A exist in higher eukaryotic organisms – and to a lesser extent in yeast – with specialized functions, providing another level of diversification for the chromatin. In *Arabidopsis*, for example, 45 core histone genes and multiple linker histones are encoded by the genome (Verbsky and Richards, 2001), However, the function of most of this histone repertoire is still unknown. Over the last few years, the roles of two evolutionary conserved H2A variants, H2AX and H2AZ, have been well characterized; it was shown that a tiny variation in the histone sequence can be very important in terms of function. Both of these variants are present in a small proportion of the nucleosomes, replacing the standard histone H2A. As mentioned in a previous chapter, a particular serine residue of the H2AX histone tail in mammals – or of the major H2A in yeast (Downs et al., 2000) – is rapidly phosphorylated in response to DSBs resulting from environmental insult, metabolic mistake, or programmed process (reviewed in Redon et al., 2002). The H2AZ variant (HTA3 or HTZ1 in *S. cerevisiae*) is present in a non-uniform specific pattern across the chromosome in various organisms, altering nucleosome stability, and is involved in transcriptional control. Accordingly, one proposed model would be that chromatin regions with a high H2AZ content, would not have to rely as much as others on remodeling for transcription, because H2AZ–H2B dimers are more easily dissociated than H2A-H2B (reviewed in Redon et al., 2002).

Within the nucleosome particle, the interaction of DNA with the histone octamer is fairly strong and the organization of the interaction is nearly identical for all DNA sequences, regardless of inherent sequence-dependent structure (Wolffe and Hayes, 1999). Together with the higher order structure of the chromatin fiber, this renders the DNA difficult to access by other proteins. Although strong when considering the whole nucleosome, the DNA-octamer interaction has an inherent flexibility at the level of each of the 14 main individual DNA-histone contacts. In the cellular context, two main aspects contribute to this flexibility: (i) the intrinsic physical properties of the nucleosomes that are mostly unaffected by the use of different histone variants or by the DNA sequence, and (ii) the active disruption or remodeling by various large protein complexes that accompanies replication and transcriptional activities in combination with or independent of histone modifications and histone chaperone activities (Wolffe and Hayes, 1999; Khorasanizadeh, 2004).

The accessibility of individual nucleotides or short stretches within the DNA sequence may greatly vary depending on whether these regions are exposed at the nucleosomal surface or hidden, the most accessible nucleotides being in the inter-nucleosomal stretch of DNA. In fact, because of the dynamic equilibrium of the nucleosome, all nucleotides oscillate between an inaccessible and a transiently accessible state (Gontijo et al., 2003), such that with the help of protein factors favoring this transient state, all nucleotides – or DNA lesions – might become accessible. Conversely, the part of the genome that is hidden in higher-order chromatin structure is less accessible to chemical mutagens than transcriptionally active or replicating regions.

Because the structure of DNA bound to histones is remarkably different from that of free DNA or of other protein-DNA complexes (Richmond and Davey, 2003), it might be important to perform experiments dealing with DNA repair factors in a nucleosomal or chromatin context, as naked DNA may not reflect the *in vivo* situation of chromatinized DNA. As a good example, the *in vitro* strand pairing activity of Rad54/Rad51 recombination proteins is induced up to 100 times in a chromatin context, as compared to activity on naked DNA (Alexiadis and Kadonaga, 2002), suggesting that eukaryotic repair factors have evolved to cope with the eukaryotic DNA packaged into chromatin.

9) The dynamic chromatin and chromatin remodeling complexes

Large regions of chromatin can assume two main states: the compacted heterochromatic

state with little accessibility and the relatively open euchromatic state that is associated with transcriptionally active regions. In both cases, the determination of the state correlates with several non-permanent specific histone marks. Also at the level of the gene, the nucleosomes harbor different chemical modifications, defining small micro-territories within the chromatin. During development at the organism level and cell-cycle progression at the cellular level, different territories within the chromatin are established, maintained, and modulated. In addition, chromatin states and marks are affected by the environment and the history of the cell. As an example, the position of nucleosomes and nuclease accessibility in the upstream regions of particular plant genes change in response to environmental and developmental cues (Paul and Ferl, 1998; Li et al., 2001). Therefore chromatin, both globally and locally, has to be considered as a dynamic responsive structure at all levels of its organization. Chromatin has to be seen as the molecular basis of both stable and transient epigenetic traits.

In the current view, three main actors can be distinguished that participate in an interconnected way in chromatin dynamics: (i) variation of the chromatin protein assortment by the use of histone variants, various linker histones and non histone components (see previous section), (ii) the so-called histone code consisting in a wealth of chemical modifications at the histone tails (discussed below), and (iii) nucleosome repositioning accomplished by large protein complexes by sliding or translocation of the nucleosome along the DNA molecule, or by nucleosome assembly or disruption (discussed at the end of this section).

The alteration of nucleosome structure via histone modifications has been first considered as a mechanism of transcriptional regulation (reviewed in Workman and Kingston, 1998). The various patterns of histone-tail decorations have been suggested to represent a “histone code” (Strahl and Allis, 2000; Nakayama et al., 2001) (Fig. 5). The major and most studied histone modifications are acetylation of various lysine residues and methylation of lysine and arginine residues (Fig. 5) (reviewed in Fischle et al., 2003; Iizuka and Smith, 2003). These phenomena have also been extensively studied in plants (reviewed in Lusser, 2002; Loidl, 2004). The acetylation of histones is regulated by the competing action of the various histone acetyltransferases (HATs) and histone deacetylases (HDACs), which are part of large complexes that share some components with the transcription machinery and are well conserved between organisms (see Pandey et al., 2002; Carrozza et al., 2003). Proteins with HAT activity include yeast HAT1, GCN5 and ESA1, human TIP60 and GCN5, (CBP)/p300 factors, and differ in term of histone

residue specificity and associated partners. These proteins acetylate lysine residues but also other non-histone proteins like p53 and retinoblastoma (Rb) in the case of the (CBP)/p300 HAT, thus participating in additional regulatory functions (Sterner and Berger, 2000). The HDAcs represent a large family of proteins subdivided in three classes according to the names of the yeast homologs: RPD3, HDA1 and SIR2. Plants have an additional class of HDAcs, the HD2-related proteins, but their roles are not yet clearly understood (Loidl and Langer, 1993; Pandey et al., 2002). This diversification of HATs and HDAcs between plants, animals and fungi may reflect the evolutionary plasticity or a functional diversification within these gene families (Pandey et al., 2002). In a simplistic view, histone modifications such as acetylation are thought to prevent neighboring nucleosomes to interact, thereby disrupting condensed chromatin states. However, some histone acetylations have been linked with other processes like silencing (see below). Moreover, several yeast mutants with increased histone acetylation show repression of a large number of genes (Bernstein et al., 2000). Consequently, although histone acetylation and deacetylation are commonly seen as a paradigm for gene activation and repression, respectively, the molecular significance of the potentially enormous diversity of histone acetylation patterns is still largely unknown.

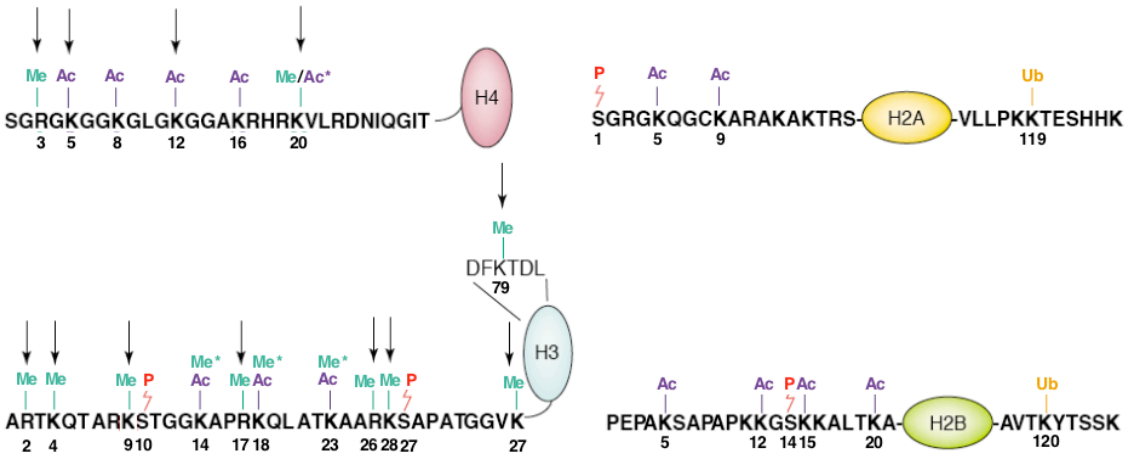

Figure 5. Known histone tail modifications. All reported post-translational core-histone modifications are depicted; most of them being in the Nt tail. Ac, acetylation; Me, methylation; P, phosphorylation; Ub, ubiquitylation. Numbers refer to the amino-acid positions from the Nt. Modifications marked with an asterisk (*) were only reported in plants. For more details see Loidl, 2004.

Histone phosphorylation is another example of a dynamic reversible chromatin

mark (Fig. 5), which can interfere with other modifications. Phosphorylation can affect the standard histones as well as histone variants like H2AX, as mentioned in a previous section. In mammals, H3 serine-10 phosphorylation inhibits H3 lysine-9 methylation (Rea et al., 2000), suggesting that such flexible marks determine more stable modifications like methylation. Histone methyl-transferases (HMT) are responsible for the methylation of arginine and lysine residues of the histone tails of H3 and H4 (Fig. 5). A few histone tail residues can be either methylated or acetylated, in an exclusive manner. Although histone demethylases are predicted to exist, not a single one was isolated so far. Being a more static process, histone methylation provides a rather stable modification, and is considered to be an epigenetic mark (reviewed in Lusser, 2002; Iizuka and Smith, 2003). For instance, H3 lysine-9 methylation is frequently found in heterochromatic regions whereas H3 lysine-4 methylation is mainly observed in transcriptionally active regions (Noma et al., 2001). As for HATs and HDAcs, in every eukaryotic organism many HMTs are responsible for the various histone methylations. The *Arabidopsis* genome contains at least 29 potential HMTs (Lusser, 2002).

Another example for the complexity of the histone code is ubiquitylation, which constitutes an unusual case and one of the least understood modifications. Both histone H2B mono-ubiquitylation and de-ubiquitylation were shown to be involved in gene activation, suggesting that the sequential ubiquitylation and de-ubiquitylation of histones as well as cooperation among different histone modifications play an important role in transcriptional regulation (Henry et al., 2003).

Many studies converged to the important point that all these histone modifications participate in a sort of cross-talk that determines the activity of the chromatin (see examples above and reviewed in (Fischle et al., 2003). This makes it difficult to determine the causes and successive events in chromatin dynamics. In plants the histone code was found to be slightly different than in other eukaryotes, and additional modification sites were found (Fig. 5) (Loidl, 2004). In addition to the cross-talk between modifications at the histone level, recent studies have revealed the existence of a histone-DNA cross-talk between histone acetylation and methylation and DNA methylation, especially in plants. As example, in *Arabidopsis*, H3 lysine-9 methylation is greatly reduced in the maintenance DNA methyltransferase *met1* mutant background in which CpG DNA methylation is abolished (Tariq et al., 2003).

Chromatin remodeling is another aspect of chromatin dynamics that is contributed by the large SWI/SNF (Switch/Sucrose non-fermenting) complexes in an energy-

dependent process. This is accompanied by re-positioning or translocation of nucleosomes along the DNA molecule. SWI/SNF complexes comprise various proteins – at least nine, as revealed by the various described complexes – such as actin, actin related proteins (ARP), SNF5 like proteins and many proteins of unknown function associated with a core ATPase unit (Martens and Winston, 2003). The ATPases belong to the SWI/SNF family of the DEAD/H (SF2) superfamily of DNA-stimulated ATPases. These ATPases are characterized by a helicase motif (it was first described in DNA helicases) consisting of seven conserved stretches of amino-acids. This motif is essentially an ATP binding and hydrolysis motif and does not imply DNA helicase activity. All studied members of the SWI/SNF family contain an ATPase activity but lack a helicase activity. Instead, it is suggested these ATPases provide to the complex, through ATP hydrolysis, the driving force that is necessary to move nucleosomes along the DNA. SWI/SNF ATPases can associate with HATs and HDACs complexes and with the transcription machinery, or at least share common factors with them (reviewed in Tsukiyama, 2002). Primarily, these complexes were found to regulate local gene activity in a complex association with the transcriptional machinery, but they seem to have many more functions (see below). Generally, the increasing amount of data on SWI/SNF ATPases suggests that chromatin remodeling plays a crucial role in establishing and maintaining spatial and temporal patterns of gene activity during development in all eukaryotes (reviewed in Lusser, 2002; Reyes et al., 2002).

There are four main conserved classes within the SWI/SNF family of proteins (Fig. 6), which can be distinguished according to the conserved domains outside the ATPase motif and are conserved in eukaryotes. Although they do not strictly belong to the SWI/SNF superfamily of proteins, the RAD54 and RAD26 like proteins, involved in DNA repair activities, are very similar and can be considered as additional SWI/SNF like classes of proteins (Fig. 6). The SWI/SNF class (from yeast SWI2/SNF2) contains a bromodomain at the C-terminus that binds to acetylated N-terminal histone tails (Hassan et al., 2002; Martens and Winston, 2003). This is consistent with the finding that HAT complexes stabilize SWI/SNF-nucleosome binding at the promoter region (Hassan et al., 2001). Proteins in this class include BRG1 and BRM in mammals, Brahma in *Drosophila* and STH1/NSP1 and SWI2/SNF2 in *S. cerevisiae*. The *Arabidopsis* SPLAYED (SYD) SWI/SNF protein appears to be involved in transcriptional activation and repression, and functions as a co-activator of LEAFY in the transcriptional regulation of the floral homeotic genes (Wagner and Meyerowitz, 2002). The ATPases of the SWI/SNF class

function mostly as transcriptional activators, and can have a redundant role with HATs (reviewed in Tsukiyama, 2002; Martens and Winston, 2003). Several studies describe the sequential recruitment of HAT and SWI/SNF complexes to promote transcription, but the order of recruitment seems to depend on the system studied, (Cosma et al., 1999; Agalioti et al., 2000; Dilworth et al., 2000). There is also substantial evidence that, in addition to their role as activators, some SWI/SNF class complexes are also involved directly in transcriptional repression of some genes (reviewed in Martens and Winston, 2003).

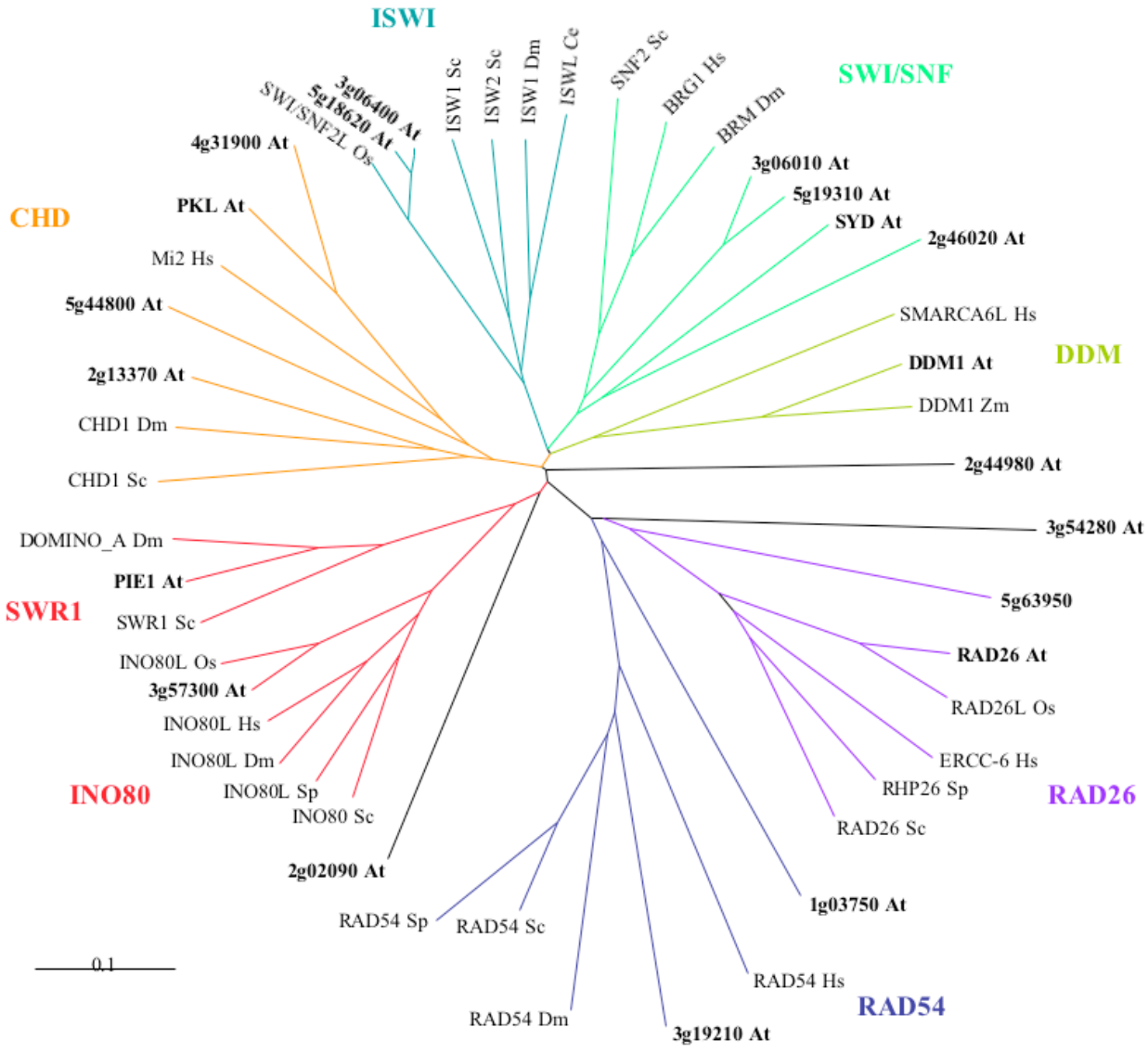

Figure 6. Phylogenetic tree of SWI/SNF related proteins. The four main SWI/SNF protein families (SWI/SNF, CHD, ISWI & INO80) are represented together with closely related families (DDM, RAD26 & RAD54). Only the conserved ATPase motifs were used to do the alignment. All *Arabidopsis* SWI/SNF related sequences were used and are depicted with their AGI number, or reported name when available. For tree building methods and accession numbers, see Materiel and Methods.

The ISWI class takes its name from the *Drosophila* ISWI (imitation switch). In *Drosophila* this unique member can belong to three different complexes that all possess chromatin-remodeling activities and are involved in transcriptional regulation, suggesting another degree of complexity in the control of chromatin remodeling by SWI/SNF complexes. The ISWI members harbor a C-terminal SANT (SWI3, ADA2, NcoR, TFIIIB) domain. The N-terminal part of the SANT domain would interact with HATs or HDAcs (You et al., 2001; Sterner et al., 2002), whereas the C-terminal part was proposed to bind acetylated histone tails (Grune et al., 2003). In *S. cerevisiae*, the ISWI2 containing complex seems to have an opposite effect to the SWI2/SNF2 complex in regulating chromatin accessibility. In addition, the *Drosophila* ISWI was found to be important for the initiation of DNA replication within the CHRAC complex and to participate in chromatin assembly in the context of the ACF (ATP-utilizing chromatin assembly and remodeling factor) complex (reviewed in Ito, 2003).

The CHD (from the mammalian Mi-2/CHD) class of complexes has two consecutive N-terminal chromodomains, that were found in other proteins to mediate interaction with methylated histone H3 (Jacobs et al., 2001). In mammals, the NURD complex combines HDAc, Mi-2 driven remodeling activity and methylated-DNA-binding proteins (Zhang et al., 1998; Wade et al., 1999), suggesting a role for the NURD complex in transcriptional repression linked with DNA methylation. The *Arabidopsis* CHD class PICKLE (PKL), seems to be a co-repressor of embryonic developmental genes (Ogas et al., 1999).

There are two main proteins in the fourth class: the yeast INO80 and SWR1 proteins that contain a characteristic large insertion in the ATPase motifs. INO80 was originally found to be required for yeast growth in the absence of inositol (Ebbert et al., 1999). The INO80 ATPase is part of a large chromatin-remodeling complex that plays a dual role in transcription and DNA metabolism (Shen et al., 2000). The INO80 complex is the unique SWI/SNF complex that does exhibit helicase activity, due to the presence of two true helicases, RVB1 and RVB2, that resemble the bacterial RuvB (see above) (Shen et al., 2000). The yeast SWR1 protein was recently found to be part of a complex required for the recruitment and exchange of the histone-variant HTZ1 (the yeast H2A-Z variant) into chromatin (Krogan et al., 2003; Mizuguchi et al., 2004). This histone-variant exchange activity constitutes a novel function for SWI/SNF complexes. Also, the SWR1 complex promotes the expression of genes near heterochromatic regions (Krogan et al., 2003). An *Arabidopsis* gene that is highly similar to *Drosophila* DOMINO and *S.*

cerevisiae SWR1 was described as PHOTOPERIOD-INDEPENDENT EARLY FLOWERING (*PIE1*). PIE1 has an arrangement of ATPase domains identical to that of INO80 and SWR1, although it has a SET domain that is absent in INO80 and was thus proposed to be an ISWI class protein. PIE1 was found to be required for FLC activation and to promote floral repression, i.e. PIE1 negatively regulates the expression of genes that promote flowering (Noh and Amasino, 2003).

Based on the presence of the seven-fold helicase motif, there are about 39 potential SWI/SNF-like proteins in *Arabidopsis* (Verbsky and Richards, 2001). Among them, about 20 unambiguously fall in the above described classes and are depicted in Fig. 6. With the exception of the three examples given above (SYD, PKL and PIE) where a developmental role was established, most of them are of unknown function. Apart from DDM1 that is described below, none of these SWI/SNF members were shown to possess ATPase and remodeling activities.

The above description of the SWI/SNF classes and several recent studies argue for a much broader role of chromatin remodeling than just transcriptional activation or repression. For instance, recently a link between chromatin remodeling related activities and gene silencing was established. As example, the *Arabidopsis* protein encoded by the *MOM1* (*MORPHEUS' MOLECULE*) gene contains motifs – including a truncated version of an ATPase motif – suggesting a role in chromatin dynamics. *MOM* is involved in the regulation of transcriptional gene silencing (Amedeo et al., 2000). A *mom1* mutation reactivates silent transgenic loci without affecting methylation of their promoter. The DNA methylation locus *DDM1* is also required for the maintenance of transcriptional gene silencing in *Arabidopsis* and encodes the only plant SWI/SNF protein for which ATPase and chromatin remodeling activities have been demonstrated so far (Jeddeloh et al., 1999; Brzeski and Jerzmanowski, 2003). The *mom1/ddm1* double mutant has an enhanced phenotype; this suggests that in plants two transcriptional silencing pathways – one independent and one dependent on methylation, through MOM1 and DDM1, respectively – exist, both of which possibly involving chromatin remodeling complexes (Mittelsten Scheid et al., 2002).

Since they regulate the expression of numerous genes in the cell, SWI/SNF complexes may play a crucial role in establishing gene expression patterns during development. In the plant model *Arabidopsis thaliana*, studies have begun to dissect the molecular basis of the epigenetic controls at work during development, and unraveled an important role for SWI/SNF complexes for the regulation of phase transitions during

development. This is well illustrated by the examples of PKL, SYD and PIE mentioned above (reviewed in Berger and Gaudin, 2003). The BRM (Brahma) complex is required for the expression of homeotic genes and is essential for development in *Drosophila* (Kennison and Tamkun, 1988). In mice, mutations in *BRM* (SNF2α) are accompanied by a compensatory BRG1 overexpression and by an increased size as compared to wild-type animals (Reyes et al., 1998). This is actually a good example of possible compensation or partial redundancy between various SWI/SNF complexes.

Besides chromatin remodeling, other multiprotein complexes were found to be linked with changes in chromatin organization. The Polycomb group (PcG) and trithorax group (trxG) proteins induce and maintain histone methylation and chromatin states at loci of homeotic genes in plants, *Drosophila* and mammals (reviewed in Simon and Tamkun, 2002; Berger and Gaudin, 2003). The HP1 (heterochromatin-associated protein 1) like proteins contain a chromodomain that mediates HP1 binding to the methylated lysine-9 of H3. HP1 like proteins have been involved in the silencing of euchromatic genes, and mammalian HP1α interacts with BRG1, a SWI2/SNF2 ATPase (Nielsen et al., 2002). The regulation of photomorphogenesis mediated by the DET1 (DE-ETIOLATED1) protein in *Arabidopsis* is another example that may involve a special type of chromatin change. DET1 acts as a photomorphogenesis repressor as part of a large protein complex with DDB1 (UV-damaged DNA-binding protein 1) and interacts directly with H2B – and especially unacetylated H2B – *in vitro* and *in vivo* (Benvenuto et al., 2002; Schroeder et al., 2002). In the presence of a light signal, HATs are recruited and acetylate H2B, probably leading to DET1 dissociation from the tail. This suggests that at least in this case H2B has a crucial role in gene regulation.

10) The chromatin context in DNA repair and recombination

The chromatin context of eukaryotic DNA may be considered as a physical barrier for the access and repair of damaged loci, although at the same time it renders the DNA less accessible to some genotoxic agents such as chemical agents (reviewed in Meijer and Smerdon, 1999; Gontijo et al., 2003). The repair machinery must have evolved to recognize and repair lesions within the chromatin context. In addition, the nucleosomal structure of the chromatin has to be disrupted before and reconstituted after complex DNA repair activities like HR, NHEJ, NER and perhaps also others.

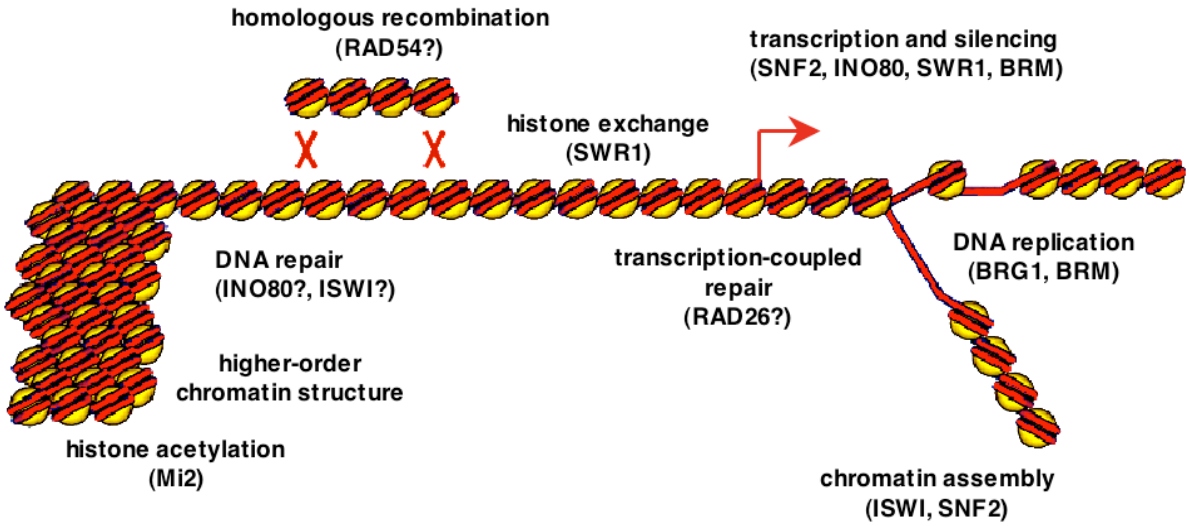

Figure 7. Multiple roles for chromatin dynamics. A non-exhaustive list of chromatin dynamics events are presented together with the known or potential (question mark) implicated SWI/SNF ATPases in brackets.

Is chromatin dynamics actively involved in the control of eukaryotic DNA repair and recombination processes? Does chromatin cooperate with the DNA repair factors and/or does it participate in the reconstitution of intact chromatin after repair? During the time of the present study, *in vitro* and *in vivo* data addressing the link between chromatin modification and DNA repair or recombination started to accumulate (reviewed in Green and Almouzni, 2002; Gontijo et al., 2003). As example, histone acetylation activities and chromatin remodeling – at least *in vitro* by the *Drosophila* ACF complex that contains an ISWI class ATPase – were found to promote NER in the precautious lesion-recognition step (Ura et al., 2001; Green and Almouzni, 2002). The three subunit complex chromatin assembly factor 1 (CAF-1) is involved in chromatin assembly upon DNA replication. In addition, it is recruited to chromatin after UV damage and seems to be specifically involved in the restoration of the chromatin context upon NER (Verreault, 2000; Green and Almouzni, 2003). Histone acetylation was also found to participate in DSB repair, together with histone phosphorylation. The TIP60 (TBP interacting protein) HAT is part of a large complex, and when expressed in a dominant-negative manner, leads to defects in the repair of DSBs (Ikura et al., 2000). Also, the signaling of DNA damage through ATM activation (see in previous section) is not initiated by binding to the actual lesion, but rather involves chromatin modifications as an intermediate (Bakkenist and Kastan, 2003). The molecular basis of one of these modifications was recently unraveled. Histone H4 lysine-16 acetylation by Sin3p facilitates DSB repair in yeast is an additional

nucleosome modification to H2AX phosphorylation that marks the chromatin around DSBs (Jazayeri et al., 2004).

Chromatin remodeling can also directly affect repair pathways, as shown by the fact that NER is directly stimulated by SWI2/SNF2 ATPase activity (Hara and Sancar, 2002). More specifically, the RAD26 and RAD54 proteins involved in DNA repair activities define two additional classes of related SWI/SNF ATPases that have similar helicase domains as the other classes (see previous section), but were not shown to possess chromatin remodeling activities (Fig. 6) (Fyodorov and Kadonaga, 2001). These are *bona fide* DNA helicases that are capable of unwinding the helical DNA structure. It is likely that RAD26 and RAD54 protein-containing complexes act in complexes remodelers specifically devoted to transcription-coupled repair and to recombination. Many other SWI/SNF members remain to be characterized and may act in a similar way in other repair pathways.

11) Aim of the thesis work

The aim of this study was to gain new insights on the regulation of HR in plants, by finding and characterizing novel *Arabidopsis* mutants with altered somatic HR frequency. To address this, we first developed a new type of screen to unravel unexpected factors involved in HR or regulating HR, by combining the powerful *in planta* somatic HR assay with the recently developed activation tagging mutagenesis approach. The key points of the project at this stage were: (i) To screen directly for dominant altered HR phenotypes at the whole plant level, (ii) to combine mutagenesis producing dominant and recessive phenotypes in one screen and (iii) to create a collection of mutagenized plants to be used for other screens. Then, I conducted a minimal analysis of all the candidates in order to get enough information to choose one candidate for a more thorough characterization and to prove and reproduce the recombination phenotype. Through this in depth characterization, I wanted to address the molecular reason for the altered recombination phenotype, using various techniques such as genotoxic stress sensitivity tests, observations of the development and oligonucleotide microarrays.

B. Experimental procedures

1) Materials

1.1) Plant material

All plants used are derived from the *Columbia*-0 ecotype of *Arabidopsis thaliana* (L.) Heynh. with exception of the *rat5* mutant that is in the *Wassilewskija* ecotype background. *mom1*-1 plants were also used (Amedeo et al., 2000). The inverted repeat GUS recombination line 1445 is similar to the previously described 1415 line (Gherbi et al., 2001). The luciferase recombination line 50B contains a similar inverted repeat construct based on the Firefly luciferase gene (Fig. 8). The 50B line is described in J.M., O.F., D. Schuermann, J. Lucht, G. Ries and B.H. in prep. The two allelic *AtINO80* mutants, *Atino80*-2 and *Atino80*-3, used in the study were obtained from the SAIL T-DNA tagged mutant collection (www.tmri.org). The VR1 luciferase expressing line is derived from the 50B line and is homozygous for the recombined reporter locus; the VR1 line was kindly provided by G. Ries.

1.2) Plant tissue culture medium

See Appendix 2 for media stock solutions. The following media were used for *in vitro* culture: Murashige and Skoog (MS) medium (Murashige and Skoog, 1962) from Duchefa or home made and germination medium (GM) (Masson and Paszkowski, 1997). GM: MS macroelements, MS microelements, MS vitamins, EDTA 75 mg/l, FeCl3·6H2O 27 mg/l, Sucrose 1 % (w/v). The pH was adjusted to 5.7 with KOH, and buffered with 0.5 g/l 2-(N-morpholino)ethanesulfonic acid (MES). Callus inducing medium (CIM) and shoot inducing medium (SIM): MS macroelements, MS microelements, B5 vitamins, EDTA 75 mg/l, FeCl3·6H2O 27 mg/l, Sucrose 2 % (w/v), MES 0.5 g/l, pH adjusted to 5.7; supplemented with 2,4-D (2,4-dichlorophenoxyacetic acid, 1 mg/l) and kinetin (0.2 mg/l) for CIM and NAA (α-naphtalene acetic acid, 0.1 mg/l) and BAP (6-benzylaminopurine, 1 mg/l) for SIM. For semi-sterile selection B5 macro- and microelements were used. When necessary, 0.8% (w/v) agar-agar (Merck), 100 µg/ml TIMENTIN® (500 mg Ticarcillinum, 20 mg Clavulanicum) and the following antibiotics were added: kanamycin (50 µg/ml), phosphinotricin (15 µg/ml), hygromycin (10 µg/ml), sulfonamide (20 µg/ml).

1.3) Bacterial strains and growth medium

Escherichia coli DH5α (Hanahan, 1983) and TOP10 electro-competent cells (Invitrogen) were used for cloning. The *Agrobacterium tumefasciens* strain C58CIRif^R containing the non-oncogenic Ti plasmid pGV3101 (Van Larebeke et al., 1974) was used for plant transformation and the tumor inducing *A. tumefasciens* strain A208 for the T-DNA integration assay (Nam et al., 1999).

E. coli were grown in Luria-Bertani medium (LB: 1% (w/v) Bacto-tryptone, 0.5% (w/v) Bacto-yeast-extract, 0.5 % (w/v) NaCl) or on LB plates (add 1.5% (w/v) Bacto-agar). For selection of plasmids, antibiotics were added as follows: ampicillin, 100 µg/ml; spectinomycin, 50 µg/ml; kanamycin, 50 µg/ml. *A. tumefasciens* were grown in YEB (0.5% (w/v) beef extract, 0.1% (w/v) yeast extract, 0.5% (w/v) peptone, 0.5% (w/v) sucrose, 2 mM $MgSO_4$) medium or on YEB plates (add 1.5% (w/v) Bacto-agar) supplemented with 50 µg/ml rifampicin. For selection of plasmids in *A. tumefasciens*: ampicillin, 100 µg/ml; spectinomycin, 100 µg/ml; kanamycin, 50 µg/ml.

1.4) Yeast strains and growth medium

For yeast complementation, the following strains were used: wild-type strain JS91.15-23: *MATα ura3 leu2 his3 trp1 can1* and *INO80* mutant strain YAB1: *MATα ura3 leu2 his3 trp1 can1 Δino80::kanMX*. These strains were kindly provided by H.-J. Schueller. For culture in liquid medium or on plates, yeast artificial medium without uracil was used. For 1 ml: HTL 10x (Histidine, Tryptophane, Leucine), 100 µl; CSM (complete supplement mixture minus Histidine, Leucine, Tryptophane and Uracile from BIO101)/YNB (yeast nitrogen base without amino-acids, DIFCO), 100 µl; glucose 20 %, 100 µl; H_2O, 700 µl.

1.5) Plasmid vectors

The following vectors were used for the study: pUC19 (New England Biolabs), pGEM®-T-Easy, (Promega), pCAMBIA 2300, pDH51 (Pietrzak et al., 1986), pGBKT7 (Clontech), pACT2, pPily, pET3d (New England Biolabs). The whole series of binary vectors (pEXhp, pEX4hp, pEX6Nubip, pEX6N35Sp) was derived from pPZP200 (GeneBank U10460, Hajdukiewicz et al., 1994).

1.6) Enzymes and reagents

The enzymes used in this study were purchased from New England Biolabs (Beverly, MA, USA), Roche Diagnostics (Rotkreuz, CH), Amersham Pharmacia Biotech (Buckinhamshire, UK), TaKaRa Bio Inc (Shiga, Japan), Gibco BRL (Grand Island, NY, USA), Promega (Madison, WI, USA), Stratagene (La Jolla, CA, USA) and Clontech (BD Biosciences, Palo Alto, CA, USA). As for the chemicals: Sigma (St Louis, MO, USA), Fluka (Buchs, CH), Merck (Darmstadt, DE), Amersham Pharmacia Biotech (Buckinhamshire, UK) and Bio-Rad (Hercules, CA, USA).

1.7) Oligonucleotides

Oligonucleotides were synthesized either by the FMI oligo synthesis service or by Microsynth (Balgach, Switzerland). Primers sequences are listed in Appendix 1.

2) Methods

2.1) Plant growth conditions

2.1.1) Soil growth conditions

Plants were grown on soil in a growth chamber at 16 h light/8 h dark cycles with 21°C during the day and 16°C during the night with 60 to 70 % humidity and light intensity of 3000 to 4000 lux. Alternatively plants were grown in a glasshouse with similar conditions but 24h light/day. After sowing, seeds were stratified at 4°C in the dark for 2 days to synchronize germination. For in soil selection of the *BAR* gene conferred resistance, seedlings were sprayed three times with a solution of glufosinate (70 µl in 100 ml) (Basta, AgrEvo) at day 4, 7 and 10 after germination.

2.1.2) Sulfonamide semi-sterile selection

Large-scale selection of sulfonamide resistant seedlings during the screen was achieved in semi-sterile conditions. For this, 900-1000 ml of liquid selective medium (B5 macroelements and B5 microelements in demineralized water with 20 mg/l sulfonamide (sulfadiazine, Sigma S8626) and fungicide (Previcur® 1 ml/l)) was used to imbibe 2 l of perlite in a 49 x 39 cm tray. About 1 g of seeds was distributed on the equalized surface. Tightly covered trays were stratified for 2 days at 4°C and transferred to growth chamber for 7-to-10 days until transformants can clearly be isolated.

2.1.3) Axenic growth conditions

In vitro growth was achieved in growth chamber at 16 h light/8 h dark cycles with 21°C during the day and 16°C during the night with temperature regulated shelves. Seeds were surface sterilized by 2 min incubation in 70% ethanol followed by 10 min incubation in bleach solution (7% hypochloride bleach (technical grade), 0.05% TWEEN-80) with occasional mixing. The seeds were then rinsed 2 or 3 times with sterile double-distilled water and resuspended in 0.08 % liquid agar (DIFCO Bacto-Agar) for easy plating. Seeds were germinated on agar plates containing MS (Duchefa) in growth chamber after 2 days at 4°C in the dark for stratification. For selection, appropriate selective agents were added to the medium (kanamycin 50 mg/l, sulfonamide 20 mg/l, phosphinotricin 15 mg/l). For selection after plant transformation, 100 mg/l of Timentin was added to the medium to inhibit bacterial growth.

2.2) *Arabidopsis* techniques

2.2.1) Plant transformation

Arabidopsis plant transformation was achieved by "floral dip" (Desfeux et al., 2000). In each pot (4x4 cm) to be infiltrated, 5 plants were transferred 7-days after germination and grown in growth rooms with either 16 h or 24 h light condition until the first plants begin to bolt (3-4 weeks). We cut back the first shoots to encourage growth of secondary shoots and to synchronize flowering. Plants were infiltrated about 5 days later, when a maximum number of unopened buds were present (depending on ecotype). In the morning of the day before infiltration a pre-culture of *A. tumefasciens* GV3101 carrying the desired binary plasmid was incubated in YEB with 10 mM $MgSO_4$, 100 mg/l rifampicin and the antibiotic to select for the maintenance of the binary vector, from a fresh plate. In the evening, a large overnight culture (250 ml in 1 l culture flasks) was inoculated in the same medium but without rifampicin. Upon harvesting of the bacteria by centrifugation, the pellet was taken up in half of the original culture volume of infiltration medium IM (10 mM $MgCl_2$, 5 % sucrose) and 0.05 % Extravon® (CIBA), in replacement of Silwet-77, was added to the suspension just before use. The inflorescences were dipped for a few seconds in the solution, and covered with a transparent plastic, returned to growth chamber and kept covered for 3 days.

2.2.2) Plant crosses

Flowering plants carrying the first siliques were used for crosses. Mature siliques, open flowers as well as small unopened-flowers from the meristematic region were removed from the mother plant. The three to five remaining flowers with immature anthers were emasculated and let grown for 2-3 days. At this stage, mature anthers from the father plant were isolated and gently applied to the surface of the sticky stigmate surface of the mother plant.

2.2.3) *Arabidopsis* callus cultures

To induce callus culture of in soil-grown *Arabidopsis* plants, tissues to be regenerated were surface-sterilized by incubation in 0.5 % Na-hypochlorite with 0.05 % TWEEN-80 for 10 min and rinsed three times in sterile water. The plant material was cut up in small pieces, and transferred for one week in a growth chamber on CIM plates that were complemented with 100 μg/ml TIMENTIN® (500 mg Ticarcillinum, 20 mg Clavulanicum) to inhibit bacterial growth, when required. The explants were transferred to SIM plates for one week, and then weekly to fresh SIM plates (extensive cell-proliferation should be obvious by this time) to produce enough material for DNA extraction and to allow shoot induction. By isolating emerging shoots and transferring them to GM plates, plants can be regenerated to produce seeds.

2.3) Homologous recombination assays

2.3.1) Luciferase activity monitoring

Plants containing the luciferase recombination reporter construct were sprayed with a solution of luciferin (Luciferin (Biosynth) 1 mM, Extravon 0.05 %) 20 and 10 minutes before recording. Two exposures of 15 min each in the dark were taken with a nitrogen cooled CCD (charged couple device) camera (Gloor instrument) that was shown to be more efficient for luciferase activity screens than an intensified CCD camera (Michelet and Chua, 1996). The CCD camera was fitted on a dark-room imaging chamber. The two pictures were combined to subtract the universal background and superimposed to a light picture to localize individual recombination events corresponding to luciferase positive sectors.

2.3.2) β-glucuronidase (GUS) activity assay

For the GUS activity, 2-3 week old *in vitro* grown plants were submitted to histochemical X-gluc staining as described previously (Jefferson 1987). The staining solution consisted of an equal mix of Ferri/FerroCN (FerriCN, 2 ml; FerroCN, 2 ml; Na-phosphate 0.1 M pH7, 50 ml; water, 46 ml) and X-Gluc (X-Gluc 100 mg in 1 ml DMF; EDTA 0.5 M pH8, 2 ml; Na-phosphate 0.1 M pH7, 50 ml; water, 47 ml; Triton-X100, 100 µl). Blue GUS positive sectors were then counted using a binocular.

2.4) Sensitivity to genotoxic agents

In all cases, 5-to-7-day-old *in vitro*-grown plants were used. For MMS, MMC and bleomycin, seedlings were transferred to liquid MS medium 24h before applying the agent for acclimation. After 7-10 days of incubation in the growth chamber, differences were evaluated visually and by measuring the plant weight. For UV-C, whole plants or only roots were exposed. To quantify the recovery of root tip growth after treatment, we compared the daily growth before and after exposure to UV-C.

For MMS sensitivity tests, a range of 0, 25, 50, 75, 100, 150 ppm of MMS in MS or GM medium was used to incubate seedlings 3 to 4 weeks at 16h light/day and 22,5°C. Effects were already visible after 1 week. For induction of HR by MMS, the procedure was the same except that plants were grown 10 more days before being transferred to liquid medium with 40ppm MMS.

2.5) T-DNA integration assay

Ten-day-old *in vitro*-grown plants were transferred to new MS plates and grown for another 10 days before cutting root segments of 2-3 mm for the assay. Preparation of tumor inducing *Agrobacterium* suspension and co-cultivation were done as described (Nam et al., 1999). After co-culture, the root segments were directly individualized on MS plates containing 100 mg/l timentin. Tumors were counted 3 weeks later.

2.6) Yeast transformation and complementation

For yeast transformation, the YEASTMAKER™ (Clontech) kit was used (lithium-acetate protocol) according to the manufacturer's instructions. For complementation, an *Arabidopsis* INO80 cDNA fragment amplified by PCR with primers inoBg5' (5'-cccaatagatctatggatccttcaagacgac) and inoSl3' (5'-ccaaacgtcgaccaattgtctaaaacctgc) and cut with *Bgl* II and *Sal* I was cloned in the *BamH* I – *Xho* I sites of p426MET25HA, the vector originally used for the yeast INO80 complementation (Ebbert et al., 1999). As positive control, I used the published vector (pRE82 vector containing the yeast INO80) (Ebbert et al., 1999). Wild-type (JS91.15-23) and *ino80* (YAB1) yeast strains were transformed with both constructs and with the empty vector. Transformants verified by PCR were used for the complementation essays as follows. Over-night cultures were adjusted to the same OD and serial dilutions were plated.

Different UV doses (0, 100 and 200 units) were applied with a Stratalinker (Stratagene). For MMS, plates with 0, 40 and 100 ppm were used.

2.7) Plasmid construction

2.7.1) Generation of binary vectors for the study

A series of binary vectors derived from pPZP200 (GenBank U10460, Hajdukiewicz et al., 1994) was constructed, containing the *bar*, *nptII* or *sul* genes for phosphinotricin, kanamycin and sulfonamide plant resistance under the control of the 1' side of the mannopine synthase bidirectional promoter (MASp). This series was designed to allow RNAi or overexpression strategies with T-DNAs that carry no repeats and are not based on the 35S promoter.

First, an *Eco* RI fragment containing the MASp/*bar* cassette was cloned in the *Eco* RI site of pPZP200 and resulting vectors carrying the *bar* gene pointing towards the LB were selected. A cloning cassette (MCS: *Nco* I, *Hind* III, *Pme* I, *Asc* I, *Avr* II) and a nopaline synthase terminator (nos!) were cloned between the 2' side of the MASp and the T-DNA RB using a PCR based approach. Then, the *bar* gene was cut with *Eco* RI and *Bam* HI and replaced by a digested PCR product containing the *sul* gene from pAC102. Alternatively, a digested PCR product containing the *nptII* gene from pCAMBIA2300 was used. The resulting MASp driven overexpression constructs were called pEX2 (*sul*) and pEX4 (*nptII*) (see map in Appendix 4).

For RNAi experiments, a PCR fragment containing the *FAD2* intron (Smith 2000, and Waterhouse personal communication) was cloned in the cloning cassette on the 2' side of the promoter leaving useful restriction sites before (*Nco* I, *Hind* III, *Xho* I) and after (*Bsr* GI, *Avr* II, *Asc* I) the intron sequence. The resulting RNAi vectors were called pEXhp (*sul*) and pEX4hp (*nptII*) (see map in Appendix 5).

By inserting the *tml* terminator from *A. tumefasciens* Ti plasmid (PCR fragment) between the MASp 2' side and the MCS, I further designed plant vectors for overexpression based on the 35S (pEX6N35SMyci) or ubiquitin (pEX6NUbi) promoter. For pEX6N35Smyci (see map in Appendix 6), the 35S promoter (cloned from a PCR fragment from pAC102) was fused at the translation start with a c-myc epitope containing an intron (from pLOLA, Ferrando et al., 2001). For pEX6NUbi (see map in Appendix 7), the ubi-263 cassette (Genschik et al., 1994) was introduced with an in frame *Nco* I site for subsequent cloning.

2.7.2) RNAi and overexpression constructs

For the three RNAi constructs for luciferase (*LUC*-IR), *RVB21* (*RVB*-IR) and *INO80* (*INO80*-IR), cDNAs were amplified by PCR with primers containing the necessary restriction sites, digested and cloned in direct and reverse orientation, respectively, before and after the intron of pEX4hp or pEXhp in a two step cloning. Primers were as follows: *LUC*-IR LucBG/Xhhp / LucN/Bahp; *RVB*-IR, rv21Nhp (5'-cttccaaccatggcttcccagtagctttatcaatgg) / rv21Xhp (cctttccctcgaggcgaaatctcttggcttg) and rv21Ahp (cttccaacctaggcttcccagtagctttatcaatgg) / rv21BGhp (cctttcctgtacaggcgaaatctcttggcttg); *INO80*-IR, inoIR5' / inoIR3' (see Appendix 1 for sequences).

2.7.3) Expression constructs

The *E. coli* INO80 protein expression constructs for antibody production were obtained by cloning restricted PCR amplified fragments from the *AtINO80* cDNA clone directly in pET3d (Biolabs). The primers contained compatible restriction sites to allow cloning between the *Nco* I and *Bam* HI sites in pET3d, a 6xHis tag and are as follows: NT (InoBsp1168+, InoBgHi1734-) and C (InoBsp2989+, InoBgHi3621-) (see sequences in Appendix 1).

2.8) Standard molecular biology techniques

2.8.1) Bacterial growth and transformation

We transformed competent *E. coli* DH5α or BL21 by heat-shock transformation. Aliquots of the competent cells were thawed on ice and transferred to Eppendorf tubes containing the plasmid DNA or the ligation mix. After 15 min on ice, heat-shock transformation was achieved by incubation of the mix for 60 sec at 42°C and followed by 5 min on ice. 800 µl LB medium was added, and the reaction was incubated 1 h at 37°C before plating. Alternatively, electrocompetent cells of *E. coli* (Invitrogen) or *A. tumefaciens* (for preparation see Hofgen and Willmitzer, 1988) were transformed using a BioRad pulser according to manufacturer's instructions.

2.8.2) Molecular biology

I used standard molecular biology and gene cloning methods (Sambrook and Russel, 2001) to generate the different constructs and vectors used, in combination with PCR techniques. I checked the integrity of the constructs by DNA restriction analysis and sequencing.

2.9) DNA analyses

2.9.1) Isolation of genomic DNA

Genomic DNA was extracted from desiccated callus material or from liquid nitrogen-frozen *in vitro*-grown plant tissues using the PhytoPure plant DNA extraction kit (Nucleon® Biosciences). The plant material was ground in liquid nitrogen and DNA were isolated according to the manufacturer's instructions. DNA were resuspended in TE and cleaned by first spinning down, transferring to a new tube and then adding 2.5 % (v/v) of the PhytoPure resin, shaking for 5 min, spinning for 5 min and transferring the supernatant to a fresh tube. The amount and quality of DNA was estimated by running it on an agarose gel in parallel with dilutions of *Hind* III digested λ-DNA and by measuring the optical density.

2.9.2) Southern blot analysis

I digested 500 ng to 1 µg of *Arabidopsis* genomic DNA and separated it on 0.7% agarose gels. The completeness of digestion was confirmed by EtBr staining. To analyze also fragments larger than 10 kb, DNA was depurinated by incubating the gel in 250mM HCl for 10 min at room temperature. After rinsing with water the DNA was denatured by gently shaking the gel in denaturation solution (0.4 N NaOH; 0.6 M NaCl) (2 x 15 min), briefly rinsed and neutralized by shaking in neutralization solution (0.5 M TRIS-HCl pH 7.5; 1.5 M NaCl) (2 x 15 min). The DNA was then transferred over night to Boehringer nylon membrane, using standard capillary transfer with 20 x SSC as transfer solution (3 M NaCl; 0.3 M Na-citrate; pH 7.0), UV crosslinked with Stratalinker, rinsed in water and dried.

2.9.3) Cloning and characterization of T-DNA insertion sites

T-DNA insertion site cloning was achieved by plasmid rescue from 0.5 µg of genomic DNA digested overnight with *Hind* III. The digested DNA was purified with chloroform, washed in ethanol and resuspended in 32 µl of water. Three ligation reactions with 16, 5 and 1 µl of DNA in a volume of 200 µl were incubated overnight at 16°C. The ligations were precipitated with ethanol, resuspended in 15 µl of water, transformed into electrocompetent TOP10 *E. coli* cells and plated on LB plates with ampicillin. Colonies were analyzed by restriction analysis of plasmid mini-prep and positive clones were sent for sequencing. The retrieved sequences were blasted against the public *Arabidopsis* genome sequence. Primers were designed to confirm the insertion site by PCR on T2 plants and/or to clone the LB junction.

Characterization of the mutated locus and of *AtINO80.* Since the mutation in *Atino80*-1 plants segregated with a single T-DNA as seen by a single band on Southern blot (data not shown), I could characterize the mutated locus by plasmid rescue cloning (Mysore 2000) on the genomic DNA. The junction on the other side was obtained by cloning and sequencing a PCR fragment. Only a few bp of the plant DNA were found to be deleted. The disrupted locus contains a putative gene spread on 10kb of genomic DNA. We cloned the corresponding *INO80* full length cDNA by combining an available EST clone (AI995363) covering the 3' part with RT-PCR amplified fragments corresponding to the 5' part of the gene. The resulting cDNA with a coding sequence of 4524bp was considered as full length because of the presence of an in frame stop codon in the 5'UTR. To distinguish plants that are wild-type, heterozygous and homozygous for the *ino80* mutation, we used PCR with primers differentiating between wild-type and mutated loci. The *INO80* transcript level was estimated by northern-blot hybridization with DIG labeled *INO80* cDNA as probe for detection. RNA was isolated with the RNeasy plant extraction kit (QIAGEN). Primers sequences for PCR and RT-PCR are available on request.

2.9.4) Genotyping

A quick DNA preparation method derived from (Klimyuk et al., 1993) was used for all genotyping. This protocol allows for PCR amplification of plant genomic sequences without extensive DNA isolation. Small amounts of *Arabidopsis* tissues were cut off and transferred to Eppendorf tube using the lid of the tube. After adding 50 µl of 250 mM NaOH, the material was roughly ground with a pipette tip and boiled for 2 min. 50 µl of 250 mM HCl and 30 µl of 500 mM Tris-HCl pH8, 0.25 % Triton X100 were subsequently added before boiling 2 min and spinning at full speed for 30 sec. One µl from the supernatant was used for a 25 µl PCR reaction. Alternatively, the samples were frozen and kept at –20°C for further use.

2.10) RNA analysis

2.10.1) RNA isolation

RNAs were isolated from *in vitro*-grown seedlings using the RNAeasy plant kit (QIAGEN). For one isolation, about 50-to-100 mg of liquid nitrogen-frozen material with 450 µl of the provided RLT buffer (with β-mercaptoethanol) were ground with one tungstene bead in a MixerMill robot for 90 sec at maximum speed. The rest of the extraction was done according to the provided instructions. After elution, the yield was estimated by OD measurement and the RNA was precipitated and resuspended in an appropriate volume. When necessary, a DNAse I treatment on a column was performed during the extraction procedure as recommended by the manufacturer.

2.10.2) RT-PCR

For RT-PCR, I used Ready-To-Go™ You-Prime First-Strand Beads (Amersham Biosciences) on 3 µg of RNA. A 25µl solution of RNA in water was denatured for 10 min at 65°C and left on ice for 2 min before transferring to the tubes containing the beads. After 1 min, 1 µl of oligo-dT (0.5 µg) and 8 µl of water were added. After 1 more min, the solution was homogenized using a vortex and incubated for 1 h at 37°C. Then, I added 32 µl of water to the reaction and stored it at –20°C.

2.10.3) RNA gel blot analysis

For northern blots, I used 10 to 20 µg of RNA. RNA samples in water were mixed with equal volume of denaturating buffer (MOPS x5, 20 µl; formamide, 100 µl; formaldehyde 32% solution, 32 µl) and denatured for 10 min at 65°C and then left for 10 min on ice before adding standard gel-loading buffer (with or without EtBr). The samples were loaded on a 1.2% agarose gel (MOPS; 1.2% agarose and 1.8% (v/v) of formaldehyde 32% solution added just before pouring; with or without EtBr) and run at 80 V. After taking a picture under UV for loading, gels were

directly transferred to a nylon membrane (see Southern blot section) without additional treatments. The membrane was crosslinked, briefly rinsed in water and used for hybridization.

2.11) Hybridization with non-radioactive probes

2.11.1) Preparation of the probe and hybridization

I used DIG-dUTP labeled DNA probes both for Southern and northern blot hybridization. Probes were prepared by standard PCR on plasmid template (500-fold diluted) or pre-amplified PCR products (100-fold diluted). PCR reaction contained 10 µl of DIG DNA labeling MIX (Roche), 5 µl PCR Buffer x10 (QIAGEN), 1 µl of both primers (from 25 µM stock solution) in a 50 µl reaction. The *INO80* probe consisted in a mixture of 5' region and 3' region probes generated with smBGhp/smAhp and smcD2997+/cDsm3748-, respectively. The ampicillin and sulfonamide probe were amplified with bla5'/bla3' and sul5'/sul3' primer pairs.

I pre-hybridized the membrane with 20 ml DIG Easy Hyb (Roche) for 2 h at 42°C. The probe (5 µl of DIG labeled PCR reaction in 10 ml DIG Easy Hyb) was denatured by heating at 68°C for 10 min, and directly filtered into the hybridization bottle after removing the pre-hybridization solution. After over night hybridization at 42°C the membrane was washed twice for 5 min with 2 x wash solution (2 x SSC; 0.1 % SDS) at room temperature and then twice for 15 min at 68°C in prewarmed 0.5 x wash solution (0.5 % SSC; 0.1 % SDS) before proceeding to chemiluminescent DIG detection.

2.11.2) Chemiluminescent detection

All steps were performed at room temperature with gentle shaking unless stated. After hybridization, membranes were first washed 5 min in 50 ml washing buffer consisting of MS-buffer (100 mM maleic acid; 150 mM NaCl; pH 7.5 with NaOH) supplemented with 0.3% TWEEN-20 and then incubated for 30 min in 50 ml blocking buffer (MS-buffer with 1% blocking reagent from Boerhinger prepared in MS-buffer). One µl of anti-DIG-AP conjugate antibody (Boehringer) (centrifuged for 60 s to remove precipitate) was added to 20 ml blocking buffer and used to incubate the membranes for 30 min. Subsequently, membranes were washed twice for 15 min in 50 ml washing buffer, and equilibrated for two minutes in AP-buffer (100 mM Tris-HCl pH 9.5; 100 mM NaCl). After removing excess of liquid, membranes were incubated in the dark for 5 min with CDP-Star chemiluminescent substrate diluted 100 fold in AP-buffer. Excess liquid was removed and the membrane was wrapped in plastic films and exposed to X-ray films.

2.11.3) Stripping of the probe from the membrane

To remove the probe from membranes for further hybridizations, DNA membranes were stripped by washing twice for 10 min in 0.2 N NaOH 0.1 % SDS at 37°C and then briefly at room temperature in 2 x SSC before drying. RNA membranes were stripped by immersion into boiling 0.1 % SDS solution with gentle shaking and left 15 min in the solution to cool down.

2.12) **Nucleosome binding** (in collaboration with Giovanna Benvenuto, Naples)

2.12.1)*In vitro* translation

The INO80 protein constructs for *in vitro* translation were obtained by cloning restricted PCR amplified fragments from the *AtINO80* cDNA clone directly in pGBKT7 (Clontech). The primers used contained compatible restriction sites to allow cloning between the *Nco* I and *Bam* HI sites in pGBKT7 and were as follows: NNT (smAT1, iBg1285-), NT (InoBsp1168+, iBg1683-), NTC (iBsp1615+, iBH2985-), C (InoBsp2989+, iBg4115 – there is a *Bam* HI site at position 3760), CCT (iBsp3691+, iBg4115-) and CT (InoBsp4060+, iBH4518-) (see sequences in Appendix 1). The fragments correspond to the coding sequence as follow: NNT (1-1285), NT (1168-1683),

NTC (1615-2985), C (2989-3760), CCT (3691-4115) and CT (4060-4518). ^{35}S-labelled INO80 proteins were generated using the TNT Quick *in vitro* transcription-coupled translation system from Promega.

2.12.2) Nucleosome preparation and binding assays

Mononucleosomes were prepared from chicken erythrocytes and immobilized to Sepharose 4B as described (Benvenuto 2002). For histone agarose binding assays equal amounts of *in vitro*-translated INO80 proteins were incubated with 10 ml of histone-agarose beads (Sigma) in 50 ml of PBS. After overnight incubation at 4°C, beads were washed three times in PBS. Subsequently the beads were resuspended in 20 ml of Laemmli buffer and resolved on 4-15% gradient SDS-PAGE (Bio-Rad). Following electrophoresis, the gels were fixed in 40% (v/v) MeOH/10% (v/v) HOAc for 30 min, with agitation, followed by a further 30 min incubation in ENLIGHTENING solution (NEN Life Sciences). The treated gels were dried on Whatman 3 MM paper using a gel dryer (Bio-Rad) and exposed to X-ray film in the presence of intensifying screens at -80°C.

For DNA binding assays *in vitro* translated INO80 proteins were incubated with 10 ml of DNA cellulose (SIGMA) in 0.3 ml PBS/0.1% Triton X-100. After 2 hours incubation at 18°C on a rotary incubator, beads were washed three times with the same buffer and treated as described above. *In vitro*-translated INO80 proteins were incubated together with 10 ml of nucleosome or BSA resin in the presence of PBS + 1 mg/ml BSA, in a final volume of 50 ml, overnight at 4°C with agitation. After binding the resin was washed three times and resuspended in 15 ml 2X Laemmli buffer. The bound proteins were resolved on 4-15% gradient SDS-PAGE. Gels were then treated as described above.

2.13) Transcriptome analysis

The transcriptome of *atino80* mutant plants was compared to that of wild-type *Arabidopsis* plants. Since the transcriptomes of 50B and wild-type plants were identical, I compared expression in the mutant with 50B and with wild-type without distinction. Plant lines used for the profiling experiment: 50B line, wild-type, *atino80*-1, *atino80*-2 and *atino80*-3 (all ecotype *Columbia*). All lines were profiled in duplicate (grown independently at 2-week-intervals). Microarray analysis was performed using Affymetrix ATH1 full-genome *Arabidopsis* GeneChips™ (Affymetrix, Santa Clara, USA) and the Chip data analysis was performed using the Affymetrix Microarray Suite v5 and GeneSpring 5.0 (Silicon Genetics).

10 µg of total RNA isolated from 2-week-old *in vitro*-grown plantlets (20-30 plants per line) was reverse transcribed using the SuperScript Choice system for cDNA synthesis (Life Technologies) according to the protocol recommended by Affymetrix (GeneChip Expression Analysis: Technical Manual (2001) p. 2.1.14-2.1.16). The oligonucleotide used for priming was 5'-ggccagtgaattgtaatacgactcactatagggaggcgg-(t)24-3' (Genset Oligo, France) as recommended by Affymetrix. Double-stranded cDNA was cleaned by phenol:chloroform extraction and the aqueous phase removed by centrifugation through Phase-lock Gel (Eppendorf). *In vitro* transcription was performed on 1 µg of cDNA using the Enzo BioArray High Yield RNA transcript labeling kit (Enzo Diagnostics, USA) following the manufacturer's protocol. The cRNA was cleaned using RNeasy clean-up columns (Qiagen). To improve the recovery from the columns the elution water was spun into the matrix at 27 g and then left for one minute prior to the standard 8000 g centrifugation recommended by Qiagen. This low-speed wetting step gave nearly double the yield of eluted RNA (E. J. Oakeley, unpublished observation). The cRNA was fragmented by heating in 1x fragmentation buffer (40 mM Tris-acetate pH 8.1, 100 mM KOAc, 30 mM MgOAc) as recommended by Affymetrix. 10 µg of fragmented cRNA were hybridized to an ATH1 GeneChip (Affymetrix) using their standard procedure (45°C, 16 hours). Washing and staining was performed in a Fluidics Station 400 (Affymetrix) using the protocol EukGE-WS2v4 and scanned in an Affymetrix GeneChip scanner. Chip data analysis was performed using the Affymetrix Microarray Suite v5 (target intensity 500 used for chip scaling) and GeneSpring 5.0 (Silicon Genetics). Changes in gene expression were assessed by looking for concordant changes between replicates using a signed Wilcoxon rank test (as recommended by Affymetrix). The

"change" p-value threshold was < 0.003 for increase and > 0.997 for decrease. After concordance analysis these values become < 9 x10^{-6} and > 0.999991 respectively. Any gene whose detection p-value was > 0.05 in all experimental conditions was discarded from the analysis as being unreliable data. Four replicates of the wild type condition and two replicates for each of the mutant alleles were processed. We calculated Affymetrix change p-values for every gene in every pair-wise comparison between the mutant and wild replicates (2 x 4 = 8) for each condition. A p-value threshold of < 0.003 was selected for a significant change. Using set analysis tools, we retained any gene whose direction of change (increase or decrease) was the same in at least 6/8 of the comparisons. The expression values for these highly concordant changes were then assessed and we generated lists of genes with changed expression (increase or decrease) in all alleles tested compared to wild type.

2.14) Sequencing

DNA sequencing reactions were performed by the in house FMI sequencing service with Dye Terminators (dRhodamine terminators, PE Applied Biosystems) using a Perkin-Elmer GeneAmp PCR system 2400, 9600 or 9700 thermocycler and analyzed using an ABI-Prism377 DNA sequencer. Alternatively, the reactions were sent for sequencing at Microsynth (Baglach CH).

2.15) Computer analysis

DNA and protein sequence comparison were performed by Blast analysis at various sites (NCBI, MIPS Arabidopsis Database (www.mips.gsf.de and TAIR). *In silico* analyses of DNA and protein sequences were mainly done with the DNAstrider, MapPlasmap, ClustalX, Treeview and Mac-BoxShade software. SWI/SNF protein sequences were aligned to the conserved ATPase motifs of budding yeast SNF2 (amino-acids 760 to 947 & 1104 to 1242) using ClustalX program. Then, I removed part of the sequences that were outside the ATPase domains and run the program again to generate alignment and tree files. The same strategy was used for ARP and RVB sequences.

C. Chapter 1

A genetic screen for homologous recombination (HR) mutants in *Arabidopsis thaliana*

1) Introduction

Little is known about the regulation of HR at the molecular level. At the time this work was initiated, no plant gene involved in the HR pathway or its regulation was characterized yet. As plants are powerful genetic tools especially for screening, we decided on designing and conducting a genetic screen to identify plant genes involved in HR. During the time of the screen, several plant genes were reported to be involved in HR (see Table 1, top). In parallel, several known mutations were shown to affect somatic HR frequency, most likely indirectly (Table 1 bottom). So far, plant HR mutants were isolated indirectly on the basis of (i) genetic screens for mutants hypersensitive to genotoxic stress and subsequent HR testing or (ii) by searching for plant homologs of DNA repair or recombination genes known from other organisms.

Using the former approach, the first *Arabidopsis* HR mutants were isolated in 1997, from a genetic screen for x-ray hypersensitive mutants. Three of these recessive *xrs* (x-ray sensitive) mutants were thoroughly characterized and exhibited various HR phenotypes (Table 1) (Masson et al., 1997; Masson and Paszkowski, 1997). Whereas both somatic and meiotic recombination events are reduced in the *xrs9* mutant, the *xrs4* mutant has a striking phenotype: HR is down-regulated and meiotic recombination is up-regulated. Unfortunately, despite the extensive phenotypic characterization, the molecular nature of the *xrs* mutations was not determined.

The *mim Arabidopsis* mutant, isolated on the basis of its hypersensitivity to the radiomimetic agent MMS, exhibits decreased levels of somatic intrachromosomal HR (see Table 1 and Mengiste et al., 1999). The wild-type *MIM* gene encodes a protein closely related to the structural maintenance of chromosomes (SMC) family and its expression is induced by genotoxic stresses. Although loss of SMC function is lethal in other eukaryotes, growth of the *Arabidopsis* mutant is normal in the absence of genotoxic treatments. Overexpression of MIM leads to increased HR levels, suggesting MIM is a

limiting factor for HR (Hanin et al., 2000). The protein encoded by *MIM* is not a classical SMC protein (SMC1 to SMC6), and may represent a new kind of SMC protein. SMC proteins play a central role in chromosome organization and dynamics. They function as specific heterodimers, complexed with other non-SMC proteins (Hirano, 1999). The less studied case is the SMC5-SMC6 heterodimer that was shown to function in DNA repair in *Schizosaccharomyces pombe* (Verkade et al., 1999), suggesting that some other non-standard SMCs may also function in DNA repair or recombination.

Since it is the only described HR mutant in a plant species different from *Arabidopsis*, it is interesting to mention the *Nicotiana tabacum Hyrec* mutant, even though the molecular nature of the mutation was not characterized (Table 1). The *Hyrec* dominant mutation leads to a more than 1000-fold increased level of mitotic recombination between homologous chromosomes (as measured by the *Sulphur* system, see Introduction 6.2), 6-to-9-fold increased extrachromosomal recombination levels, while leaving intrachromosomal HR unaffected (Gorbunova et al., 2000). In addition, *Hyrec* plants are resistant to gamma-irradiation but not to UV-C.

The second approach used to isolate plant HR mutants is by reverse genetic strategies, i.e. identifying known repair and recombination genes from other species such as yeast and human. Although numerous genes were characterized this way (see Table 2 and below), the importance of these genes for HR in plants was not tested so far, with the exception of *RAD50*. The absence of *RAD50* expression in *Arabidopsis* correlates with increased levels of HR (Gherbi et al., 2001). *AtRAD50* is necessary for telomere maintenance and its disruption leads to sterility and MMS hypersensitivity (Gallego et al., 2001; Gallego and White, 2001). Like in yeast, the *Arabidopsis* RAD50 protein was shown to interact with MRE11 (Daoudal-Cotterell et al., 2002).

In addition, several previously characterized unrelated mutants were tested for altered HR frequency during the time of this study (Table 1, bottom). One of these mutants, *uvr2*-1 is defective for the photorepair of the UV induced lesions CPDs (cyclobutane pyrimidine dimers), but somatic HR is only slightly increased. For the others, which are impaired in reactive oxygen species (ROS) scavenging and in plant defense, the effect on HR is most likely through increased DNA damage in the mutant background.

mutant	*gene (AGI)*	*pathway*	*mutagen*	*method*	*repair phenotype, comments*	*reference*
xrs4	ND	ND	EMS	x-ray sensitivity genetic screen	x-ray, MMS & MMC sensitive, decreased HR and increased meiotic recombination	(Masson et al., 1997; Masson and Paszkowski, 1997)
xrs9	ND	ND	EMS	x-ray sensitivity genetic screen	x-ray and MMS sensitive, decreased somatic and meiotic recombination	(Masson et al., 1997; Masson and Paszkowski, 1997)
xrs11	ND	ND	EMS	x-ray sensitivity genetic screen	x-ray and MMC, defective in x-ray mediated HR induction	(Masson et al., 1997; Masson and Paszkowski, 1997)
Hyrec*	ND	HR	ND	spontaneous	γ-ray resistant, increased interhomologs HR, intrachromosomal HR unchanged.	(Gorbunova et al., 2000)
mim	At5g61460	chromatin	T-DNA	MMS sensitivity genetic screen	MMS, UV-C, MMC, x-ray sensitivity, decreased HR	(Mengiste et al., 1999; Hanin et al., 2000)
rad50	At2g31970	NHEJ	T-DNA	homology to known protein	MMS sensitivity, sterility, telomeric defect, increased HR	(Gallego et al., 2001; Gallego and White, 2001; Gherbi et al., 2001)
bru	At3g18730	ND	T-DNA	sensitivity genetic screen	MMS, MMC, UV-C and bleomycin sensitivity, increased HR, TGS release	(Takeda et al., 2004)
centrin	At4g37010	NER	T-DNA	increased HR genetic screen	UV-C sensitive, increased HR, defective in UV-damaged DNA repair	(Molinier et al., 2004b)
uvr2-1/phr1	At1g12370	photorepair		known UV-B sensitive mutant	defective in CPDs photorepair, UV-B sensitive, slightly increased HR	(Landry et al., 1997; Ries et al., 2000a; Ries et al., 2000b)
cim3	ND	plant defense		uncharacterized defense mutant	constitutively activated systemic acquired resistance, increased HR	(Lucht et al., 2002)
vtc1/soz1	At2g39770	vitamin-C		known UV-B sensitive mutant	ascorbic-acid deficient, UV-B and H_2O_2 sensitive, increased HR	(Conklin et al., 1996; Filkowski et al., 2004)
tt4/chs	At5g13930	flavonoid		known UV-B sensitive mutant	chalcone synthase deficient, UV-B sensitive, increased HR	(Li et al., 1993; Filkowski et al., 2004)
tt5/chi	At3g55120	flavonoid		known UV-B sensitive mutant	chalcone isomerase deficient, UV-B sensitive, increased HR	(Li et al., 1993; Filkowski et al., 2004)

Table 1. Plant mutants with altered homologous recombination frequency. In the top part of the Table, DNA repair and recombination mutants are listed with the expected impaired pathway and a summary of their phenotype. Previously described mutants that were later tested for HR are listed in the bottom part. All mutants are in *Arabidopsis thaliana* except *Hyrec* (*) that is in *Nicotiana tabacum*. CPDs, cyclobutane pyrimidine dimmers; HR, homologous recombination; MMC, mitomycin C; ND, not determined; NER, nucleotide excision repair; NHEJ, non-homologous end-joining; TGS, transcriptional gene silencing.

Also, a few other *Arabidopsis* repair gene mutants have been identified. Although HR was not tested in these mutants, it is expected that most of the affected proteins – based on the similarity with known proteins – could interfere to some extent with HR, as it was reported for RAD50 (Table 1 & 2 and Gherbi et al., 2001). Mutants in the *Arabidopsis* homolog of the NHEJ ligase *LIG4* were reported (West et al., 2000; van Attikum et al., 2003); homologs of the *Ku70* and *Ku80* genes involved NHEJ and telomere maintenance have been identified and characterized in *Arabidopsis* (Riha et al., 2002; Tamura et al., 2002; Riha and Shippen, 2003). An *Arabidopsis RAD51* was also reported as well as the *RAD51* related genes *AtXRCC3* and *AtRAD51C* (Doutriaux et al.,

1998; Osakabe et al., 2002; Bleuyard and White, 2004). In addition, six RecQ like homologs were described in *Arabidopsis* that may be involved in DNA replication, repair and recombination (Hartung et al., 2000). SPO11 involved in meiotic recombination also has *Arabidopsis* counterparts (Tables 2 & 3). Homologs of NER and MMR genes – that may also affect recombination – were reported in *Arabidopsis* (Tables 2 & 3): *UVH1* was isolated in a screen for mutants hypersensitive to UV, and appeared to be the homolog of the NER yeast *Rad1* gene (Liu et al., 2000; Dubest et al., 2002), and *Arabidopsis* MSH genes were characterized with respect to heterodimerization and DNA substrate specificity (Culligan and Hays, 1997, 2000).

mutant	*AGI*	*pathway*	*phenotype*	*repair defect, comments*	*reference*
"sunscreen"					
fah1	At4g36220	ferulic acid		UV-B, ferulic acid hydroxylase 1	(Landry et al., 1995)
vtc1/soz1	At2g39770	vitamin-C		UV-B & H_2O_2, HR, ascorbic-acid deficient	(Conklin et al., 1996; Filkowski et al., 2004)
tt4/chs	At5g13930	flavonoid		UV-B, HR, chalcone synthase deficient	(Li et al., 1993; Filkowski et al., 2004)
tt5/chi	At3g55120	flavonoid		UV-B, HR, chalcone isomerase deficient	(Li et al., 1993; Filkowski et al., 2004)
DNA repair					
uvi1		photorepair		UV-B resistant	(Tanaka et al., 2002)
uvr2-1/phr1	At1g12370	photorepair		UV-B, defective in CPDs photorepair	(Landry et al., 1997; Ries et al., 2000a; Ries et al., 2000b)
uvr3	At3g15620	photorepair		UV-B, 6-4 photolyase	(Nakajima et al., 1998)
ros1	At2g36490	BER	normal	MMS, H2O2, causes TGS, DNA glycosylase/lyase	(Gong et al., 2002)
rad1/uvh1*/XPF*	At5g41150	NER		UV-B, UV-C, γ-ray, cisplatin, ineffective *in vitro* repair	(Fidantsef et al., 2000; Gallego et al., 2000; Liu et al., 2000; Dubest et al., 2002; Li et al., 2002)
*rad2****/uvh3****/XPG*	At3g28030	NER		UV, H2O2, IR	(Liu et al., 2001)
rad5	At5g22750			γ-ray, T-DNA integration	(Nam et al., 1998)
*rad3****/uvh6****/XPD*	At1g03190		development	UV, UV photoproduct repair	(Liu et al., 2003)
*rad10****/ercc1/uvr7***	At3g05210	NER		γ-ray, not UV	(Hefner et al., 2003)
*rad25/****AtXPB1***	At5g41370	NER	development	MMS, germination synchrony	(Costa et al., 2001)
centrin	At4g37010	NER		UV-C, HR, UV-damaged DNA repair	(Molinier et al., 2004b)
xrs4	ND	ND		x-ray, MMS & MMC, HR	(Masson et al., 1997; Masson and Paszkowski, 1997)
xrs9	ND	ND		x-ray & MMS, HR	(Masson et al., 1997; Masson and Paszkowski, 1997)
bru	At3g18730	ND		MMS, MMC, UV-C & bleomycin, HR, TGS release	(Takeda et al., 2004)
mim	At5g61460	chromatin		MMS, UV-C, MMC, x-ray, HR	(Mengiste et al., 1999; Hanin et al., 2000)
rev3	At1g67500	translesion synthesis		UV-B, MMC & γ-ray, DNA polymerase ς catalytic subunit	(Sakamoto et al., 2003)
msh2	At3g18525	MMR	normal	microsatellite instability	(Leonard et al., 2003)
ku70	At1g16970	NHEJ	development	MMS, IR, telomere maintenance	(Bundock et al., 2002; Riha et al., 2002; Riha and Shippen, 2003)
ku80	At1g48050	NHEJ		bleomycin, MMS, NHEJ, T-DNA integration not affected	(West et al., 2002; Friesner and Britt, 2003; Gallego et al., 2003)
lig4	At5g57160	NHEJ?	normal	MMS, x-rays, T-DNA integration not impaired	(West et al., 2000; van Attikum et al., 2003; Friesner and Britt, 2003)
rad50	At2g31970	HR/NHEJ	sterility	MMS, telomeric defect	(Gallego et al., 2001; Gallego and White, 2001; Gherbi et al., 2001)
mre11	At5g54260	HR/NHEJ		MMS, IR, telomere maintenance	(Bundock and Hooykaas, 2002)
top6B*/bin3*	At3g20780	ND	early death	increased nuclear DNA strand breaks, reduced mitotic index	(Hartung et al., 2002; Sugimoto-Shirasu et al., 2002)
BRCA2*	2 genes*	HR?	sterility	MR	(Siaud et al., 2004)
mei1	At1g77320	MR	sterility	MR (correct sequence: AJ511367)	(Grelon et al., 2003)
spo11-1		MR			(Grelon et al., 2001)
xrcc3	At5g57450	MR	sterility	bleomycin, MMC, MMS	(Bleuyard and White, 2004)
Signaling					
atm	At3g48190	signaling	sterility	γ-ray, MMS, not UV, MR	(Garcia et al., 2003)
atr	At5g40820	signaling	normal	hydroxyurea, aphidicolin, UV-B	(Culligan et al., 2004)
mkp1	At3g55270	signaling		MMS, UV-C	(Ulm et al., 2001)
myb4	At4g38620	signaling		UV-B, Myb transcription factor	(Jin et al., 2000)
uvr8	At5g63860	signaling		UV-B, RCC-1 like protein	(Kliebenstein et al., 2002)
xrs11	ND	signaling?		x-ray & MMC, HR induction	(Masson et al., 1997; Masson and Paszkowski, 1997)

Table 2. Mutants in *Arabidopsis* genes homologous to known DNA repair or recombination genes. The pathway to which the gene potentially contributes is given when known, together with the general phenotype (recessive lethal mutation, sterility, no effect, etc) of the mutant plants and their genotoxic stress or/and DNA repair phenotype (hypersensitivity unless stated). (*) The

mutant was obtained by RNAi against the two highly homologous *Arabidopsis BRCA2* genes (At4g00020/10 & At5g01630). IR, ionizing radiations; BER, base excision repair; MMR, mismatch repair; MR, meiotic recombination. Other abbreviations as in Table 1.

gene	*AGI*	*pathway*	*activity / comments*	*reference*
BRCA1	At4g21070	HR	induced by IR	(Lafarge and Montane, 2003)
MSH3	At4g25540	MMR	heterodimer with AtMSH2, *in vitro* MMR activity	(Culligan and Hays, 2000)
MSH6	At4g02070	MMR	heterodimer with AtMSH2, *in vitro* MMR activity	(Culligan and Hays, 2000; Wu et al., 2003)
MSH7	At3g24492	MMR	heterodimer with AtMSH2, *in vitro* MMR activity	(Culligan and Hays, 2000; Wu et al., 2003)
OGG1	At1g21710	8-oxoG	AtOGG1 has 8-oxoG lyase activity	(Garcia-Ortiz et al., 2001; Morales-Ruiz et al., 2003)
RAD6	At2g02760	signaling	AtRAD6/AtUBC2	(Zwirn et al., 1997)
RAD23	At1g79650	NER		(Cao et al., 2000)
RAD51	At5g20850	HR		(Ries et al., 2000b)
RAD51B	At2g28560	HR		(Doutriaux et al., 1998)
RAD51C	At2g45480	HR		(Doutriaux et al., 1998)
RAD51D	At1g07747	HR		(Doutriaux et al., 1998)
RAD54	At3g19210	HR		
RECQL1				(Hartung et al., 2000)
RECQL2			interacts with WRNexo protein	(Hartung et al., 2000)
RECQL3				(Hartung et al., 2000)
RECQL4A				(Hartung et al., 2000)
RECQL4B				(Hartung et al., 2000)
RECQsim				(Hartung et al., 2000)
WRNexo	At4g13870		homologous to exonuclease domain of human *WRN*	(Plchova et al., 2003)
XPB2	At5g41360	NER	highly similar to XPB1	(Costa et al., 2001)
XRCC2	At5g64520			(Doutriaux et al., 1998)
ZDP	At3g14890	SSB repair	ZDP recognizes SSBs and catalyzes removal of 3' end blocking lesions	(Petrucco et al., 2002)

Table 3. Additional *Arabidopsis* genes homologous to repair genes. Non-exhaustive list of reported *Arabidopsis* genes with homology to DNA repair genes from other organisms. Only genes for which no mutations were characterized are listed. SSB, single-strand breaks. Other abbreviations as for Table 1.

Although these studies are necessary and may even unravel plant specific properties for these known repair or recombination genes, they represent a biased way of looking at plant genes involved in or regulating recombination. Most of the genes obtained by this way are involved in the basic machinery of HR, whereas very few are involved in the regulation of the pathway or in the interplay with the chromatin structure. Also, recent studies revealed that mutations in such genes often give rise to severe developmental phenotype in combination with hypersensitivity to genotoxic stress (see Table 2 and ref. within). Since most plant stresses affect HR frequency (see General Introduction), this is

problematic when it comes to the assessment of an *in vivo* function in homologous recombination.

2) Results

2.1) A direct genetic screen for *Arabidopsis* mutants with altered somatic HR

2.1.1) Design of the HR mutant screen

In contrast to the indirect approaches described above, we decided to use a direct screening strategy to identify plant mutants exhibiting altered frequencies of somatic recombination. We chose *Arabidopsis thaliana* for its convenience for genetic studies and the presence of a complete sequencing project. Also, in order to screen directly for altered recombination phenotypes, we took advantage of the HR reporter system that was developed in our group, in combination with the firefly luciferase gene to allow a direct and non-lethal screen for mutants with altered somatic HR levels.

As a background for the screen, we chose the intrachromosomal HR reporter line 50B, that was not previously reported. When the recombination screen was started, the 50B line was the only luciferase based reporter line available for *Arabidopsis* ecotype *Columbia* This line harbors as a single transgene (G. Ries, personal communication) a HR construct based on the Firefly luciferase gene (Fig. 8) that is similar to the previously published GUS constructs (see General Introduction and Swoboda et al., 1994). Intrachromosomal recombination events between the two inverted repeats restore a functional luciferase gene (Fig. 8). The functionality of the luciferase gene can be assayed by detection of light emission after application of the substrate D-luciferin using a high-sensitivity CCD camera (Fig. 9A) (Millar et al., 1992; Millar et al., 1995; Millar and Kay, 1996). A similar luciferase-based reporter system was used recently to analyze interchromosomal recombination in *Arabidopsis* plants (Jelesko et al., 1999).

To be appropriate for the screen, the reporter line must fulfill several requirements for the distribution of recombination events. The number of recombination-spots/plant has to be centered on the average value and plants that do not follow the distribution curve must be extremely rare. To evaluate this, I counted luciferase spots on 175 50B plants grown under similar conditions to those used for the screen. As a result, the average number of luciferase sectors on 50B plants is well centered on 2 spots/plant, and I found only one plant with 6 spots and none with more (Fig. 9B).

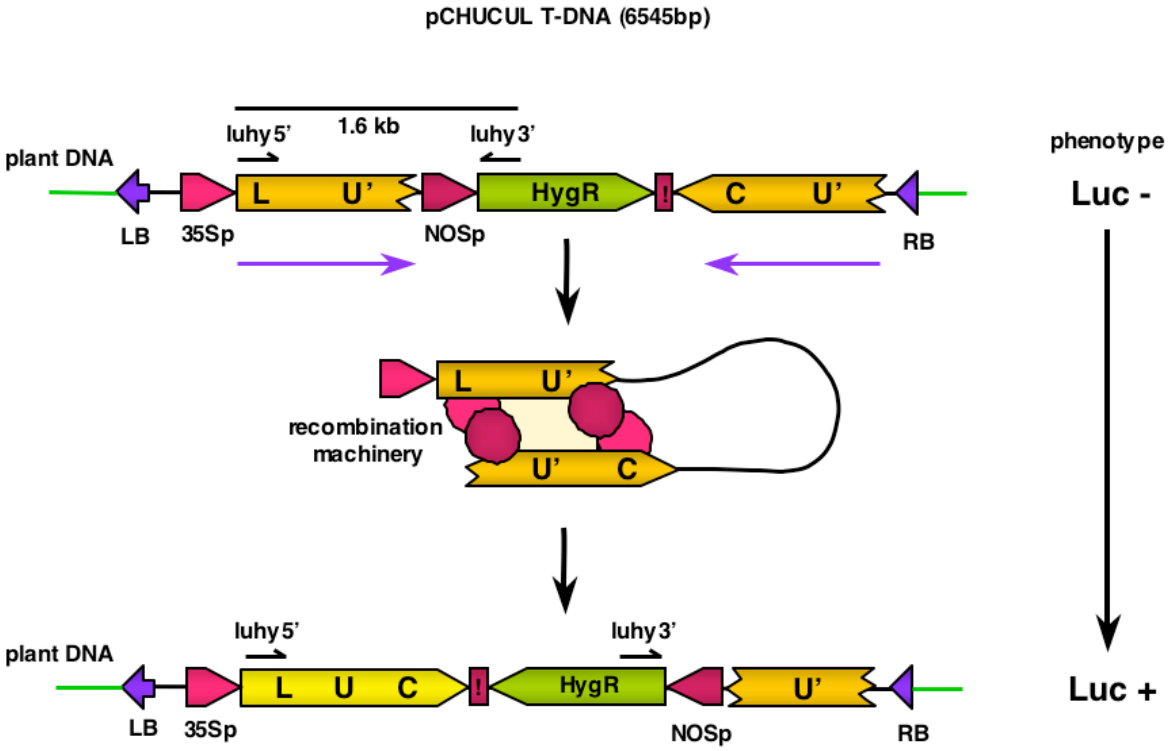

Figure 8. **The 50B line contains the integrated T-DNA region of pCHUCUL as an intrachromosomal HR reporter construct.** The luciferase construct integrated in the *Arabidopsis* genome consists of two inactive fragments (LU, UC) of a Firefly luciferase reporter gene sharing an identical stretch of 1147bp (U). HR between the inverted repeats restores a functional luciferase gene (LUC+). PCR with the luhy5'/luhy3' primer pair gives a 1.6 kb positive signal specific for the unrecombined configuration. 35Sp, CaMV viral promoter driving the luciferase gene expression. The hygromycin resistance gene (HygR) is under the control of a nopaline synthase promoter (NOSp) and allows for the selection of plants harboring the integrated construct. LB and RB, left and right borders of the T-DNA construct.

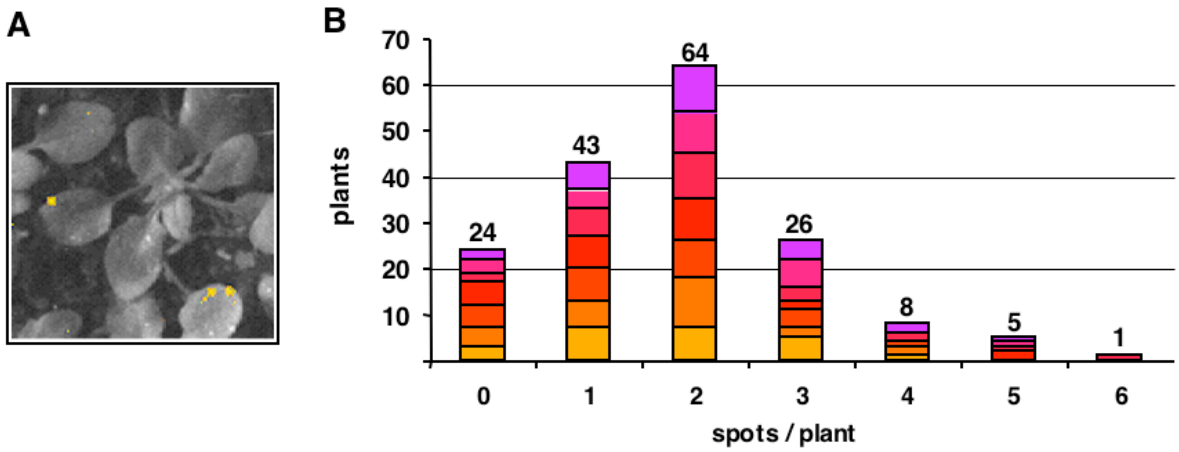

Figure 9. Distribution of luciferase sectors in the line 50B. (A) Composite picture of 50B plants showing luciferase sectors (from the dark luciferase picture) on the leaves of the plants (black & white light picture). **(B)** Distribution of the luciferase sectors in the line 50B. 7 trays (colors) with 25 plants each were counted. Plants were three-week-old and grown in soil.

As a mutagenizing agent, I used the T-DNA from the pAC102 binary vector that was kindly provided by B. Reis. This T-DNA harbors a complete 35S promoter sequence close to the right border and facing outwards (Fig. 10A). It also carries two resistance genes – also under the control of the 35S promoter – that allow for the selection of plant transformants with sulfonamide or phosphinotricine (basta). In addition, the sequence between the right border and an internal *Hind* III site contains the complete pUC plasmid sequence allowing cloning of T-DNA/plant genomic DNA junction by plasmid rescue (see below).

Such a system carrying a promoter or enhancer facing outwards the T-DNA is known as activation tagging mutagenesis and enables direct screening for dominant mutations in T1, in addition to standard T-DNA mutagenesis for recessive mutations. The insertion of the pAC102 T-DNA in a given gene locus (Fig. 10B) may result in various effects. Insertion upstream of a promoter may result in overexpression of the gene (Fig. 10C). Insertion after the gene in antisense orientation may lead to gene inactivation by an antisense effect (Fig. 10D). A knock-in insertion in the transcribed region (Fig. 10E) give rise to a potentially recessive null allele but may also result in (i) overexpression of a truncated part of the gene giving rise to a dominant-negative or positive effect or/and in (ii) an additional dominant antisense effect. Therefore we could expect dominant mutations by screening in the T1 generation and recessive mutations in the T2 generation. Because of this we decided to harvest seeds from all individual transformants to allow a second screen for recessive HR mutants or for other dominant or recessive phenotypes in the T2 generation.

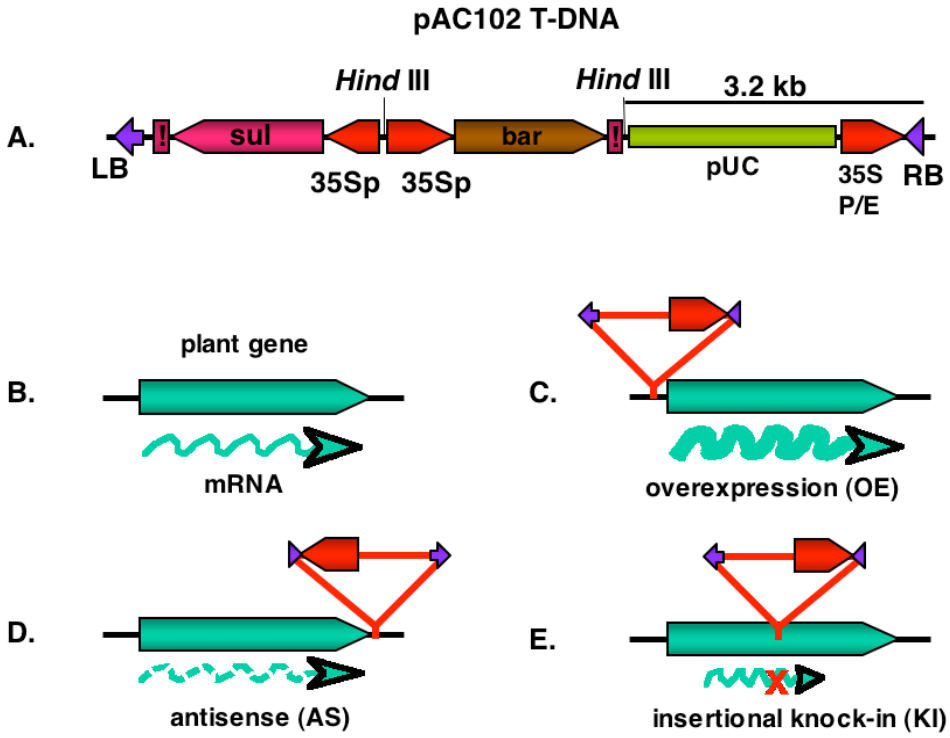

Figure 10. **T-DNA activation construct and potential effect on targeted genes.** **(A)** The pAC102 T-DNA region. Sul, sulfonamide resistance gene; bar phosphinotricine resistance gene; pUC, pUC plasmid sequence for plasmid rescue containing the ampicillin gene; !, transcription terminators. **(B)** Plant gene with wild-type level of RNA expression. **(C)** Activation of gene expression by insertion upstream of the coding sequence. **(D)** Reduction of the mRNA level by antisense effect. **(E)** Abolishment of gene expression by knock-in insertion.

To determine a reasonable size for the screen, we calculated the probability (*P*) to hit any *Arabidopsis* gene. Considering that about 1.5 T-DNAs would integrate in each transformant and that the *Arabidopsis* genome contains 25000 genes on about 100000 kb of DNA, we used the formula $P=1-(1-f)^N$ (Clarke and Carbon, 1979), where f is the fraction target length / genome length and *N* the number of insertions. According to this method, we can expect a saturation probability of about 70% by screening about 20000 T1 transformants, which we considered as suitable.

2.1.2) Supertransformation of the 50B line and selection of the T1 transformants

To produce the mutagenized population of reporter line to be used for the screen, we transformed by floral dipping (i.e. without vacuum infiltration) 33 trays of *Arabidopsis* representing 924 pots with about 5 plants each. From these, we harvested 386.4 g of

seeds. I selected all of them for sulfonamide resistance (conferred by the integrated activation-tagging T-DNA) in semi-sterile condition by batch of 1 g and obtained 23270 resistant seedlings as potential independent transformants. This represents a mean transformation efficiency of 5-transformants / transformed-plant or 705-transformants / transformed-*Arabidopsis*-tray. I observed a large variation in transformation efficiency (Table 4), but it could not be attributed to a particular parameter such as the influence of temperature and length of plant/agrobacterium incubation (Table 4). This is perhaps because the most important parameter (that was no measured) was the dilution with seeds coming from early or late flowers that were not subjected to dipping.

tray	*incubation*	*seed yield*	*resistant plants /g-seeds*	*total/g*
1	2 days 22°C	10.6 g	38	
2		11.8 g	52	≈45
3	2 days 14°C	13.5 g	73	
4		12.4 g	51	≈62
5	2 days 22°C	14.0 g	43	
6		13.2 g	71	≈57
7	2 days 16°C	12.0 g	38	
8		9.25 g	33	
9		11.6 g	23	≈31
10	2 days 16°C	6.4 g	30	
11		11.1 g	38	
12		10.7 g	25	
13		11.8 g	21	
14		11.8 g	12	
15		10.3 g	34	
16		12.9 g	24	
17		11.2 g	**11**	≈24
18	2 days 16°C	15.3 g	38	
19		14.7 g	24	
20		14.4 g	37	
21		14.1 g	37	
22		14.9 g	32	
23		13.3 g	46	≈35
24	2 days 16°C	10.9 g	52	
25		13.5 g	34	
26		11.1 g	31	≈39
27	4 days 16°C	11.4 g	101	
28		10.0 g	96	
29		12.0 g	82	≈93
30	2 days 16°C	11.3 g	151	
31		10.2 g	**247**	
32		13.8 g	183	
33		11.1 g	163	≈184
			Average	≈60

Table 4. Efficiency of transformation for the screen. The conditions for the *Agrobacterium*/*Arabidopsis* "coculture" or incubation are listed with the amount of seeds harvested for each of the 33 trays of 50B plants. The efficiency is given in reference to harvested seeds. An extreme value is in bold. Total/g, average of transformant plants/g of seeds for each condition.

2.1.3) Luciferase-based screening for HR altered phenotypes

Since I looked for dominant phenotypes, I tested HR directly on the primary transformants. Selected transformants were transferred (i) to soil for one week to allow the 4 first true leaves to develop and then (ii) again in new square trays with 25 plants each according to the size of the plants. At 20-to-25-days after germination I submitted

the trays to luciferase imaging. To discriminate mutant candidates from the other transformants, I first considered T1 transformants with two luciferase sectors or more. I compared the number of spots on these plants with the average number of spots per plant for the 24 other transformants on the same tray. I considered as mutant candidates the plants that exhibited more than 10 times the average level of recombination sectors. At two times during the screen, I had trays with a severe increase of luciferase sectors for all the plants, often in a gradient from one side of the tray to the other. However, nothing particular had happened to these plants that could explain this phenomenon. As it was unlikely to have so many candidates in the same tray, I did not consider these plants.

Out of a total of 789 trays representing 19520 plants that were screened, I found 46 candidates. The difference between these 19520 plants to the 23270 selected plants actually screened (see above) results from plants that died in the time lapse between the transfer to soil and the luciferase imaging. To confirm the increased level of luciferase sectors in these T1 plants, I tested them again one to three weeks after the initial test. The 37 plants that passed this step were chosen for further characterization and sorted in three classes according to their relative increase in HR (Table 5). Class 1 candidates have a strong increase of luciferase sectors or look fully luciferase positive, i.e. they exhibit a potential recombination increase above 50-fold (see as examples *up23* & *to24* Fig. 11). The second class consists of candidates with an increase in luciferase sectors ranging from 15- to 50-fold and the third class contains candidates with a moderate recombination increase (10-to-15-fold).

Whereas some candidates exhibited an increased number of spots throughout the whole plant (see *to24* Fig. 11C & 11D and others Table 5), other candidates had an increase only on rosette leaves (see *up23* Fig. 11A & 11B and 8 other candidates on Table 5), juvenile leaves (Table 5, *cq2*, *hw17*, *ms19*, *adx23* & *yl19*) or only on one leaf (Table 5, mostly class 3 candidates).

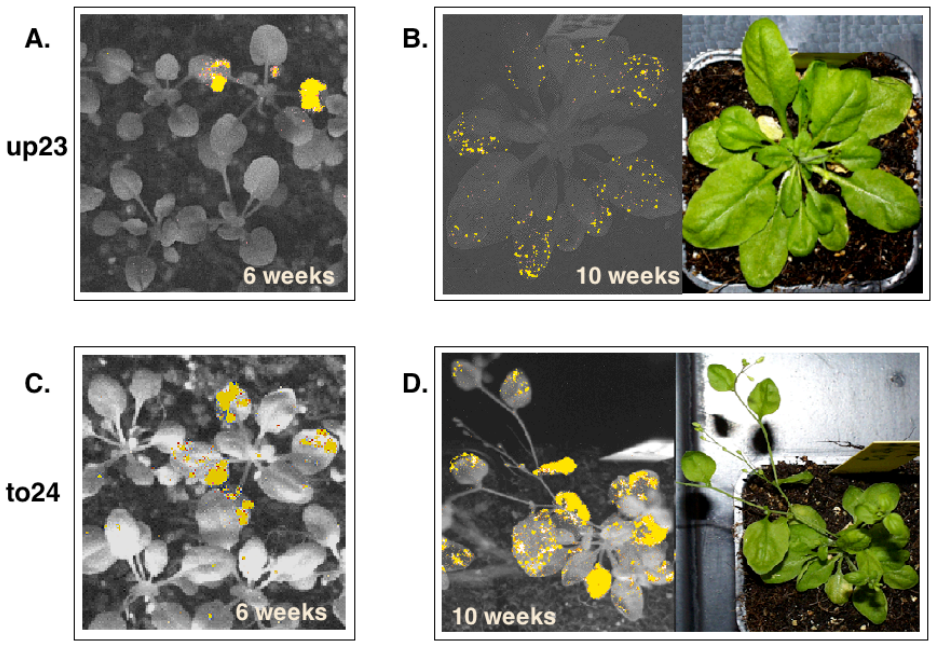

Figure 11. HR mutant candidates with a strong increase of luciferase sectors. Luciferase pictures of *up23* and *to24* candidates in their original trays **(A)** & **(C)**, and 4 weeks later **(B)** & **(D)**.

plant	*increase*	*comments*
class 1		
ea10	ND	LUC+ plant
hs24	>50	whole plant
to24	≈50	whole plant
up23	≈50	rosette leaves
class 2		
cq2	≈40	juvenile leaves
hi5	≈15	rosette leaves
hs13	≈20	
hw17	≈20	juvenile leaves
kp25	≈15	rosette leaves
lb21	≈20	
mn8	≈20	bushy
ms19	≈20	juvenile leaves
sm22	≈20	rosette leaves
sr15	≈15	rosette leaves
sq4	≈30	
xg20	≈15	
xw13	≈20	2 leaves
ack14	≈25	

plant	*increase*	*comments*
adx23	≈20	mostly juvenile leaves
ado7	≈25	one leaf
xv12	≈20	rosette leaves
zo15	≈30	4 leaves
adp12	≈15	
yj23	≈40	
yl19	≈30	mostly juvenile leaves
class 3		
fp8	≈10	one leaf
jr19	≈10	
js2	≈10	one leaf
qh3	≈10	
vw4	≈10	rosette leaves
yk24	≈10	
zq20	≈10	3 leaves
zq24	≈10	whole plant
abx20	≈10	
acp6	≈10	rosette leaves
adq16	≈10	one leaf
adx21	≈10	one leaf

Table 5. Recombination phenotype of the T1 candidates. All candidates are listed. The recombination increase was estimated against non-candidate transformants (see text). Comments refer to the part of the plant that exhibited the increased level of luciferase sectors, and to potential luciferase positive plants (LUC+).

2.2) Characterization of the HR mutant candidates

2.2.1) Guidelines for the characterization

To get molecular data about the candidates already in the first generation, I amplified material by inducing calli from leaves or stem sections for all the candidates. I used this material to isolate genomic DNA for the molecular characterization of the mutation (Southern blot and plasmid rescue) and as a rescue in case the candidate plant was sterile (Fig. 12). In parallel, I checked the candidate's offspring for HR phenotype and T-DNA marker segregation. I then genotyped these T2 plants according to the determined mutation(s) to follow the insertion site segregation and to isolate homozygous lines (Fig. 12). I finally combined all these data to determine on which candidates a more thorough analysis should be undertaken.

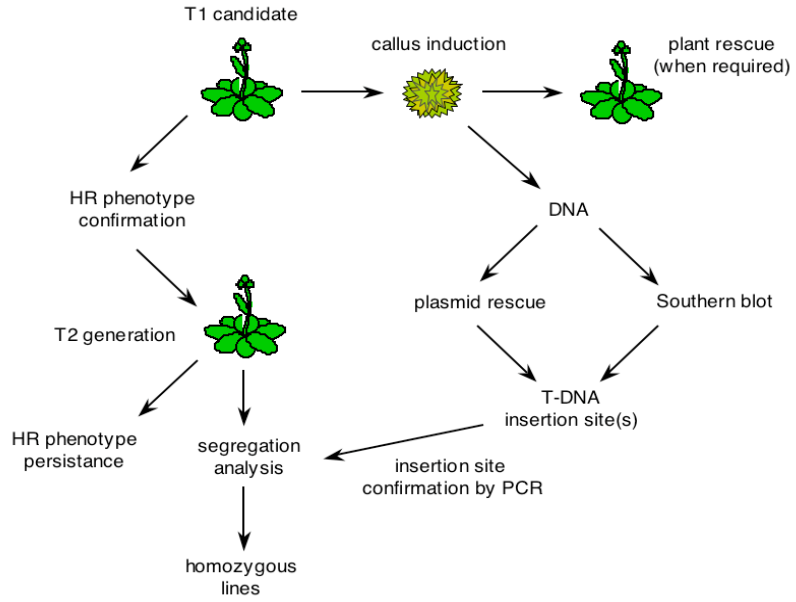

Figure 12. General scheme for the characterization of HR mutant candidates.

2.2.2) Developmental phenotype

I looked at the growth and developmental phenotype for all the candidates. Since these plants were unique, I could not conclude at this stage that the observed phenotypes were linked to the recombination phenotype. I could use it as a guideline for further characterization in offspring plants. Nine of the candidates were sterile (Table 6). In most cases it was not solely a deficiency in fertility, but it was accompanied by severe developmental and growth defects (as example, see *jr19* and *sq4* Figure 13A & 13B). A small percentage of sterility is expected in primary *Arabidopsis* transformants. For this screen, the proportion of sterile transformants (actually, plants that die late in

development or did not produce seeds) was around 1 % (189 plants). In contrast, 24 % of the HR mutant candidates were sterile, which represents a 25-fold enrichment compared to the internal control. However, this trait it not equally distributed between the classes, as class 1 candidates all produced seeds, 3 out of 21 plants in class 2 were sterile, whereas 5 of the 12 class 3 candidates were sterile. Although sterility does not seem to be a general trait of recombination-up candidates, this suggests that sterile plants with developmental or growth defects might be more prone to moderate HR increase and/or that many recombination genes are also involved in growth and development.

A few candidates displayed developmental or growth abnormalities (Table 6), but this is again not to be considered as a common feature of recombination candidates. Indeed during the screen I recovered plants with similar developmental and growth phenotypes that did not exhibit altered HR phenotypes, although such phenotypes were much more frequent in the candidates (data not shown).

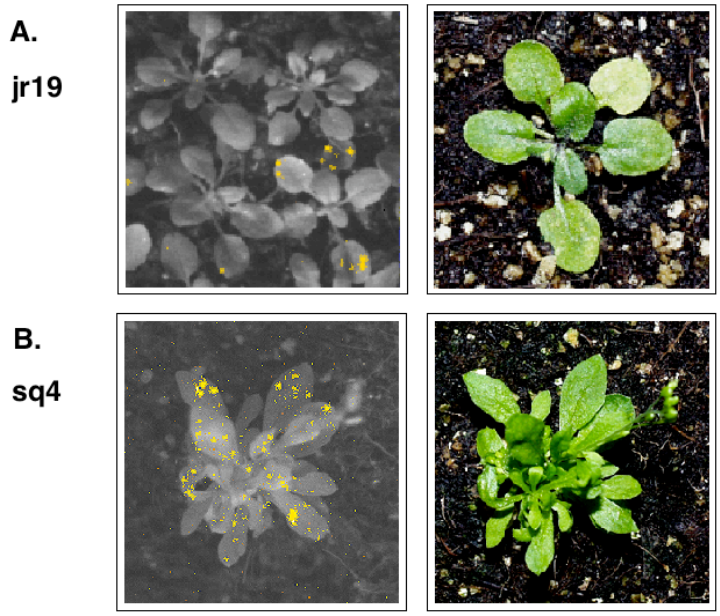

Figure 13. Candidates with moderate increased HR. (A) The *jr19* plant exhibited an increased HR phenotype only on the first true leaves of the rosette and a sterile phenotype. **(B)** The *sq4* candidate had an increased HR phenotype associated with sterility and with a bushy phenotype.

2.2.3) Persistence of the phenotype and isolation of homozygous lines

To further characterize the HR phenotype of the candidates, I assessed the HR frequency in the T2 plants derived from each candidate and compared it to HR in 50B plants. I germinated T2 seeds from the candidates and from the 50B line in soil and monitored HR events 2-weeks and 4-weeks post germination on 18 plants each (candidate and control)

on the same picture. Strikingly, none of the candidates retained the same level of increased HR in the second generation compared to the original T1 phenotype. In most cases, HR frequency was indistinguishable in candidates and 50B control plants. However, as we expected persistent phenotypes, the settings of this experiment (18 plants only, 50B line instead of out-segregant controls) were such that changes in HR frequency below 2-to-4-fold could not be addressed accurately. As an exception, the *hw17* candidate did retain a moderate recombination-up phenotype in the T2 generation (Fig. 22B); it showed an about 20-fold higher recombination frequency than control T1 plants (see below), and an about 2-to-4-fold increase, compared to the control, in the offspring.

Because of the complex T-DNA used for mutagenesis, harboring three copies of the 35S promoter, progressive silencing of the activation tagging 35S (close to the right border) and the consecutive loss of promoter-enhancer effect could possibly explain the disappearance of the phenotype. A loss of phenotype in the second generation for half of the candidates was also reported in the activation tagging screen by the group of D. Weigel, together with a progressive attenuation of the phenotype through generations (Weigel et al., 2000).

To attempt to recover the initial HR phenotype from a potential silencing effect, I tried several methods. First, I treated *in vitro*-grown candidates and control plants with the demethylating agent 5-azacytidine 7-to-14-days before HR monitoring. I did not see any recovery of the recombination-up phenotype by this method, although the induction of HR by 5-azacytidine was so strong (10-to-30-fold) already in the control that it may have masked the recovery. As another approach to recover the phenotype, I crossed some of the candidates at the homozygous stage (*to24*, *sm22*, *vw4*, *up23* and *kp25*) with the *mom*-1 mutant that was shown to reactivate previously transcriptionaly silent genes (Amedeo et al., 2000). I compared the resulting F2 plants with 50B line plants for the occurrence of luciferase spots and found no significant increase in the crossed plants.

Despite this phenotype problem, we decided to isolate homozygous lines, and to study the segregation of the potential HR phenotype-causing mutation; this facilitated further work on the candidates and allowed to collect more information for the choice of interesting candidates. First, I analyzed the segregation of the mutagenizing T-DNA in T2 plants by sulfonamide selection. This gives the apparent number of loci with an active sulfonamide resistance gene, as a single locus is expected to segregate about 3-to-1 and 2 loci are expected to segregate about 15-to-1 for resistance-to-sensitivity (Table 6, third column). Important distortions in the segregation may mean that the candidate has a male

or female gametophytic defect, or has an embryo lethal phenotype. I confirmed these indications by segregation analysis in the T3 generation, and used them subsequently in combination with molecular data (see below) to isolate lines homozygous for the mutations.

Unexpectedly, I found 9 candidates with a T2 generation that was 100% sensitive to sulfonamide (Table 6). The molecular analysis (Southern blot and plasmid rescue, see below) suggested that only 3 of those contain an integrated pAC102 T-DNA. The 6 others could be untransformed 50B that passed the selection. It is therefore possible that the recombination increase is not due to a mutation but to the stressing environment that represent the selection for such wild-type plants. Thus, I considered these plants as potential false candidates (*lb21*, *sr15*, *xg20*, *adp12*, *yj23* & *yl19*). Despite of this, one of them had an interesting developmental and recombination phenotype in the second generation (*xg20*, see in a later section).

2.2.4) Genomic insertion sites of the mutagenizing T-DNA

The mutagenizing T-DNA of pAC102 allows for plasmid rescue of T-DNA RB/plant-genomic junctions using *Hind* III digested genomic DNA of the candidates because of the pUC plasmid sequence present between a *Hind* III site and the RB (Fig. 10A). For a standard T-DNA integration, we expect after the RB sequence the *Arabidopsis* genomic sequence of the integration site up to the next genomic *Hind* III site. The expected size and number of junctions to rescue can be deduced from Southern blot analysis using *Hind* III restriction and the ampicillin sequence from pUC as a probe, as this should allow the detection of the very same fragments that can be rescued after ligation. I performed Southern blot analysis with 1 µg of *Hind* III digested genomic DNA probing for sulfonamide (sul) or ampicillin (bla) resistance genes for all candidates (Table 6, and Fig. 14). In addition to help for the plasmid rescue, Southern blot analysis also revealed the complexity and multiplicity of T-DNA insertions.

For plasmid rescue, I first ligated *Hind* III digested genomic DNA in conditions that favor intramolecular ligation, to restore a functional pUC vector harboring the T-DNA RB/plant-genomic DNA junction. Restriction analysis of plasmids recovered in *E. coli* cells revealed the sizes of the junction fragments. This was also important in cases in which two bands were seen on Southern blots, and to chose clones with different junction fragments (*hw17* and *sq4* Fig. 14 as examples). As extreme examples, *vw4* has clearly one 4.2 kb band (Fig. 14) that corresponds with the 4.2 kb rescued plasmid (Fig. 36),

whereas *mn8* has a minimum of 5 bands (Fig. 14), and all but one rescued plasmids contain T-DNA and vector sequences only (Fig. 25).

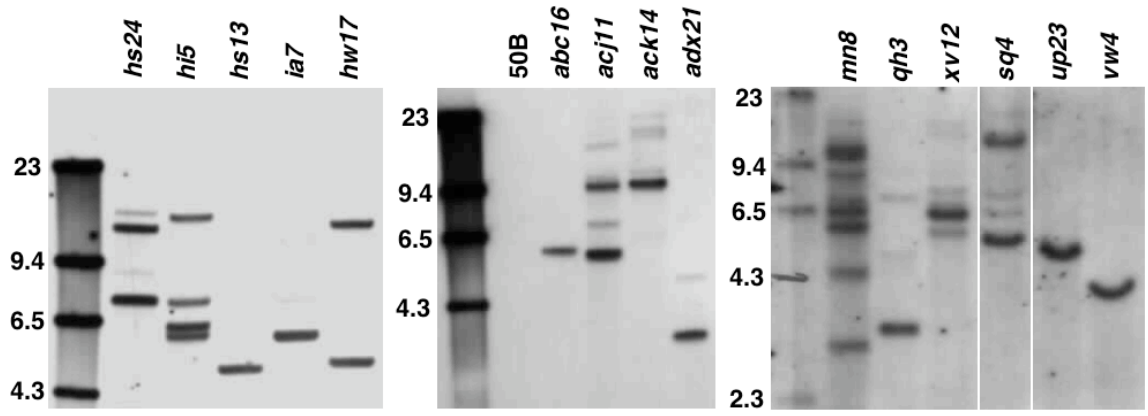

Figure 14. Southern blot analysis of some T1 candidates. T1 genomic DNA of the HR mutant candidates was digested with *Hind* III and hybridized with DIG-labeled *bla* (ampicillin gene) probe. The size of DIG-labeled DNA ladder in kb is given on the left.

To characterize the genomic loci of the T-DNA insertions, I sequenced two or three rescued clones of each restriction pattern and analyzed them using Blast analysis on the potential plant sequence against the *Arabidopsis* genome database. The insertion sites of the candidates were distributed on the whole genome except on chromosome IV and a region of chromosome I that has a similar size (Fig. 15). However, with such a small number of insertion sites this may not be significant. The insertion site analysis is given for all candidates on Table 6 and more precisely for each candidate in a section below.

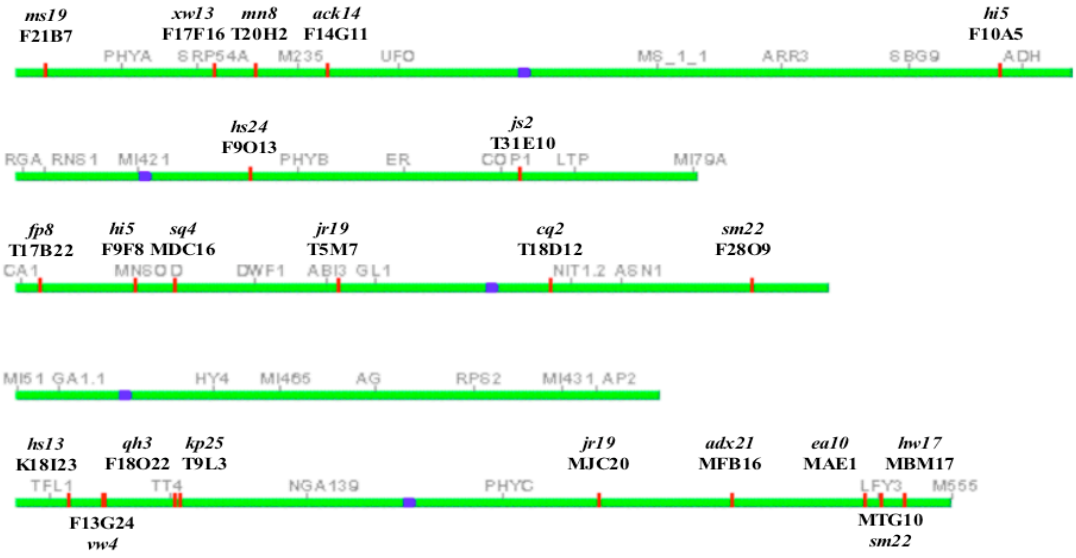

Figure 15. Schematic representation of T-DNA insertions on the five chromosomes of *Arabidopsis*. The BAC or P1 clone name corresponding to the locus of insertion is given for each candidate. Blue boxes, centromeres; gray labels, markers.

Of the 25 junctions rescued, only 11 have a conserved RB sequence followed by the genomic sequence. Five harbor a deletion of the RB sequence from a few bp up to 385 bp or more, that is often associated with insertion of unrelated DNA. In addition, two insertions contain the whole pAC102 backbone vector region from RB to LB, which may result from RB skipping during T-DNA processing in *Agrobacterium* (*ea10*, Fig. 16; *hs24* see specific section). Moreover *hs24* also harbors the whole LB region with the sulfonamide resistance gene after the pUC sequence that replaced the RB region (Fig. 18). The latter and other observed rearrangements or complicated insertions (data not shown) are probably reminiscent of recombination or annealing events between the 3 copies of the 35S promoter of the T-DNA (Fig. 10A). Also two RB-to-RB and one LB-LB tandem insertions were found (*to24* & *up23*, Table 6 and see also in next section; *hi5*, Fig. 20). Additional rearrangements, especially at the LB side may exist, as only four LB junctions were analyzed.

2.3) State of work and description of the candidates

2.3.1) Current art for all the candidates

I list below, in a descriptive way, all available information on the candidates. Table 6 summarizes information and state of work (segregation, sterility, insertion site and available homozygous lines) for all candidates, whereas information on recombination can be found in Table 5. In the following sections, where candidates are grouped by recombination classes, we describe additional data for some candidates and give a schematic representation of the loci into which T-DNAs are integrated.

plant	Southern	segregation (n)	insertion region	chromosome	RB insertion or deletion + vector sequence	potential target	comments
class 1							
ea10	3	8.3 (56)	MAE1	V		*At5g60810*, At5g60820	H
			F17A17	III	v(5kb)	At3g07900, At3g07890	H
hs24	3	0.3 (98)	F9O13	II	v(≈2kb) +RB skipping	*At2g15620*	H
to24	1	3 (82)		ND	RB-RB	?	
up23	1	9.7 (32)		ND	RB-RB with deletion	?	H
class 2							
cq2	1	3 (21)	T18D12	III	v(20bp)	*transposable element*	H
hi5	4	4.1 (77)	F10A5	I	LB-LB, d(RB), i(250bp)	At1g75600, *At1g75610*	H
			F9F8	III	i(150bp)	At3g10960, At3g10970	
hs13	1	all S (137)	K18I23	V		At5g05460, At5g05470	
hw17	2	11,5 (149)	MBM17	V	genomic deletion	*At5g63950*, At5g63960	embryonic lethal
			repeats	ND		?	
kp25	1	1.2 (90)	T9L3	V		*At5g14840*, At5g14850	H
lb21	0	all S (43)					
mn8	5	sterile	*T20H2	I		*At1g20220*, At1g20225	
ms19	2	all S (160)	F21B7	I		At1g03457, At1g03470	
sm22	2	3,1 (45)	*F28O9	III		At3g57290, *At3g57300*	H
			MTG10	V		At5g62000,	
sr15	0	all S (53)					
sq4	1	sterile	*MDC16 (III)	III	dRB(270bp)	At3g13980, At3g13990	
xg20	0	all S					lethal
xw13	2	3 (79)	F17F16 (I)	I	dRB(385bp), i(40bp)	At1g16930.1, *At1g16920.1*	H(1)
ack14	1	2.4 (40)	F14G11 (I)	I	dRB, i(56bp)	At1g25580, At1g25682	
adx23	ND	3 (109)		ND			H
ado7	ND	sterile		ND			
xv12	1	all S (19)		ND	RB-RB		
zo15	ND	ND		ND			
adp12	0	all S (22)					
yj23	0	all S (47)					
yl19	0	all S (27)					
class 3							
fp8	1	4.3 (114)	T17B22 (III)	III		At3g03110, *At3g03120*	
jr19	>2	sterile	T5M7 (III)	III		*At3g25670*, At3g25680	
			MJC20 (V)	V		At5g42010, At5g42020	
js2	1	4.9 (77)	T31E10 (II)	II		At2g34550, At2g34560	
qh3	1	sterile	F18O2 (V)	V	i(30bp)	At5g14230	
vw4	1	2 (30)	*F13G24 (V)	V	dRB(68bp) + i20bp	At5g08050, At5g08060	H
yk24	ND	ND		ND			
zq20	ND	sterile		ND			
zq24	ND	sterile		ND			
abx20	ND	sterile		ND			
acp6	ND	4,0 (129)		ND			
adq16	ND	3.3 (82)		ND			
adx21	1	2.9 (81)	MFB16 (V)	V		*At5g50710*	

Table 6. T-DNA insertion sites and potential target genes. For each T1 candidate the number of *Hind* III bands containing the ampicillin gene is reported as determined by Southern blotting (Southern column). For about 100 *in vitro*-grown T2 seedlings, the ratio of resistant to sensitive plants towards sulfonamide was calculated (unless the T1 plant was sterile). On the insertion column, the region of integration of the T-DNA(s) is reported as determined by plasmid rescue. For some candidates, the LB junction (*) was also determined by PCR and sequencing. Associated rearrangements are indicated with their size: d, deletion; i, insertion; v, vector sequence; RB-RB and LB-LB, head-to-head and tail-to-tail tandem T-DNA insertion, respectively. The two closest genes to the insertion are listed as potential target genes. Genes in italic have the T-DNA integrated in the coding region. H, homozygous line, when available.

2.3.2) T-DNA insertion sites and selected candidates

2.3.2.1) Candidates from the class 1

- ea10

For *ea10,* two insertion sites were found by plasmid rescue, one each on chromosome V and III (Fig. 16). This is in agreement with segregation for sulfonamide resistance versus sensitivity close to 15/1 (data not shown). In addition, a minimum of 4 bands is seen on Southern blot, suggesting that at least one of the T-DNA integration results from a complex event. The insertion on chromosome V maps to the region of the P1 clone MAE1, and the insertion on chromosome III maps to BAC clone F17A17. As for this latter junction, the sequence recovered after the RB consists of the pAC102 binary backbone from the RB to about the LB (4536 to 9020 bp). Then follows a short direct repeat of 19 bp, followed by a stretch of T-DNA LB region in reverse orientation (9676 to 9614 bp), before the junction with plant genomic DNA (Fig. 16). Combined with the fact that several clones from plasmid rescue contained T-DNA regions, this suggests that complex T-DNA rearrangements are associated with one of these insertions.

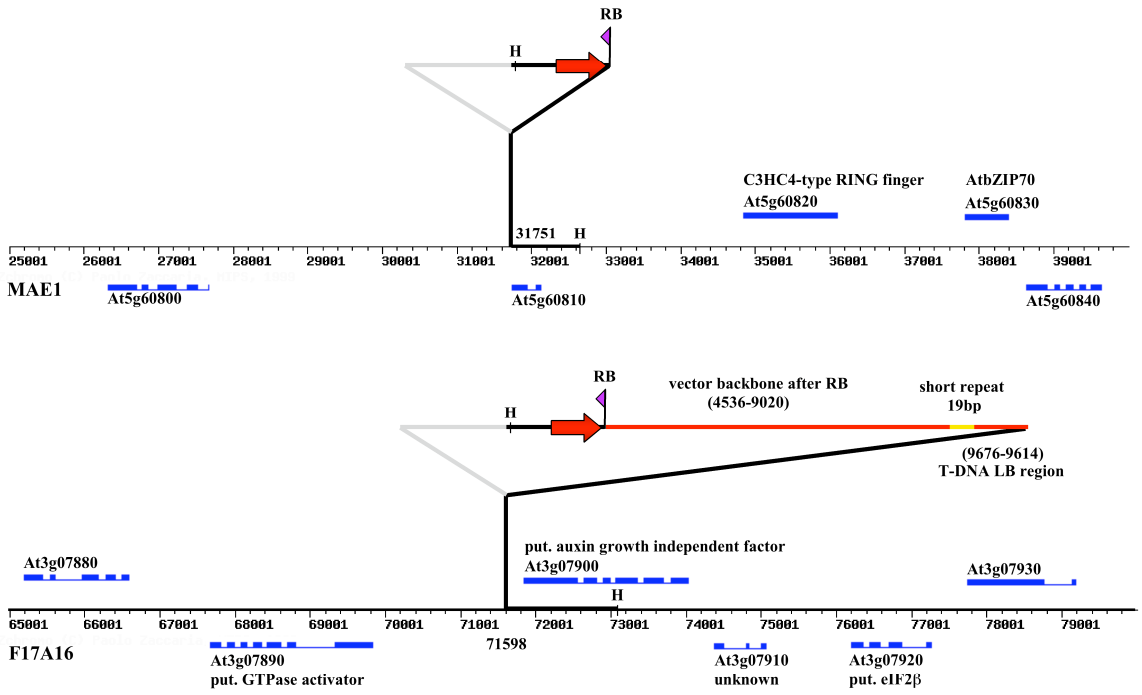

Figure 16. ***ea10*** **has T-DNAs inserted in chromosome V, P1 clone MAE1 and in chromosome III, BAC clone F17A16.** The inserted T-DNAs are represented according to plasmid rescue, PCR and Southern blot data. Regions in grey have not been analyzed. Predicted or known genes in direct or reverse orientation are depicted along the genomic region of the insertion. The red arrow represents the 35S promoter enhancer. LB & RB, T-DNA left and right borders; H, *Hind* III restriction sites flanking the rescued junction.

On the first luciferase record picture, *ea10* plants exhibited a strong luciferase activity on the whole plant that was confirmed at a later stage where in addition stem leaves, flowers and siliques were also luciferase positive (data not shown). This phenotype was maintained and segregating in the second generation (Fig. 17). Such a strong luciferase activity on the whole plant can be explained either by a dramatic increase of HR events or by a HR event at the reporter locus early in T1 development or late in the T0 generation. This may produce a luciferase plus plant with one functional allele of the luciferase reporter in the whole plant. Alternatively, this reporter locus event may be linked with or mask a recombination-up phenotype. To test this, I looked at the correlation between the segregation of the phenotype (Fig. 17), the segregation of the mutation and the segregation of the recombined locus in the second generation. PCR primers (luhy5' & luhy3') that specifically amplify the unrecombined reporter locus were used (Fig. 8), thereby allowing the identification of plants homozygous for the recombined locus by absence of a PCR product. Indeed, plants with a strongly increased luciferase activity are fully recombined plants (Table 7). In addition, plants 7 and 13 segregate as wild-type for the T-DNA despite their strong luciferase activity. The other *ea10* plants with many luciferase sectors or strong luciferase activity may be heterozygous for the recombined reporter locus (Plants 18, 19 & 21 on Table 7). This strongly suggests that *ea10* was heterozygous for a recombined reporter allele that is responsible for the observed luciferase phenotype. I cannot exclude, however, that a recombination-up phenotype was originally the cause of this transmittable recombination event.

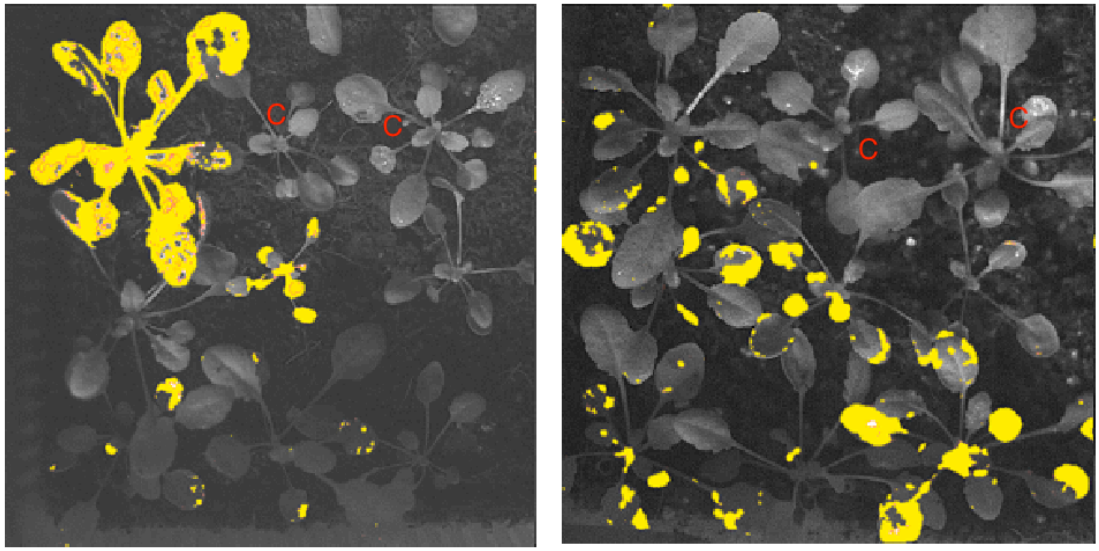

Figure 17. **Segregation of the luciferase phenotype of *ea10* plants in T2 generation.** Three-week-old segregating *ea10* plants were submitted to luciferase imaging. The two pictures are representative of the various patterns observed. C, 50B control plants.

plant	PCR sul	PCR luhy	PCR adh	luc phenotype	plant	PCR sul	PCR luhy	PCR adh	luc phenotype
1	+	-	+	full	16	+	+	+	+
2	+	+	+	+	17	+	+	+	-
3	+	-	+	++	18	+	+	+	++
4	+	-	+	++	19	+	+	+	++
5	+	+	+	-	20	+	+	+	-
6	+	+	+	+	21	+	+	+	++
7	-	-	+	full	22	+	+	+	+
8	+	+	+	+	23	+	-	+	full
9	+	+	+	+	24	+	+	+	-
10	+	-	+	full	25	+	-	+	++
11	+	+	+	+	50B	-	-	+	-
12	+	+	+	-	50B	-	-	+	-
13	-	-	+	full	50B	-	-	+	-
14	+	-	+	full	50B	-	-	+	-
15	+	+	+	-					

Table 7. Segregation of the luciferase phenotype and T-DNA insertions in *ea10* progeny plants show that *ea10* has a recombined reporter locus. A segregating T2 population of *ea10* plants was submitted to luciferase imaging and PCR genotyping together with 50B as control. Presence (+) and absence (-) of a PCR product is reported for primer pair specific of the T-DNA sulfonamide gene (sul, sul5' and sul3'), the unrecombined luciferase substrate (luhy, luhy5' and luhy3') and the endogenous *ADH* (alcool dehydrogenase) gene as control (adh, adh5' and adh3'). For the luciferase activity: Full, fully positive plant; ++, many active sectors; +, a few sectors; -, no sectors.

- hs24

The initial Southern blot analysis shows 3 bands (plus a faint one from incomplete digestion) for *hs24* (Fig. 14) that still co-segregate in the T3 generation, suggesting that they represent linked T-DNA insertions or a single complex insertion (data not shown). The 7 kb band corresponds to the rescued junction on chromosome II (Fig. 18), whereas the two others could be associated with other rescued plasmids that contain pAC102 backbone sequence (probably from RB skipping). Only one-fourth of the T2 plants were sulfonamide resistant. Also, in T3 these families exhibited a 1.5-to-1 resistant/sensitive ratio, suggesting that some of the plants with the insert(s) are not viable. Indeed, the T-DNA integration disrupted the *NIR1* gene (nitrite reductase), important because of its involvement in the second step of nitrate assimilation, but nothing is known about the phenotype of *NIR1* mutants (Lin and Cheng, 1997; Takahashi et al., 2001).

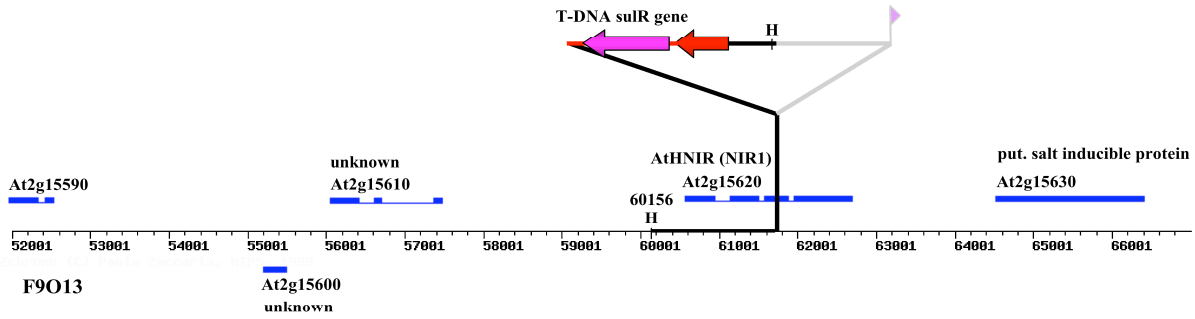

Figure 18. ***hs24*** **T-DNA insertion site in chromosome II, region of BAC F9O13.** The insertion site is likely to be complex and to contain vector backbone sequences (see text). Comments and conventions as for Fig. 16.

- *to24* and *up23*

The mutant candidate *up23* exhibited more than 50-fold increased recombination levels on all rosette leaves (Fig. 11A & 11B). I observed a similar increase for *to24*, but on the whole plant (Fig. 11C & 11D). Development and fertility were in both cases similar to that of wild-type plants. I was not successful in cloning plant T-DNA junctions for these candidates and got only vector sequences. In both *to24* and *up23*, the activation tagging T-DNA seem to be integrated as two copies in a head-to-head conformation (RB-RB), i.e. the 35S promoter-enhancer from each T-DNA facing each other. For *up23*, the 5 kb band on Southern blot (Fig. 14), together with PCR analysis of genomic DNA and rescued plasmids (data not shown), suggest an important deletion at the RB/RB junction. For *to24*, the 6.5 kb band seen by Southern blot (data not shown), is of the expected size for a RB/RB tandem integration (two times the *Hind* III-RB sequence, Fig. 10A).

2.3.2.2) Candidates from the class 2

-*cq2*

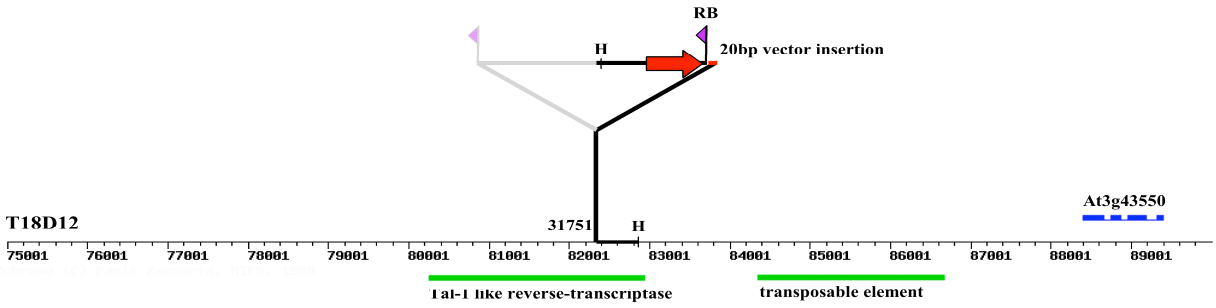

Figure 19. ***cq2*** **T-DNA insertion site in chromosome III, region of BAC T18D12.** Comments and conventions as for Fig. 16.

- hi5

The *hi5* plant exhibited 10 spots per leaf for all rosette leaves, but no spots were seen on axillary stem leaves. Four *Hind* III bands were seen on the Southern blot, but only one locus was recorded through segregation analysis (Fig. 14 and data not shown).

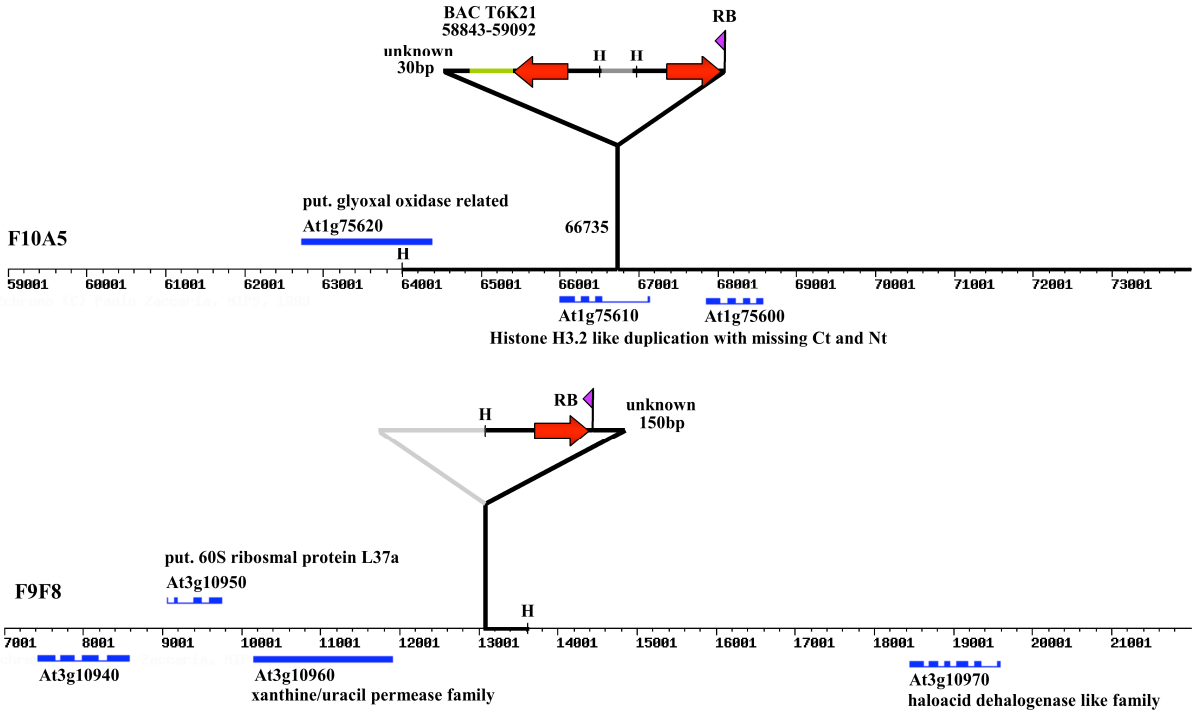

Figure 20. ***hi5*** **T-DNA insertion sites in chromosome I, region of BAC F10A5 and chromosome III, region of BAC F9F8.** Comments and conventions as for Fig. 16.

- hs13

The Southern blot analysis gave a 4.7 kb band (Fig. 7), that is similar in size with the rescued plasmid (Fig. 14).

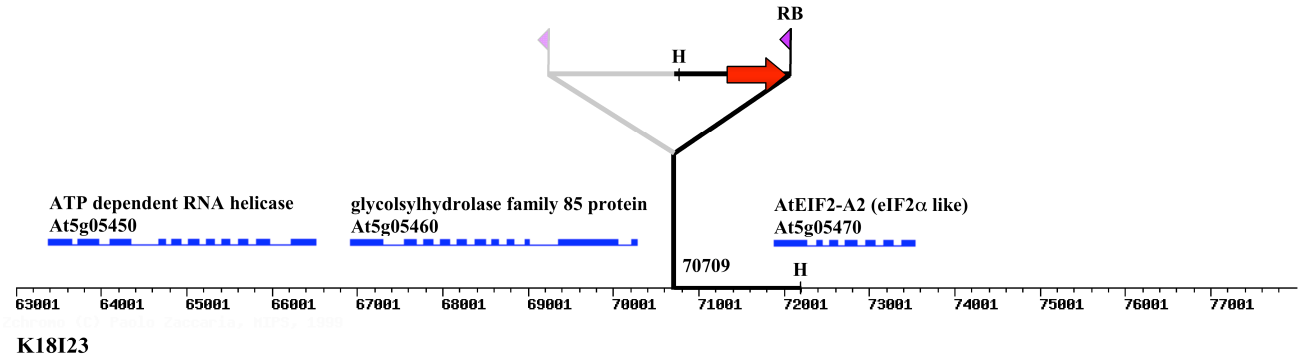

Figure 21. ***hs13*** **T-DNA insertion site in chromosome V, region of BAC K18I23.** Comments and conventions as for Fig. 16.

- hw17

The original picture of the *hw17* plant shows 10-to-20 luciferase spots on 5 leaves (Fig. 22A), which were confirmed 2 weeks later. The overall development of *hw17* was normal. As already mentioned above, the recombination-up phenotype of *hw17* was maintained in the T2 generation (Fig. 22B). The genetic and molecular characterization of this mutation is the subject of another thesis work. Two T-DNA insertion sites were found (see Fi. 14 for the Southern blot and data not shown). One T-DNA integrated in the region of BAC MBM17 in a potential RAD26 like ATPase gene (Fig. 23), and the second T-DNA insertion site is in genomic region containing ribosomal repeats, but could not be attributed to a precise genomic location (data not shown from plasmid rescue).

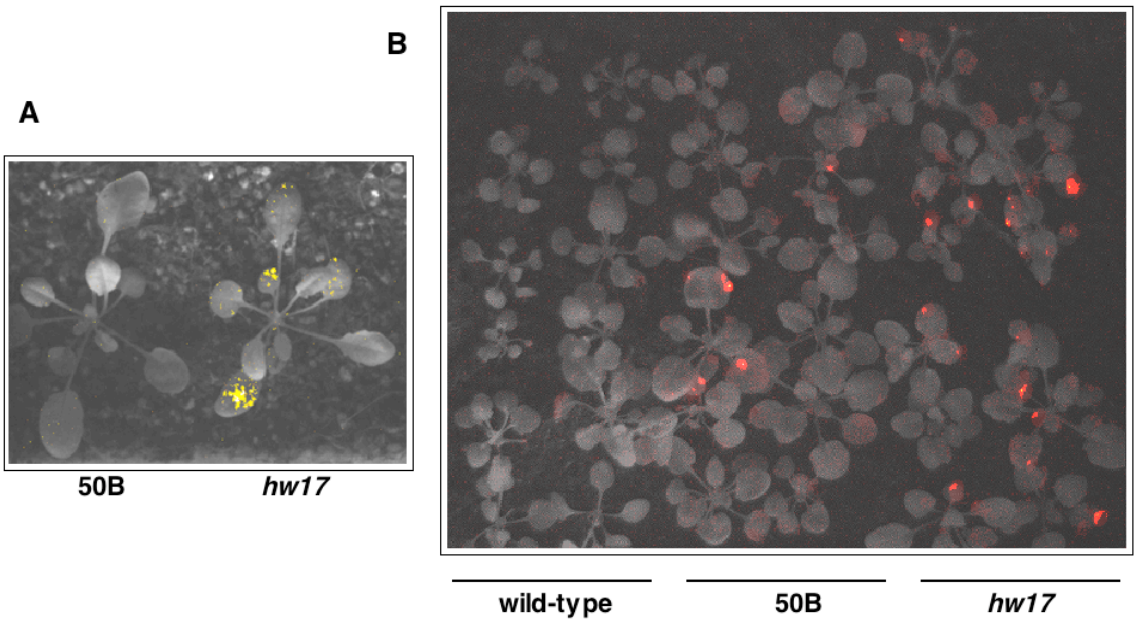

Figure 22. The recombination-up phenotype of *hw17* is maintained in the T2 generation.
(A) Original combined luciferase picture of *hw17* candidate together with a 50B control plant. **(B)** Persistance of the recombination-up phenotype in the T2 generation. A combined picture of a segregating *hw17* T2 population compared with 50B and wild-type control plants.

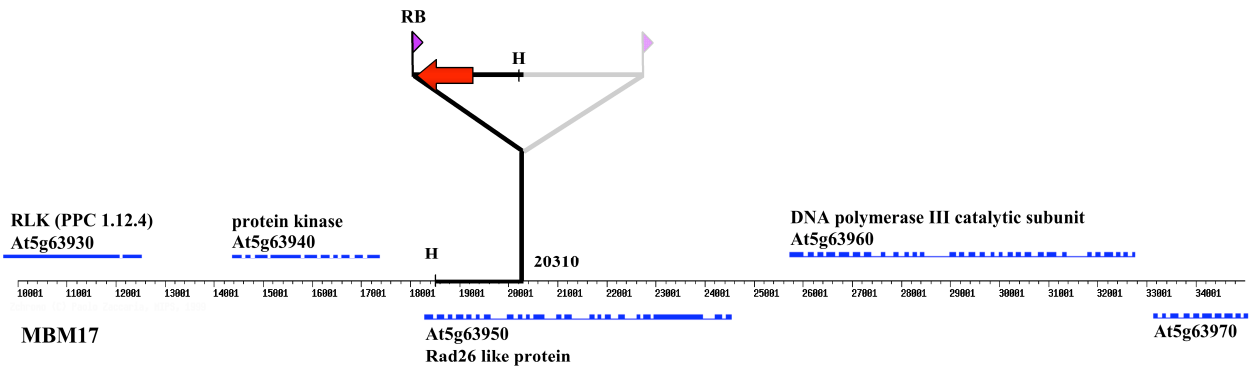

Figure 23. *hw17* T-DNA insertion site in chromosome V, region of P1 clone MBM17. Comments and conventions as for Fig. 16.

- *kp25*

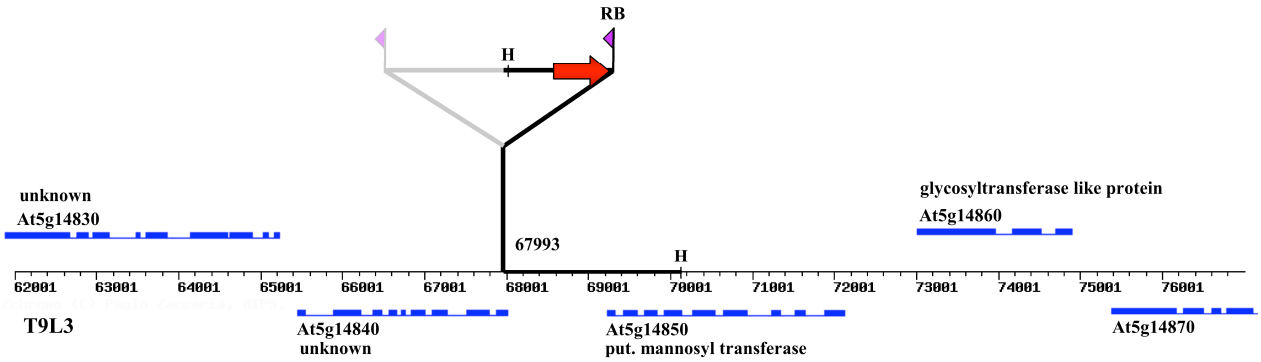

Figure 24. ***kp25* T-DNA insertion site in chromosome V, region of BAC T9L3.** Comments and conventions as for Fig. 16.

- *mn8*

The original *mn8* plant was very small (2-3 cm) and exhibited a strong bushy phenotype with more than 20 recombination spots. The few flowers that developed were all sterile and all attempts of cross-pollination to rescue a putative male or female defect failed. Small bushy plants were regenerated from the callus that mimics the original *mn8* phenotype, and also never set-up seeds. Therefore, no further analysis is possible except using reverse genetics approaches with the candidate genes. I saw at least 5 bands by Southern blot analysis (Fig. 14), but I could only rescue one genomic junction. Additional clones contained only vector sequences and 50 bp from the chromosome V centromeric region, suggesting a complex integration pattern at this site or at another position. As for the rescued insertion in BAC T20H2, the T-DNA integrated in the At1g20220 gene locus without associated deletion (PCR of the LB junction and sequencing, data not shown) (Fig. 25). Although the locus encodes for a protein of unknown function, the next gene *At1g20200* is essential for development (embryo defective 2719) and may contribute to the observed *mn8* developmental phenotype, perhaps through a dominant-negative effect.

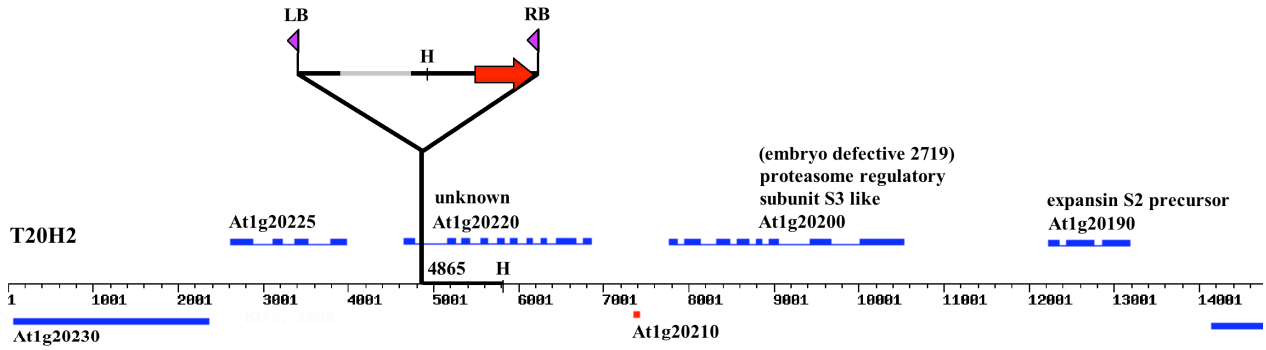

Figure 25. ***mn8* T-DNA insertion site in chromosome I, region of BAC T20H2.** Comments and conventions as for Fig. 16.

- *ms19*

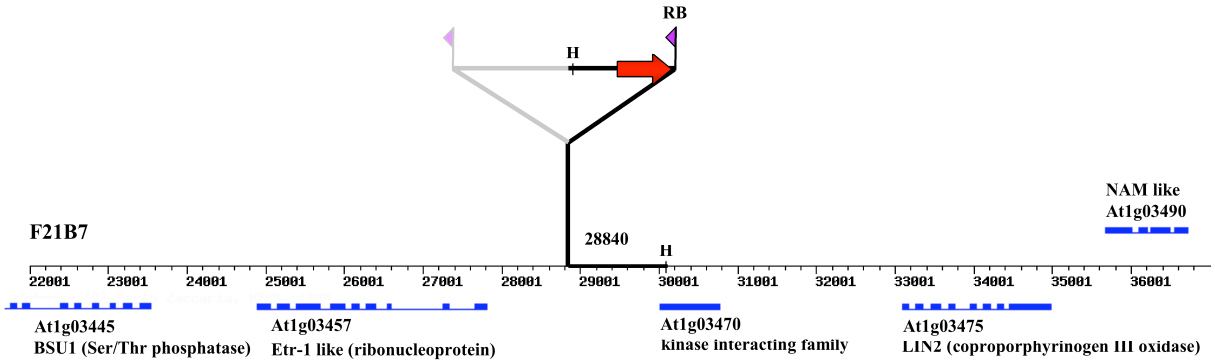

Figure 26. ***ms19*** **T-DNA insertion site in chromosome I, region of BAC F21B7.** Comments and conventions as for Fig. 16.

- *sm22*

The characterization of this candidate constitutes the subject for second chapter of this thesis work. Two T-DNA insertion sites were found for sm22 (Fig. 27). The insertion in the region of BAC F28O9 led to the disruption of a potential *Arabidopsis* INO80 ATPase homolog that could potentially have been accompanied by an antisense effect on the first exons of the gene. The second insertion site is in P1 clone MTG10 region and does not possess an active sulfonamide resistance as seen by segregation analysis and PCR genotyping. The *sm22* mutant was interesting in the sense that HR frequency was much higher than that in 50B plants in the first assay. When checked in further generations using the wild-type segregants as control, this *sm22* line exhibited a stable decreased recombination phenotype in a semi-dominant manner that segregated with the F28O9 insertion site (see chapter 2).

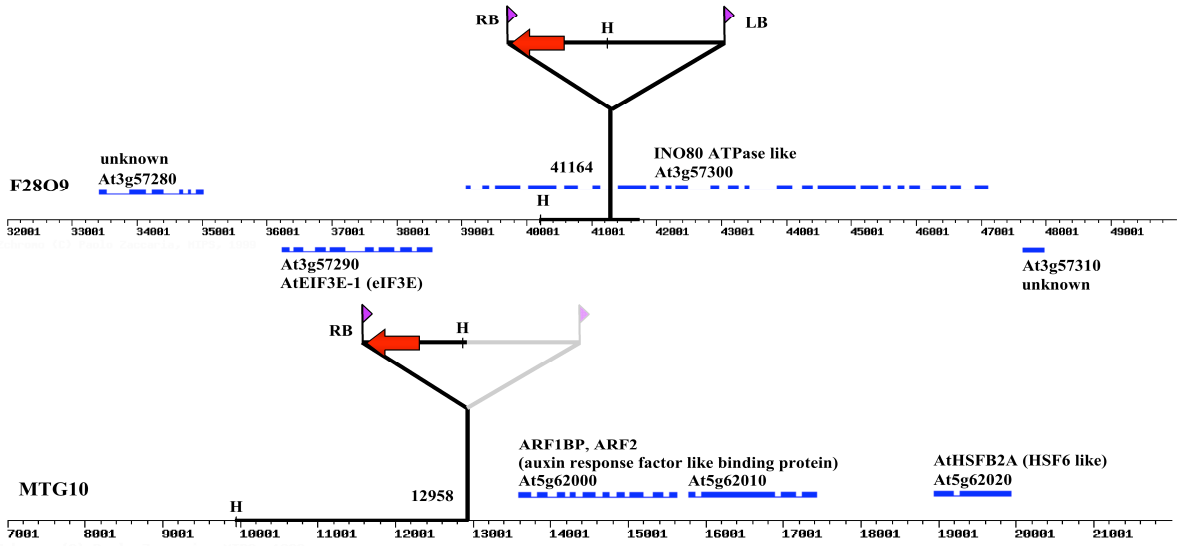

Figure 27. ***sm22*** **T-DNA insertion sites in chromosome III, region of BAC F28O9 and chromosome V, region of P1 clone MTG10.** Comments and conventions as for Fig. 16.

- sq4

The *sq4* candidate was a dwarf plant with a bushy phenotype associated with sterility that exhibited 5-to-10 spots on each leaf (Fig. 13B). Southern blot analysis revealed a 5.8 kb and a ≈13 kb band (Fig. 14). The 5.8 kb band corresponds to a rescued junction on chromosome III in the region of P1 clone MDC16 (Fig. 28), where 2/3 of the 35S promoter are missing. As the corresponding LB junction was obtained by PCR and sequencing (data not shown), it is likely that another T-DNA insertion that could not be rescued is associated with the ≈13 kb band. The T-DNA insertion in MDC16 may have affected the nearby At3g13990 locus, that encodes a protein with RCC motifs (Fig. 28).

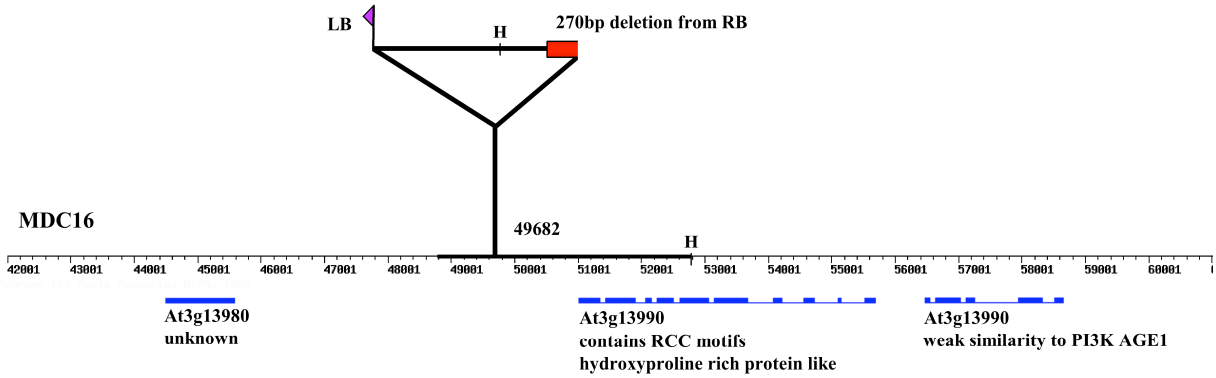

Figure 28. ***sq4*** **T-DNA insertion site in chromosome III, region of P1 clone MDC16.** Comments and conventions as for Fig. 9.

- xg20

The *xg20* candidate (Fig. 29A) exhibited an intriguing T2 segregation: on sulfonamide selective medium, all the T2 seedlings were sensitive and when T2 *xg20* seeds were germinated without selection on MS medium, some seedlings show a strong developmental phenotype (Fig. 29B) that was accompanied in most cases by numerous luciferase sectors (Fig. 29C). Although this suggests that the recombination-up phenotype is maintained, further analysis led to the conclusion that such phenotype was not linked with a T-DNA insertion (Southern blot, PCR and sulfonamide selection, data not shown).

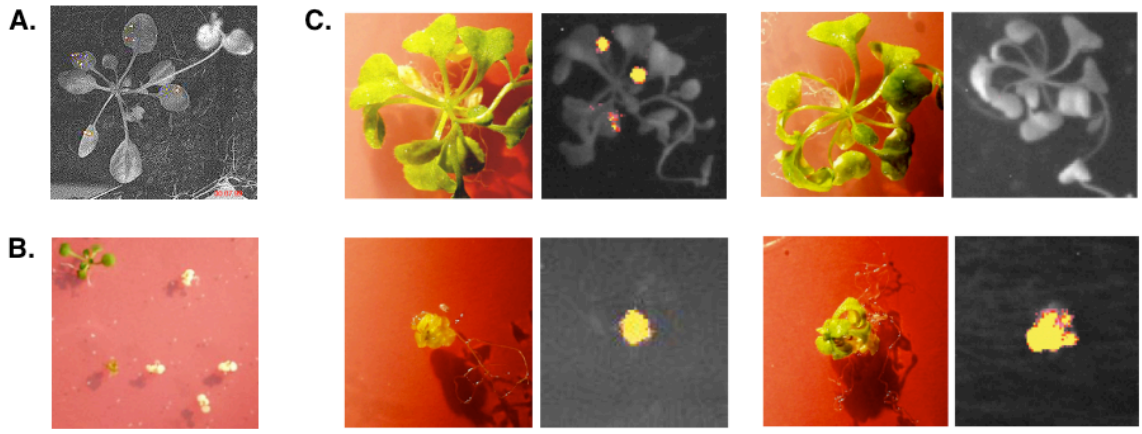

Figure 29. Developmental and luciferase phenotype of *xg20*. (A) Original T1 luciferase image of *xg20*. **(B)** T2 *xg20 in vitro*-grown seedlings germinated on non selective MM medium. **(C)** Luciferase and light images of 3-week-old plants with the developmental phenotype (bottom) or not (top). Same plants as in (B).

- xw13

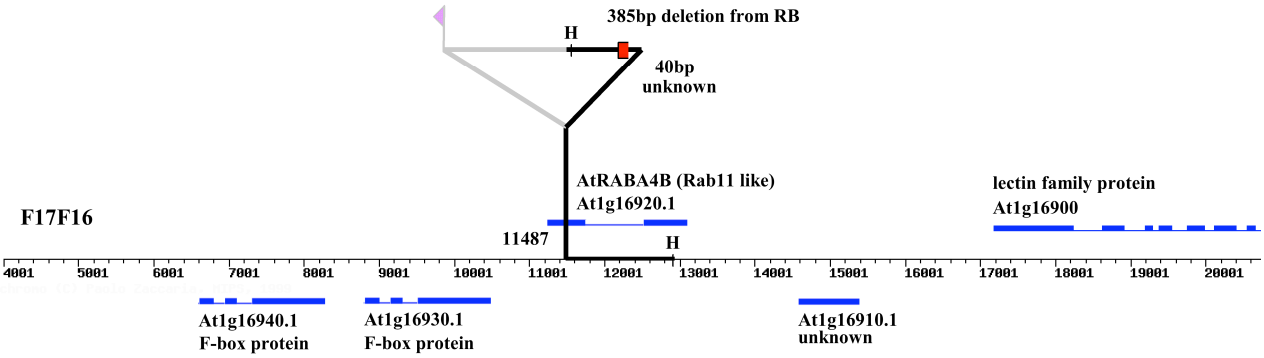

Figure 30. ***xw13* T-DNA insertion site in chromosome I, region of BAC F17F16.** Comments and conventions as for Fig. 16.

- ack14

The 9.5 kb band from Southern blot analysis (Fig. 14) corresponds to the size of the *Hind* III digested rescued plasmid, although the latter contains only 1 kb of genomic DNA. To explain the 5 kb excess in size for the rescued plasmid, the rescued T-DNA RB region must contain rearranged vector sequences between the deleted RB – that was sequenced (Fig. 31) and the *Hind* III of the pUC region. This T-DNA integration may have led to the overexpression of the *At1g25590* locus (Fig. 31).

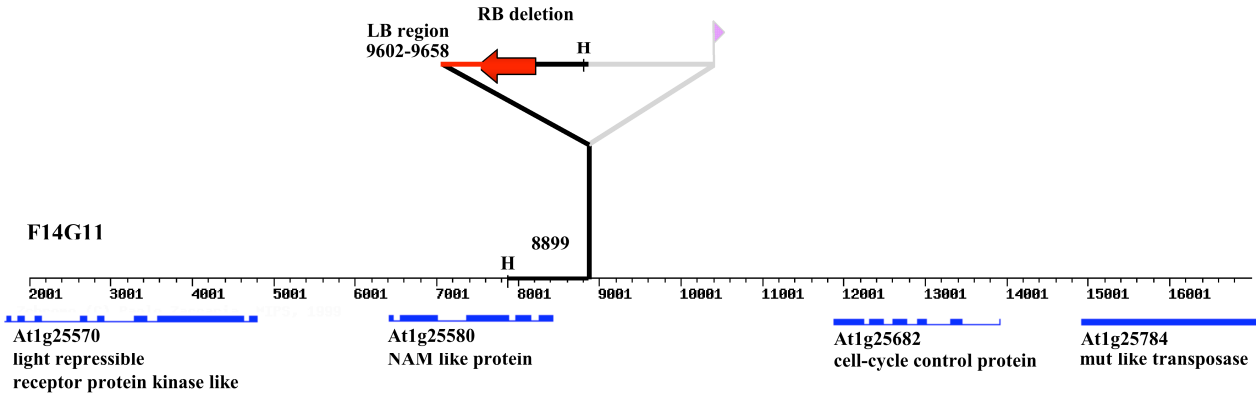

Figure 31. *ack14* T-DNA insertion site in chromosome I, region of BAC F14G11. Additional rearrangements present in the rescued 9.5 kb *Hind* III fragment that would explain its size were not determined. NAM, *NO APICAL MERISTEM* (transcription factor) gene. Comments and conventions as for Fig. 16.

2.3.2.3) **Candidates from the class 3**

- fp8

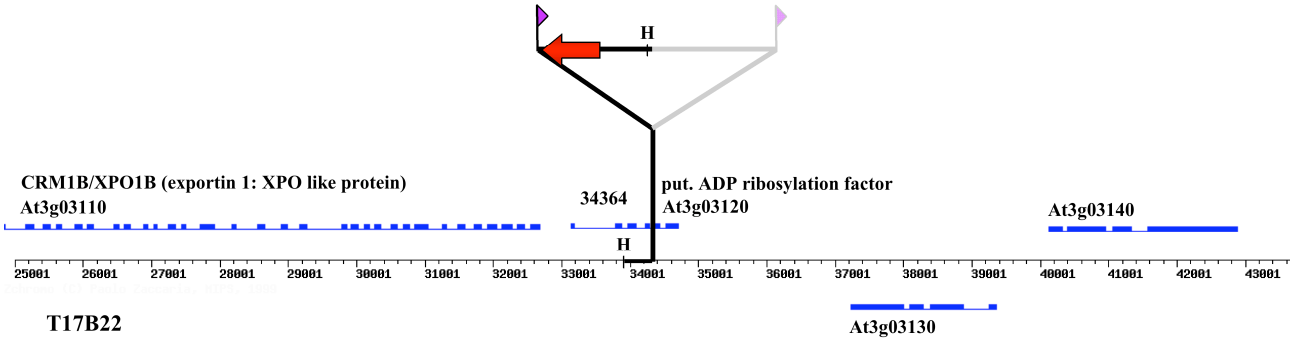

Figure 32. *fp8* T-DNA insertion site in chromosome III, region of BAC T17B22. Comments and conventions as for Fig. 16.

- jr19

The increased number of luciferase spots was only seen on the first true leaves of *jr19* (Fig. 13A). The plant had a normal development, but was sterile. In addition, two RB junctions were rescued (Fig. 33) and the Southern blot analysis revealed a complex pattern of bands (data not shown). It was therefore too speculative to work on the genes near the two insertion sites that may have contributed to the recombination increase.

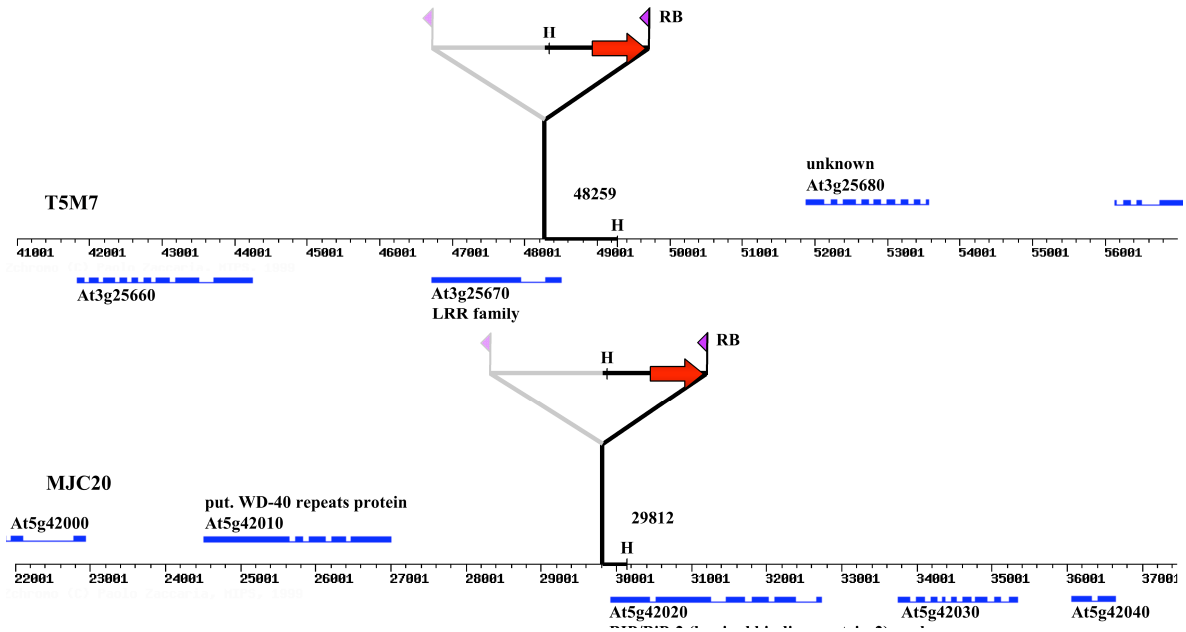

Figure 33. ***jr19*** **T-DNA insertion site in chromosome III, region of BAC T5M7 and on chromosome V, region of P1 clone MJC20.** WD-40, family of transcription factor**.** Comments and conventions as for Fig. 16.

- js2

The original *js2* plant exhibited many spots on one leaf. The 4.2 kb rescued plasmid corresponds to the unique band seen on the Southern blot (data not shown). In agreement, T2 generation *js2* plants segregated as a single locus for sulfonamide resistance. Two genes could be affected by the T-DNA inserted in the BAC T31E10 region (Fig. 34): A gibberelin-2 oxidase like gene (*At2g34550*) in antisense orientation and the promoter region of a gene with similarity to katanin and mei-1 (*At2g34560*). MEI-1 is an ATPase with similarity to the microtubule-severing protein katanin and is required together with MEI-2 for meiotic spindle formation in *Caenorhabditis elegans* (Srayko et al., 2000).

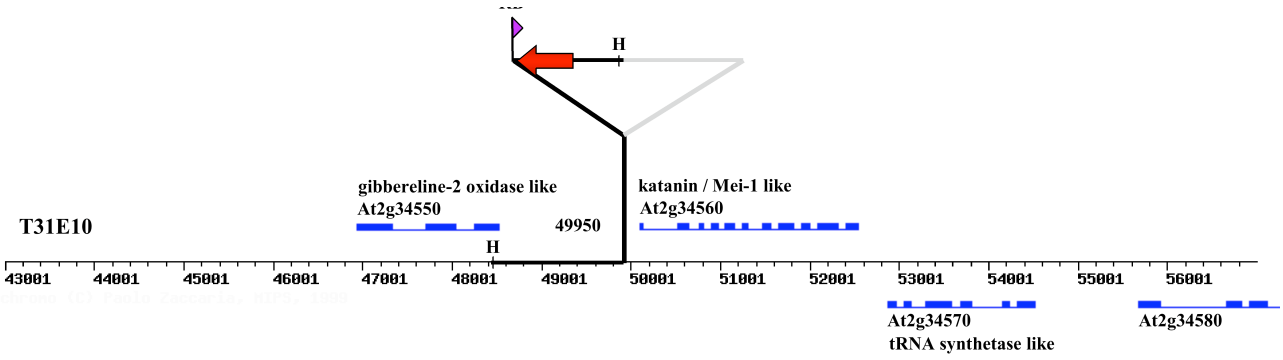

Figure 34. ***js2*** **T-DNA insertion site in chromosome II, region of BAC T31E10.** Mei-1, see text. Comments and conventions as for Fig. 16.

- qh3

We observed an increased level of recombination spots on *qh3* juvenile leaves as well as on adult stem leaves (data not shown). Southern blot analysis revealed one 3.3 kb *Hind* III band that corresponds to the rescued sequence containing 30 bp of genomic DNA (Fig. 14 & 35). In order to retrieve a longer stretch of genomic DNA, I selected for larger inserts in plasmid rescue using partially digested DNA and I could rescue an additional 1655 bp *Hind* III sequence that confirmed mapping to chromosome V, BAC F18O22 (Fig. 35). The T-DNA is integrated at the *At5g14230* locus that encodes a member of the large family of ankyrin repeats containing proteins. In addition, an antisense effect is also possible on the next gene (*At5g14240*) that encodes a phosducin like signaling protein. Phosducins are involved in signaling by interfering with G proteins, and yeast homologs play an essential role in cell growth (Flanary et al., 2000). On the other side of the insertion, no genes are predicted, although it is interesting to note that the second gene in this direction at an approximate distance of 20 kb is a SWIb complex BAF60b like gene.

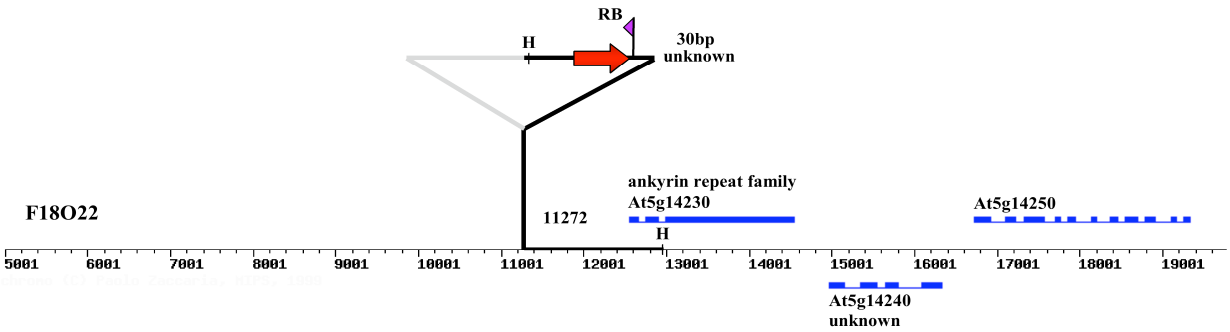

Figure 35. ***qh3* T-DNA insertion site in chromosome V, region of BAC F18O22.** 20 bp of unknown origin between the RB and genomic DNA. Comments and conventions as for Fig. 16.

- vw4

Despite a moderate increase in recombination, *vw4* has a T-DNA integrated in a region containing interesting potential repair genes (Fig. 36). The predicted At5g08010 protein is distantly related to the SMC family (see General Introduction) – most closely to SMC4. The predicted At5g08020 protein belongs to the small RPA (Replication Protein A) family in *Arabidopsis*. Besides their role in replication, RPA proteins have been reported to be participate in recombination and repair processes (see examples in Sugiyama and Kowalczykowski, 2002; Wolner et al., 2003). Both of these genes are expressed, as shown by RT-PCR (data not shown) and the presence of available ESTs

(www.mips.gsf.de). I cloned the corresponding cDNAs in plant expression vectors to look at their potential impact on recombination levels.

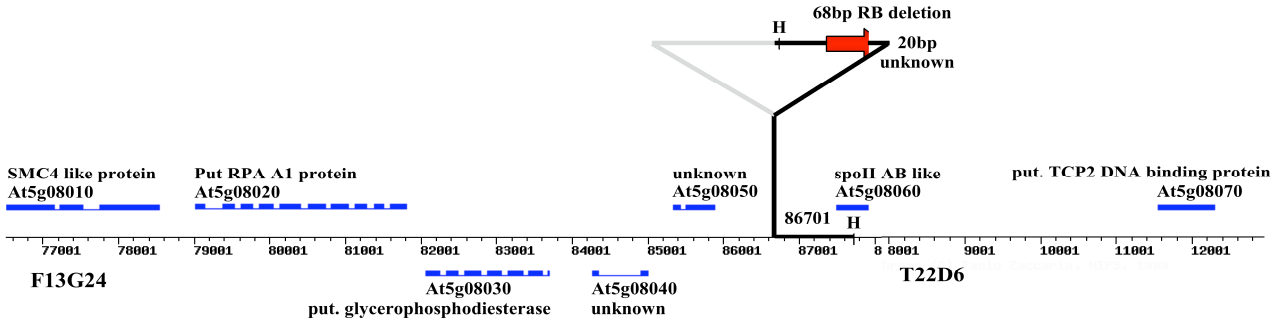

Figure 36. ***vw4*** **T-DNA insertion site in chromosome V, region of BAC F13G24 and T22D6.** Comments and conventions as for Fig. 16.

- adx21

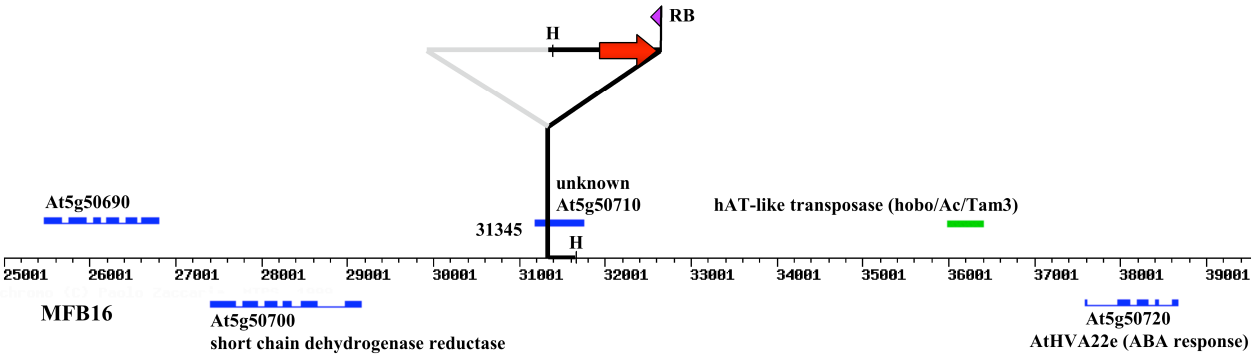

Figure 37. ***adx21*** **T-DNA insertion site in chromosome V, region of P1 clone MFB1.** The short ORF in which the T-DNA is integrated has no similarity to any known protein. ABA, Abscissic acid. Comments and conventions as for Fig. 16.

3) Summary of the screen

I performed a genetic screen for *Arabidopsis thaliana* mutants with altered somatic recombination levels using a stably integrated luciferase based intrachromosomal HR substrate. As a mutagenic agent, I used a T-DNA construct designed for activation tagging. Out of 19520 individual transformants tested, 37 exhibited an altered HR phenotype. Nine of them were sterile and/or exhibited important developmental or growth phenotypes that precluded the formation progeny seeds, which is more than the average number of sterile plants expected. However, in most cases the altered recombination phenotype was lost in the offspring. To characterize the mutations, I cloned all the T-DNA insertion sites by plasmid rescue and determined the potential

target genes. I discuss the genes likely to be responsible for the observed phenotype. Two candidates were chosen for a thorough analysis, *sm22* that is the subject of the second chapter of this thesis work and *hw17* that is the subject of another thesis work.

D. Chapter 2

The *Arabidopsis ino80* mutant links homologous recombination and chromatin remodeling

1) Introduction

Homologous recombination (HR) in eukaryotic organisms serves a dual role in providing genetic flexibility by creating novel sequence assortments upon meiosis and in maintaining genome integrity through DNA repair in somatic tissues (Paques and Haber, 1999). HR represents an alternative pathway to non-homologous end-joining (NHEJ) for the repair of double-strand breaks (DSB). The repair by NHEJ involves direct ligation that may not preserve the integrity of the genetic information and that thus may be deleterious for the cell. The HR pathway is more precise but requires a DNA template homologous to the damaged molecule, that can be the sister chromatid, the homologous chromosome or any segment of DNA that has enough sequence similarity to the DNA to be repaired. The choice of a pathway to repair DSBs is thus crucial for genome integrity and evolution, especially in plants where the germline is only determined late during development. In higher eukaryotes such as animals and plants HR-mediated repair is rare compared to NHEJ mediated repair (Paques and Haber, 1999; Britt and May, 2003). Very little is known on what influences the choice of the pathway taken, but chromatin structure at the site of a lesion likely will play a major role in the recruitment of repair enzymes and thereby the choice of repair pathway. The repair of DSBs by HR involves numerous steps that include recognition and recruitment of the homologous sequences, strand invasion, DNA synthesis and resolution of complex structures. Although the proteins directly participating in HR repair are well studied – in particular in yeast and prokaryotes – the regulation of these steps remains more elusive (Paques and Haber, 1999; West, 2003). As a complicated multi-step process, eukaryotic HR may even involve different steps of chromatin remodeling. As a consequence, various proteins that are not part of the core of the recombination machinery may directly participate in the regulation of HR.

I described in the first chapter the direct genetic screen for mutants with altered HR frequencies that I carried out in *Arabidopsis*, and the rough characterization of the mutant candidates obtained. In this second chapter, I present the characterization of *atino80*-1, a

mutant with decreased HR frequency. I show evidence that the *Arabidopsis AtINO80* is a positive regulator of HR while leaving other repair pathways unaffected. The binding of AtINO80 protein to mononucleosome *in vitro* supports the idea that INO80 positively regulates HR through modification of chromatin structure at sites of DNA repair by HR. In addition, the *Arabidopsis AtINO80* seems to have a role in the transcriptional regulation of a subset of the genome. INO80 mostly regulates general metabolism genes, whereas very few stress response genes and no repair related genes are affected. Moreover, I present evidence for the existence of the other INO80 complex partners in *Arabidopsis*.

2) Results

2.1) The *atino80*-1 mutant line is deficient in somatic HR

As a reporter system to identify genes involved in HR we developed an *Arabidopsis* line called 50B carrying a firefly luciferase recombination substrate stably integrated in the genome (Fig. 8). As with the previously described β-glucuronidase system (Swoboda et al., 1994), somatic HR events can be directly monitored, but in this case in living tissues (Fig. 9A). By screening a population of 20,000 *Arabidopsis* transformants of the HR reporter line mutagenized by T-DNA insertion (see chapter 1), I identified one line with a decreased HR frequency (Fig. 38A & 38B).

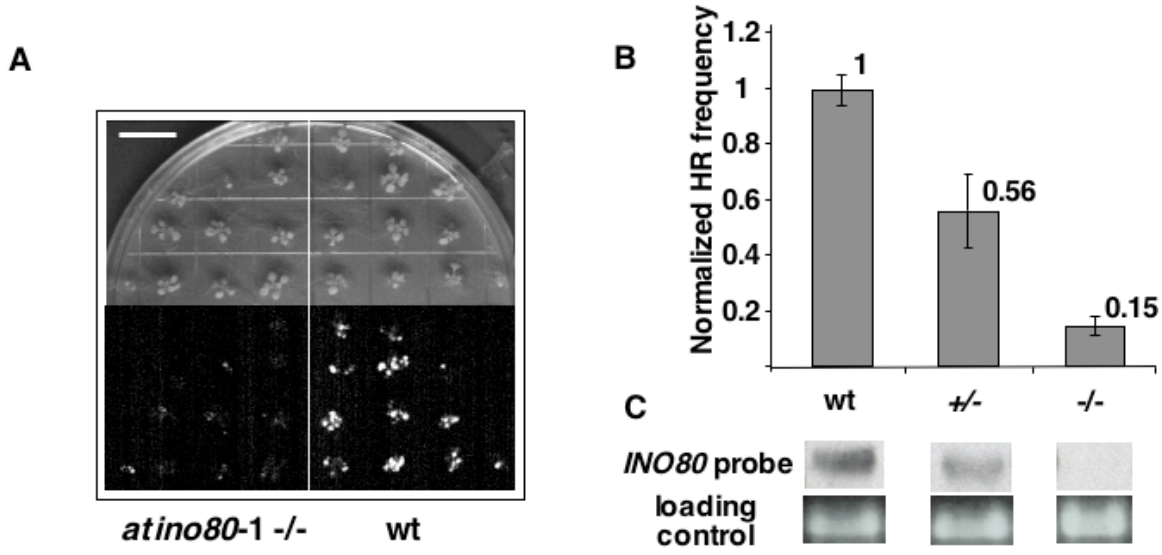

Figure 38. The *atino80*-1 mutant line is deficient in somatic HR. (**A**) Somatic HR sectors on 14-day-old *in vitro*-grown *atino80*-1 and control plants (50B). Top, light image; bottom, luciferase-imaging picture. Scale bar = 2cm. (**B**) *INO80* transcript level correlates positively with HR frequency. wt, wild-type out-segregants; +/-, heterozygous; -/-, homozygous for the *ino80* mutation. Recombination spots were counted on 20-day-old plants and HR frequency was normalized against the mean value of that in wild type plants. Error bars = s.e.m. (**C**) *INO80* transcript level. Northern blot hybridization with RNA isolated from the corresponding plants shown in (B). Ribosomal RNA revealed by ethidium bromide staining of the gel before hybridization was used as a loading control.

The phenotype behaved as a semi-dominant trait over several generations, and co-segregated with a simple T-DNA insertion (data not shown). By cloning the T-DNA/plant-genome junctions, the mutation was assigned to the *At5g57300* gene locus. No rearrangements or deletions associated with T-DNA integration were observed. I subsequently cloned a full-length cDNA of 4.7 kb expressed from this locus and found that the gene consists of 23 exons and 22 introns (Fig. 39). In the mutant, the T-DNA is integrated in the 6th exon, creating a null allele. *At5g57300* encodes a 1507 amino acids long protein that is the unique *Arabidopsis* candidate for INO80 (see below). INO80 defines the small INO80 subclass of SWI/SNF family ATPases (Shen et al., 2000). Accordingly, the *At5g57300* gene was named *INO80* (or *AtINO80*) and the mutant *atino80*-1.

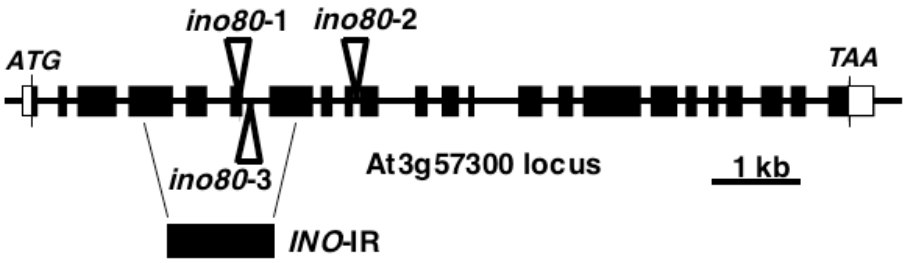

Figure 39. *AtINO80* gene organization and *ino80* mutations. Gene organization and location of the T-DNA insertions in the *atino80*-1, *atino80*-2 & *atino80*-3 alleles. Black boxes, exons; *INO*-IR, sequence used for the RNAi constructs.

To quantify the HR deficiency, I compared wild-type out-segregants with homozygous and heterozygous mutants originating from the same mother plant. Interestingly, *INO80*$^{+/-}$ heterozygous plants contain about half the *INO80* wild-type transcript level (Fig. 38C). I used this property as a tool to compare HR in different situations. As shown in Fig. 38B, the HR frequency in heterozygous and homozygous *atino80*-1 is 56% and 15%, respectively, of that in the wild type. In addition to showing that the mutation is semi-dominant, this clearly indicates a direct correlation between HR frequency and *INO80* mRNA level. These data suggest AtINO80 is a positive regulator of HR activity, acting in a dose-dependent manner. However, in the *atino80*-1 mutant, in which the *INO80* transcript cannot be detected (Fig. 38C), HR still takes place (Fig. 38B), suggesting that this residual HR activity is the INO80-independent basic level of recombination activity and that *INO80* is not absolutely required for HR. Alternatively, an undetectable *INO80* transcript level may be responsible for the remaining HR activity, even in the mutant with an insertion of the T-DNA in the *AtINO80* gene.

2.2) Development of a RNAi system suitable for the assessment of the mutant candidates

To ask whether the reduced HR levels solely reflect *INO80* deficiency in the mutant, I wanted to down-regulate the *INO80* transcript level in the 50B recombination reporter line using an RNAi approach. Also, we were interested to use such system with other mutant candidates. As no suitable vectors were available at that time for such strategy, I designed my own RNAi vectors called pEXhp (carrying a sulfonamide resistance gene for selection in plants) and pEX4hp (carrying a kanamycin resistance gene) that are similar to those of Waterhouse (P. Waterhouse, personal communication, see also Smith et al., 2000; Stoutjesdijk et al., 2002). The T-DNA region of these vectors harbor an expression cassette driven by the constitutive MAS (mannopine synthase) 2' promoter that contains the *FAD2* (Fatty acid desaturase-2 *Arabidopsis* gene) intron flanked by restriction sites (Appendix 5). A 200-800 bp region of the gene of interest can be cloned in reverse orientation before and after the intron to allow the expression of double-stranded RNA homologous to the gene of interest. To test the strategy, I cloned a 695 bp region – from position 576 to 1271 – of the luciferase gene in pEXhp (Fig. 40A), and transformed the resulting construct by floral dipping in the VR1 line that constitutively expresses the luciferase gene. As shown Fig. 40B, more than 95 % of the independent T1 transformants exhibit a strong reduction of luciferase activity. Therefore, pEXhp and pEX4hp can be used to efficiently down-regulate gene expression by double-strand RNA (dsRNA) production.

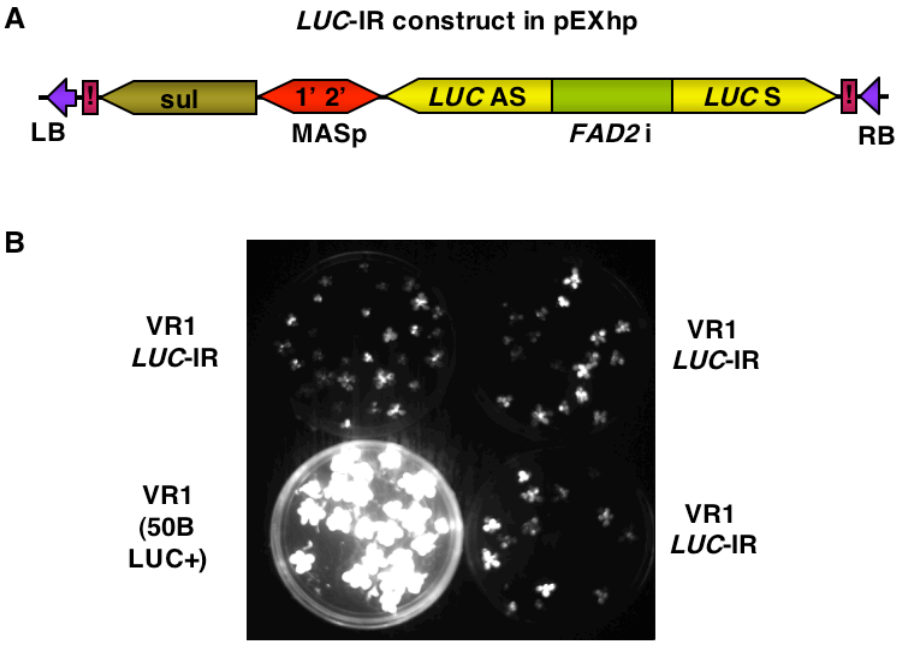

Figure 40. Validation of the RNAi strategy with the luciferase gene. (A) *LUC*-IR construct. T-DNA region of the pEXhp RNAi vector with the indirect (*LUC* AS) and direct (*LUC* S)

complementary sequences of the luciferase gene. *FAD2* i; *Arabidopsis FAD2* gene intron. **(B)** Luciferase picture of 2-week-old *in vitro*-grown T1 transformants of the VR1 line carrying the *LUC*-IR T-DNA and of VR1 control plants.

2.3) The HR phenotype is caused by *INO80* and is locus-independent

To ask whether the reduced HR levels solely reflect *INO80* deficiency in the mutant, I down-regulated the *INO80* transcript level in the 50B recombination reporter line with constructs producing double-stranded RNA homologous to the 5' region of *INO80* (*INO*-IR, see Fig. 39). The *INO*-IR sequence extends from position 549 to 1000 of the coding sequence and was amplified from the *INO80* cDNA. Using the system described above, in which the expression of the double-strand RNA is under the control of the constitutive mannopine synthase promoter (Fig. 41A, top construct), I transformed reporter line plants with either the *INO*-IR construct or an empty vector. Upon selection in the next generation, individual transformants were isolated and grown *in vitro*. After 2 weeks, HR frequency was monitored and plants were pooled for RNA extraction. *INO80* transcript levels were strongly reduced in the pool of transformants carrying the *INO*-IR construct (Fig. 41B). HR frequency was also significantly reduced in these plants (Fig. 41C), showing that, indeed, the reduced HR phenotype of *atino80*-1 is due to decreased *INO80* expression. In addition, the steady state mRNA level at the recombination reporter locus was not changed in the mutant or RNAi plants, showing that the observed HR phenotype is not due to transcriptional effects at the reporter locus (data not shown). The use of a similar *INO80*-IR RNAi construct where the expression of the dsRNA is driven by the strong constitutive 35S promoter (Fig. 41A, bottom construct), resulted in the same effect – i.e. decreased HR levels (data not shown).

To test whether the influence of *INO80* on HR is specifically restricted to the 50B reporter locus, I studied the effect of *INO80* down-regulation in the independent recombination line 1445, in which the recombination substrate has the same structure but is based on the β-glucuronidase (GUS) reporter gene and is certainly integrated in a different genomic location (Gherbi et al., 2001). In agreement with the 50B locus results, RNAi-mediated down-regulation of *INO80* in the line 1445 results in decreased HR frequency, demonstrating the effect of *INO80* on HR to be locus-independent (Figure 41C).

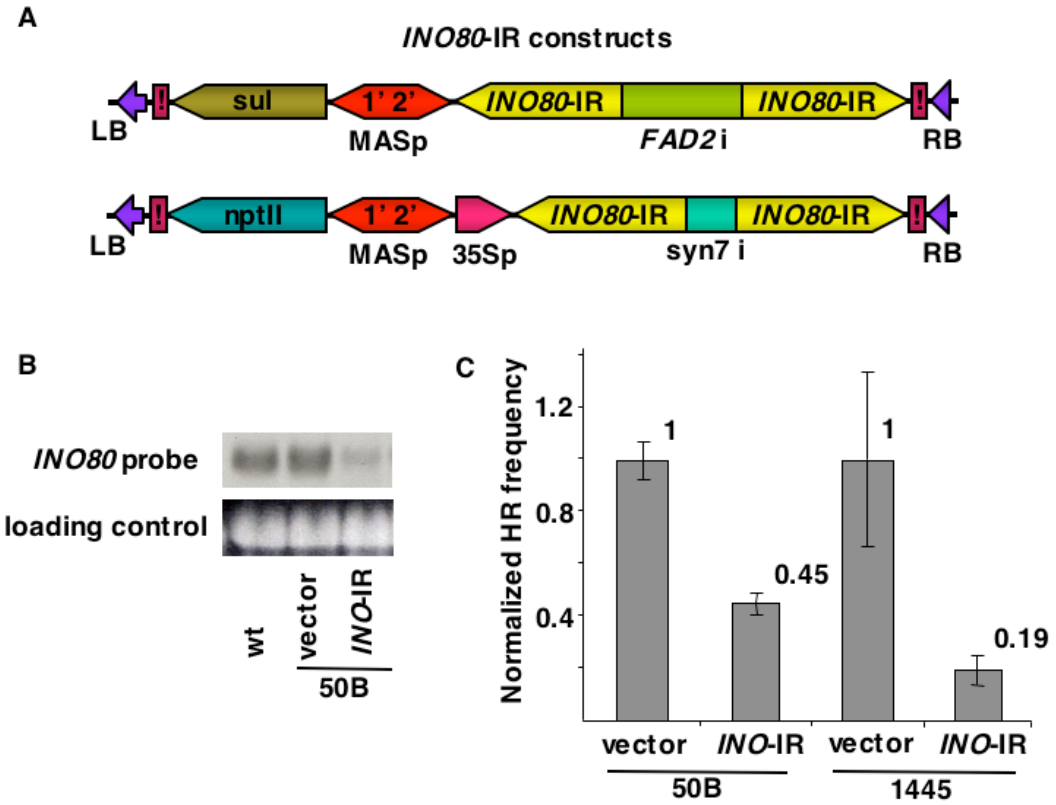

Figure 41. The HR phenotype is caused by *INO80* and is locus independent. (**A**) RNAi constructs used to down-regulate *AtINO80* expression level driven by the mannopine synthase promoter (MASp, top) or the 35S promoter (35Sp, bottom). *FAD2* i, see Fig. 40; *INO*-IR, see Fig. 39; syn7 i; synthetic intron (Goodall and Filipowicz, 1989, 1991). (**B**) Inhibition of *AtINO80* expression in 50B reporter line. Northern blot probed with DIG-labeled *INO80* cDNA showing reduction of *INO80* transcript level in pooled *INO*-IR plants (20 plants). wt, wild-type *Arabidopsis* RNA; vector and *INO*-IR, RNA from pooled plants (20 plants) transgenic for the empty vector and the *INO*-IR construct, respectively, in the 50B background. Loading control, ethidium bromide stained rRNA. (**C**) The HR phenotype is reproducible and is not locus-dependent. Plants similar to those in (B) were tested for HR. In addition, the β-glucuronidase HR reporter line 1445 was used in a similar experimental setup. After counting recombination spots, HR frequency in *INO*-IR plants was normalized to the mean value of that in 50B or 1445 vector control plants, respectively (Error bars = s.e.m.).

2.4) *Atino80*-1 plants display a mild developmental phenotype

Although homozygous *atino80*-1 plants display overall normal vegetative and reproductive development, a slight tendency towards reduced size is observed (data not shown). In addition, *atino80*-1 plants produce more lateral branching from the rosette while lateral branching on the stem is not affected (Fig. 42A & 42B). Moreover, the total length of lateral shoots per plant is increased (Fig. 42C). I observed no difference at any of the rosette stages. Examination of silique contents together with the segregation of the mutated locus clearly indicates that the *atino80*-1 allele has no effect on embryogenesis or on early development. Also, fertility of *atino80*-1 plants is normal and the *atino80*-1

phenotype does not alter in subsequent generations (data not shown), suggesting that no severe defects occur during meiosis, and that there are no gross epigenetic or genetic changes that accumulate over time and generations.

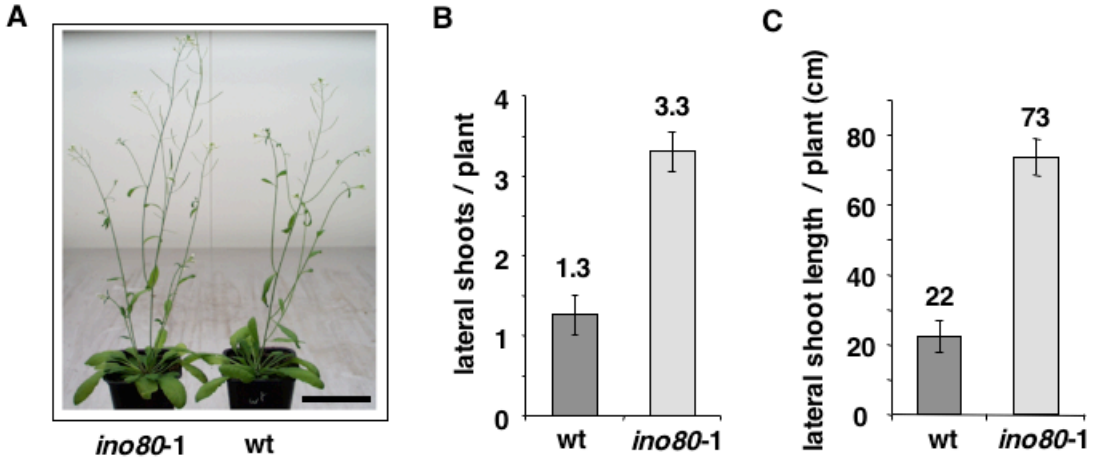

Figure 42. *atino80*-1 has a mild branching phenotype. (**A**) Development of *atino80*-1 homozygous plants compared with that of wild-type out-segregants (*INO80*$^{+/+}$). Scale bar = 5cm. (**B**) & (**C**) Quantification of the increased branching of *ino80*-1 plants. The number of lateral shoots emerging from the rosette (left) and the total length of these lateral shoots (right) was meseared for *ino80*-1 plants (n=20) and wild-type out-segregants (wt, n=19) plants. Numbers are the mean value ±s.e.m per plant for one representative experiment out of three.

2.5) Characterization of two additional *ino80* T-DNA insertion alleles

Two additional T-DNA insertion mutants in *AtINO80* were obtained from the SAIL collection. Both have the T-DNA inserted in the 5' part of the gene (Fig. 39). The two alleles harbour a complex T-DNA pattern that cosegregates as one locus with the junction in the *INO80* gene (Southern blot analysis, and PCR genotyping, data not shown). In addition, I could not detect the INO80 transcript by northern blot analysis in homozygous *ino80*-2 and *ino80*-3 plants, although a shorter transcript is produced in *ino80*-2. Plants homozygous for either of these alleles exhibit a strong although slightly different developmental phenotype, (Fig. 43A). *Atino80*-2 homozygous plants have a 1-week-delay in flowering and produce many thin flowering shoots with small siliques (Fig. 43B). In addition, heterozygous plants exhibit a semi-dominant phenotype of reduced-sterility. *Atino80*-3 homozygous plants have pale-green leaves and flower 2-3 weeks later than wild-type plants (Fig. 43C); their flowering shoots are short and weak. Both alleles exhibit a strongly reduced seed yield, which was never observed in *ino80*-1 plants. However, *atino80*-2 and *atino80*-3 *in vitro*-grown seedlings are similar to wild-type and *atino80*-1 seedlings up to 15 days after germination and thus can be compared at this stage (Fig. 44).

The observed stronger phenotype of *ino80*-2 and *ino80*-3 can be explained by either (i) the contribution of another impaired gene in these alleles, (ii) a possible compensation for *INO80* deficiencies in *ino80*-1 or/and (iii) an incomplete loss of function in *ino80*-1 but not in *ino80*-2 and *ino80*-3. Indeed, whole-transcriptome analysis of the three alleles (see later section) revealed a slight decrease in the expression of the gene upstream of *INO80*, *At3g57290*, the ATG of which is less than 500 bp from *INO80*. This gene incodes the *Arabidopsis* translation initiation factor3-E1 (eIF3E1). Thus, it is likely that a change in its expression can have important consequence for the plant growth and development, as it may affect the whole translation initiation machinery.

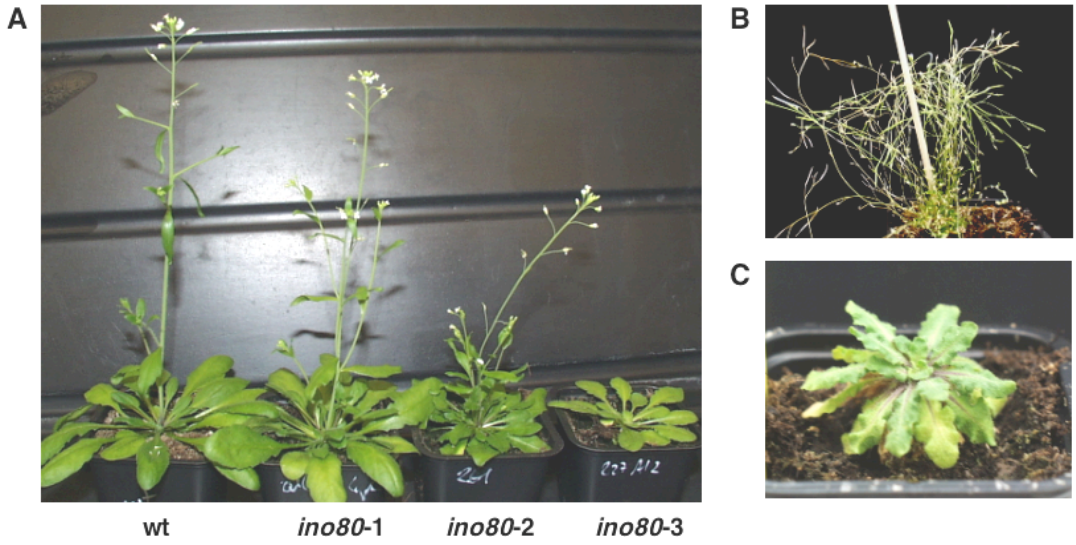

Figure 43. Developmental phenotype of *atino80*-2 and *atino80*-3. (A) Four-week-old wild-type (wt), original mutant *atino80*-1, *atino80*-2 and *atino80*-3 plants. **(B)** Eight-week-old *atino80*-2 plant showing numerous weak shoots with small siliques. **(C)** Six-week-old *atino80*-3 plant just prior to flowering exhibiting a late edged-leave phenotype.

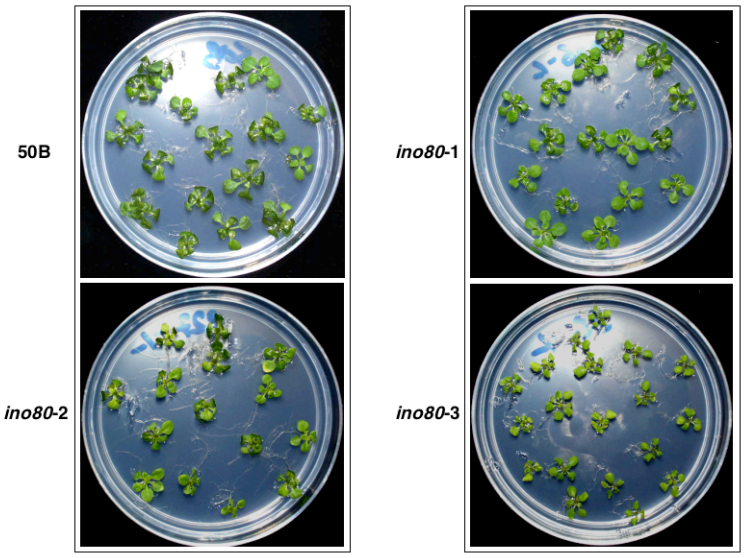

Figure 44. Phenotypes of young seedlings of the different *ino80* alleles. Homozygous lines of the three *ino80* alleles were grown *in vitro* for two weeks in parallel with 50B control plants.

2.6) The *Arabidopsis AtINO80* gene product is a bona fide INO80 SWI/SNF protein that binds to mononucleosomes *in vitro*

Members of the INO80 subclass of the SWI/SNF family are closely related to the DDM1 (Jeddeloh et al., 1999; Brzeski and Jerzmanowski, 2003) and SWR1 ATPases (Krogan et al., 2003), and are found in all eukaryotes (Fig. 45A and see also Fig. 6). SWI/SNF ATPases act in large complexes and mainly affect chromatin structure, although DDM1 also affects DNA methylation and the SWR1 complex was recently shown to catalyze histone H2AZ variant exchange in yeast (Mizuguchi et al., 2004). SWI/SNF family proteins are defined by their ATPase domain which is actually divided in seven distinct and well defined motifs that are conserved with other ATPases like helicases (Richmond and Peterson, 1996; Hall and Matson, 1999). By comparing the *Arabidopsis* INO80 sequence with known SWI/SNF proteins I could verify that all the motifs are present. To determine the position of AtINO80 and the 19 closest proteins of *Arabidopsis* within the SWI/SNF superfamily, I aligned their sequences and removed parts that exceed the two blocks of ATPase motifs defined as amino-acids 760-947 & 1104-1242 of the yeast SNF2 sequence. The ATPase domains of INO80 subfamily members share between 65 and 80 % identity at the protein level, whereas identity to other SWI/SNF members is between 30 and 50 % (Fig. 45A and data not shown).

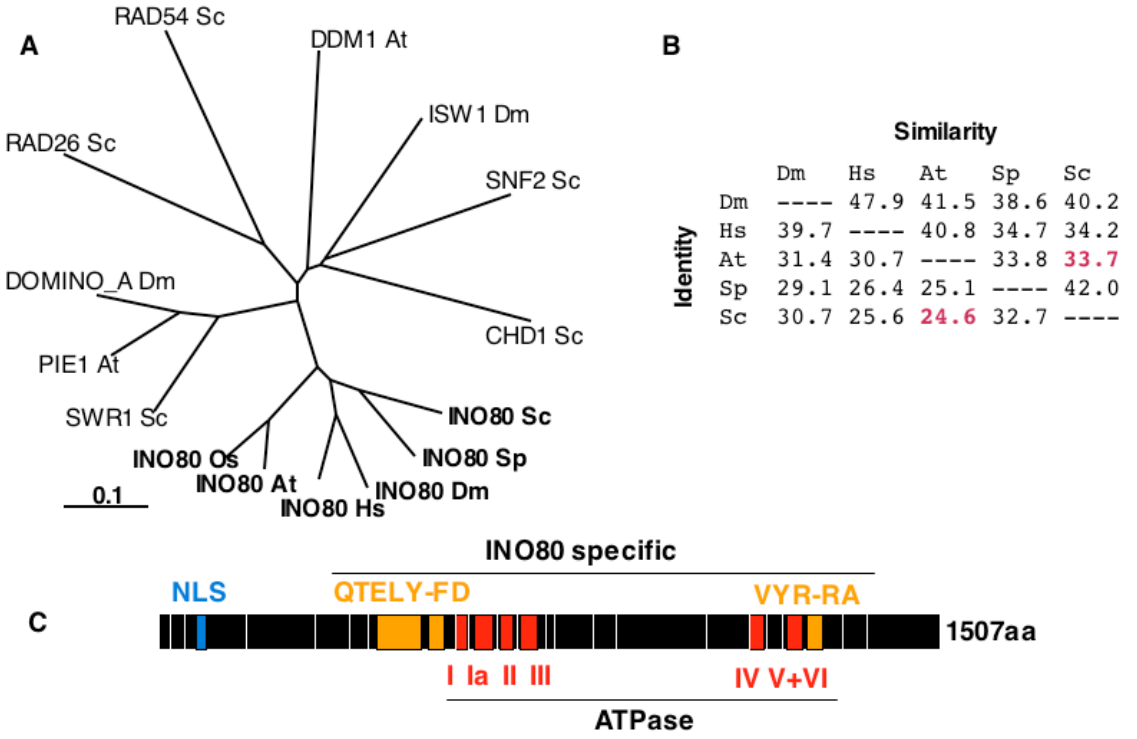

Figure 45. The *Arabidopsis* INO80 protein. (**A**) Phylogenic tree of the INO80 SWI/SNF ATPase subfamily of proteins. The tree was obtained by aligning the ATPase domains of proteins

representative of the SWI/SNF subfamilies together with INO80 subfamily members. For more details and sequences used, see Materiel and Methods. At, *Arabidopsis thaliana*; Dm, *Drosophila melanogaster*; Hs, *Homo sapiens*; Os, *Oriza sativa*; Sc, *Saccharomyces cerevisiae*; Sp, *Schizosaccharomyces pombe*. (**B**) Yeast *yINO80* and *AtINO80* share 24.6% identity and 33.7% similarity at the whole protein level. Identity/Similarity matrix for the full-length protein sequences of the INO80 subfamily of SWI/SNF ATPase (nomenclature as above). The matrix was generated with the programs ClustalX and MacBoxshade. (**C**) Structure of AtINO80 protein. The ATPase motifs are represented in two blocks from I to III and from IV to VI. QTELY-FD and VYR-RA, the two INO80-specific conserved regions; NLS, nuclear localization signal; Vertical white lines, intron positions.

Apart from the ATPase domains, large stretches of amino acids are conserved specifically in the INO80 subfamily (Shen et al., 2000) (Fig. 45C). Two closely spaced regions (QTELY and FD in Fig. 45C) located before, and one (VYR-RA), after the ATPase motif, are of particular interest as candidates for an INO80-specific function. By aligning the ATPase domains of all potential *Arabidopsis* SWI/SNF proteins with members of the different SWI/SNF subfamilies, I found that AtINO80 undoubtedly groups within the small INO80 subclass (Fig. 45A) and is the unique *Arabidopsis* INO80 candidate (Fig. 6). Further, *Arabidopsis* INO80 contains an N-terminal NLS that is conserved in the rice sequence. Thus, the sequence conservation of AtINO80 and its position in the SWI/SNF family identify it as the *Arabidopsis* INO80 ortholog.

Because the corresponding yeast protein is part of a chromatin remodeling complex, we asked whether AtINO80 has affinity for chromatin. Since we did not succeed to express the complete protein in *E. coli* or insect cells, probably because of its size (data not shown), we generated parts of the protein separately and tested their binding to mononucleosomes. Six different constructs were made, taking into account the different domains and the conservation at the amino-acid sequence level (Fig. 46A & 46B). The *in vitro* translated products of these constructs were then tested for retention on resin-immobilized chicken mononucleosomes; the resin retained all sub-regions of INO80 with the exception of the C-terminal CT construct (Fig. 46C). To discriminate potentially unspecific binding to DNA from binding to histones, we tested the retention of the proteins by DNA and by histones (Fig. 46D). The data clearly show that fragments NNT, NTC and C bind preferentially to the histone part of nucleosomes. This is the first evidence for an INO80 protein interacting directly with the histone component of chromatin.

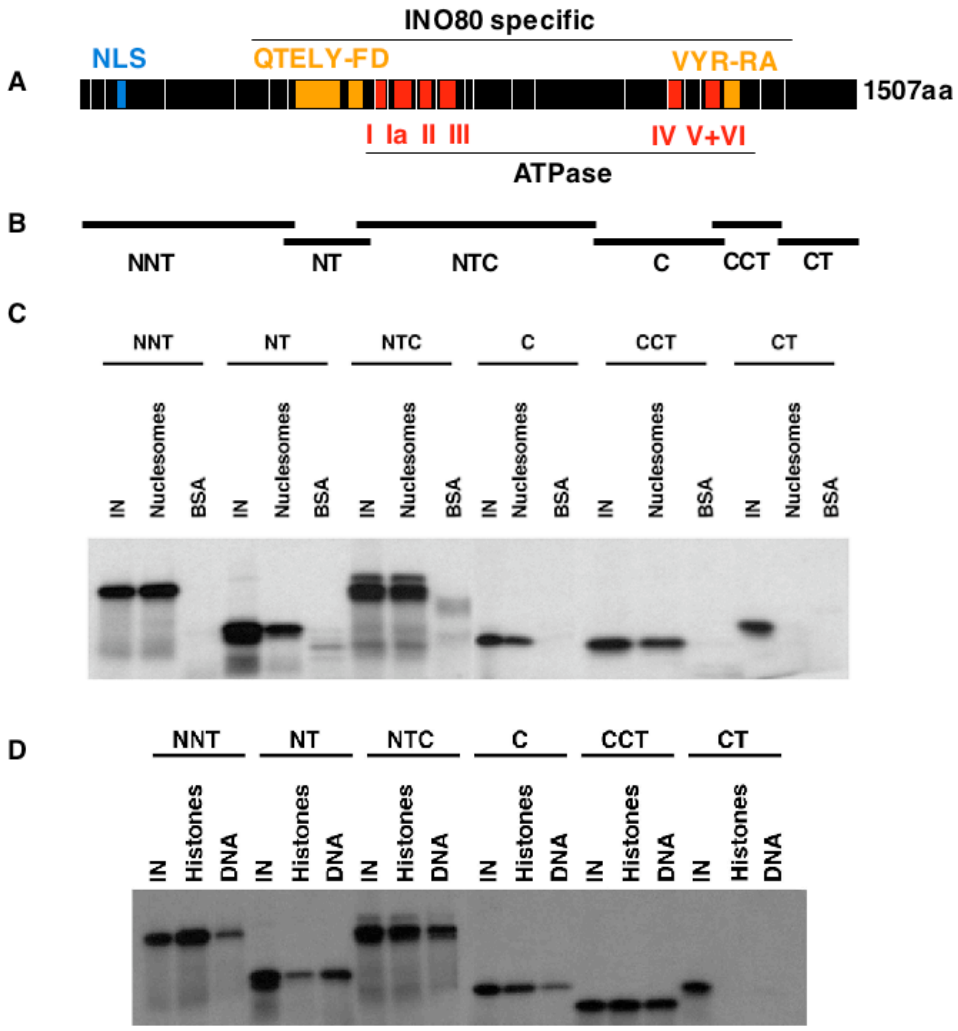

Figure 46. INO80 binds to munonucleosomes *in vitro*. (**A**) (**B**) Constructs used for *in vitro* translation, depicted with respect to their location in the INO80 protein sequence. (**C**) SDS-PAGE analysis of binding of in vitro-translated ^{35}S-labelled INO80 fragments to resin-immobilized chicken erythrocyte mononucleosomes. IN, INO80 input; Nucleosomes, INO80 retained on the resin-immobilized mononucleosomes; BSA, INO80 retained on BSA resin. (**D**) ^{35}S-labelled INO80 fragments binding to histone agarose and DNA cellulose. Control binding for the experiment shown in (C). Histone, INO80 retention on histone-agarose beads; DNA, INO80 retention on DNA cellulose.

In budding yeast, the INO80 ATPase is part of a large chromatin-remodeling complex that plays a dual role in transcription and DNA metabolism (Shen et al., 2000). Recently, the yINO80 complex was reported to be regulated by inositol polyphosphates that have a major role in the communication of environmental signals (Shen et al., 2003b; Steger et al., 2003). Two helicases essential for viability of yeast, RVB1 and RVB2, provide helicase activity to the yINO80 complex, and take part in many nuclear functions (Jonsson et al., 2001). We found plant counterparts for RVB1 and RVB2 in the *Arabidopsis* genome (see latter section). Interestingly, among the actin related proteins (ARP4, ARP5 and ARP8) associated with the yINO80 complex, ARP5 and ARP8 appear

to be specific to this complex and have been proposed to be directly involved in the chromatin remodeling process (Shen et al., 2003a). An ARP gene family has also been reported for *Arabidopsis* and potential ARP5 and ARP8 genes can be found among them (see later section and McKinney et al., 2002; Kandasamy et al., 2003). It is thus likely that an INO80 complex similar to that in *S. cerevisiae*, exists in plants. Taken together with the nucleosome binding, this suggests *Arabidopsis* INO80 is a *bona fide* chromatin remodeling component.

2.7) *atino80*-1 plants are not hypersensitive to genotoxic agents

To test whether repair pathways other than HR are affected in the *atino80*-1 background, we subjected *atino80*-1 plants to various genotoxic stresses. In higher eukaryotes like *Arabidopsis*, DNA breaks resulting from genotoxic agents are repaired predominantly by mechanisms other than HR, such as the NHEJ pathway (Paques and Haber, 1999; Britt and May, 2003). *atino80*-1 plants as well as the two allelic mutants behaved identically to wild type plants towards treatment with bleomycin - a DSB-causing agent -, UV-C, Mitomycin-C and methyl methanesulfonate (MMS) (Fig. 47A & 47B and data not shown), suggesting that the pathways used to repair DNA damage resulting from these agents are not dependent on *INO80* activity in *Arabidopsis*. This in turn may imply that not only NHEJ, but also nucleotide excision repair, base excision repair and mismatch repair are unaffected in *atino80*-1 plants. In addition, MMS does not induce the steady state level of *AtINO80* transcripts (RT-PCR and microarray data not shown) as it does in yeast (Jelinsky and Samson, 1999).

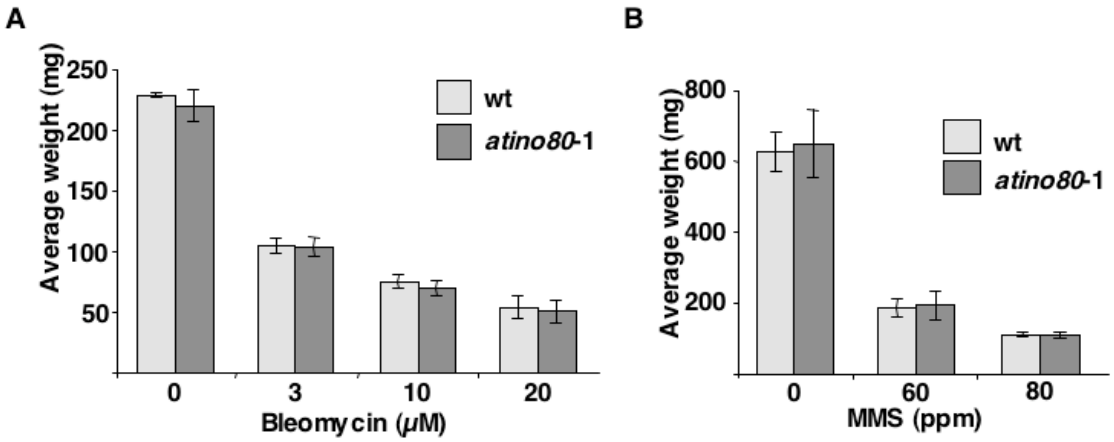

Figure 47. *atino80*-1 plants are not hypersensitive to genotoxic stresses. (**A**) Treatment with the double-strand break (DSB) causing agent bleomycin. Seven-day-old *in vitro*-grown seedlings were submitted to various doses of bleomycin in liquid culture in 96-well plates. After 7 days, the

fresh weight was measured for samples of 12 plants each. Values are the mean ± s.d. for one experiment out of three repeats. (**B**) Exposure to the genotoxic agent MMS. Plants were grown as above and exposed to MMS for 7 days in liquid culture in 24-well plates. Weight was measured as above; the graph represents one out of 3 repeats ± s.d.

2.8) The *atino80*-1 mutation does not affect the efficiency of T-DNA integration

To further evaluate the repair pathways affected in *atino80*-1 plants, we tested DNA repair of in a chromatin context using an *in vivo* T-DNA integration assay. The T-DNA of *Agrobacterium tumefaciens* is generally thought to integrate into the plant genome via a particular illegitimate repair process (Mysore et al., 2000; van Attikum et al., 2003; Britt and May, 2003). To test for T-DNA integration we used a root transformation assay with an *Agrobacterium* strain containing an oncogenic T-DNA (Nam et al., 1999). Again, *atino80*-1 plants behaved as the control plants did (Fig. 48), supporting the hypothesis that *AtINO80* is not involved in the illegitimate repair pathway.

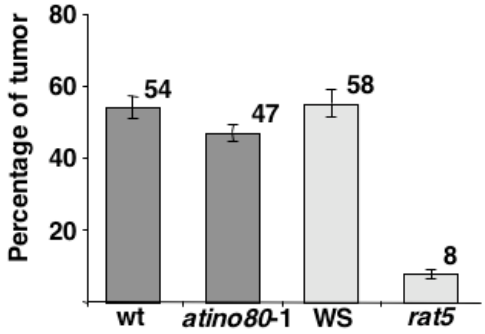

Figure 48. T-DNA integration is unaffected by the *ino80* mutation. Root transformation assay. The percentage of roots segments carrying tumors was counted 3 weeks after co-cultivation with a tumor inducing *Agrobacterium* strain. Values are the mean ± s.e.m. of one out of three repeats. The *rat5* control is a mutant deficient in T-DNA integration (Mysore et al., 2000). WS, *Wassilewskija* ecotype plants as control for the *rat5* mutant.

2.9) The *ino80* mutation does not reactivate the transcriptionally silent information (TSI) loci

Over the last years, several studies pointed towards a direct link between repair activities and transcriptional gene silencing (TGS). DDM1, an ATPase of the SWI/SNF family related to the RAD54 and RAD26 subfamilies (Fig. 45A and 6), was shown to participate in TGS (Mittelsten Scheid et al., 1998; Jeddeloh et al., 1999). Mutations in the endonuclease III domain nuclear protein *ROS1* gene, cause enhanced sensitivity to the genotoxic agents MMS and H_2O_2 together with transcriptional silencing of a transgene and its homologous endogenous gene (Gong et al., 2002). More recently, the *Arabidopsis BRU* gene was found to affect both DNA repair activities and TGS (Takeda et al., 2004). To address the potential involvement of INO80 in TGS, I looked at the expression of

endogenous targets of TGS in the *ino80* mutant or in RNAi lines. As shown Fig. 49, neither the *ino80*-1 mutant at the homozygous or heterozygous stage, nor the *INO*-IR RNAi lines were able to release silencing of the pericentromeric repeats TSI (transcriptionally silent information) that were shown to be reactivated in a number of TGS mutants (Steimer et al., 2000; Jackson et al., 2002; Saze et al., 2003). As a control I used RNA isolated from *mom1*, a mutant in which silencing at TSI is released (Steimer et al., 2000). This result is a good indication that the *Arabidopsis* INO80 is not involved in endogenous TGS, although I cannot exclude that loci silenced through a different mechanism are reactivated.

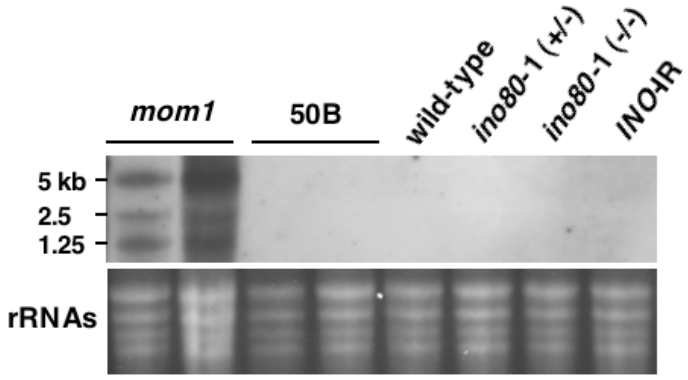

Figure 49. The *ino80* mutation does not reactivate transcriptionally silent TSI loci. Northern blot hybridization with RNA isolated from *in vitro*-grown seedlings probed with a DIG-labeled *TSI-A* fragment (Steimer et al., 2000). *mom1*, positive control (Amedeo et al., 2000; Steimer et al., 2000); 50B, RNA from the HR reporter line 50B; *ino80*-1, RNA from plants heterozygous (+/-) or homozygous (-/-) for the *ino80*-1 mutation in the 50B background; *INO*-IR, RNA from pooled plants transgenic for the *INO*-IR construct in the 50B background. Ribosomal RNA (rRNAs) revealed by EtBr staining of the gel before hybridization was used as a loading control.

2.10) *AtINO80* regulates a subset of the *Arabidopsis* transcriptome

To further investigate the implications of the *ino80* mutation for transcriptional regulation, I compared the genome-wide transcription profiles of plants from the three alleles of *ino80* with those of wild-type plants. Using whole genome *Arabidopsis* Affymetrix oligonucleotide microarrays and considering genes that are commonly regulated in the three alleles, I found that the *ino80* mutation affected a subset of about 0.5% of the *Arabidopsis* transcriptome (Fig. 50). As a good internal control, 50B and wild-type transcriptomes were essentially identical with no gene significantly changed. Applying a 1.5 fold-change cut-off, 29 genes were activated in absence of INO80, whereas 67 genes were repressed (Appendix 7). The regulated genes are involved mainly in general metabolism with very few genes involved in stress response and signaling. We found no

bias to particular chromosomal location, telomeres, or individual chromosomes in the genomic distribution of INO80-activated or repressed genes (Fig. 51). This resembles the situation of the yeast *ino80* mutant, but not that of the closely related yeast SWR1 ATPase mutant (Mizuguchi et al., 2004). Up- or downregulation of some of these genes may be responsible for the mild branching phenotype of the *atino80* mutant (see Discussion). In addition, I checked specifically a list of 302 known or putative genes involved in repair or recombination and found that their expression was not substantially changed in any of the three allelic mutants (Figure 50 and data not shown).

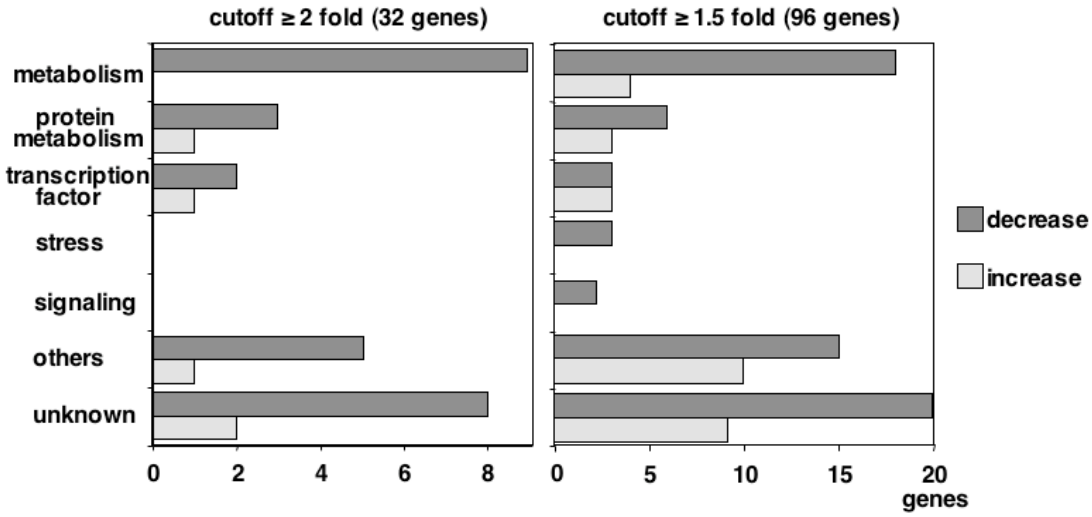

Figure 50. INO80 regulates a small subset of the *Arabidopsis* transcriptome. Affymetrix profiling of 2-week-old *ino80* mutant plants from the 3 alleles compared with wild-type plants. The distribution of genes with increased (white) or decreased (black) expression level in functional categories is represented. Genes with fold changes in expression level in *ino80* versus wild-type plants higher than 2 (left panel) or 1.5 (right panel) were used. The chromosomal distribution of the regulated genes is given in Fig. 51.

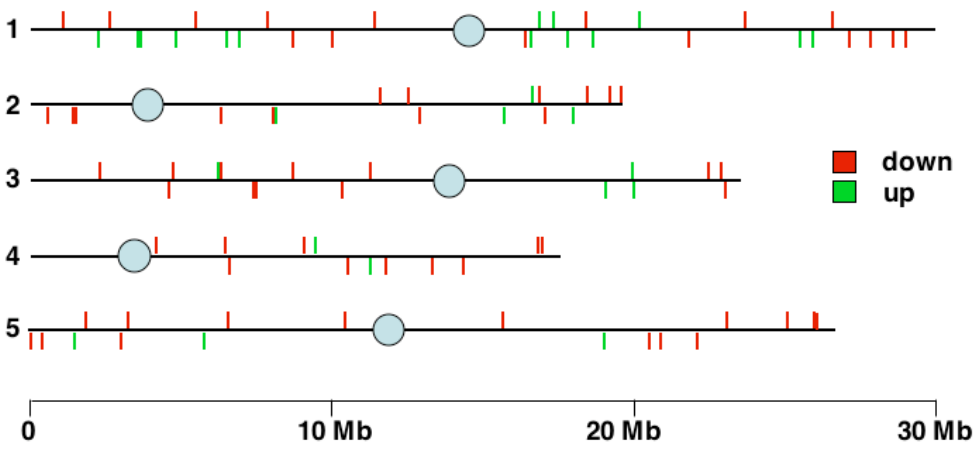

Figure 51. INO80 regulated genes are evenly distributed along chromosomes. Chromosomal distribution of genes commonly regulated in the three alleles of INO80. The blue balls represent the centromeric regions. Genes above or below the chromosomal line are in sense or antisense transcriptional orientation, respectively.

Taken together, this shows that *INO80* most likely does not exert its recombination-promoting function via general transcriptional activation or repression. Rather, *INO80* appears to be a positive dose-dependent regulator of HR, probably through chromatin remodeling. However, these data suggest a second function for *Arabidopsis* INO80 as a global regulator of transcription for a subset of the transcriptome. This is in agreement with INO80 being a member of the SWI/SNF superfamily of chromatin factors and a dual function in transcription and DNA metabolism (Shen et al., 2000).

2.11) Genome-wide gene expression upon MMS exposure is very similar in *atino80*-1 and control plants

In contrast to the situation in yeast, the *atino80* mutant is not hypersensitive to genotoxic stress. Therefore I wanted to analyze more precisely the physiological consequences of genotoxic stress on *atino80* plants. For this, I investigated whether transcriptional changes in response to MMS are different in wild-type and *ino80* by conducting a time course experiment. Two-week-old *in vitro*-grown seedlings of *ino80* and wild-type plants were acclimated to liquid media for one day. One hour after the light was switched on, MMS (at a final concentration of 40 ppm) was applied to half of the plants, and samples of 30 plants each were harvested at time 0, 4 h and 8 h. I chose 40 ppm of MMS as this dose is sufficient to induce the expression of *AtRAD51* but is not lethal for the plant (RT-PCR, data not shown). The experiment was done twice. After RNA isolation, we performed full-genome Affymetrix chip profiling of all duplicate samples and looked at transcriptional changes over time in presence or absence of MMS. The study of transcriptome dynamics in absence of MMS contributes to information on genes that are regulated by the photoperiod in wild-type and *ino80* plants. In the first analysis, I performed an ANOVA test to select genes with the most significant changes. A large number of genes are changed after 4 h (650 genes) and 8 h (911 genes) in wild-type (Fig. 52A); these genes are likely photoperiod-regulated genes. A similarly large number of genes are changed after 4 h (707 genes) and 8 h (914 genes) in the *ino80* background (Fig. 52A). These genes are essentially the same as those changed in wild-type as very few genes differ between wild-type and *ino80* at each time point (30 genes at 0 h, 24 genes at 4 h and 8 h, Fig. 52A). Again, this experiment suggests INO80 regulates a small subset of the *Arabidopsis* transcriptome. However, a smaller number of genes are regulated compared to the previous experiment (see above section); this most likely reflects the high stringency of

this analysis and a different variability (physiological state of the samples, number of replicates, allelic mutants). Surprisingly, there is very little overlap between genes changed in *ino80* compared to wild-type at 0, 4 and 8 h (data not shown) even though most of these genes have a similar trend – but below significance – at the different time points. To investigate this further, I looked in a less stringent way at genes up- or down-regulated in *ino80* at the three time points by fold-change filtering without ANOVA testing. Again, a very small number of genes (24 increased and 10 decreased) are common in the three time points (Fig. 52C & 52D). This suggests that the subset of the transcriptome regulated by INO80 changes over the photoperiod. Alternatively, it may be due to the adaptation to the new conditions, as plants were acclimated in liquid culture 1 day before the treatment.

In presence of MMS the situation is similar (Fig. 52B), with about 900 genes regulated at 4 h and about 1200 at 8 h. Further, the small number of genes that are different between wild-type and *ino80* plants also only partially overlap. However, many more genes are different at 4 h (149 genes, Fig. 52B) than at another time point or without MMS, indicating a potential involvement of INO80 in the control of MMS regulated genes at 4 h.

A no MMS (986 genes)

		ino80	wt		
		0 h	0 h	4 h	8 h
wt	0 h	30	-	650	911
	0 h	-	**30**	678	926
ino80	4 h	707	672	**24**	187
	8 h	914	910	249	**24**

B 40 ppm MMS (1412 genes)

		ino80	wt		
		0 h	0 h	4 h	8 h
wt	0 h	54	-	894	1235
	0 h	-	**54**	908	1230
ino80	4 h	888	850	**149**	249
	8 h	1235	1215	456	**37**

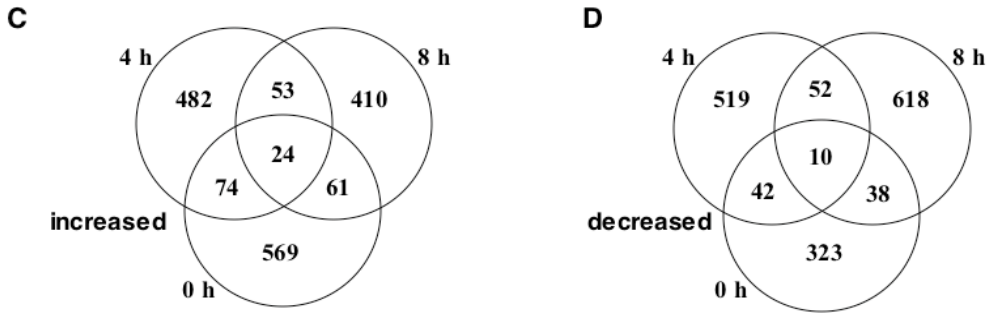

Figure 52. Comparison of the *ino80* and wild-type transcriptome of plants treated with MMS. (A) Transcriptional changes over the photoperiod. All untreated samples were used to generate lists of genes that are significantly changed (up or down), as tested by ANOVA and Turkey post-hoc analysis. **(B)** Transcriptional changes upon MMS treatment. The same analysis as above was used for treated samples (40 ppm MMS) and untreated samples at time 0. **(C)** Ven

diagram comparison of genes increased 1.5-fold in *ino80* compared to wild-type at time 0, 4 & 8 h. Genes present and exhibiting a raw data value above 50 in at least one condition were used to generate the lists by fold-change filtering. **(D)** Same as (C) but decreased in *ino80.*

2.12) Ectopic overexpression of *AtINO80* in *Arabidopsis*

As down-regulation of *INO80* expression results in decreased HR levels in a dose-dependent manner, it was of interest to test the influence of increased *INO80* expression on recombination and development. For this, I designed two constructs allowing a strong ectopic expression of *INO80* from the cDNA sequence. With the first construct, in the pEX6N35SMyci vector (see Appendix 6), the constitutive 35S promoter drives the expression of INO80 fused at its N-terminus to a c-myc epitope containing an intron. In the second construct, in pEX6NUbi (see Appendix 5), INO80 expression is under the control of the strong ubiquitin promoter (Genschik et al., 1994). I transformed the GUS HR reporter lines 1445 and 1418 with these constructs. GUS staining of pooled 2-week-old transformants did not show any significant change of HR levels in overexpression construct plants compared to vector transformed plants (data not shown). However, also northern blot analysis of pooled T1 plants or T2 families did not reveal any overexpressing lines. As the overexpression vectors were successfully tested *in planta* for GUS overexpression, these data may indicate that *INO80* overexpression is not tolerated by the plants. Indeed, I did find one pEX6N35SMyci *INO80* line that overexpresses INO80 as demonstrated by northern blot analysis and that exhibited strongly increased recombination levels. In addition, plants from this line were smaller than those from the other lines. However, since only few seeds were available for this line, I could not yet test whether this increase is significant.

3) Potential components of a plant INO80 complex

3.1) The yeast INO80 complex

SWI/SNF complexes are major players in chromatin modifications, together with histone acetyl-transferases (HATs) and histone deacetylases (HDAcs). These complexes show some degree of connectivity, share a number of proteins and act mainly as positive or negative transcriptional regulators through chromatin remodeling activities that result in changed accessibility to the transcriptional machinery or to transcriptional regulators (see General Introduction for more information).

As already mentioned, the yeast INO80 complex contains about 12 polypeptides. Besides the RVBs and ARPs proteins that are discussed below, actin (Act1p), Nhp10p (a protein of unknown function that contains a high mobility group HMG motif) and Anc1p/Taf14p (subunit of TFIID, TFIIF, and SWI/SNF complexes, involved in RNA polymerase II transcription initiation and in chromatin modification) also belong to the complex (Shen et al., 2003a). Further, there are a couple of INO80 complex specific proteins (Ies) of unknown function. These are Ies1p, Ies3p and in complexes isolated under low salt conditions, Ies2p, Ies4p, Ies5p & Ies6p (Shen et al., 2003a). A search for *Arabidopsis* homologs did not reveal clear candidates for any of them (not shown). This is in sharp contrast to the RVBs and ARPs for which homologs were found. However, considering that yeast and *Arabidopsis* INO80 share only 24 % identity on the whole sequence, it might be difficult to identify homologs for such small proteins.

3.2) Eukaryotic RVBs Helicases

3.2.1) RVB homologues in *Arabidopsis*

The prokaryotic counterpart of RVB1 and RVB2, the RuvB helicase, is a motor protein that drives branch migration of Holliday junctions during HR (see General Introduction and Yamada et al., 2001; West, 2003). Eukaryotic RVBs and RuvB proteins share highly conserved A and B Walker domains, indicative of proteins that bind nucleotide triphosphates (Kanemaki et al., 1997; Gohshi et al., 1999). Indeed, the presence of RVBs in a wide range of eukaryotes ranging from yeast to mammals, suggests that this basic helicase activity is conserved among the eukaryotes. Also, in yeast and mammals at least, RVB function is essential for the survival of the organism. Despite a confusing nomenclature, central but very diverse functions were attributed to eukaryotic RVBs mainly in transcription, DNA repair and development (see General Discussion).

Searching the *Arabidopsis* genome with yeast *RVB1* & *RVB2* sequences, I could identify three genes with 60.4 to 65.4 % identity at the protein level with the yeast proteins (Fig. 53A & 53B). As for other organisms, the *Arabidopsis* RVB homologues fall in two groups defined by yeast RVB1 and RVB2 (Fig. 53A). The *Arabidopsis RVB1* gene has a complex gene oganization with 11 introns, whereas *RVB21* and *RVB22* have only one intron each in the center of the gene (Fig. 53C). Together with their very high similarity (82.7 % at the protein level, Fig. 53B), this probably indicates that *RVB21* and *RVB22* arose by a recent gene duplication, as shown for many *Arabidopsis* genes (Blanc

et al., 2000). Although I could not detect *RVBs* transcripts by standard northern blot hybridization (data not shown), RT-PCR analysis and microarray data clearly indicate that the three genes are transcriptionaly expressed, although at very low level in the case of *RVB22* (Table 8 and data not shown).

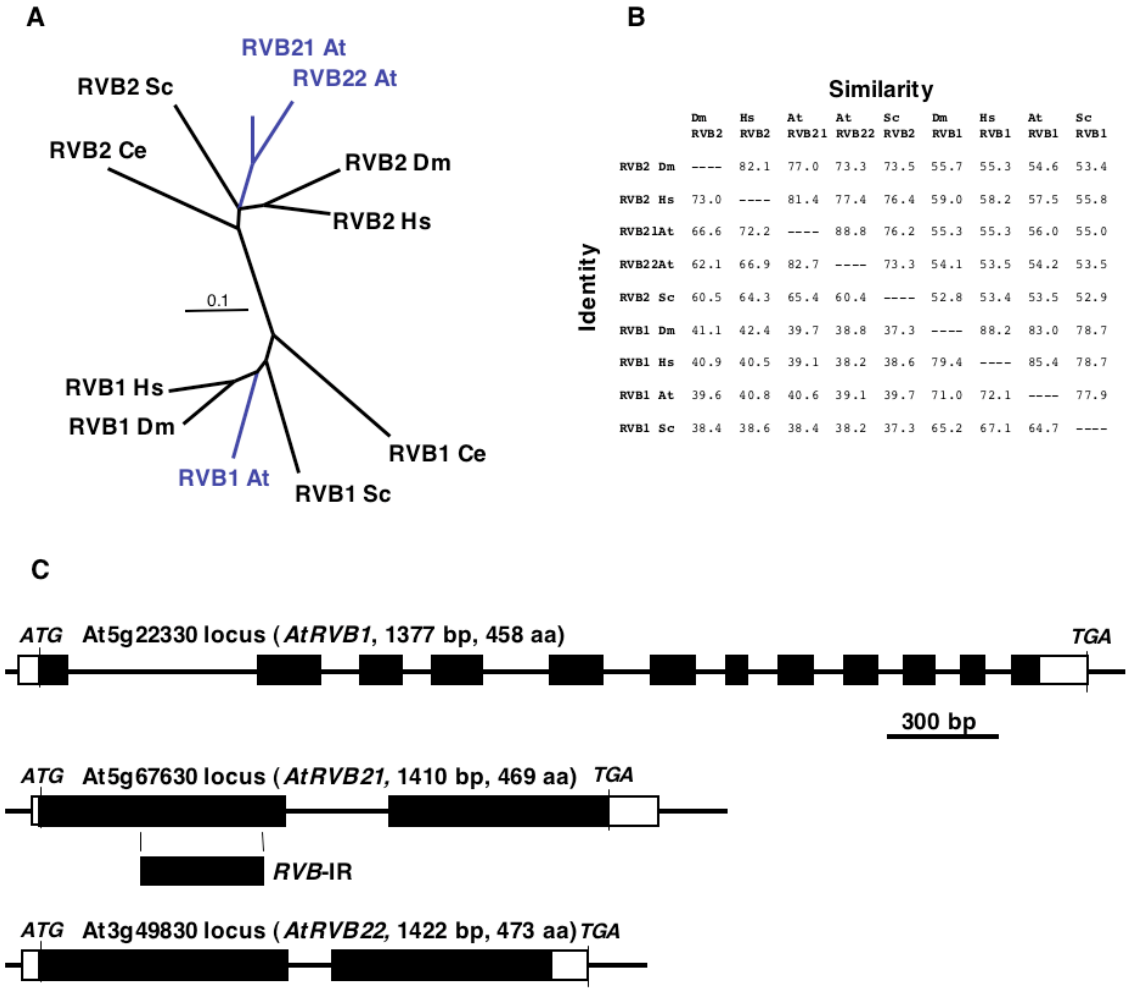

Figure 53. *Arabidopsis* RVB gene organization. (A) Protein phylogenetic tree of RVB1 and RVB2 in eukaryotes. Full-length protein sequences were used. In *Arabidopsis*, the RVB2 has two very closely related homologues. Accession numbers: RVB1 Hs (NP_003698), RVB1 Dm (AAF54514), RVB1 At (from *At5g22330*), RVB1 Sc (NP_010476), RVB1 Ce (CAB02793), RVB2 Hs (NP_006657), RVB2 Dm (AAF49182), RVB21 At (from *At5g67630*), RVB22 At (from *At3g49830*), RVB2 Sc (NP_015089), RVB2 Ce (AAF98631). At, *A. thaliana*; Ce, *C. elegans*; Sc, *S. cerevisiae*; Dm, *D. melanogaster*; Hs, *H. sapiens*. **(B)** Amino acid sequence conservation in the RVB family of helicases. Identity/Similarity matrix for the full-length RVB protein sequences. Nomenclature as in (A). **(C)** Organization of the *Arabidopsis* RVB genes. *RVB*-IR, sequence used for RNAi construct. Black box represent exons (separated by introns). White box are 5' and 3' UTR (untranslated region).

To evaluate RVB genes function in *Arabidopsis*, I pursued two parallel experimental approaches. First, I addressed the effect of down-regulating *RVB* expression by RNAi or by gene knockout (see below). Second, I investigated the potential involvement

of the RVB proteins in an *Arabidopsis* INO80 complex by looking at various potential interactions between RVB and RVB proteins and between RVBs and INO80 by yeast-two-hybrid using the pACT2 and pGBKT7 vectors (data not shown). Due to the length of the proteins we expressed fragments consisting of the INO80 truncations described above (Fig. 46B) and of two overlapping constructs for each of the RVBs. However, interactions were found for neither of the tested combinations. This may mean that INO80 and RVB do not interact directly in the complex (this was not tested in *S. cerevisiae*) or that the expressed proteins do not have the proper configuration to interact. Alternatively, INO80 and RVBs may not participate in the same complex in *Arabidopsis*.

3.2.2) RVBs are essential in *Arabidopsis*

To investigate the function of *Arabidopsis* RVBs, I down-regulated the transcript level of the three RVBs in the 50B recombination reporter line with constructs producing double-stranded RNA homologous to a highly conserved region of all three *RVBs* (*RVB*-IR from *RVB21* gene, see Fig. 53C). The *RVB*-IR sequence extending from position 258 to 595 of *RVB21* coding sequence was amplified from the *RVB21* cDNA and cloned in the pEXhp RNAi vector (see above and Appendix 4). I transformed reporter line plants with either the *RVB*-IR construct or an empty vector. Upon selection in the next generation, individual transformants were isolated and grown *in vitro*. Plants carrying the *RVB*-IR construct had small dark green unexpanded leaves and grew very slowly, in contrast with vector transformed plants (Fig. 54). All *RVB*-IR transformants stayed at this stage for 3-4 weeks and died without having produced seeds. Due to the strong phenotype of these RNAi plants, it was not possible to analyze HR levels. In parallel, I analyzed two allelic mutants in the RVB1 gene obtained from the SAIL collection (SAIL_397_C11 & SAIL_867_G11, Fig. 55C). Their developmental phenotype was normal at the heterozygous stage, but I could not recover homozygous plants for the T-DNA insertion (data not shown). In addition, the Basta resistance carried by the T-DNA segregated as 2/1 for resistance/sensitivity indicative of a homozygous lethal phenotype (data not shown). This further suggests that *RVB1* is essential in *Arabidopsis*. As the *ino80* mutation does not result in such defect, it is tempting to speculate that the *Arabidopsis* RVB1 has an essential role independent of its potential implication in the INO80 complex.

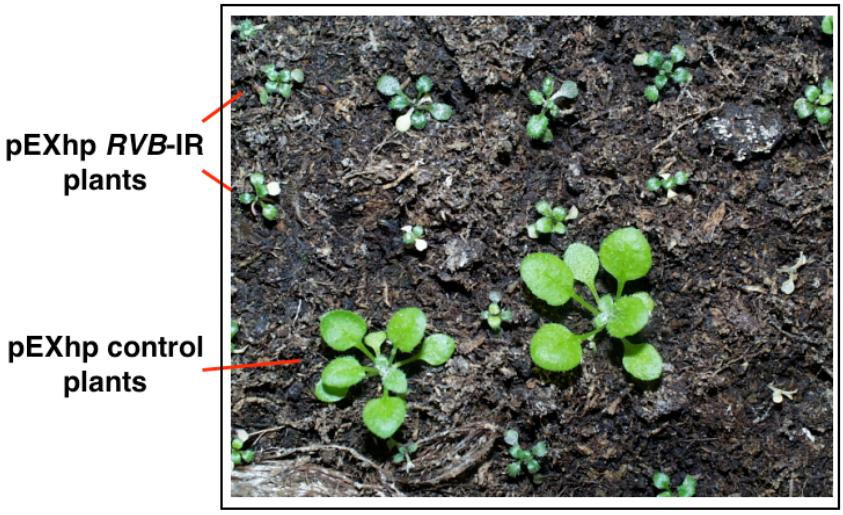

Figure 54. The RVB family is essential in *Arabidopsis*. In the T1 generation, plants carrying pEXhp *RVB*-IR T-DNA stay very small compared to empty vector transformed plants. Three-week-old independent T1 transformants of pEXhp *RVB*-IR or pEXhp alone were selected *in vitro* and transferred to soil.

3.3) Actin related proteins (ARPs)

3.3.1) The ARP protein family

The actin related protein (ARP) family regroups distantly related proteins that share the actin-fold motif defined as a common tertiary structure and a mostly not tested ATP-binding domain (Boyer and Peterson, 2000). In yeast, 10 ARPs were found numbered according to their increased divergence from conventional actin (Fig. 55A). Some ARPs are cytoplasmic (ARP2/ARP3, ARP1 & ARP10) and involved in actin related activities, whereas the others were recently reported as components of various chromatin remodeling complexes (Fig. 55B) and thus may play important functions in the nucleus (Boyer and Peterson, 2000). For instance the ARP4 protein, component of the yeast INO80 complex, is shared by at least 3 other complexes, making its function difficult to elucidate (Fig. 55B). Interestingly, ARP4 interacts with the core histones and especially with H2A through its insertion domain II in the conserved ATPase motifs (Harata et al., 1999).

3.3.2) *Arabidopsis ARP* genes and INO80

Very little is known about *Arabidopis* ARP function, with the exception of the ARP2/3 complex and its implication in development (Mathur et al., 2003). However, the ARP gene family was thoroughly characterized and a recent review points to interesting peculiarities of plant ARP gene members (Kandasamy et al., 2004). Also, localization studies were performed for AtARP7 and AtARP9 (Szerlong et al., 2003). There are two homologs for Arp4p that are shared by a number of complexes including INO80 (Fig.

55A & 55B). As for the INO80 complex specific Arp5 and Arp8 proteins, homologs exist but no data are available on their possible contribution to an *Arabidopsis* INO80 complex (Fig. 55A & 55B). Using RT-PCR analysis, I found both *ARP5* (*At3g12380*) and *ARP8* (*At5g43500*) expressed, although most (about 80 %) *ARP8* transcripts were incompletely spliced in the 3' region (data not shown, primer sequences in Appendix 1). In addition, due to the poor sequence conservation, the orthology is not clear (data not shown).

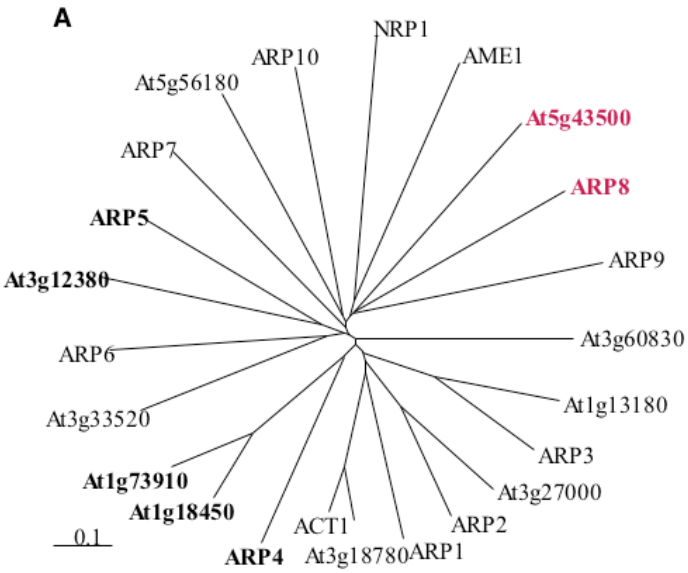

B

Arabidopsis		*S. cerevisiae*		
AGI	**Kandasamy et al., 2004**		**localization**	**complex**
-	-	ARP1	cytoplasmic	dynactin
At3g27000	AtARP2	ARP2	cytoplasmic	ARP2/ARP3
At1g13180	AtARP3	ARP3	cytoplasmic	ARP2/ARP3
At1g18450 At1g73910	AtARP4 AtARP4A	ARP4	nuclear	INO80, NuA4, HAT, SWR1
At3g12380	AtARP5	ARP5	nuclear	INO80
At3g33520	AtARP6	ARP6	nuclear	SWR1
At3g60830	AtARP7	-	-	-
-	-	ARP7	nuclear	SWI/SNF, RSC
At5g43500	AtARP9	ARP8	nuclear	INO80
-	-	ARP9	nuclear	SWI/SNF, RSC
At5g56180	AtARP8	ARP10	cytoplasmic	Dynactin

Figure 55. The ARP gene family. (A) Phylogenic tree of yeast and *Arabidopsis* ARPs proteins. ARPs in the INO80 complex are in bold. Complete sequences were used to preserve domains specific of each ARP. At, *Arabidopsis*; all other proteins are from *S. cerevisiae*. Yeast accession numbers can be found at www.yeastgenome.org. **(B)** Yeast and *Arabidopsis* ARPs. Subcellular localization and known complexes of yeast ARPs. Nomenclature and complex attribution according to the current literature (Kandasamy et al., 2004; Mizuguchi et al., 2004).

The characterization of the ARPs that are present in the potential *Arabidopsis* INO80 complex may help to isolate an INO80 complex and uncover its function. Because the yeast Arp4p belongs to many complexes and is essential, I concentrated on analyzing the *Arabidopsis* ARP5 and ARP8 candidates. Taking advantage of the time-course profiling experiment described above, I looked whether the expression of any of the *Arabidopsis ARPs* would be affected by the INO80 mutation (Table 8). Indeed, the only *ARP* which exhibits altered expression in *ino80* is *At5g43500*, the potential Arp8p ortholog (Fig. 55). This gene, that I called *ARP8* (*AtARP9* according to Kandasamy et al., 2004), shows consistently increased transcript levels in the *ino80* background over the three time points analyzed.

			0 h				4 h				8 h			
AGI	**name**	**ANOVA**	***ino80***		**wt**		***ino80***		**wt**		***ino80***		**wt**	
AT5G43500	*ARP8* (*AtARP9*)	0.10	**425**	**P**	**269**	**P**	**563**	**P**	**316**	**P**	**598**	**P**	**382**	**P**
AT3G27000	*ARP2* (*AtARP2*)	0.22	176	A	178	A	233	A	141	A	195	A	155	A
AT3G46520	*Actin* 12	0.22	5	A	12	A	17	A	34	A	7	A	23	A
AT3G49830	*RVB22*	0.31	4	A	29	A	9	A	16	A	6	A	5	A
AT5G67630	*RVB21*	0.93	544	P	522	P	552	P	580	P	593	P	614	P
AT3G33520	*ARP6* (*AtARP6*)	0.93	708	P	730	P	727	P	689	P	752	P	713	P
AT3G12380	*ARP5* (*AtARP5*)	0.93	265	P	270	P	340	P	323	P	310	P	326	P
AT5G22330	*RVB1*	0.93	448	P	421	P	545	P	480	P	471	P	509	P
AT3G60830	*ARP* (*AtARP7*)	0.93	427	P	472	P	473	P	463	P	453	P	486	P
AT1G73910	*ARP4* (*AtARP4A*)	0.93	27	A	23	A	46	A	34	A	19	A	39	A
AT1G13180	*ARP3* (*AtARP3*)	0.93	222	P	191	P	285	P	260	P	287	P	312	P
AT1G18450	*ARP4* (*AtARP4*)	0.93	874	P	895	P	858	P	891	P	794	P	788	P
AT5G56180	*ARP10* (*AtARP8*)	0.93	499	P	520	P	375	P	437	P	478	P	410	P

Table 8. Transcript profiling of ARPs and RVBs in wild-type and *ino80*-1 plants. A list of *Arabidopsis ARPs* and *RVB* genes was checked in the time course transcriptome analysis described above. The raw mean data values with their flags (P, present; A, absent) are given for wild-type (wt) and *ino80*-1 (*ino80*) in absence of MMS.

4) Summary

HR serves a dual role in providing genetic flexibility and in maintaining genome integrity. Little is known about the regulation of HR and other repair pathways in the context of chromatin. We report on a mutant in the *Arabidopsis INO80* ortholog of the SWI/SNF ATPase family, which shows a reduced frequency of HR. In contrast, sensitivity to genotoxic agents and efficiency of T-DNA integration remain unaffected. This suggests that INO80 is a positive regulator of HR, while not affecting other repair pathways. Further, transcriptionaly silent TSI loci are not reactivated in absence of INO80, suggesting that *Arabidopsis* INO80 function is independent of transcriptional silencing. Using whole genome expression studies by microarray profiling I show evidence that INO80 regulates a small subset of *Arabidopsis* genes, suggesting a dual role for INO80 in transcription and repair by HR. Moreover, the recombination-promoting function of INO80 is not likely to involve general transcriptional regulation, and the transcriptional regulation of repair related genes is unaffected in the mutant. This is the first report of INO80 function in a higher eukaryote. Mononucleosome binding studies support that INO80 positively regulates HR through modification of chromatin structure at sites of DNA repair by HR. Finally, I provide evidence for the existence and/or connectivity with INO80 of other INO80 complex partners in *Arabidopsis*.

E. General Discussion

1) Genetic screening for HR mutants

As HR serves a dual role in providing genetic flexibility and in maintaining genome integrity (Paques and Haber, 1999), the choice of a pathway to repair DSBs is crucial, especially in plants where the germline is only determined late during development (see General Introduction). Although the proteins directly participating in HR repair are well studied – in particular in yeast and prokaryotes – the regulation of these steps, the potential associated chromatin remodeling events and the global control of HR remain more elusive (Paques and Haber, 1999; West, 2003). As a consequence, the discovery of factors affecting or involved in HR will provide important information both for the understanding of genome integrity and evolution and for the improvement of HR based gene technology approaches.

So far, the isolation of genes involved in recombination or regulating recombination in plants was achieved through indirect approaches. These are mostly genetic screens for genotoxic stress hypersensitivity (Masson and Paszkowski, 1997; Mengiste et al., 1999; Takeda et al., 2004) and reverse genetic approaches directed at *Arabidopsis* homologs of yeast recombination and repair genes (Gherbi et al., 2001), in combination with subsequent tests for altered HR levels. Even though these approaches proved to be successful (See Chapter 1, Introduction), they represent a biased way to look for HR components. Specifically, they cannot unravel genes solely involved in the HR repair pathway or genes involved in plant specific repair activities or control pathways. Genes isolated in this thesis work may help to fill this gap, as we describe the first direct screen for HR mutants in plants.

The outcome of the screen can be considered in several ways. First, as a collection of new mutants that will help to characterize HR and its regulation in plants, but also in other eukaryotes as this type of genetic approach was not used in higher eukaryotes so far. In addition we can assess the screen in terms of success and of problems in order to establish further genetic screens for HR mutants. Concerning the type of candidate genes found – although we did not prove the causality in most cases – it can be first noticed that

no known repair genes or genes with obvious implications in HR were found. Also, about half of the candidate genes are of totally unknown function and do not show similarity with any known gene. Interestingly, several genes related to functions in chromatin dynamics were found. For one mutant, *sm22*/*ino80*-1, the gene was proved to be responsible for the altered recombination phenotype. Other chromatin related proteins are potential candidates for HR-related activities; they include a non standard SMC protein, designated as SMC4 like in *vw4*, a protein containin RCC-1 domains, a tandem histone H3.2 and an additional SWI/SNF family ATPase. Standard SMC proteins (SMC1-SMC6) are involved in chromosome condensation and cohesion, but also in DNA repair function in yeast (see Chapter 1, Introduction). The gene responsible for the decrease in HR level in the *mim* mutant was also shown to encode a protein belonging to the SMC family (Mengiste et al., 1999). As another example, the ATPase mutated in *hw17* is very interesting as its closest yeast homolog is Rad26p, which defines a small subfamily of SWI/SNF ATPases involved in transcription-coupled repair (TCR) (van Gool et al., 1994; Tijsterman and Brouwer, 1999; Bucheli et al., 2001). TCR forms a subpathway of the nucleotide excision repair (NER) pathway and deals with bulky-type DNA damage induced by UV and various chemicals. The most probable *Arabidopsis* RAD26 ortholog, according to sequence homology (AtRAD26 on Fig. 6), is different from the *hw17* ATPase (At5g63950), suggesting that the latter has a function different from RAD26. As the *hw17* ATPase belongs to a small, plant specific group of ATPases it is tempting to speculate that it may be involved in plant specific repair activities. Once a number of these new genes are confirmed as causing the HR phenotype, their roles in structure and/or dynamics of chromatin events controlling HR will become apparent. A few other candidate proteins from the screen may play a role in DNA accessibility and/or metabolism; these are an RPA like protein (*vw4*) and a DNA polymerase δ (*hw17*). The latter has been proved to influence HR levels (D. Schuermann, personal communication).

During the time of this study, efficient systems to inhibit gene expression by RNAi were developed and seem to be a solution of choice to rapidly prove a gene function. In plants, RNAi is mostly achieved by producing double-stranded RNA homologous to the gene to be down-regulated *in vivo*. The RNAi system that we developed according to J. M. Waterhouse (Smith et al., 2000; Stoutjesdijk et al., 2002), proved to be efficient for a quick assessment of gene function postulated from the screen, either directly in the first generation after integration of the RNAi construct (this work) or

in the second generation (characterization of a mutant obtained in a further screen, Molinier et al., 2004).

Although non-lethal screening with the luciferase reporter proved to be convenient and efficient for the initial discovery of HR mutant candidates, it was much more difficult to handle when we came to the persistence of the phenotype. In theory, only luciferase spots on plants within a single image can be compared, because of the detection variability between luciferase image capture. Nevertheless, we could establish conditions that help to avoid this unwanted effect. According to my observations it is more convenient – in terms of time and experimental design – to prove phenotypes using GUS based systems, as we did it for a further genetic screen (Molinier et al., 2004b). Therefore, the advantage of the non-lethal luciferase based approach seems to be negligible to me when I take in account the confirmation and characterization of the phenotype of the candidates, compared to the GUS-based approach where the phenotype can be assessed in a non-lethal way using only a few leaves (Molinier et al., 2004b).

The problems with phenotype persistence that I encountered with this genetic screen may stem from the activation tagging approach itself, or from the particular construct I used. Indeed, the particular arrangement with direct and indirect repeats of the 35S promoter/enhancer sequence in the pAC102 T-DNA (Annex 3) is prone to induce silencing effects. In addition, with the activation tagging strategy itself, it cannot be excluded that plant cells react to undesired changes of gene expression leading to a progressive loss of the activation tagging effect. However, the activation tagging approach with four repeats of the 35S enhancer sequence has been proved to be a successful strategy in *Arabidopsis* using the construct developed by D. Weigel (Weigel et al., 2000). Examples showing a gain of function with visible phenotypes are the activation of a *MYB* factor gene, the patatin and leafy petiole genes (Borevitz et al., 2000; van der Graaff et al., 2000; Huang et al., 2001). However, problems of phenotype persistence have been associated also with this approach and a recent study reports that plants containing more than a single T-DNA insertion exhibit methylation of the 35S enhancer resulting in dramatic decrease of 35S enhancer activity (Chalfun-Junior et al., 2003). This may explain that in some activation tagged lines the 35S enhancer is silenced due to methylation. As an alternative, an activation tagging approach based on a simplified version of the pAC102 vector could be designed, with no repeat of the 35S promoter, as repeats seem be responsible for some of the encountered difficulties.

2) The phenotypes of the *Arabidopsis ino80* mutation

A small number of *Arabidopsis* mutants with decreased levels of HR were isolated: The EMS mutants *xrs4* and *xrs9*, the mutated genes of which were not characterized (Masson and Paszkowski, 1997) and *mim*, in which an SMC-like protein is down-regulated (Mengiste et al., 1999) (see Chapter 1, Introduction). In a mutant, decreased HR levels may either correlate with increased illegitimate recombination when the affected factor is involved in the choice of DSB repair pathway (see General Introduction) or with unchanged levels of illegitimate recombination when an HR-specific factor was hit. Alternatively, decreased HR frequencies can be accompanied by a general weakness of DNA repair pathways. The fact that *ino80*-1 plants exhibit unchanged sensitivity towards genotoxic agents inducing DSBs likely indicates that illegitimate repair is not affected by the absence of INO80, as DSBs are prominently repaired by NHEJ in plants (Britt and May, 2003; Hanin and Paszkowski, 2003). This hypothesis is strengthened by the result that *ino80*-1 has no defects in T-DNA integration, a process shown to rely on the NHEJ pathway in plants (van Attikum et al., 2001; Friesner and Britt, 2003), although recent studies suggest that some components of the NHEJ pathway are not required for T-DNA integration in *Arabidopsis* (van Attikum et al., 2003; Gallego et al., 2003).

Significantly, all previously reported plant HR mutants are also altered in genotoxic stress responses, i.e., repair pathways other than HR (Masson and Paszkowski, 1997; Mengiste et al., 1999; Gorbunova et al., 2000; Gherbi et al., 2001), making *Atino80*-1 the first reported plant mutant that is specifically affected in HR. DNA repair or recombination may be modified or regulated by higher order chromatin structure (Mengiste et al., 1999; Qin and Parthun, 2002; Ura and Hayes, 2002; Birger et al., 2003; Downs et al., 2003), mainly concerning the involvement of chromatin modifications at various levels and steps in nucleotide excision repair (Green and Almouzni, 2002; Ura and Hayes, 2002). Thus, INO80 represents the first described positive regulator of HR probably acting through chromatin events.

The fact that I observed no difference in sensitivity towards various genotoxic agents for *atino80* plants is in sharp contrast to observations in budding yeast, in which the *ino80* mutation leads to hypersensitivity to all genotoxic agents tested (UV-C, ionizing radiation, γ-rays, MMS and hydroxyurea) (Ebbert et al., 1999; Shen et al., 2000). Except for the G2 phase, in which the sister chromatid is available as template for repair by HR, DNA breaks in haploid yeast cells are thought to be mainly repaired by the

illegitimate pathway. Although no specific repair pathway was tested in the *S. cerevisiae ino80* mutant, the repair preference difference in yeast and plants suggests distinct roles for INO80 in the two organisms. Alternatively, the difference in response to genotoxic agents of the *ino80* mutation may reflect the different repair preferences of yeast and *Arabidopsis*, where HR and NHEJ, respectively, are the prevalent repair pathways (Paques and Haber, 1999; Britt and May, 2003). In this scenario, INO80 activity might then contribute to the minor repair pathway in both organisms.

The fact that *ino80*-1 mutants do not accumulate developmental defects over generation and are not affected in fertility is in agreement with the above indications of *INO80* being a positive regulator of HR, but not an essential component of HR in *Arabidopsis*. It may also indicate that *INO80* is not involved in meiotic recombination. The increased branching of *ino80*-1, together with slightly reduced height is reminiscent of the effect of increased cytokinin concentrations (Heyl and Schmulling, 2003). Such phenotype may result either from a defect in auxin metabolism or signaling, or from an increased cytokinin effect. *Arabidopsis* cytokinin mutants were shown to have similar phenotypes (Werner et al., 2003). Indeed, another *Arabidopsis* SWI/SNF ATPase, PKL (Fig. 6), has been suggested to play a role in giberellin hormone dependent responses (Henderson et al., 2004)

3) A dual function for the *Arabidopsis* INO80

The general common function of SWI/SNF ATPase chromatin remodeling complexes can be described as transcriptional regulation. In yeast, mammals and *Drosophila*, ATPase and chromatin remodeling activities, as well as a role in the control of transcriptional activities, has been characterized for a number of these complexes. In plants SWI/SNF complexes were not yet characterized and ATPase activity has only been reported for DDM1. Nevertheless, several mutants in SWI/SNF family members were described in *Arabidopsis,* with an associated function in transcriptional regulation: SPLAYED (SYD) is involved in transcriptional activation and repression, and is a co-activator of LEAFY for the transcriptional activation of homeotic genes (Wagner and Meyerowitz, 2002); PICKLE (PKL), seems to be a co-repressor of embryonic developmental genes (Ogas et al., 1999); PHOTOPERIOD-INDEPENDENT EARLY FLOWERING (PIE1) negatively regulates the expression of genes that promote flowering (Noh and Amasino, 2003). However global changes at the transcriptome level were not tested (see General Introduction for more details and Fig. 6). The yeast ortholog of PIE1 – SWR1 – promotes the expression of

genes near heterochromatic regions through recruitment and exchange into chromatin of the histone-variant HTZ1 (the yeast H2A-Z variant) (Krogan et al., 2003; Mizuguchi et al., 2004). PIE1, SWR1 and the *Drosophila* Domino-A protein actually represent the subfamily of SWI/SNF proteins most closely related to that of INO80 (see Fig. 6). In strong contrast to *syd*, *pkl* and *pie1*, *atino80*-1 plants exhibit only a mild developmental phenotype, although developmental defects are stronger in the *atino80*-2 and *atino80*-3 alleles.

By looking at the whole transcriptome by microarray analysis in *atino80* mutants (Chapter 2, 2.10), I discovered that about 0.5% of the *Arabidopsis* genes are differentially regulated, with a similar number of genes up- and down-regulated. This represents about 100 genes regulated by INO80 using a 1.5 fold-change cut-off. In a second experiment (Chapter 2, 2.11), I found fewer genes significantly regulated. Nonetheless, I could see a consistent trend (up- or down-regulated) for many genes although under the statistically significant level (by comparing time points and between experiments, data not shown). This suggests, that more genes than found are regulated by INO80 – but in a fine-tuning manner, raising the possibility that INO80 participates in the regulation of a subset of the transcriptome in a cooperative manner with other transcriptional activators or repressors. Alternatively, it may mean that the important transcriptional function of INO80 is compensated for by other chromatin remodeling complexes in the mutant. This is remarkable since changes of small amplitude (1.25 fold) – although consistent – were also reported for the transcriptome of the yeast *ino80* mutant (Mizuguchi et al., 2004). Indeed, in yeast, 61 and 71 genes were activated and repressed more than 2 fold, respectively, whereas 263 and 278 genes were activated and repressed more than 1.5 fold, respectively, with very few genes over a 3-fold-change. Also, I found no bias to particular chromosomal location, telomeres, or individual chromosomes in the genomic distribution of INO80-activated or repressed genes, again resembling the situation of the yeast *ino80* mutant, but not that of the closely related yeast SWR1 ATPase mutant (Mizuguchi et al., 2004). The observation that a subset of the transcriptome regulated by INO80 changes over the photoperiod, may also strengthen the above hypothesis, as it again suggests that INO80 is involved in a fine-tuning regulation, in this case with photoperiod dependent transcriptional regulators.

Interestingly, in *Arabidopsis*, the regulated genes are mainly involved in general metabolism with very few genes involved in stress response and signaling. As for the yeast *ino80*, no bias towards repair or stress related genes, was reported, in agreement with my

Arabidopsis data. Also, as discussed in a previous section, some of the regulated genes may be responsible for the mild developmental phenotype of *atino80*.

As a conclusion, my results suggest a second function for INO80 in *Arabidopsis* as a fine gene regulator of a subset of the transcriptome. This is in agreement with INO80 being a member of the SWI2/SNF2 superfamily of chromatin factors and with the dual function of yINO80 in transcription and DNA metabolism (Shen et al., 2000). Taken together with the recombination data, this shows that *INO80* most likely does not exert its recombination-promoting function via general transcriptional activation or repression. Rather, *INO80* appears to be a positive dose-dependent regulator of HR, probably through chromatin remodeling in parallel with its function in transcriptional regulation.

4) A potential *Arabidopsis* INO80 complex

In budding yeast, the INO80 ATPase is part of a large chromatin-remodeling complex that plays a dual role in transcription and DNA metabolism (Shen et al., 2000). Two heli-cases essential for viability of yeast, RVB1 and RVB2, provide helicase activity to the yINO80 complex, and take part in many nuclear functions (Jonsson et al., 2001). Other proteins in the complex include ARP4, ARP5 and ARP8, the latter having been proposed to contribute to the chromatin remodeling activity of the complex (Shen et al., 2003a).

In yeast, RVB1, RVB2 are functionally coupled and present together with ARP4 and ACT1 in the INO80 complex, but also in the NuA4 HAT (histone acetyltransferase) complex and the recently discovered SWR1 ATPase complex (Jonsson et al., 2001; Krogan et al., 2003; Mizuguchi et al., 2004). RVBs are directly implicated in general transcriptional regulation; they control over 5% of the transcriptome, with a similar number of genes being repressed and activated (Jonsson et al., 2001); they interact with the TATA-binding protein (TBP) both *in vitro* and *in vivo* and seem to be important in recruiting it to the promoter (Ohdate et al., 2003). Further, RVB2 is required for cell cycle progression and RNA Polymerase II directed transcription (Lim et al., 2000). In mammals, TIP48/TIP49a (RVB1 like) and TIP49/TIP49b (RVB2 like) bind to each other and are part both of a large ATPase/helicase complex involved in c-Myc-mediated oncogenesis and apoptosis and of the TIP60 HAT complex involved in DNA repair and apoptosis (Qiu et al., 1998; Kanemaki et al., 1999; Ikura et al., 2000; Wood et al., 2000). Furthermore, TIP49b was recently described to regulate the activity of Activating Transcription Factor 2 (ATF2) that is implicated in transcriptional control of stress-responsive genes response to

stress and DNA damage (Cho et al., 2001). Although apparently unrelated, there is strong evidence that mammalian RVBs bind to snoRNAs (small nucleolar RNAs) (Watkins et al., 2002). In *Drosophila*, the RVB homologs Pontin52 and Reptin52 also bind to the TBP and are implicated in an additional mechanism for the control of the Wingless/Wnt pathway (Bauer et al., 1998; Bauer et al., 2000). However, in none of the mentioned reports is thereany indication of eukaryotic RVBs involved in a process resembling the prokaryotic RuvB function in HR.

As also found in other organisms, the *Arabidopsis RVB* gene family seems to be necessary for plant development as RNAi against all three genes resulted in small transformants with slow growth that died without having set seeds. This is strengthened by the embryonic lethality of two *RVB1* mutant alleles. Thus, the absence of *RVB* in *Arabidopsis* results in more dramatic effect than that of *INO80*. Although our data are not yet conclusive, they represent the only study on plant *RVB* genes so far, and suggest RVB proteins have important functions in *Arabidopsis* apart from their potential involvement in the INO80 complex.

Interestingly, among the actin related proteins (ARP4, ARP5 and ARP8) associated with the yINO80 complex, ARP5 and ARP8 appear to be specific to this complex and have been proposed to be directly involved in the chromatin remodeling process (Shen et al., 2003a). The finding that the *Arabidopsis* ARP8 gene candidate is induced in the *ino80*-1 mutant background is not only interesting as an indication that it is part of the INO80 complex but also for the implication it may have to the *ino80*-1 phenotype. It is well possible that this up-regulation acts as a sort of compensation mechanism for the loss of INO80, and may therefore hide a part of the INO80 deficient phenotype. Indeed, the yeast Arp8p associates with some components of the complex in absence of INO80, suggesting that Arp8p can have a function in absence of INO80 (Shen et al., 2003a). The two other *Arabidopsis ino80* alleles do not show altered expression of the *ARP8* gene candidate. Perhaps the increased developmental phenotype seen in these alleles is not solely due to misregulation of *At3g57290* (translation initiation factor, see Chapter 2) but would also represent a stronger *ino80* specific phenotype because it would not be compensated.

I have shown that the *Arabidopsis* genome encodes potential orthologs of all ARP and RVB of the yeast INO80 complex. Together with the results presented for the corresponding genes, this suggests the existence of an *Arabidopsis* INO80 complex similar to that of yeast. Alternatively, it can well be that the plant INO80 complex contains

additional or different proteins. These proteins may be responsible for the specific function of the plant INO80.

5) Contribution of an AtINO80 complex to DSB repair

The preferred target for the *Arabidopsis* INO80 is HR whereas yeast INO80 seems to be involved in illegitimate recombination (because yino80 is hypersensitive to DSB inducing agents. At least two explanations may be offered: (i) INO80 has a different repair function in yeast and *Arabidopsis*, i.e. NHEJ and HR, repectively, or (ii) INO80 acts at DSB independently of the subsequent repair pathway used, that is, in an early step of DSB processing. In both cases, the INO80 complex is likely to be recruited to its site of action through an as yet unknown mechanism. One possibility would be that INO80 or the INO80 complex recognizes special marks at damaged loci, especially since a SWI/SNF ATPase INO80 is likely to be involved in chromatin rearrangements at the damaged locus rather than directly in the enzymatic steps of HR.

The presence of the RuvB helicase homologs RVB1 and RVB2 in the yINO80 complex suggests a potential direct involvement of INO80 in the migration of Holliday junctions, as the prokaryotic RuvB is directly involved in this process (see General Introduction). However, recent studies in this field disfavor such hypothesis. Indeed, eukaryotic organisms seem to have evolved complex mechanisms for the resolution of Holliday junctions, involving proteins like RAD51C in mammals, XPF in *Drosophila* and Mus81p in fission yeast (Heyer et al., 2003; Hollingsworth and Brill, 2004; Liu et al., 2004). Further, the size of the fraction containing the resolution activity isolated from mammalian cells precludes the involvement of RVB like proteins (Constantinou et al., 2001; Heyer et al., 2003). Finally, none of studies on RVB function have revealed such a role, although a large number of functions have been described (see above).

DNA double-strand breaks (DSBs) are generally accepted to be the most biologically significant lesion by which ionizing radiation causes cancer and hereditary disease. The response of eukaryotic cells to DSBs in genomic DNA includes the sequestration of many factors into nuclear foci that will influence the choice of the repair pathway crucial for genome integrity and evolution (see General Introduction). In higher eukaryotes HR-mediated repair is rare compared to NHEJ mediated repair, but the preference for NHEJ or HR may also depend on the phase of the cell cycle (see General Introduction and Paques and Haber, 1999; Britt and May, 2003). Very little is known on what influences the choice of the pathway taken, but chromatin structure at the site of a lesion likely will play a major

role in the recruitment of repair enzymes and thereby the choice of repair pathway.

Until very recently, the events leading to the processing of DSBs and the determination of the repair pathway used remained a black box in DNA repair. The discovery of a precocious step of phosphorylation and acetylation of chromatin at DNA breaks sheds light on this missing link. Upon DNA damage, a histone H2A variant, H2AX, becomes extensively phosphorylated within 1–3 minutes and forms foci at break sites. A number of studies have shown that this is an evolutionarily conserved cellular response to DSB (Modesti and Kanaar, 2001; Redon et al., 2002). In yeast, the phosphorylation of the standard H2A (HTA1 and HTA2) replaces H2AX phosphorylation (Wyatt et al., 2003). DNA damage induced phosphorylated H2AX (γ-H2AX) foci colocalize with repair factors like RAD50 and RAD51 or the tumor suppressor protein BRCA1 in mammals. NFBD1, a nuclear protein containing a forkhead-associated motif and two BRCT motifs forms nuclear foci that also colocalize with γ-H2AX (Shang et al., 2003; Xu and Stern, 2003), suggesting that DSB repair is accompanied by changes in chromatin structure. Further, the use of wortmannin, an inhibitor of the phosphoinositide-3 family of protein kinases abolishes the formation of these foci, suggesting these kinases mediate the response (Paull et al., 2000).

There is evidence that foci of γ-H2AX quantitatively correspond to DSBs and can thus allow the quantification of the repair of individual DSBs (Rothkamm and Lobrich, 2003). This allowed the investigation of DSB repair after low radiation doses (1 mGy) in nondividing primary human fibroblasts, and revealed that some DSBs remain unrepaired for many days, in strong contrast to the efficient DSB repair at higher doses (Rothkamm and Lobrich, 2003). γ-H2AX may not constitute the primary or only signal required for the redistribution of repair complexes to damaged chromatin, but may function to concentrate proteins at DNA lesions (Celeste et al., 2003). Another important signal in this context might be acetylation of histone H4 lysine-16 that occur early aftert DSBs are created and is mediated by Sin3p in yeast (Jazayeri et al., 2004). It is very tempting to speculate that the INO80 complex recognizes such histone marks and contributes to repair by modifying chromatin at damaged chromosomal sites.

Despite the evidence of H2AX phosphorylation and histone acetylation events in the precocious processing of DSBs in many organisms, none of these modifications were so far reported in plants. I indeed did find two potential H2A variants with the H2AX specific C-terminal motif (Redon et al., 2002) in the *Arabidopsis* genome, but no further information is available on them. This renders the hypothesis of INO80 recruitment by

such marks difficult to address in plants. In addition, plants lack a system allowing analysis of recruitment of factors like INO80 to DSBs. However, in a recent review, a study showing that the yeast INO80 complex is recruited to DSBs, supports this model (Peterson and Cote, 2004). Interestingly, the same review mentioned evidence for the recruitment of another SWI/SNF complex, SWR1, at DSBs, suggesting that multiple chromatin remodeling events are at work, either in a concerted manner or directing specific repair machines towards particular kinds of damage or to particular broken chromosomal sites.

The information on the dual role of *Arabidopsis* INO80 suggests a schematic working model for the INO80 function (Fig. 56). The putative *Arabidopsis* INO80 complex would act as chromatin remodeler that activates or represses transcription of a subset of genes. After a DSB is created, it is processed and the region of the break is progressively marked with histone modifications like H2AX phosphorylation. This may facilitate repair by the major DSB repair pathway (NHEJ in most cases in *Arabidopsis*) and, in parallel, promote the recruitment of chromatin remodeling complexes like the INO80 complex to the damaged region. The chromatin remodeling activity of the INO80 complex would then favor repair of the DSB by the minor pathway (HR in most cases in *Arabidopsis*). The necessity of an active recruitment of INO80 to the damaged region remains to be tested.

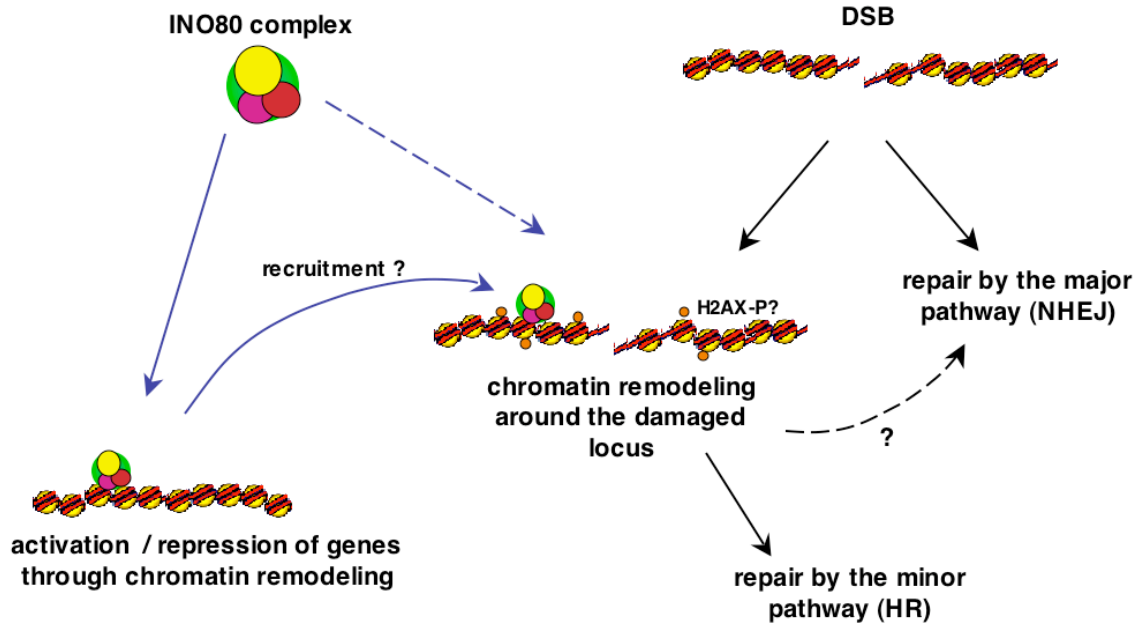

Figure 56. Working model for INO80 function in *Arabidopsis*. The duality of INO80 function in transcription and DNA repair is represented. In *Arabidopsis* no equivalent of phosphorylated histone H2AX (H2AX-P) was shown so far. DSB, DNA double-strand break; NHEJ, non-homologous end-joining; HR, homologous recombination.

6) Gene targeting in plants; a possible contribution from this work

The precise manipulation of the genome of higher plants is still a major challenge. Some advances have been made recently for the creation of point mutations at predetermined positions by chimeric RNA/DNA oligonucleotides (Hohn and Puchta, 1999; Zhu et al., 1999). However, the targeted insertion of longer stretches of DNA sequence at any desired location (knock-in) or the replacement of predetermined plant genomic sequences by heterologous DNA (knock-out) via HR is at present not possible as a routine technique (Hanin and Paszkowski, 2003). Since the original successful HR directed gene targeting event in plant was reported (Paszkowski et al., 1988), only a few studies have appeared in the literature that describe successful gene targeting in higher plants (Lee et al., 1990; Offringa et al., 1990; Miao and Lam, 1995). In all cases the numbers of targeted events were very low; with 10^{-3} to 10^{-5} desired events compared to illegitimate integration events gene targeting remains a major exercise (Hohn and Puchta, 1999; Mengiste and Paszkowski, 1999). In mammals, gene targeting applied to mouse embryonic stem (ES) cells is now a routine technique for the study of gene function, mostly used to generate knockout mice. However, the development of HR mediated gene targeting in human ES cells was only recently established with the use of an electroporation approach (Zwaka and Thomson, 2003).

Positive-negative selection and extension of the region of sequence homology failed in increasing the low relative frequency of gene targeting (Thykjaer et al., 1997; Gallego et al., 1999). One promising strategy to facilitate gene targeting in higher plants would be to shift the balance between illegitimate and HR events towards the latter, by facilitating HR events in plants by genetic manipulation. Another strategy in plants, is to express heterologous proteins known to be involved in HR. Overproduction of the bacterial resolvase RuvC was shown to increase somatic inter-and intrachromosomal recombination, as well as extrachromosomal recombination (Shalev et al., 1999), but no gene targeting studies were reported yet with this system. Expression of the bacterial RecA protein had similar effects (Reiss et al., 1996), but subsequent experiments did not show an increase of gene targeting events (Reiss et al., 2000). One problem in plants may come from the preferential use of the synthesis dependent strand annealing SDSA mechanism (see General Introduction) for recombinational repair of DSBs over the classical DSB repair mechanism (Ray and Langer, 2002). Recently a reliable system to

detect gene targeting events in *Arabidopsis* was developed using an endogenous gene encoding the protoporphyrinogen oxidase (PPO), involved in chlorophyll and heme syntheses with a highly stringent selection procedure. Although the frequency of targeted events was not higher than reported previously, one third of selected events were due to true gene targeting, which makes it a system of choice to evaluate the frequency of gene targeting events (Hanin et al., 2001).

Besides improvements to the gene targeting technique itself, i.e. homology, selection, delivery and developmental stage used (reviewed in Puchta, 2002; Hanin and Paszkowski, 2003), the combined use of plant components that influence and/or control HR levels may help to increase the gene targeting efficiency. For instance, genes isolated from such genetic screen as the one described in this work, could be tested for their influence on homology directed gene targeting efficiency in the PPO system developed by Hanin et al. This could be achieved by manipulating the endogenous level of these genes either in a stable situation by the use of mutants, overexpressing plants or RNAi plants, or transciently by providing in *cis* RNAi or overexpression constructs. Alternatively, HR promoting factors could be provided together with the gene targeting construct.

In the case of INO80, we need to test first whether increased *INO80* expression levels would increase HR levels, and only then the gene targeting frequency could be analyzed. However, so far INO80 overexpression in plants did not yield plants with increased levels of the desired mRNA.

7) Conclusion and experimental perspectives

As a prolongation of this work, I would design experimental approaches to address the following points.

- Concerning the screen, I would design a further genetic screen for HR mutants using the lessons from the one described in this thesis (see above). It is indeed on the basis of this first screen that J. Molinier designed a successful activation tagging based genetic screen for mutants intermolecular HR (Fritsch, O., Molinier, J., Schuermann D., Lucht, J., Ries, G. and Hohn, B. Identification of new plant factors involved in homologous recombination by direct genetic screens, manuscript in preparation, and Molinier et al., 2004b)

- I found it disappointing that no plants overexpressing INO80 were recovered in overexpression experiments. I propose (i) to overexpress a tagged version of INO80 in an

ino80 mutant background, to discriminate between expression and overexpression problems and (ii) to overcome the potential deleterious effect of ectopically elevated INO80 levels by the use of an inducible promoter.

- I will devote important efforts to unravel the composition of the *Arabidopsis* INO80 complex. For this I will try either to immunoprecipitate the complex from ino80 mutants complemented with tagged versions of INO80 or look for potential interaction *in vitro* using proteins expressed in yeast, *E. coli* or in an *in vitro* translation and transcription coupled system.

- To further investigate the so far contrasting specificities of plant and yeast INO80 for DNA repair, I will compare yeast and *Arabidopsis* INO80 function by combining transcriptome analysis, genotoxic stress response and DNA repair assays. In the same context and with similar experimental approaches, I will consider the contribution of ARP8 to the INO80 function in *Arabidopsis* (using RNAi and mutants) and compare it with yeast, as my data suggest a possible connection/cooperation between ARP8 and INO80 function (see the potential contribution of the *Arabidopsis* ARP8 to the *ino80* phenotype).

- Finally, I will be interested to look how the observed differences between yeast and *Arabidopsis* INO80 function in repair correlate with the potential mechanism of recruitment of INO80 to DSB in both organisms. This can be achieved by ChIP (chromatin immunoprecipitation) methods combined with a chromosomal break assay, but will require anti-INO80 antibodies or plants with tagged versions of INO80.

References

Agalioti, T., Lomvardas, S., Parekh, B., Yie, J., Maniatis, T., and Thanos, D. (2000). Ordered recruitment of chromatin modifying and general transcription factors to the IFN-beta promoter. Cell **103,** 667-678.

Alexiadis, V., and Kadonaga, J.T. (2002). Strand pairing by Rad54 and Rad51 is enhanced by chromatin. Genes Dev **16,** 2767-2771.

Amedeo, P., Habu, Y., Afsar, K., Mittelsten Scheid, O., and Paszkowski, J. (2000). Disruption of the plant gene *MOM* releases transcriptional silencing of methylated genes. Nature **405,** 203-206.

van Attikum, H., Bundock, P., and Hooykaas, P.J. (2001). Non-homologous end-joining proteins are required for Agrobacterium T-DNA integration. Embo J **20,** 6550-6558.

van Attikum, H., Bundock, P., Overmeer, R.M., Lee, L.Y., Gelvin, S.B., and Hooykaas, P.J. (2003). The Arabidopsis AtLIG4 gene is required for the repair of DNA damage, but not for the integration of Agrobacterium T-DNA. Nucleic Acids Res **31,** 4247-4255.

Baker, B.S., Carpenter, A.T., Esposito, M.S., Esposito, R.E., and Sandler, L. (1976a). The genetic control of meiosis. Annu Rev Genet **10,** 53-134.

Baker, B.S., Boyd, J.B., Carpenter, A.T., Green, M.M., Nguyen, T.D., Ripoll, P., and Smith, P.D. (1976b). Genetic controls of meiotic recombination and somatic DNA metabolism in *Drosophila melanogaster*. Proc Natl Acad Sci U S A **73,** 4140-4144.

Bakkenist, C.J., and Kastan, M.B. (2003). DNA damage activates ATM through intermolecular autophosphorylation and dimer dissociation. Nature **421,** 499-506.

Bauer, A., Huber, O., and Kemler, R. (1998). Pontin52, an interaction partner of beta-catenin, binds to the TATA box binding protein. Proc Natl Acad Sci U S A **95,** 14787-14792.

Bauer, A., Chauvet, S., Huber, O., Usseglio, F., Rothbacher, U., Aragnol, D., Kemler, R., and Pradel, J. (2000). Pontin52 and reptin52 function as antagonistic regulators of beta-catenin signalling activity. Embo J **19,** 6121-6130.

Bennett, C.B., Westmoreland, T.J., Snipe, J.R., and Resnick, M.A. (1996). A double-strand break within a yeast artificial chromosome (YAC) containing human DNA can result in YAC loss, deletion or cell lethality. Mol Cell Biol **16,** 4414-4425.

Benvenuto, G., Formiggini, F., Laflamme, P., Malakhov, M., and Bowler, C. (2002). The photomorphogenesis regulator DET1 binds the amino-terminal tail of histone H2B in a nucleosome context. Curr Biol **12,** 1529-1534.

Berger, F., and Gaudin, V. (2003). Chromatin dynamics and *Arabidopsis* development. Chromosome Res **11,** 277-304.

Bernstein, B.E., Tong, J.K., and Schreiber, S.L. (2000). Genomewide studies of histone deacetylase function in yeast. Proc Natl Acad Sci U S A **97,** 13708-13713.

Bilang, R., Peterhans, A., Bogucki, A., and Paszkowski, J. (1992). Single-stranded DNA as a recombination substrate in plants as assessed by stable and transient recombination assays. Mol Cell Biol **12,** 329-336.

Birger, Y., West, K.L., Postnikov, Y.V., Lim, J.H., Furusawa, T., Wagner, J.P., Laufer, C.S., Kraemer, K.H., and Bustin, M. (2003). Chromosomal protein HMGN1 enhances the rate of DNA repair in chromatin. Embo J **22,** 1665-1675.

Blanc, G., Barakat, A., Guyot, R., Cooke, R., and Delseny, M. (2000). Extensive duplication and reshuffling in the Arabidopsis genome. Plant Cell **12,** 1093-1101.

Bleuyard, J.Y., and White, C.I. (2004). The Arabidopsis homologue of Xrcc3 plays an essential role in meiosis. Embo J **23,** 439-449.

Borevitz, J.O., Xia, Y., Blount, J., Dixon, R.A., and Lamb, C. (2000). Activation tagging identifies a conserved MYB regulator of phenylpropanoid biosynthesis. Plant Cell **12,** 2383-2394.

Boyer, L.A., and Peterson, C.L. (2000). Actin-related proteins (Arps): conformational switches for chromatin-remodeling machines? Bioessays **22,** 666-672.

Britt, A.B., and May, G.D. (2003). Re-engineering plant gene targeting. Trends Plant Sci **8,** 90-95.

Brzeski, J., and Jerzmanowski, A. (2003). Deficient in DNA methylation 1 (DDM1) defines a novel family of chromatin-remodeling factors. J Biol Chem **278,** 823-828.

Bucheli, M., Lommel, L., and Sweder, K. (2001). The defect in transcription-coupled repair displayed by a Saccharomyces cerevisiae rad26 mutant is dependent on carbon source and is not associated with a lack of transcription. Genetics **158,** 989-997.

Bundock, P., and Hooykaas, P. (2002). Severe developmental defects, hypersensitivity to DNA-damaging agents, and lengthened telomeres in Arabidopsis MRE11 mutants. Plant Cell **14,** 2451-2462.

Bundock, P., van Attikum, H., and Hooykaas, P. (2002). Increased telomere length and hypersensitivity to DNA damaging agents in an Arabidopsis KU70 mutant. Nucleic Acids Res **30,** 3395-3400.

Burk, L.G., and Menser, H.A. (1964). A dominant *aurea* mutation in tobacco. Tob. Sci. **8,** 101-104.

Cao, X., Springer, N.M., Muszynski, M.G., Phillips, R.L., Kaeppler, S., and Jacobsen, S.E. (2000). Conserved plant genes with similarity to mammalian de novo DNA methyltransferases. PNAS **97,** 4979-4984.

Carrozza, M.J., Utley, R.T., Workman, J.L., and Cote, J. (2003). The diverse functions of histone acetyltransferase complexes. Trends Genet **19,** 321-329.

Celeste, A., Fernandez-Capetillo, O., Kruhlak, M.J., Pilch, D.R., Staudt, D.W., Lee, A., Bonner, R.F., Bonner, W.M., and Nussenzweig, A. (2003). Histone H2AX phosphorylation is dispensable for the initial recognition of DNA breaks. Nat Cell Biol **5,** 675-679.

Chalfun-Junior, A., Mes, J.J., Mlynarova, L., Aarts, M.G., and Angenent, G.C. (2003). Low frequency of T-DNA based activation tagging in Arabidopsis is correlated with methylation of CaMV 35S enhancer sequences. FEBS Lett **555,** 459-463.

Cho, S.G., Bhoumik, A., Broday, L., Ivanov, V., Rosenstein, B., and Ronai, Z. (2001). TIP49b, a regulator of activating transcription factor 2 response to stress and DNA damage. Mol Cell Biol **21,** 8398-8413.

Christianson, M.L. (1975). Mitotic crossing-over as an important mechanism of floral sectoring in *Tradescantia*. Mutation Research **28,** 389- 395.

Clarke, L., and Carbon, J. (1979). Methods Enzymol **68,** 396 ff.

Clikeman, J.A., Khalsa, G.J., Barton, S.L., and Nickoloff, J.A. (2001). Homologous recombinational repair of double-strand breaks in yeast is enhanced by MAT heterozygosity through yKU-dependent and -independent mechanisms. Genetics **157,** 579-589.

Conklin, P.L., Williams, E.H., and Last, R.L. (1996). Environmental stress sensitivity of an ascorbic acid-deficient Arabidopsis†mutant. PNAS **93,** 9970-9974.

Constantinou, A., Davies, A.A., and West, S.C. (2001). Branch migration and Holliday junction resolution catalyzed by activities from mammalian cells. Cell **104,** 259-268.

Constantinou, A., Chen, X.B., McGowan, C., and West, S.C. (2002). Holliday junction resolvases in human cells: two activities with distinct substrate specificities. Embo J **21,** 5577-5585.

Cosma, N.P., Tanaka, T., and Nasmyth, K. (1999). Ordered recruitment of transcription and chromatin remodeling factors to a cell-cycle and developmentally regulated promoter. Cell **97,** 299-311.

Costa, R.M., Morgante, P.G., Berra, C.M., Nakabashi, M., Bruneau, D., Bouchez, D., Sweder, K.S., Van Sluys, M.A., and Menck, C.F. (2001). The participation of AtXPB1, the XPB/RAD25 homologue gene from Arabidopsis thaliana, in DNA repair and plant development. Plant J **28,** 385-395.

Culligan, K., Tissier, A., and Britt, A. (2004). ATR Regulates a G2-Phase Cell-Cycle Checkpoint in Arabidopsis thaliana. Plant Cell.

Culligan, K.M., and Hays, J.B. (1997). DNA mismatch repair in plants - an *Arabidopsis thaliana* gene that predicts a protein belonging to the MSH2 subfamily of eukaryotic MutS homologs. Plant Physiol **115,** 833-839.

Culligan, K.M., and Hays, J.B. (2000). *Arabidopsis* MutS homologs-AtMSH2, AtMSH3, AtMSH6, and a novel AtMSH7-form three distinct protein heterodimers with different specificities for mismatched DNA. Plant Cell **12,** 991-1002.

Daoudal-Cotterell, S., Gallego, M.E., and White, C.I. (2002). The plant Rad50-Mre11 protein complex. FEBS Lett **516,** 164-166.

van der Graaff, E., Dulk-Ras, A.D., Hooykaas, P.J., and Keller, B. (2000). Activation tagging of the LEAFY PETIOLE gene affects leaf petiole development in Arabidopsis thaliana. Development **127,** 4971-4980.

Desfeux, C., Clough, S.J., and Bent, A.F. (2000). Female reproductive tissues are the primary target of Agrobacterium-mediated transformation by the Arabidopsis floral-dip method. Plant Physiol **123,** 895-904.

Dilworth, F.J., Fromental-Ramain, C., Yamamoto, K., and Chambon, P. (2000). ATP-driven chromatin remodeling activity and histone acetyltransferases act sequentially during transactivation by RAR/RXR *in vitro*. Mol Cell **6,** 1049-1058.

Doutriaux, M.P., Couteau, F., Bergounioux, C., and White, C.I. (1998). Isolation and characterization of the RAD51 and DMC1 homologs from Arabidopsis thaliana. Mol Gen Genet **257,** 283-291.

Downs, J.A., Lowndes, N.F., and Jackson, S.P. (2000). A role for *Saccharomyces cerevisiae* histone H2A in DNA repair. Nature **408,** 1001-1004.

Downs, J.A., Kosmidou, E., Morgan, A., and Jackson, S.P. (2003). Suppression of homologous recombination by the Saccharomyces cerevisiae linker histone. Mol Cell **11,** 1685-1692.

Dubest, S., Gallego, M.E., and White, C.I. (2002). Role of the AtRad1p endonuclease in homologous recombination in plants. EMBO Rep **3,** 1049-1054.

Ebbert, R., Birkmann, A., and Schuller, H.J. (1999). The product of the *SNF2/SWI2* paralogue *INO80* of *Saccharomyces cerevisiae* required for efficient expression of various yeast structural genes is part of a high-molecular-weight protein complex. Mol Microbiol **32,** 741-751.

Ellis, J., Dodds, P., and Pryor, T. (2000). Structure, function and evolution of plant disease resistance genes. Curr Opin Plant Biol **3,** 278-284.

Evans, E., and Alani, E. (2000). Roles for mismatch repair factors in regulating genetic recombination. Mol Cell Biol **20,** 7839-7844.

Ferrando, A., Koncz-Kalman, Z., Farras, R., Tiburcio, A., Schell, J., and Koncz, C. (2001). Detection of in vivo protein interactions between Snf1-related kinase subunits with intron-tagged epitope-labelling in plants cells. Nucl. Acids. Res. **29,** 3685-3693.

Fidantsef, A.L., Mitchell, D.L., and Britt, A.B. (2000). The Arabidopsis UVH1 gene is a homolog of the yeast repair endonuclease RAD1. Plant Physiol **124,** 579-586.

Filkowski, J., Kovalchuk, O., and Kovalchuk, I. (2004). Genome stability of vtc1, tt4, and tt5 Arabidopsis thaliana mutants impaired in protection against oxidative stress. Plant J **38,** 60-69.

Fischle, W., Wang, Y., and Allis, C.D. (2003). Histone and chromatin cross-talk. Curr Opin Cell Biol **15,** 172-183.

Flanary, P.L., DiBello, P.R., Estrada, P., and Dohlman, H.G. (2000). Functional analysis of Plp1 and Plp2, two homologues of Phosducin in yeast. J Biol Chem **275,** 18462-18469.

Friedberg, E.C. (2003). DNA damage and repair. Nature **421,** 436-440.

Friesner, J., and Britt, A.B. (2003). Ku80- and DNA ligase IV-deficient plants are sensitive to ionizing radiation and defective in T-DNA integration. Plant J **34,** 427-440.

Fritsch, O., Hohn, B., Kovalchuk, I., and Kovalchuk, O. (2000). Des bio-indicateurs de pollution radioactive [Bioindicators of radioactive pollution]. Biofutur **205,** 48-51.

Frohnmeyer, H., and Staiger, D. (2003). Ultraviolet-B Radiation-Mediated Responses in Plants. Balancing Damage and Protection. Plant Physiol. **133,** 1420-1428.

Fyodorov, D.V., and Kadonaga, J.T. (2001). The many faces of chromatin remodeling: SWItching beyond transcription. Cell **106,** 523-525.

Gallego, F., Fleck, O., Li, A., Wyrzykowska, J., and Tinland, B. (2000). AtRAD1, a plant homologue of human and yeast nucleotide excision repair endonucleases, is involved in dark repair of UV damages and recombination. Plant J **21,** 507-518.

Gallego, M.E., and White, C.I. (2001). RAD50 function is essential for telomere maintenance in Arabidopsis. Proc Natl Acad Sci U S A **98,** 1711-1716.

Gallego, M.E., Sirand-Pugnet, P., and White, C.I. (1999). Positive-negative selection and T-DNA stability in Arabidopsis transformation. Plant Mol Biol **39,** 83-93.

Gallego, M.E., Bleuyard, J.Y., Daoudal-Cotterell, S., Jallut, N., and White, C.I. (2003). Ku80 plays a role in non-homologous recombination but is not required for T-DNA integration in Arabidopsis. Plant J **35,** 557-565.

Gallego, M.E., Jeanneau, M., Granier, F., Bouchez, D., Bechtold, N., and White, C.I. (2001). Disruption of the Arabidopsis RAD50 gene leads to plant sterility and MMS sensitivity. Plant J **25,** 31-41.

Ganal, M.W., and Tanksley, S.D. (1996). Theor Appl Genet **92,** 101-108.

Garcia, V., Salanoubat, M., Choisne, N., and Tissier, A. (2000). An *ATM* homologue from *Arabidopsis thaliana*: complete genomic organisation and expression analysis. Nucleic Acids Res **28,** 1692-1699.

Garcia, V., Bruchet, H., Camescasse, D., Granier, F., Bouchez, D., and Tissier, A. (2003). AtATM is essential for meiosis and the somatic response to DNA damage in plants. Plant Cell **15,** 119-132.

Garcia-Ortiz, M.V., Ariza, R.R., and Roldan-Arjona, T. (2001). An OGG1 orthologue encoding a functional 8-oxoguanine DNA glycosylase/lyase in Arabidopsis thaliana. Plant Mol Biol **47,** 795-804.

Garcia-Rubio, M., Huertas, P., Gonzalez-Barrera, S., and Aguilera, A. (2003). Recombinogenic effects of DNA-damaging agents are synergistically increased by transcription in *Saccharomyces cerevisiae*. New insights into transcription-associated recombination. Genetics **165,** 457-466.

Genschik, P., Marbach, J., Uze, M., Feuerman, M., Plesse, B., and Fleck, J. (1994). Structure and promoter activity of a stress and developmentally regulated polyubiquitin-encoding gene of Nicotiana tabacum. Gene **148,** 195-202.

Gherbi, H., Gallego, M.E., Jalut, N., Lucht, J.M., Hohn, B., and White, C.I. (2001). Homologous recombination in planta is stimulated in the absence of Rad50. EMBO Rep **2,** 287-291.

Gohshi, T., Shimada, M., Kawahire, S., Imai, N., Ichimura, T., Omata, S., and Horigome, T. (1999). Molecular cloning of mouse p47, a second group mammalian RuvB DNA helicase-like protein: homology with those from human and Saccharomyces cerevisiae. J Biochem (Tokyo) **125,** 939-946.

Gong, Z., Morales-Ruiz, T., Ariza, R.R., Roldan-Arjona, T., David, L., and Zhu, J.K. (2002). ROS1, a repressor of transcriptional gene silencing in Arabidopsis, encodes a DNA glycosylase/lyase. Cell **111,** 803-814.

Gontijo, A.M.d.M.C., Green, C.M., and Almouzni, G. (2003). Repairing DNA damage in chromatin. Biochimie **85,** 1133-1147.

Gonzalez-Barrera, S., Garcia-Rubio, M., and Aguilera, A. (2002). Transcription and double-strand breaks induce similar mitotic recombination events in *Saccharomyces cerevisiae*. Genetics **162,** 603-614.

Goodall, G.J., and Filipowicz, W. (1989). The AU-rich sequences present in the introns of plant nuclear pre-mRNAs are required for splicing. Cell **58,** 473-483.

Goodall, G.J., and Filipowicz, W. (1991). Different effects of intron nucleotide composition and secondary structure on pre-mRNA splicing in monocot and dicot plants. Embo J **10,** 2635-2644.

van Gool, A.J., Verhage, R., Swagemakers, S.M., van de Putte, P., Brouwer, J., Troelstra, C., Bootsma, D., and Hoeijmakers, J.H. (1994). RAD26, the functional S. cerevisiae homolog of the Cockayne syndrome B gene ERCC6. Embo J **13,** 5361-5369.

Gorbunova, V., Avivi-Ragolski, N., Shalev, G., Kovalchuk, I., Abbo, S., Hohn, B., and Levy, A.A. (2000). A new hyperrecombinogenic mutant of *Nicotiana tabacum*. Plant J **24,** 601-611.

Green, C.M., and Almouzni, G. (2002). When repair meets chromatin. First in series on chromatin dynamics. EMBO Rep **3,** 28-33.

Green, C.M., and Almouzni, G. (2003). Local action of the chromatin assembly factor CAF-1 at sites of nucleotide excision repair in vivo. Embo J **22,** 5163-5174.

Grelon, M., Vezon, D., Gendrot, G., and Pelletier, G. (2001). AtSPO11-1 is necessary for efficient meiotic recombination in plants. Embo J **20,** 589-600.

Grelon, M., Gendrot, G., Vezon, D., Pelletier, G., Mathilde, G., Ghislaine, G., Daniel, V., and Georges, P. (2003). The Arabidopsis MEI1 gene encodes a protein with five BRCT domains that is involved in meiosis-specific DNA repair events independent of SPO11-induced DSBs. Plant J **35,** 465-475.

Grune, T., Brzeski, J., Eberharter, A., Clapier, C.R., Corona, D.F., Becker, P.B., and Muller, C.W. (2003). Crystal structure and functional analysis of a nucleosome recognition module of the remodeling factor ISWI. Mol Cell **12,** 449-460.

Hajdukiewicz, P., Svab, Z., and Maliga, P. (1994). The small, versatile pPZP family of Agrobacterium binary vectors for plant transformation. Plant Mol Biol **25,** 989-994.

Hall, M.C., and Matson, S.W. (1999). Helicase motifs: the engine that powers DNA unwinding. Mol Microbiol **34,** 867-877.

Hanahan, D. (1983). Studies on transformation of *Escherichia coli* with plasmids. J Mol Biol **166,** 557-580.

Hanin, M., and Paszkowski, J. (2003). Plant genome modification by homologous recombination. Curr Opin Plant Biol **6,** 157-162.

Hanin, M., Mengiste, T., Bogucki, A., and Paszkowski, J. (2000). Elevated levels of intrachromosomal homologous recombination in Arabidopsis overexpressing the MIM gene. Plant J **24,** 183-189.

Hanin, M., Volrath, S., Bogucki, A., Briker, M., Ward, E., and Paszkowski, J. (2001). Gene targeting in Arabidopsis. Plant J **28,** 671-677.

Hara, R., and Sancar, A. (2002). The SWI/SNF chromatin-remodeling factor stimulates repair by human excision nuclease in the mononucleosome core particle. Mol Cell Biol **22,** 6779-6787.

Harata, M., Oma, Y., Mizuno, S., Jiang, Y.W., Stillman, D.J., and Wintersberger, U. (1999). The nuclear actin-related protein of Saccharomyces cerevisiae, Act3p/Arp4, interacts with core histones. Mol Biol Cell **10,** 2595-2605.

Hartung, F., Plchova, H., and Puchta, H. (2000). Molecular characterisation of RecQ homologues in Arabidopsis thaliana. Nucleic Acids Res **28,** 4275-4282.

Hartung, F., Angelis, K.J., Meister, A., Schubert, I., Melzer, M., and Puchta, H. (2002). An archaebacterial topoisomerase homolog not present in other eukaryotes is indispensable for cell proliferation of plants. Curr Biol **12,** 1787-1791.

Hassan, A.H., Neely, K.E., and Workman, J.L. (2001). Histone acetyltransferase complexes stabilize swi/snf binding to promoter nucleosomes. Cell **104,** 817-827.

Hassan, A.H., Prochasson, P., Neely, K.E., Galasinski, S.C., Chandy, M., Carrozza, M.J., and Workman, J.L. (2002). Function and selectivity of bromodomains in anchoring chromatin-modifying complexes to promoter nucleosomes. Cell **111,** 369-379.

Hays, J.B. (2002). *Arabidopsis thaliana*, a versatile model system for study of eukaryotic genome-maintenance functions. DNA Repair (Amst) **1,** 579-600.

Hefner, E., Preuss, S.B., and Britt, A.B. (2003). Arabidopsis mutants sensitive to gamma radiation include the homologue of the human repair gene ERCC1. J Exp Bot **54,** 669-680.

Henderson, J.T., Li, H.-C., Rider, S.D., Mordhorst, A.P., Romero-Severson, J., Cheng, J.-C., Robey, J., Sung, Z.R., de Vries, S.C., and Ogas, J. (2004). PICKLE Acts throughout the Plant to Repress Expression of Embryonic Traits and May Play a Role in Gibberellin-Dependent Responses. Plant Physiol. **134,** 995-1005.

Henry, K.W., Wyce, A., Lo, W.S., Duggan, L.J., Emre, N.C., Kao, C.F., Pillus, L., Shilatifard, A., Osley, M.A., and Berger, S.L. (2003). Transcriptional activation via sequential histone H2B ubiquitylation and deubiquitylation, mediated by SAGA-associated Ubp8. Genes Dev **17,** 2648-2663.

Heyer, W.D., Ehmsen, K.T., and Solinger, J.A. (2003). Holliday junctions in the eukaryotic nucleus: resolution in sight? Trends Biochem Sci **28,** 548-557.

Heyl, A., and Schmulling, T. (2003). Cytokinin signal perception and transduction. Curr Opin Plant Biol **6,** 480-488.

Hirano, T. (1999). SMC-mediated chromosome mechanics: a conserved scheme from bacteria to vertebrates? Genes Dev **13,** 11-19.

Hoeijmakers, J.H. (2001). Genome maintenance mechanisms for preventing cancer. Nature **411,** 366-374.

Hofgen, R., and Willmitzer, L. (1988). Storage of competent cells for Agrobacterium transformation. Nucleic Acids Res **16,** 9877.

Hohn, B., and Puchta, H. (1999). Gene therapy in plants. Proc Natl Acad Sci U S A **96,** 8321-8323.

Hollingsworth, N.M., and Brill, S.J. (2004). The Mus81 solution to resolution: generating meiotic crossovers without Holliday junctions. Genes Dev. **18,** 117-125.

Huang, S., Cerny, R.E., Bhat, D.S., and Brown, S.M. (2001). Cloning of an Arabidopsis patatin-like gene, STURDY, by activation T-DNA tagging. Plant Physiol **125,** 573-584.

Iizuka, M., and Smith, M.M. (2003). Functional consequences of histone modifications. Curr Opin Genet Dev **13,** 154-160.

Ikura, T., Ogryzko, V.V., Grigoriev, M., Groisman, R., Wang, J., Horikoshi, M., Scully, R., Qin, J., and Nakatani, Y. (2000). Involvement of the TIP60 histone acetylase complex in DNA repair and apoptosis. Cell **102,** 463-473.

Ira, G., Malkova, A., Liberi, G., Foiani, M., and Haber, J.E. (2003). Srs2 and Sgs1-Top3 suppress crossovers during double-strand break repair in yeast. Cell **115,** 401-411.

Ito, T. (2003). Nucleosome assembly and remodeling. Curr Top Microbiol Immunol **274,** 1-22.

Jackson, J.P., Lindroth, A.M., Cao, X., and Jacobsen, S.E. (2002). Control of CpNpG DNA methylation by the KRYPTONITE histone H3 methyltransferase. Nature **416,** 556-560.

Jacobs, S.A., Taverna, S.D., Zhang, Y., Briggs, S.D., Li, J., Eissenberg, J.C., Allis, C.D., and Khorasanizadeh, S. (2001). Specificity of the HP1 chromodomain for the methylated N-terminus of histone H3. Embo J **20,** 5232-5241.

Jansen, M., Gaba V., Greenberg BM. (1998). Higher plants and UV-B radiation: balancing damage, repair and acclimation. trends in plant science **3,** 131-135.

Jazayeri, A., McAinsh, A.D., and Jackson, S.P. (2004). Saccharomyces cerevisiae Sin3p facilitates DNA double-strand break repair. PNAS **101,** 1644-1649.

Jeddeloh, J.A., Stokes, T.L., and Richards, E.J. (1999). Maintenance of genomic methylation requires a SWI2/SNF2-like protein. Nat Genet **22,** 94-97.

Jelesko, J.G., Harper, R., Furuya, M., and Gruissem, W. (1999). Rare germinal unequal crossing-over leading to recombinant gene formation and gene duplication in Arabidopsis thaliana. Proc Natl Acad Sci U S A **96,** 10302-10307.

Jelinsky, S.A., and Samson, L.D. (1999). Global response of Saccharomyces cerevisiae to an alkylating agent. Proc Natl Acad Sci U S A **96,** 1486-1491.

Jin, H., Cominelli, E., Bailey, P., Parr, A., Mehrtens, F., Jones, J., Tonelli, C., Weisshaar, B., and Martin, C. (2000). Transcriptional repression by AtMYB4 controls production of UV-protecting sunscreens in Arabidopsis. Embo J **19,** 6150-6161.

Johnson, R.D., and Jasin, M. (2000). Sister chromatid gene conversion is a prominent double-strand break repair pathway in mammalian cells. Embo J **19,** 3398-3407.

Jonsson, Z.O., Dhar, S.K., Narlikar, G.J., Auty, R., Wagle, N., Pellman, D., Pratt, R.E., Kingston, R., and Dutta, A. (2001). Rvb1p and Rvb2p are essential components of a chromatin remodeling complex that regulates transcription of over 5% of yeast genes. J Biol Chem **276,** 16279-16288.

Kadyk, L.C., and Hartwell, L.H. (1992). Sister chromatids are preferred over homologs as substrates for recombinational repair in *Saccharomyces cerevisiae*. Genetics **132,** 387-402.

Kandasamy, M.K., McKinney, E.C., and Meagher, R.B. (2003). Cell cycle-dependent association of *Arabidopsis* actin-related proteins AtARP4 and AtARP7 with the nucleus. Plant J **33,** 939-948.

Kandasamy, M.K., Deal, R.B., McKinney, E.C., and Meagher, R.B. (2004). Plant actin-related proteins. Trends Plant Sci **9,** 196-202.

Kanemaki, M., Kurokawa, Y., Matsu-ura, T., Makino, Y., Masani, A., Okazaki, K., Morishita, T., and Tamura, T.A. (1999). TIP49b, a new RuvB-like DNA helicase, is included in a complex together with another RuvB-like DNA helicase, TIP49a. J Biol Chem **274,** 22437-22444.

Kanemaki, M., Makino, Y., Yoshida, T., Kishimoto, T., Koga, A., Yamamoto, K., Yamamoto, M., Moncollin, V., Egly, J.M., Muramatsu, M., and Tamura, T. (1997). Molecular cloning of a rat 49-kDa TBP-interacting protein (TIP49) that is highly homologous to the bacterial RuvB. Biochem Biophys Res Commun **235,** 64-68.

Kennison, J.A., and Tamkun, J.W. (1988). Dosage-dependent modifiers of polycomb and antennapedia mutations in *Drosophila*. Proc Natl Acad Sci U S A **85,** 8136-8140.

Khanna, K.K., and Jackson, S.P. (2001). DNA double-strand breaks: signaling, repair and the cancer connection. Nat Genet **27,** 247-254.

Khorasanizadeh, F. (2004). The nucleosome: from genomic organization to genomic regulation. Cell **116,** 259-272.

Kliebenstein, D.J., Lim, J.E., Landry, L.G., and Last, R.L. (2002). Arabidopsis UVR8 regulates ultraviolet-B signal transduction and tolerance and contains sequence similarity to human regulator of chromatin condensation 1. Plant Physiol **130,** 234-243.

Klimyuk, V.I., Carroll, B.J., Thomas, C.M., and Jones, J.D. (1993). Alkali treatment for rapid preparation of plant material for reliable PCR analysis. Plant J **3,** 493-494.

Kovalchuk, I., Kovalchuk, O., and Hohn, B. (2001a). Biomonitoring the genotoxicity of environmental factors with transgenic plants. Trends Plant Sci **6,** 306-310.

Kovalchuk, I., Kovalchuk, O., Arkhipov, A., and Hohn, B. (1998). Transgenic plants are sensitive bioindicators of nuclear pollution caused by the Chernobyl accident. Nat Biotechnol **16,** 1054-1059.

Kovalchuk, I., Kovalchuk, O., Kalck, V., Boyko, V., Filkowski, J., Heinlein, M., and Hohn, B. (2003). Pathogen-induced systemic plant signal triggers DNA rearrangements. Nature **423,** 760-762.

Kovalchuk, O., Titov, V., Hohn, B., and Kovalchuk, I. (2001b). A sensitive transgenic plant system to detect toxic inorganic compounds in the environment. Nat Biotechnol **19,** 568-572.

Krejci, L., Van Komen, S., Li, Y., Villemain, J., Reddy, M.S., Klein, H., Ellenberger, T., and Sung, P. (2003). DNA helicase Srs2 disrupts the Rad51 presynaptic filament. Nature **423,** 305-309.

Krogan, N.J., Keogh, M.C., Datta, N., Sawa, C., Ryan, O.W., Ding, H., Haw, R.A., Pootoolal, J., Tong, A., Canadien, V., Richards, D.P., Wu, X., Emili, A., Hughes, T.R., Buratowski, S., and Greenblatt, J.F. (2003). A Snf2 family ATPase complex required for recruitment of the histone H2A variant Htz1. Mol Cell **12,** 1565-1576.

Lafarge, S., and Montane, M.H. (2003). Characterization of Arabidopsis thaliana ortholog of the human breast cancer susceptibility gene 1: AtBRCA1, strongly induced by gamma rays. Nucleic Acids Res **31,** 1148-1155.

Landry, L.G., Chapple, C.C., and Last, R.L. (1995). Arabidopsis mutants lacking phenolic sunscreens exhibit enhanced ultraviolet-B injury and oxidative damage. Plant Physiol **109,** 1159-1166.

Landry, L.G., Stapleton, A.E., Lim, J., Hoffman, P., Hays, J.B., Walbot, V., and Last, R.L. (1997). An Arabidopsis photolyase mutant is hypersensitive to ultraviolet-B†radiation. PNAS **94,** 328-332.

Lebel, E.G., Masson, J., Bogucki, A., and Paszkowski, J. (1993). Stress-induced intrachromosomal recombination in plant somatic cells. Proc Natl Acad Sci U S A **90,** 422-426.

Lee, K.Y., Lund, P., Lowe, K., and Dunsmuir, P. (1990). Homologous recombination in plant cells after Agrobacterium-mediated transformation. Plant Cell **2,** 415-425.

Leonard, J.M., Bollmann, S.R., and Hays, J.B. (2003). Reduction of stability of arabidopsis genomic and transgenic DNA-repeat sequences (microsatellites) by inactivation of AtMSH2 mismatch-repair function. Plant Physiol **133,** 328-338.

Li, A., Schuermann, D., Gallego, F., Kovalchuk, I., and Tinland, B. (2002). Repair of damaged DNA by Arabidopsis cell extract. Plant Cell **14,** 263-273.

Li, G., Chandrasekharan, M.B., Wolffe, A.P., and Hall, T.C. (2001). Chromatin structure and phaseolin gene regulation. Plant Mol Biol **46,** 121-129.

Li, J., Ou-Lee, T.M., Raba, R., Amundson, R.G., and Last, R.L. (1993). Arabidopsis Flavonoid Mutants Are Hypersensitive to UV-B Irradiation. Plant Cell **5,** 171-179.

Liang, F., Han, M., Romanienko, P.J., and Jasin, M. (1998). Homology-directed repair is a major double-strand break repair pathway in mammalian cells. Proc Natl Acad Sci U S A **95,** 5172-5177.

Lichten, M., and Goldman, A.S. (1995). Meiotic recombination hotspots. Annu Rev Genet **29,** 423-444.

Lim, C.R., Kimata, Y., Ohdate, H., Kokubo, T., Kikuchi, N., Horigome, T., and Kohno, K. (2000). The Saccharomyces cerevisiae RuvB-like protein, Tih2p, is required for cell cycle progression and RNA polymerase II-directed transcription. J Biol Chem **275,** 22409-22417.

Lin, Y., and Cheng, C.L. (1997). A chlorate-resistant mutant defective in the regulation of nitrate reductase gene expression in Arabidopsis defines a new HY locus. Plant Cell **9,** 21-35.

Lindahl, T., and Wood, R.D. (1999). Quality control by DNA repair. Science **286,** 1897-1905.

Liu, Y., Masson, J.Y., Shah, R., O'Regan, P., and West, S.C. (2004). RAD51C is required for Holliday junction processing in mammalian cells. Science **303,** 243-246.

Liu, Z., Hall, J.D., and Mount, D.W. (2001). Arabidopsis UVH3 gene is a homolog of the Saccharomyces cerevisiae RAD2 and human XPG DNA repair genes. Plant J **26,** 329-338.

Liu, Z., Hossain, G.S., Islas-Osuna, M.A., Mitchell, D.L., and Mount, D.W. (2000). Repair of UV damage in plants by nucleotide excision repair: Arabidopsis UVH1 DNA repair gene is a homolog of Saccharomyces cerevisiae Rad1. Plant J **21,** 519-528.

Liu, Z., Hong, S.W., Escobar, M., Vierling, E., Mitchell, D.L., Mount, D.W., and Hall, J.D. (2003). Arabidopsis UVH6, a homolog of human XPD and yeast RAD3 DNA repair genes, functions in DNA repair and is essential for plant growth. Plant Physiol **132,** 1405-1414.

Loidl, J., and Langer, H. (1993). Evaluation of models of homologue search with respect to their efficiency on meiotic pairing. Heredity **71 (Pt 4),** 342-351.

Loidl, P. (2004). A plant dialect of the histone language. Trends Plant Sci **9,** 84-90.

Lucht, J.M., Mauch-Mani, B., Steiner, H.Y., Metraux, J.P., Ryals, J., and Hohn, B. (2002). Pathogen stress increases somatic recombination frequency in *Arabidopsis*. Nat Genet **30,** 311-314.

Luger, K. (2003). Structure and dynamic behavior of nucleosomes. Curr Opin Genet Dev **13,** 127-135.

Lusser, A. (2002). Acetylated, methylated, remodeled: chromatin states for gene regulation. Curr Opin Plant Biol **5,** 437-443.

Malkova, A., Ross, L., Dawson, D., Hoekstra, M.F., and Haber, J.E. (1996). Meiotic recombination initiated by a double-strand break in rad50 delta yeast cells otherwise unable to initiate meiotic recombination. Genetics **143,** 741-754.

Martens, J.A., and Winston, F. (2003). Recent advances in understanding chromatin remodeling by Swi/Snf complexes. Curr Opin Genet Dev **13,** 136-142.

Masson, J.E., and Paszkowski, J. (1997). Arabidopsis thaliana mutants altered in homologous recombination. Proc Natl Acad Sci U S A **94,** 11731-11735.

Masson, J.E., King, P.J., and Paszkowski, J. (1997). Mutants of Arabidopsis thaliana hypersensitive to DNA-damaging treatments. Genetics **146,** 401-407.

Mathur, J., Mathur, N., Kernebeck, B., and Hulskamp, M. (2003). Mutations in actin-related proteins 2 and 3 affect cell shape development in Arabidopsis. Plant Cell **15,** 1632-1645.

McKinney, E.C., Kandasamy, M.K., and Meagher, R.B. (2002). Arabidopsis contains ancient classes of differentially expressed actin-related protein genes. Plant Physiol **128,** 997-1007.

Meijer, M., and Smerdon, M.J. (1999). Accessing DNA damage in chromatin: insights from transcription. Bioessays **21,** 596-603.

Mengiste, T., and Paszkowski, J. (1999). Prospects for the precise engineering of plant genomes by homologous recombination. Biol Chem **380,** 749-758.

Mengiste, T., Revenkova, E., Bechtold, N., and Paszkowski, J. (1999). An SMC-like protein is required for efficient homologous recombination in Arabidopsis. Embo J **18,** 4505-4512.

Miao, Z.H., and Lam, E. (1995). Targeted disruption of the TGA3 locus in Arabidopsis thaliana. Plant J **7,** 359-365.

Michelet, B., and Chua, N.H. (1996). Improvement of Arabidopsis Mutant Screens Based on Luciferase Imaging *in planta*. Plant Mol Biol Rep **14,** 320-329.

Millar, A.J., and Kay, S.A. (1996). Integration of circadian and phototransduction pathways in the network controlling CAB gene transcription in Arabidopsis. Proc Natl Acad Sci U S A **93,** 15491-15496.

Millar, A.J., Short, S.R., Chua, N.H., and Kay, S.A. (1992). A novel circadian phenotype based on firefly luciferase expression in transgenic plants. Plant Cell **4,** 1075-1087.

Millar, A.J., Straume, M., Chory, J., Chua, N.H., and Kay, S.A. (1995). The regulation of circadian period by phototransduction pathways in Arabidopsis. Science **267,** 1163-1166.

Mittelsten Scheid, O., Afsar, K., and Paszkowski, J. (1998). Release of epigenetic gene silencing by trans-acting mutations in Arabidopsis. Proc Natl Acad Sci U S A **95,** 632-637.

Mittelsten Scheid, O., Probst, A.V., Afsar, K., and Paszkowski, J. (2002). Two regulatory levels of transcriptional gene silencing in *Arabidopsis*. Proc Natl Acad Sci U S A **99,** 13659-13662.

Mizuguchi, G., Shen, X., Landry, J., Wu, W.H., Sen, S., and Wu, C. (2004). ATP-driven exchange of histone H2AZ variant catalyzed by SWR1 chromatin remodeling complex. Science **303,** 343-348.

Modesti, M., and Kanaar, R. (2001). DNA repair: spot(light)s on chromatin. Curr Biol **11,** R229-232.

Molinier, J., Ries, G., Bonhoeffer, S., and Hohn, B. (2004a). Interchromatid and Interhomolog Recombination in Arabidopsis thaliana. Plant Cell **16,** 342-352.

Molinier, J., Fritsch, O., Ramos, C., and Hohn, B. (2004b). CENTRIN2 Modulates Homologous Recombination and Nucleotide Excision Repair in *Arabidopsis*. Plant Cell **16,** in press.

Morales-Ruiz, T., Birincioglu, M., Jaruga, P., Rodriguez, H., Roldan-Arjona, T., and Dizdaroglu, M. (2003). Arabidopsis thaliana Ogg1 protein excises 8-hydroxyguanine and 2,6-diamino-4-hydroxy-5-formamido-pyrimidine from oxidatively damaged DNA containing multiple lesions. Biochemistry **42,** 3089-3095.

Murashige, T., and Skoog, F. (1962). A revised medium for rapid growth and bio assays with tobacco tissue culture. Physiol Plant **15,** 473-497.

Mysore, K.S., Nam, J., and Gelvin, S.B. (2000). An Arabidopsis histone H2A mutant is deficient in Agrobacterium T-DNA integration. Proc Natl Acad Sci U S A **97,** 948-953.

Nachman, M.W. (2002). Variation in recombination rate across the genome: evidence and implications. Curr Opin Genet Dev **12,** 657-663.

Nakajima, S., Sugiyama, M., Iwai, S., Hitomi, K., Otoshi, E., Kim, S., Jiang, C., Todo, T., Britt, A., and Yamamoto, K. (1998). Cloning and characterization of a gene (UVR3) required for photorepair of 6-4 photoproducts in Arabidopsis thaliana. Nucl. Acids. Res. **26,** 638-644.

Nakayama, J., Rice, J.C., Strahl, B.D., Allis, C.D., and Grewal, S.I. (2001). Role of histone H3 lysine 9 methylation in epigenetic control of heterochromatin assembly. Science **292,** 110-113.

Nam, J., Mysore, K.S., and Gelvin, S.B. (1998). Agrobacterium tumefaciens transformation of the radiation hypersensitive Arabidopsis thaliana mutants uvh1 and rad5. Mol Plant Microbe Interact **11,** 1136-1141.

Nam, J., Mysore, K.S., Zheng, C., Knue, M.K., Matthysse, A.G., and Gelvin, S.B. (1999). Identification of T-DNA tagged Arabidopsis mutants that are resistant to transformation by Agrobacterium. Mol Gen Genet **261,** 429-438.

Nassif, N., Penney, J., Pal, S., Engels, W.R., and Gloor, G.B. (1994). Efficient copying of nonhomologous sequences from ectopic sites via P-element-induced gap repair. Mol Cell Biol **14,** 1613-1625.

Nielsen, B.L., Sanchez, C., Ichinose, H., Cervino, M., Lerouge, T., Chambon, P., and Losson, R. (2002). Selective interaction between the chromatin-remodelling factor BRG1 and the heterochromatin-associated protein HP1alpha. EMBO J **21,** 5797-5806.

Noh, Y.-S., and Amasino, R.M. (2003). *PIE1*, an ISWI Family Gene, Is Required for *FLC* Activation and Floral Repression in Arabidopsis. Plant Cell **15,** 1671-1682.

Noma, K., Allis, C.D., and Grewal, S.I. (2001). Transitions in distinct histone H3 methylation patterns at the heterochromatin domain boundaries. Science **293,** 1150-1155.

Offringa, R., de Groot, M.J., Haagsman, H.J., Does, M.P., van den Elzen, P.J., and Hooykaas, P.J. (1990). Extrachromosomal homologous recombination and gene targeting in plant cells after *Agrobacterium* mediated transformation. Embo J **9,** 3077-3084.

Ogas, J., Kaufmann, S., Henderson, J., and Somerville, C. (1999). PICKLE is a CHD3 chromatin-remodeling factor that regulates the transition from embryonic to vegetative development in Arabidopsis. Proc Natl Acad Sci U S A **96,** 13839-13844.

Ohdate, H., Lim, C.R., Kokubo, T., Matsubara, K., Kimata, Y., and Kohno, K. (2003). Impairment of the DNA binding activity of the TATA-binding protein renders the transcriptional function of Rvb2p/Tih2p, the yeast RuvB-like protein, essential for cell growth. J Biol Chem **278,** 14647-14656.

Osakabe, K., Yoshioka, T., Ichikawa, H., and Toki, S. (2002). Molecular cloning and characterization of RAD51-like genes from Arabidopsis thaliana. Plant Mol Biol **50,** 71-81.

Pandey, R., Muller, A., Napoli, C.A., Selinger, D.A., Pikaard, C.S., Richards, E.J., Bender, J., Mount, D.W., and Jorgensen, R.A. (2002). Analysis of histone acetyltransferase and histone deacetylase families of *Arabidopsis thaliana* suggests functional diversification of chromatin modification among multicellular eukaryotes. Nucleic Acids Res **30,** 5036-5055.

Paques, F., and Haber, J.E. (1999). Multiple pathways of recombination induced by double-strand breaks in *Saccharomyces cerevisiae*. Microbiol Mol Biol Rev **63,** 349-404.

Parniske, M., Hammond-Kosack, K.E., Golstein, C., Thomas, C.M., Jones, D.A., Harrison, K., Wulff, B.B., and Jones, J.D. (1997). Novel disease resistance specificities result from sequence exchange between tandemly repeated genes at the Cf-4/9 locus of tomato. Cell **91,** 821-832.

Paszkowski, J., Baur, M., Bogucki, A., and Potrykus, I. (1988). Gene targeting in plants. Embo J **7,** 4021-4026.

Paul, A.L., and Ferl, R.J. (1998). Permeabilized *Arabidopsis* protoplasts provide new insight into the chromatin structure of plant alcohol dehydrogenase genes. Dev Genet **22,** 7-16.

Paull, T.T., Rogakou, E.P., Yamazaki, V., Kirchgessner, C.U., Gellert, M., and Bonner, W.M. (2000). A critical role for histone H2AX in recruitment of repair factors to nuclear foci after DNA damage. Curr Biol **10,** 886-895.

Peterson, C.L., and Cote, J. (2004). Cellular machineries for chromosomal DNA repair. Genes Dev. **18,** 602-616.

Petrucco, S., Volpi, G., Bolchi, A., Rivetti, C., and Ottonello, S. (2002). A nick-sensing DNA 3'-repair enzyme from Arabidopsis. J Biol Chem **277,** 23675-23683.

Pietrzak, M., Shillito, R.D., Hohn, T., and Potrykus, I. (1986). Expression in plants of two bacterial antibiotic resistance genes after protoplast transformation with a new plant expression vector. Nucl. Acids. Res. **14,** 5857-5868.

Plchova, H., Hartung, F., and Puchta, H. (2003). Biochemical characterization of an exonuclease from Arabidopsis thaliana reveals similarities to the DNA exonuclease of the human Werner syndrome protein. J Biol Chem **278,** 44128-44138.

Puchta, H. (2002). Gene replacement by homologous recombination in plants. Plant Mol Biol **48,** 173-182.

Puchta, H., and Hohn, B. (1996). From centiMorgans to base pairs: homologous recombination in plants. Trends Plant Sci. **1,** 340-348.

Puchta, H., Swoboda, P., and Hohn, B. (1995a). Induction of intrachromosomal homologous recombination in whole plants. Plant J. **7,** 203-210.

Puchta, H., Swoboda, P., Gal, S., Blot, M., and Hohn, B. (1995b). Somatic intrachromosomal homologous recombination events in populations of plant siblings. Plant Mol Biol **28,** 281-292.

Qin, S., and Parthun, M.R. (2002). Histone H3 and the histone acetyltransferase Hat1p contribute to DNA double-strand break repair. Mol Cell Biol **22,** 8353-8365.

Qiu, X.B., Lin, Y.L., Thome, K.C., Pian, P., Schlegel, B.P., Weremowicz, S., Parvin, J.D., and Dutta, A. (1998). An eukaryotic RuvB-like protein (RUVBL1) essential for growth. J Biol Chem **273,** 27786-27793.

Ray, A., and Langer, M. (2002). Homologous recombination: ends as the means. Trends Plant Sci **7,** 435-440.

Rea, S., Eisenhaber, F., O'Carroll, D., Strahl, B.D., Sun, Z.W., Schmid, M., Opravil, S., Mechtler, K., Ponting, C.P., Allis, C.D., and Jenuwein, T. (2000). Regulation of chromatin structure by site-specific histone H3 methyltransferases. Nature **406,** 593-599.

Redon, C., Pilch, D., Rogakou, E., Sedelnikova, O., Newrock, K., and Bonner, W. (2002). Histone H2A variants H2AX and H2AZ. Curr Opin Genet Dev **12,** 162-169.

Reiss, B., Klemm, M., Kosak, H., and Schell, J. (1996). RecA protein stimulates homologous recombination in plants. Proc Natl Acad Sci U S A **93,** 3094-3098.

Reiss, B., Schubert, I., Kopchen, K., Wendeler, E., Schell, J., and Puchta, H. (2000). RecA stimulates sister chromatid exchange and the fidelity of double-strand break repair, but not gene targeting, in plants transformed by Agrobacterium. Proc Natl Acad Sci U S A **97,** 3358-3363.

Reyes, J.C., Hennig, L., and Gruissem, W. (2002). Chromatin-remodeling and memory factors. New regulators of plant development. Plant Physiol **130,** 1090-1101.

Reyes, J.C., Barra, J., Muchardt, C., Camus, A., Babinet, C., and Yaniv, M. (1998). Altered control of cellular proliferation in the absence of mammalian brahma (SNF2alpha). Embo J **17,** 6979-6991.

Richmond, E., and Peterson, C.L. (1996). Functional analysis of the DNA-stimulated ATPase domain of yeast SWI2/SNF2. Nucleic Acids Res **24,** 3685-3692.

Richmond, T.J., and Davey, C.A. (2003). The structure of DNA in the nucleosome core. Nature **423,** 145-150.

Richter, T.E., and Ronald, P.C. (2000). The evolution of disease resistance genes. Plant Mol Biol **42,** 195-204.

Ries, G., Buchholz, G., Frohnmeyer, H., and Hohn, B. (2000a). UV-damage-mediated induction of homologous recombination in *Arabidopsis* is dependent on photosynthetically active radiation. Proc Natl Acad Sci U S A **97,** 13425-13429.

Ries, G., Heller, W., Puchta, H., Sandermann, H., Seidlitz, H.K., and Hohn, B. (2000b). Elevated UV-B radiation reduces genome stability in plants. Nature **406,** 98-101.

Riha, K., and Shippen, D.E. (2003). Ku is required for telomeric C-rich strand maintenance but not for end-to-end chromosome fusions in Arabidopsis. Proc Natl Acad Sci U S A **100,** 611-615.

Riha, K., Watson, J.M., Parkey, J., and Shippen, D.E. (2002). Telomere length deregulation and enhanced sensitivity to genotoxic stress in Arabidopsis mutants deficient in Ku70. Embo J **21,** 2819-2826.

Rothkamm, K., and Lobrich, M. (2003). Evidence for a lack of DNA double-strand break repair in human cells exposed to very low x-ray doses. Proc Natl Acad Sci U S A **100,** 5057-5062.

Sakamoto, A., Lan, V.T., Hase, Y., Shikazono, N., Matsunaga, T., and Tanaka, A. (2003). Disruption of the AtREV3 gene causes hypersensitivity to ultraviolet B light and gamma-rays in Arabidopsis: implication of the presence of a translesion synthesis mechanism in plants. Plant Cell **15,** 2042-2057.

Salomon, S., and Puchta, H. (1998). Capture of genomic and T-DNA sequences during double-strand break repair in somatic plant cells. Embo J **17,** 6086-6095.

Sambrook, J., and Russel, D.W. (2001). Molecular cloning, a laboratory manual. Cold Spring Harbor Laboratory Press, New York.

Saze, H., Mittelsten Scheid, O., and Paszkowski, J. (2003). Maintenance of CpG methylation is essential for epigenetic inheritance during plant gametogenesis. Nat Genet **34,** 65-69.

Schroeder, D.F., Gahrtz, M., Maxwell, B.B., Cook, R.K., Kan, J.M., Alonso, J.M., Ecker, J.R., and Chory, J. (2002). De-etiolated 1 and damaged DNA binding protein 1 interact to regulate Arabidopsis photomorphogenesis. Curr Biol **12,** 1462-1472.

Shalev, G., Sitrit, Y., Avivi-Ragolski, N., Lichtenstein, C., and Levy, A.A. (1999). Stimulation of homologous recombination in plants by expression of the bacterial resolvase ruvC. Proc Natl Acad Sci U S A **96,** 7398-7402.

Shang, Y.L., Bodero, A.J., and Chen, P.L. (2003). NFBD1, a novel nuclear protein with signature motifs of FHA and BRCT, and an internal 41-amino acid repeat sequence, is an early participant in DNA damage response. J Biol Chem **278,** 6323-6329.

Shen, X., Mizuguchi, G., Hamiche, A., and Wu, C. (2000). A chromatin remodelling complex involved in transcription and DNA processing. Nature **406,** 541-544.

Shen, X., Ranallo, R., Choi, E., and Wu, C. (2003a). Involvement of actin-related proteins in ATP-dependent chromatin remodeling. Mol Cell **12,** 147-155.

Shen, X., Xiao, H., Ranallo, R., Wu, W.H., and Wu, C. (2003b). Modulation of ATP-dependent chromatin-remodeling complexes by inositol polyphosphates. Science **299,** 112-114.

Shinagawa, H., and Iwasaki, H. (1996). Processing the holliday junction in homologous recombination. Trends Biochem Sci **21,** 107-111.

Siaud, N., Dray, E., Gy, I., Gerard, E., Takvorian, N., and Doutriaux, M.P. (2004). Brca2 is involved in meiosis in Arabidopsis thaliana as suggested by its interaction with Dmc1. Embo J **23,** 1392-1401.

Simon, J.A., and Tamkun, J.W. (2002). Programming off and on states of gene expression: transcriptional control during *Drosophila* development. Curr Opin Genet Dev **12,** 210-218.

Smith, G.R. (2001). Homologous Recombination Near and Far from DNA Breaks: Alternative Roles. Annu Rev Genet **35,** 243-274.

Smith, N.A., Singh, S.P., Wang, M.B., Stoutjesdijk, P.A., Green, A.G., and Waterhouse, P.M. (2000). Total silencing by intron-spliced hairpin RNAs. Nature **407,** 319-320.

Srayko, M., Buster, D.W., Bazirgan, O.A., McNally, F.J., and Mains, P.E. (2000). MEI-1/MEI-2 katanin-like microtubule severing activity is required for Caenorhabditis elegans meiosis. Genes Dev. **14,** 1072-1084.

Steger, D.J., Haswell, E.S., Miller, A.L., Wente, S.R., and O'Shea, E.K. (2003). Regulation of chromatin remodeling by inositol polyphosphates. Science **299,** 114-116.

Steimer, A., Amedeo, P., Afsar, K., Fransz, P., Mittelsten Scheid, O., and Paszkowski, J. (2000). Endogenous targets of transcriptional gene silencing in Arabidopsis. Plant Cell **12,** 1165-1178.

Sterner, D.E., and Berger, S.L. (2000). Acetylation of histones and transcription-related factors. Microbiol Mol Biol Rev **64,** 435-459.

Sterner, D.E., Wang, X., Bloom, M.H., Simon, G.M., and Berger, S.L. (2002). The SANT domain of Ada2 is requiredd for normal acetylation of histones by the yeast SAGA complex. J Biol Chem **277,** 8178-8186.

Stoutjesdijk, P.A., Singh, S.P., Liu, Q., Hurlstone, C.J., Waterhouse, P.A., and Green, A.G. (2002). hpRNA-mediated targeting of the Arabidopsis FAD2 gene gives highly efficient and stable silencing. Plant Physiol **129,** 1723-1731.

Strahl, B.D., and Allis, C.D. (2000). The language of covalent histone modifications. Nature **403,** 41-45.

Sugimoto-Shirasu, K., Stacey, N.J., Corsar, J., Roberts, K., and McCann, M.C. (2002). DNA topoisomerase VI is essential for endoreduplication in Arabidopsis. Curr Biol **12,** 1782-1786.

Sugiyama, T., and Kowalczykowski, S.C. (2002). Rad52 protein associates with replication protein A (RPA)-single-stranded DNA to accelerate Rad51-mediated displacement of RPA and presynaptic complex formation. J Biol Chem **277,** 31663-31672.

Swoboda, P., Hohn, B., and Gal, S. (1993). Somatic homologous recombination in planta: the recombination frequency is dependent on the allelic state of recombining sequences and may be influenced by genomic position effects. Mol Gen Genet **237,** 33-40.

Swoboda, P., Gal, S., Hohn, B., and Puchta, H. (1994). Intrachromosomal homologous recombination in whole plants. Embo J **13,** 484-489.

Symington, L.S. (2002). Role of RAD52 Epistasis Group Genes in Homologous Recombination and Double-Strand Break Repair. Microbiol Mol Biol Rev **66,** 630-670.

Szerlong, H., Saha, A., and Cairns, B.R. (2003). The nuclear actin-related proteins Arp7 and Arp9: a dimeric module that cooperates with architectural proteins for chromatin remodeling. Embo J **22,** 3175-3187.

Takahashi, M., Sasaki, Y., Ida, S., and Morikawa, H. (2001). Nitrite reductase gene enrichment improves assimilation of NO(2) in Arabidopsis. Plant Physiol **126,** 731-741.

Takeda, S., Tadele, Z., Hofmann, I., Probst, A.V., Angelis, K.J., Kaya, H., Araki, T., Mengiste, T., Scheid, O.M., Shibahara, K.-i., Scheel, D., and Paszkowski, J. (2004). BRU1, a novel link between responses to DNA damage and epigenetic gene silencing in Arabidopsis. Genes Dev. **18,** 782-793.

Tamura, K., Adachi, Y., Chiba, K., Oguchi, K., and Takahashi, H. (2002). Identification of Ku70 and Ku80 homologues in Arabidopsis thaliana: evidence for a role in the repair of DNA double-strand breaks. Plant J **29,** 771-781.

Tanaka, A., Sakamoto, A., Ishigaki, Y., Nikaido, O., Sun, G., Hase, Y., Shikazono, N., Tano, S., and Watanabe, H. (2002). An ultraviolet-B-resistant mutant with enhanced DNA repair in Arabidopsis. Plant Physiol **129,** 64-71.

Tariq, M., Saze, H., Probst, A.V., Lichota, J., Habu, Y., and Paszkowski, J. (2003). Erasure of CpG methylation in Arabidopsis alters patterns of histone H3 methylation in heterochromatin. Proc Natl Acad Sci U S A **100,** 8823-8827.

Thykjaer, T., Finnemann, J., Schauser, L., Christensen, L., Poulsen, C., and Stougaard, J. (1997). Gene targeting approaches using positive-negative selection and large flanking regions. Plant Mol Biol **35,** 523-530.

Tijsterman, M., and Brouwer, J. (1999). Rad26, the yeast homolog of the cockayne syndrome B gene product, counteracts inhibition of DNA repair due to RNA polymerase II transcription. J Biol Chem **274,** 1199-1202.

Tsukiyama, T. (2002). The in vivo functions of ATP-dependent chromatin-remodelling factors. Nat Rev Mol Cell Biol **3,** 422-429.

Ulm, R., Revenkova, E., di Sansebastiano, G.P., Bechtold, N., and Paszkowski, J. (2001). Mitogen-activated protein kinase phosphatase is required for genotoxic stress relief in Arabidopsis. Genes Dev **15,** 699-709.

Ura, K., and Hayes, J.J. (2002). Nucleotide excision repair and chromatin remodeling. Eur J Biochem **269,** 2288-2293.

Ura, K., Araki, M., Saeki, H., Masutani, C., Ito, T., Iwai, S., Mizukoshi, T., Kaneda, Y., and Hanaoka, F. (2001). ATP-dependent chromatin remodeling facilitates nucleotide excision repair of UV-induced DNA lesions in synthetic dinucleosomes. Embo J **20,** 2004-2014.

Van Komen, S., Reddy, M.S., Krejci, L., Klein, H., and Sung, P. (2003). ATPase and DNA helicase activities of the *Saccharomyces cerevisiae* anti-recombinase Srs2. J Biol Chem **278,** 44331-44337.

Van Larebeke, N., Engler, G., Holsters, M., Van den Elsacker, S., Zaenen, I., Schilproot, R.A., and Schell, J. (1974). Large plasmids in *Agrobacterium tumefasciens* essential for crown gall-inducing ability. Nature **252,** 169-170.

Veaute, X., Jeusset, J., Soustelle, C., Kowalczykowski, S.C., Le Cam, E., and Fabre, F. (2003). The Srs2 helicase prevents recombination by disrupting Rad51 nucleoprotein filaments. Nature **423,** 309-312.

Verbsky, M.L., and Richards, E.J. (2001). Chromatin remodeling in plants. Curr Opin Plant Biol **4,** 494-500.

Verkade, H.M., Bugg, S.J., Lindsay, H.D., Carr, A.M., and O'Connell, M.J. (1999). Rad18 is required for DNA repair and checkpoint responses in fission yeast. Mol Biol Cell **10,** 2905-2918.

Verreault, A. (2000). De novo nucleosome assembly: new pieces in an old puzzle. Genes Dev **14,** 1430-1438.

Wade, P.A., Gegonne, A., Jones, P.L., Ballestar, E., Aubry, F., and Wolffe, A.P. (1999). Mi-2 complex couples DNA methylation to chromatin remodelling and histone deacetylation. Nat Genet **23,** 62-66.

Wagner, D., and Meyerowitz, E.M. (2002). SPLAYED, a novel SWI/SNF ATPase homolog, controls reproductive development in Arabidopsis. Curr Biol **12,** 85-94.

Walbot, V. (1996). Sources and consequences of phenotypic and genotypic plasticity in flowering plants. Trends Plant Sci. **1,** 27-32.

Walbot, V., and Evans, M.M. (2003). Unique features of the plant life cycle and their consequences. Nat Rev Genet **4,** 369-379.

Wang, G., Hyne, V., Chao, S., Henry, Y., De Buyser, J., Gale, M.D., and Snape, J.W. (1995). Theor Appl Genet **91,** 744-746.

Watkins, N.J., Dickmanns, A., and Luhrmann, R. (2002). Conserved stem II of the box C/D motif is essential for nucleolar localization and is required, along with the 15.5K protein, for the hierarchical assembly of the box C/D snoRNP. Mol Cell Biol **22,** 8342-8352.

Weigel, D., Ahn, J.H., Blazquez, M.A., Borevitz, J.O., Christensen, S.K., Fankhauser, C., Ferrandiz, C., Kardailsky, I., Malancharuvil, E.J., Neff, M.M., Nguyen, J.T., Sato, S., Wang, Z.Y., Xia, Y., Dixon, R.A., Harrison, M.J., Lamb, C.J., Yanofsky, M.F., and Chory, J. (2000). Activation tagging in Arabidopsis. Plant Physiol **122,** 1003-1013.

Werner, T., Motyka, V., Laucou, V., Smets, R., Van Onckelen, H., and Schmulling, T. (2003). Cytokinin-deficient transgenic Arabidopsis plants show multiple developmental alterations indicating opposite functions of cytokinins in the regulation of shoot and root meristem activity. Plant Cell **15,** 2532-2550.

West, C.E., Waterworth, W.M., Jiang, Q., and Bray, C.M. (2000). Arabidopsis DNA ligase IV is induced by gamma-irradiation and interacts with an Arabidopsis homologue of the double strand break repair protein XRCC4. Plant J **24,** 67-78.

West, C.E., Waterworth, W.M., Story, G.W., Sunderland, P.A., Jiang, Q., and Bray, C.M. (2002). Disruption of the Arabidopsis AtKu80 gene demonstrates an essential role for AtKu80 protein in efficient repair of DNA double-strand breaks in vivo. Plant J **31,** 517-528.

West, S.C. (1997). Processing of recombination intermediates by the RuvABC proteins. Annu Rev Genet **31,** 213-244.

West, S.C. (2003). Molecular views of recombination proteins and their control. Nat Rev Mol Cell Biol **4,** 435-445.

Wolffe, A.P., and Hayes, J.J. (1999). Chromatin disruption and modification. Nucleic Acids Res **27,** 711-720.

Wolner, B., van Komen, S., Sung, P., and Peterson, C.L. (2003). Recruitment of the recombinational repair machinery to a DNA double-strand break in yeast. Mol Cell **12,** 221-232.

Wood, M.A., McMahon, S.B., and Cole, M.D. (2000). An ATPase/helicase complex is an essential cofactor for oncogenic transformation by c-Myc. Mol Cell **5,** 321-330.

Workman, J.L., and Kingston, R.E. (1998). Alteration of nucleosome structure as a mechanism of transcriptional regulation. Annu Rev Biochem **67,** 545-579.

Wu, S.Y., Culligan, K., Lamers, M., and Hays, J. (2003). Dissimilar mispair-recognition spectra of Arabidopsis DNA-mismatch-repair proteins MSH2*MSH6 (MutSalpha) and MSH2*MSH7 (MutSgamma). Nucleic Acids Res **31,** 6027-6034.

Wyatt, H.R., Liaw, H., Green, G.R., and Lustig, A.J. (2003). Multiple roles for Saccharomyces cerevisiae histone H2A in telomere position effect, Spt phenotypes and double-strand-break repair. Genetics **164,** 47-64.

Xu, X., and Stern, D.F. (2003). NFBD1/KIAA0170 is a chromatin-associated protein involved in DNA damage signaling pathways. J Biol Chem **278,** 8795-8803.

Yamada, K., Kunishima, N., Mayanagi, K., Ohnishi, T., Nishino, T., Iwasaki, H., Shinagawa, H., and Morikawa, K. (2001). Crystal structure of the Holliday junction migration motor protein RuvB from Thermus thermophilus HB8. Proc Natl Acad Sci U S A **98,** 1442-1447.

Yang, S., Kuo, C., Bisi, J.E., and Kim, M.K. (2002). PML-dependent apoptosis after DNA damage is regulated by the checkpoint kinase hCds1/Chk2. Nat Cell Biol **4,** 865-870.

You, A., Tong, J.K., Grozinger, C.M., and Schreiber, S.L. (2001). CoREST is an integral component of the CoREST-human histone deacetylase complex. Proc Natl Acad Sci U S A **98,** 1454-1458.

Young, N.D. (2000). The genetic architecture of resistance. Curr Opin Plant Biol **3,** 285-290.

Zhang, Y., LeRoy, G., Seelig, H.P., Lane, W.S., and Reinberg, D. (1998). The dermatomyositis-specific autoantigen Mi-2 is a component of a complex containing histone deacetylase and nucleosome remodeling activities. Cell **95,** 279-289.

Zhu, T., Peterson, D.J., Tagliani, L., St Clair, G., Baszczynski, C.L., and Bowen, B. (1999). Targeted manipulation of maize genes in vivo using chimeric RNA/DNA oligonucleotides. Proc Natl Acad Sci U S A **96,** 8768-8773.

Zwaka, T.P., and Thomson, J.A. (2003). Homologous recombination in human embryonic stem cells. Nat Biotechnol **21,** 319-321.

Zwirn, P., Stary, S., Luschnig, C., and Bachmair, A. (1997). Arabidopsis thaliana RAD6 homolog AtUBC2 complements UV sensitivity, but not N-end rule degradation deficiency, of Saccharomyces cerevisiae rad6 mutants. Curr Genet **32,** 309-314.

Abbreviations

35Sp	Cauliflower mosaic virus 35S promoter
BAC	Bacterial artificial chromosome
BER	Base excision repair
bp	Base-pair
CaMV	Cauliflower mosaic virus
CCD	Camera coupled-device
CPD	Cyclobutane pyrimidine dimers
Ct	Carboxy-terminal end
DSB	Double-strand break
EDTA	Ethylenediamine tetracetic acid
EMS	Ethylmethane sulfonate
EST	Expressed sequence tag
EtBr	Ethidium bromide
GUS	beta-glucuronidase (gene)
HAT	Histone acetyltransferase
HDAc	Histone deacetylase
H2O2	Hydrogen peroxide
HR	Homologous recombination
HygR	Hygromycin resistance (gene)
IR	Ionizing radiation
kb	Kilo base-pair
LB	T-DNA left border
LUC	Luciferase (gene)
MAS(p)	Mannopine synthase (promoter)
MMC	Mitomycin-C
MMR	Mismatch repair
MMS	Methylmethane sulfonate
MR	meiotic recombination
MS	Murashigue and Skoog medium
mRNA	messenger RNA
ND	Not determined
NER	Nucleotide excision repair
NHEJ	Non-homologous end-joining
NOS	Nopaline synthase
NOSp	Nopaline synthase promoteur
nptII	Neomycin phosphotransferase II gene
Nt	Amino-terminal end
PCR	Polymerase chain reaction
P/E	Promoter/enhancer
ORF	Open reading frame
RB	T-DNA right border
RNAi	RNA interference
ROS	Reactive oxygen species
rpm	rotation per minute
SDS	Sodium dodecyl sulfate
SDSA	Synthesis dependent strand annealing
SMC	Structural maintenance of chromosomes
SSB	Single-strand break
ssDNA	Single-strand DNA
sul	Sufonamide (gene)
SWI/SNF	Switch/sucrose non-fermenting
TCR	Transcription-coupled repair
T-DNA	Transfered-DNA
TGS	Transcriptional gene silencing
Tris	tris-(hydroxymethyl)-aminomethane
TSI	Transcriptionally silent information

Appendix

Appendix 1: Table of oligonucleotides

Name	Sequence (5'-3')
inoT5'	tggagaaggggatacatacg
inoT3'	acgtacagcccaaggatcg
102RB (rbnos#5)	gatcagattgtcgtttcccgcc
inoIR5'(InoBG/Xhhp)	cctttccctcgagtgtacatctttgctttcagcttcttcg
inoIR3'(InoN/Bahp)	cttccaaggatccatggtttggacattggtgatggtg
iBsp1615+	ttaccatcatgaagctacgccaaacttctg
iBsp3691+	ttaccatcatgacaaagatgctgaacattctcg
iBH4518-	ccattcggatccagcggagctacttggatcg
iBg4115-	ccattcagatctgataccacatccgcagctc
iBH2985-	ccattcggatccgtgaaaagccaaatgctc
iBg1683-	ccattcagatcttgctcgagccagaaactg
iBg1285-	ccattcagatctcctctcttctgccatctgc
smAT1	accatcatgatggatccttcaagacgac
InoBsp1168+	ttaccatcatgaaggtgggtagatcatac
InoBsp2989+	ttaccatcatgatggatctatcaccatcagaag
InoBsp4060+	ttaccatcatgactggagggcatgttcag
InoBgHi1734-	ttggaagatctctagtgatggtgatggtgatgagtctgaactgttgatgtaacag
InoBgHi3621-	ttggaagatctctagtgatggtgatggtgatgcttcccagagtccgtgagc
smBGhp	cctttcctgtacatgcaatgaattctgccattc
smAhp	cttccaacctaggtttggcgtagcttcatatattc
smcD2987+	tgatggatctatcaccatcag
cDsm3748-	ggtgggattccaatcactttc
smcDAvr	ctcacctaggaaccaattgtctaaaacctgc
sm5UT	ctagaagcttttaaggattaagactctcc
sul5'	gtgactacagtcagccgtgc
sul3'	aatatcgggatagagcgcag
luhy5'	ggaagacgccaaaaacataaag
luhy3'	gacatatccacgccctccta
act2-5	tggacaagtcataaccatcggagc
act2-3	tgtgaacaatcgatggacctgac
Arp5.1.5'	ccaccaagatcttcatgatggcagaactgctatttgagac
Arp5.1.3'	caacaaggtacctaggaattcacaaatagttgtatcgaatttg
Arp5.2.5'	ccaccaggatcctcatgatcctgaagaaagtatgg
Arp5.2.3'	caacaaggtacctaggaattcaccacatgagtcttgacttg
Arp5.3.5'	ccaccaggatccccatggaagcatcagttgttgatg
Arp5.3.3'	caacaaggtacctaggaattcagaaacatttcctgtgaaccac
Arp8.5'	ccaccaggatccccatggcaaaaccaaaatccaattc
Arp8.3'	cacaactcgaggtacctaggaagcttctaggggttgatgaagtacat
Fad5'	ccgatcaagcttccaattctcgagctccatctccaggtccgtcg
Fad3'	cgaatccctaggcaatttctgtacacccatgtttctgagaaaacc
adh5'	ttcacttctctctgtcacaccg
adh3'	gatgcaacgaatactctctccc
bla5'	tttgccttcctgtttttgct
bla3'	aactttatccgcctccatcc
dTanchor	gaccacgcgtatcgatgtcgacttttttttttttttt(a/c/g)
MCS5'nos	catccatggcaagcttagtttaaacacacctaggcgcgcctttcttaagattgaatcctg
ubi5'	acccaaggagctcactacgttagagcgctaacg
ubi3'	ggaggtaagcttgttgccatggccatgcctcctctaagacg
tml5'	ccactcgagtcatgattcccgtcgccgacacc
tml3'	caaacccaagcttccaactgagctctggttgttgcatcatagagg
LucN/Bahp	cttccaaggatccatggtgcactgatcatgaactcctc
LucBG/Xhhp	cctttccctcgagtgtacagctatgtctccagaatgtagc

Appendix 2: Media stock solutions

MS macroelements (10x):

NH_4NO_3	16.5 mg/l
KNO_3	19 mg/l
$CaCl_2 \cdot 2H_2O$	4.4 mg/l
$MgSO_4 \cdot 7H_2O$	3.7 mg/l
KH_2PO_4	1.7 mg/l
H_20	fill up to 1 l

B5 macroelements (10x):

$(NH_4)_2SO_4$	1.34 mg/l
KNO_3	25 mg/l
$CaCl_2 \cdot 2H_2O$	1.5 mg/l
$MgSO_4 \cdot 7H_2O$	2.5 mg/l
NaH_2PO_4	1.3 mg/l
H_20	fill up to 1 l

B5 microelements (1000x):

KI	0.75 g/l
H_3BO_3	3 g/l
$MnSO_4 \cdot H_2O$	10 g/l
$ZnSO_4 \cdot 7H_2O$	2 g/l
$Na_2MoO_4 \cdot 2H_2O$	0.25 g/l
$CuSO_4 \cdot 5H_2O$	25 mg/l
$CoCl_2 \cdot 6H_2O$	25 mg/l
H_20	fill up to 1 l

MS microelements (1000x):

KI	0.83 g/l
H_3BO_3	6.2 g/l
$MnSO_4 \cdot H_2O$	16.9 g/l
$ZnSO_4 \cdot 7H_2O$	8.6 g/l
$Na_2MoO_4 \cdot 2H_2O$	0.25 g/l
$CuSO_4 \cdot 5H_2O$	25 mg/l
$CoCl_2 \cdot 6H_2O$	25 mg/l
H_20	fill up to 1 l

MS vitamins (100x):

Nicotinic acid	50 mg/l
Pyridoxine HCl	50 mg/l
Thiamine HCl	10 mg/l
Glycine	0.2 g/l
myo-Inositol	10 g/l
H_20	fill up to 1 l

B5 vitamins (100x):

Nicotinic acid	0.1 g/l
Pyridoxine HCl	0.1 g/l
Thiamine HCl	1 g/l
myo-Inositol	10 g/l
H_20	fill up to 1 l

Appendix 3: pAC102 vector and T-DNA region map

Single sites are shown. Bold names, multiple sites.

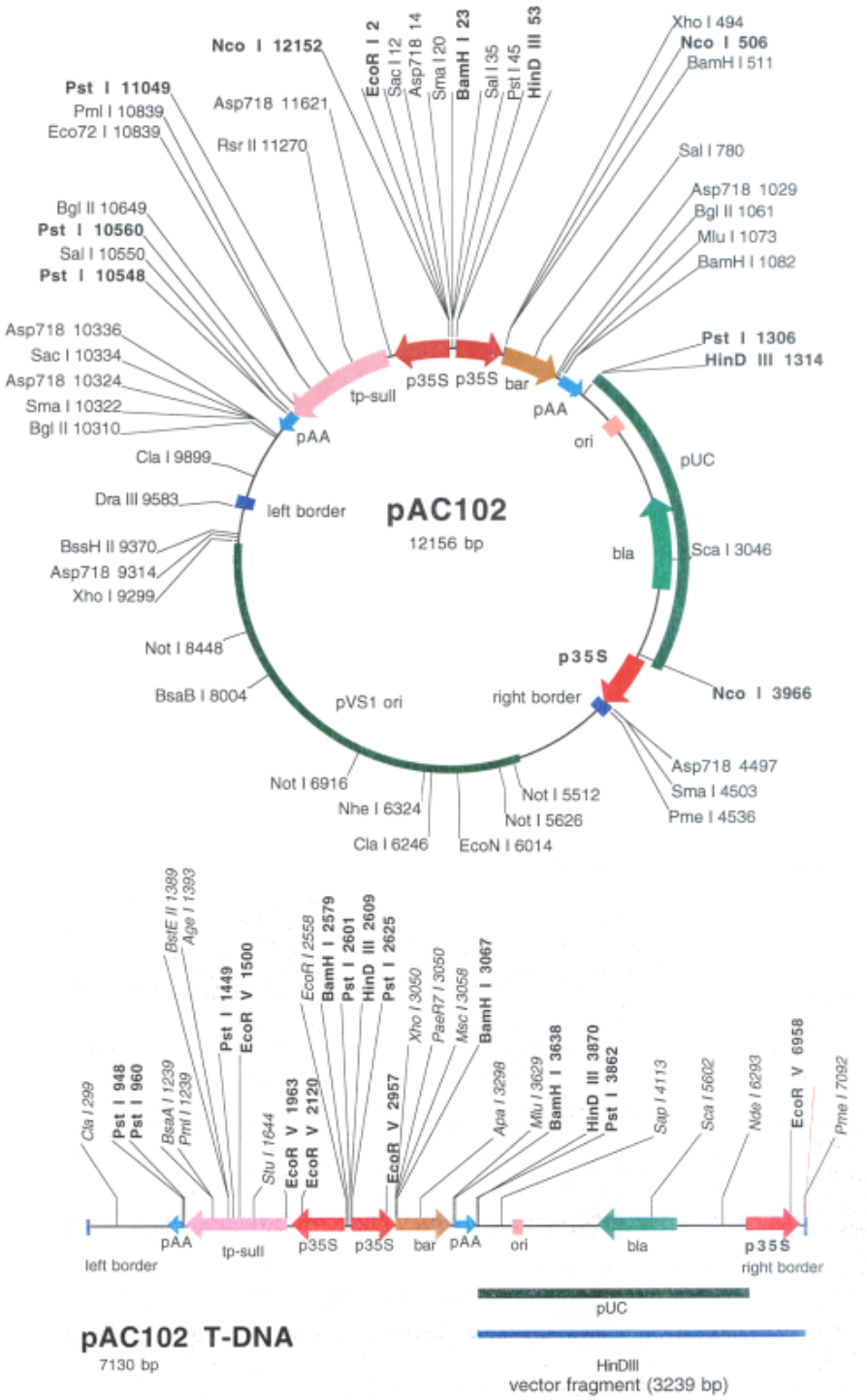

Appendix 4: pEX2 and pEX4 vector map

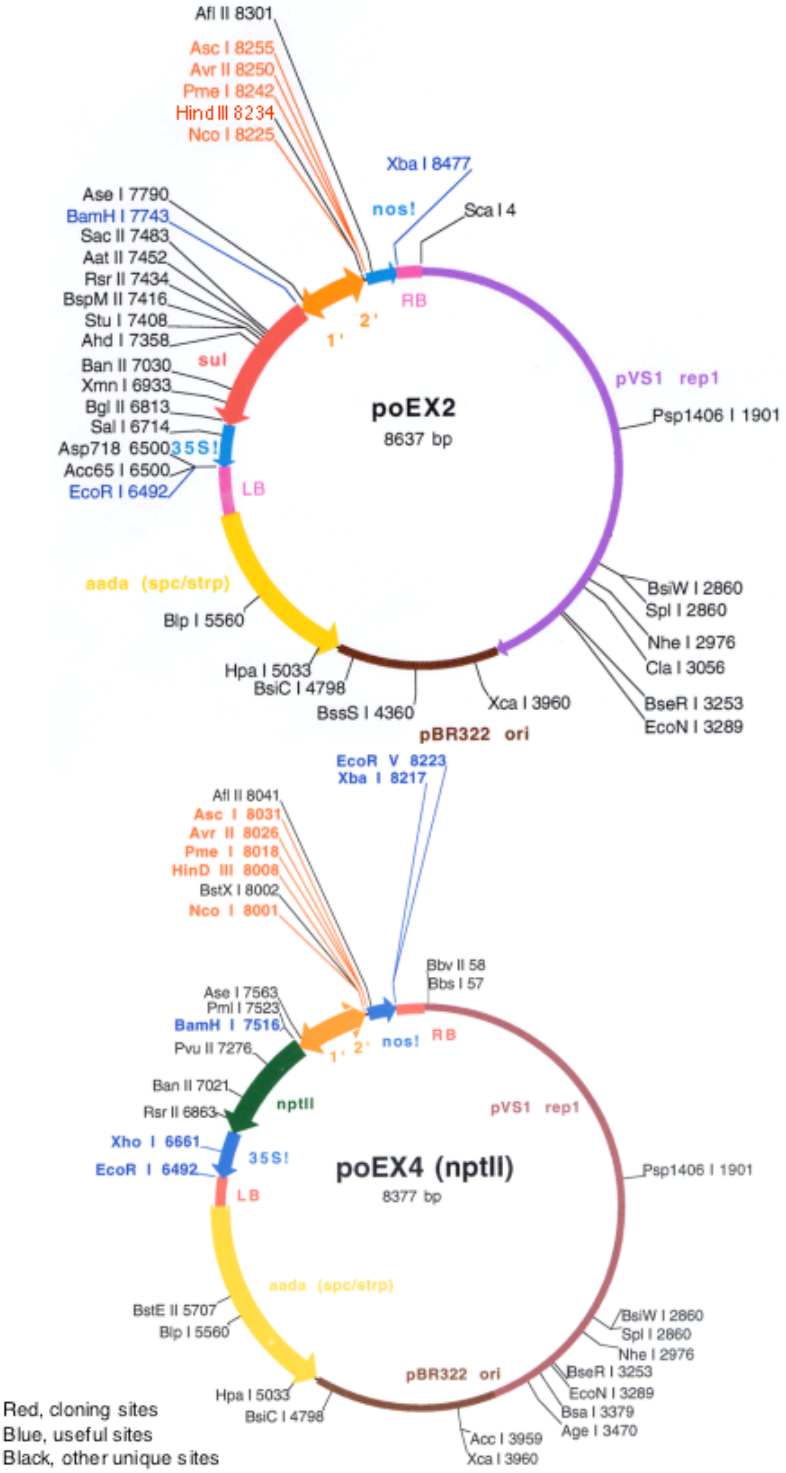

Appendix 5: pEXhp and pEX4hp vector map

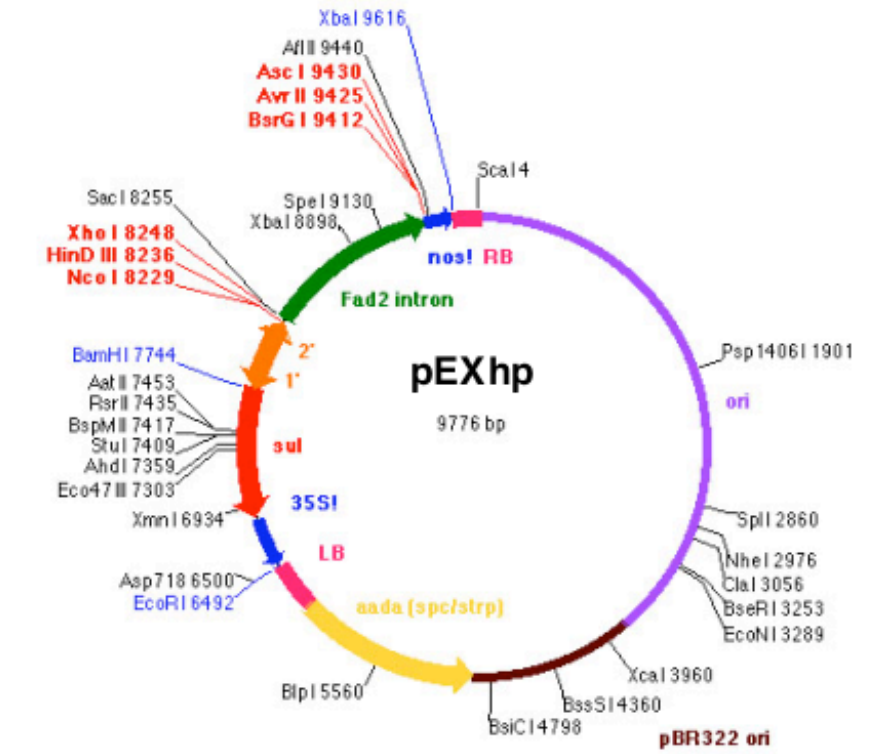

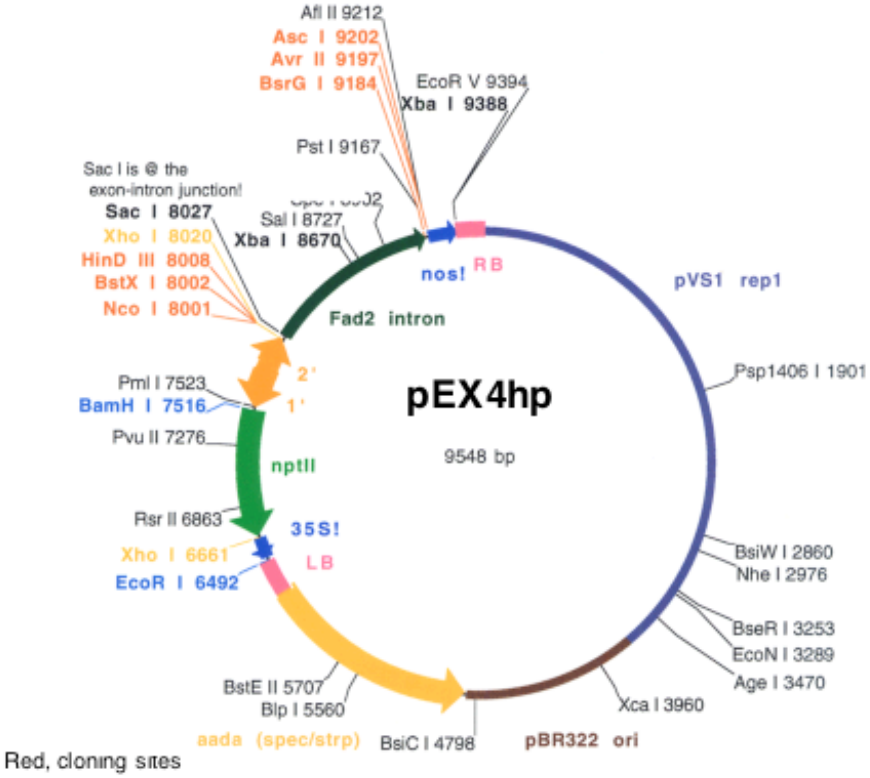

Red, cloning sites
Blue, useful sites
Black, other unique sites

Appendix 6: pEX6N35SpMyci vector map

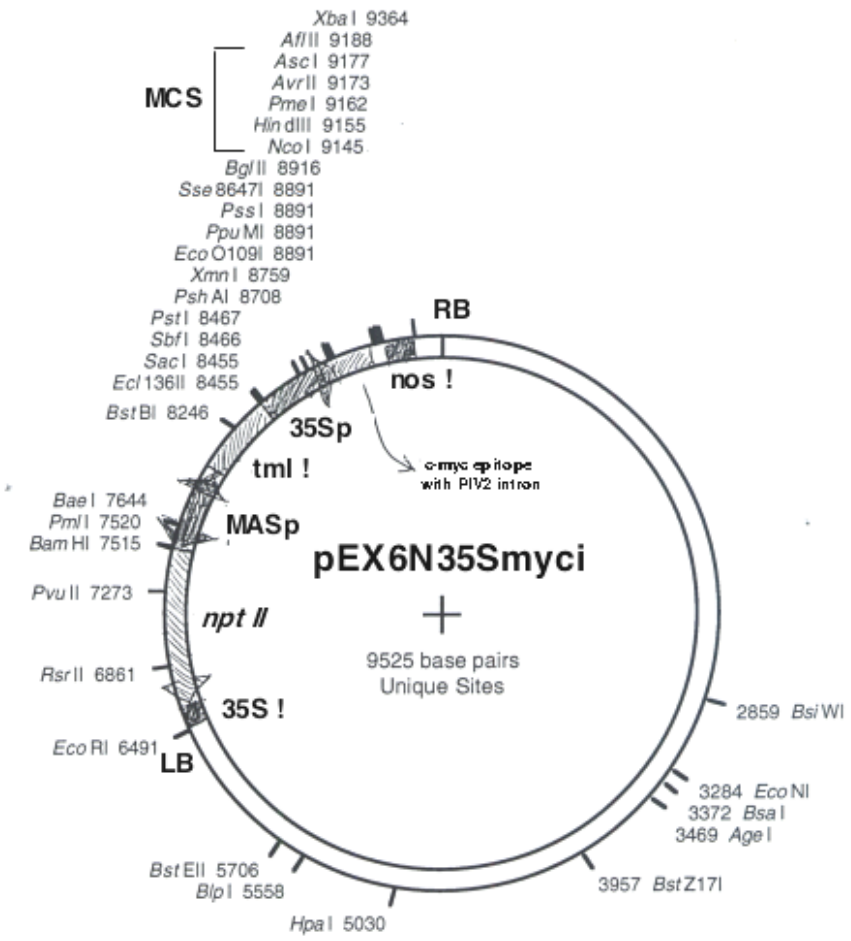

Appendix 7: pEX6Nubip vector map

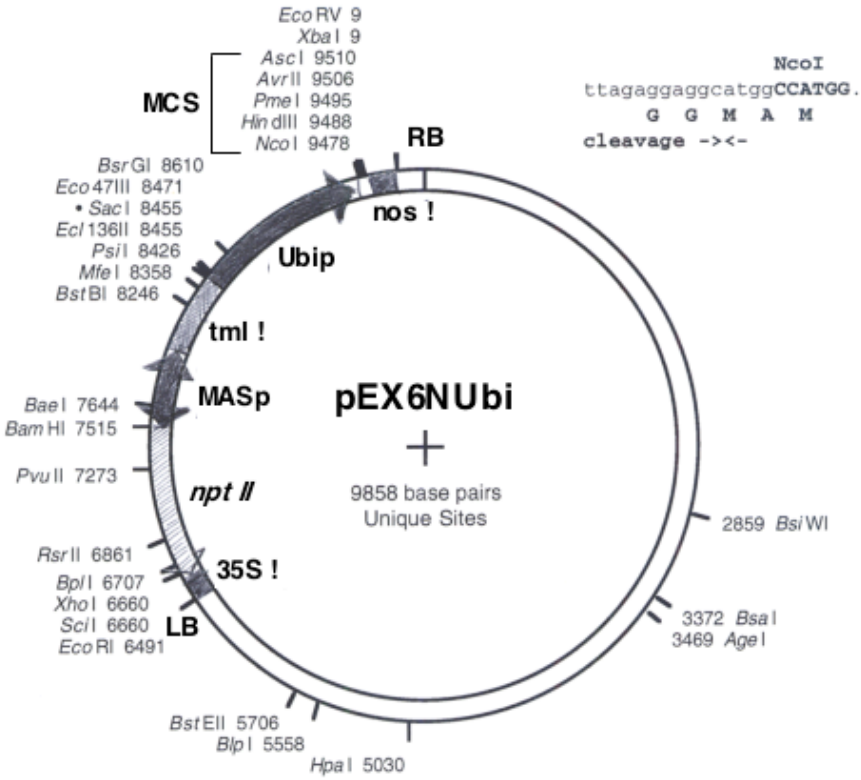

Appendix 8: Genes regulated by the three *ino80* alleles

List of genes with decreased expression in *ino80* plants (67 genes)

AGI number	FC	ANOVA	probe set	funct. Cat.	description	*ino80* -2 raw	flags	*ino80*-3 raw	flags	*ino80* -1 raw	flags	wt raw	flags
AT2G40570	5.39	0.0026	255821_at	protein metabolism	Initiator tRNA phosphoribosyl-transferase, putative	24.9 (22.7 to 27.1)	A	60.15 (25.3 to 95)	P,A	55.6 (48.3 to 62.9)	P,A	288 (266 to 302)	P
AT3G24100	3.43	0.0009	257239_at	unknown	four F5 (4F5) protein family (69aa)	142.2 (115.1 to 169.3)	P	180.2 (151.8 to 208.6)	P	174 (156.6 to 191.4)	P	578.425 (523.3 to 668.2)	P
AT4G12830	3.33	0.0360	254783_at	others	2-hydroxy-6-oxohepta-2,4-dienoate hydrolase, putative	190.9 (190.4 to 191.4)	P	359.1 (350.2 to 368)	P	185.15 (93.7 to 276.6)	P,A	541.5 (353.1 to 731.7)	P
AT4G57700	3.27	>0.05	247881_at	unknown	unknown protein family (ipir|D64592) (352aa)	80.6 (62.8 to 98.4)	P	79.3 (45.1 to 113.5)	P,A	78.75 (35.9 to 121.6)	P,A	211.775 (166 to 245.2)	P
AT3G18390	3.08	0.0002	257717_at	metabolism RNA	similar to maize crs1, required for atpF splicing	189.3 (170.7 to 207.9)	P	324.65 (286.2 to 363.1)	P	226.2 (202.2 to 250.2)	P	672.125 (635.1 to 724)	P
AT1G73250	2.62	>0.05	260094_at	metabolism	GER1 (GDP-ketodeoxy-D-mannose-epimerase-reductase)	128.3 (113.5 to 143.1)	P,A	131.1 (109.5 to 152.7)	P	114.85 (56.2 to 173.5)	P,A	251.85 (228.9 to 287.3)	P
AT4G13250	2.52	0.0173	254764_at	metabolism lipid	Short-chain dehydrogenase-reductase (SDR) family, putative	608.35 (544.1 to 672.6)	P	799.7 (551.3 to 1,048.1)	P	650.05 (493.5 to 806.6)	P	1,560.175 (1,245.8 to 1,812.4)	P
AT5G01220	2.41	0.0060	251143_at	metabolism lipid	putative protein SspIX protein	547.2 (451.3 to 643.1)	P	975 (750.8 to 1,199.2)	P	293.8 (274.9 to 312.7)	P	687.9 (622 to 761.6)	P
AT5G38850	2.30	0.0011	249427_at	protein metabolism	40S ribosomal protein S9-like	625.5 (564.3 to 686.7)	P	420 (406.5 to 433.5)	P	328 (288.8 to 367.2)	P	726.675 (693.7 to 750.6)	P
AT1G08840	2.26	0.0039	264781_at	metabolism RNA	SIGB, RNA polymerase sigma subunit SigB	313.3 (310.2 to 316.4)	P	419.45 (308.4 to 530.5)	P	341.5 (298.6 to 384.4)	P	744.5 (650.1 to 817.3)	P
AT5G63430	2.26	0.0104	247386_at	transcription factor	putative transcription factor	140.9 (123.2 to 158.6)	P	292.4 (254.7 to 330.1)	P	161.85 (109 to 214.7)	P	336.2 (313.3 to 389.8)	P
AT3G20375	2.25	0.0060	256741_at	transcription factor	putative transcription factor	192.7 (191.4 to 194)	P	84.55 (67.5 to 101.6)	P	94.05 (74.2 to 113.9)	P,A	203.2 (170.2 to 256.9)	P
AT5G66880	2.22	0.0009	247111_at	others	unknown protein, membrane protein	546.15 (508.1 to 584.2)	P	240.15 (200.5 to 279.8)	P	319.65 (299.2 to 340.1)	P	688.05 (672 to 715)	P
AT5G51260	2.21	0.0001	248440_at	metabolism	acid phosphatase	117.05 (113.2 to 120.9)	P	190.95 (184.5 to 197.4)	P	218.1 (201.7 to 234.5)	P	468.975 (414.2 to 531.2)	P
AT2G14910	2.19	0.0001	266614_at	unknown	unknown protein, seed maturation?	1,398.25 (1,369.2 to 1,427.3)	P	2,008.9 (1,890 to 2,127.8)	P	2,028.05 (1,926.5 to 2,129.6)	P	4,297.075 (4,142.1 to 4,506.9)	P
AT2G04230	2.16	0.0009	257447_at	protein metabolism	F-box protein, putative	145.9 (141.4 to 150.4)	P	48.85 (42.9 to 54.8)	P,A	109.65 (85.8 to 133.5)	P	225.5 (202.2 to 268.9)	P
AT5G06210	2.14	0.0014	250721_at	metabolism RNA	contains RRM1 motif and similarity to RNA-binding protein	464.85 (424.4 to 505.3)	P	235.15 (209.1 to 261.2)	P	271.65 (239 to 304.3)	P	563.624 (493.9 to 661.5)	P
AT1G44790	2.08	0.0014	261336_at	others	unknown protein, cation transport?	317.05 (286.6 to 347.5)	P	298.3 (285.8 to 310.8)	P	343.25 (290.1 to 396.4)	P	687.175 (616.6 to 782.3)	P
	2.07	0.0041	244921_s_at	unknown	unknown protein	193.8 (173.3 to 214.3)	P	161.9 (148.2 to 175.6)	P	153.6 (124.7 to 182.5)	P	302.925 (278.2 to 325.8)	P
AT2G04360	2.05	0.0075	263859_at	unknown	unknown protein	505.5 (496.5 to 514.5)	P	572.5 (559.5 to 585.5)	P	417.7 (318.7 to 516.7)	P	806.5 (747 to 842.4)	P
AT1G60260	2.04	0.0002	264270_at	others	beta-glucosidase, putative	148.9 (148.5 to 149.3)	P,M	186.05 (182.9 to 189.2)	P,A	142.8 (132.1 to 153.5)	A	281.95 (267.6 to 297.4)	P
AT1G27925	2.02	0.0002	257222_at	protein metabolism	DegP protease almost identical to DegP protease precursor	1,030.95 (1,001.9 to 1,060)	P	1,501.45 (1,443.3 to 1,559.6)	P	1,105.5 (1,019.4 to 1,191.6)	P	2,162.4 (2,079.4 to 2,260.1)	P
AT3G14210	2.01	0.0045	257008_at	others	Lipase/Acylhydrolase with GDSL motif (myrosinase-associated)	6,460.75 (5,468.6 to 7,452.9)	P	6,353.25 (5,497.7 to 7,208.8)	P	5,727.5 (5,041.5 to 6,413.5)	P	11,108.449 (10,404 to 12,345.1	P
AT1G15980	2.01	0.0014	261788_at	unknown	unknown protein	684 (614.5 to 753.5)	P	1,931.65 (1,765.6 to 2,097.7)	P	1,537.3 (1,208.3 to 1,866.3)	P	2,958.625 (2,385.8 to 3,396.3)	P
AT3G60910	2.01	0.0001	251391_at	unknown	unknown protein	563.75 (541.9 to 585.6)	P	494.75 (470 to 519.5)	P	522.9 (488.9 to 556.9)	P	1,015.55 (968.2 to 1,073.6)	P
AT1G28670	2.00	0.0014	262733_s_at	metabolism lipid	identical to lipase AAA93262 Arabidopsis	805.4 (758.8 to 852)	P	1,031.45 (1,026.5 to 1,036.4)	P	585.8 (556.3 to 615.3)	P	1,136.825 (982.1 to 1,226.5)	P
AT3G07580	2.00	0.0023	250815_at	unknown	unknown protein	178.4 (155.6 to 201.2)	P	241.8 (231.4 to 252.2)	P	255 (228.7 to 281.3)	P	497.425 (384.9 to 608.6)	P
AT4G18370	1.97	0.0121	254669_at	protein metabolism	IIhoA protease precursor, putative	1,104.05 (986.2 to 1,221.9)	P	878.9 (703.1 to 1,054.7)	P	666.6 (601.4 to 731.8)	P	1,269.65 (1,155.1 to 1,454.4)	P
AT2G30460	1.95	0.0020	267520_at	others	integral membrane protein, putative	171.5 (164 to 179)	P	259.55 (211.8 to 307.3)	P	239.7 (212.2 to 267.2)	P	452.1 (429.2 to 501.7)	P
AT3G21110	1.92	0.0027	256978_at	metabolism	phosphoribosylaminoimidazole-succinocarboxamide synthase, putativ	175.3 (164 to 186.6)	P	236 (233 to 239)	P	192 (169.9 to 214.1)	P	359.15 (310.9 to 408.3)	P
AT5G19500	1.88	0.0001	245943_at	others	permease family protein, putative	207.15 (200.4 to 213.9)	P	291.8 (288.8 to 294.8)	P	238.7 (224.8 to 252.6)	P	434 (408.7 to 446.3)	P
AT5G02150	1.88	0.0007	251022_at	stress	Hsp70 binding protein, putative	231 (217.5 to 244.5)	P	86.1 (81 to 91.2)	P	165.65 (152.1 to 179.2)	P	302.5 (251.9 to 350.2)	P
AT4G24930	1.86	0.0002	254137_at	others	thylakoid lumenal 17.9 kDa protein, putative	740.6 (706.4 to 774.8)	P	1,294.95 (1,257.2 to 1,332.7)	P	921.15 (850.7 to 991.6)	P	1,659.725 (1,553.2 to 1,762.4)	P
AT1G64740	1.86	0.0020	262885_at	others	similar to alpha-tubulin 6	436.65 (425.2 to 448.1)	P	349.95 (294.7 to 405.2)	P	392.85 (379.6 to 406.1)	P	709.175 (664.3 to 758.3)	P
AT1G64910	1.85	0.0002	266767_at	unknown	similar to plastid-lipid associated protein PAP/fibrillin family	332.45 (322.6 to 342.3)	P	615.45 (572.1 to 658.8)	P	501.95 (467.7 to 616.2)	P	1,064 (960.9 to 1,219.6)	P
AT5G04350	1.83	0.0002	263668_at	fluorescent biosynth	ACC oxidase (Similar to Arabidopsis 2A6), putative	709.9 (777.7 to 822.1)	P	1,037.3 (1,035.4 to 1,039.2)	P	915 (838.1 to 991.9)	P	1,622.25 (1,537.6 to 1,731)	P
AT2G02400	1.83	0.0014	266202_at	phenylprop pathway	cinnamoyl-CoA reductase, putative	281.35 (271.4 to 291.3)	P	285.3 (256.8 to 313.8)	P	282.75 (248.6 to 316.9)	P	497.85 (461 to 527.3)	P
AT3G21280	1.76	0.0041	258045_at	protein metabolism	ubiquitin-specific protease 7 (UBP7), putative	178.65 (160.1 to 198.1)	P	209.05 (168 to 250.1)	P	208.05 (168.6 to 247.5)	P	351.15 (334 to 374.3)	P
AT1G31910	1.74	0.0001	246286_at	metabolism	phosphoenolpyruvate kinase, putative	1,550.9 (1,508.6 to 1,593.2)	P	1,918 (1,875.3 to 1,960.7)	P	1,793.25 (1,740.9 to 1,845.6)	P	3,028.725 (2,894.7 to 3,157.8)	P
AT5G52110	1.73	0.0038	248401_at	unknown	unknown protein	99 (91.3 to 106.7)	P,A	129.7 (101.8 to 157.6)	P,M	173.7 (167.1 to 180.3)	P	296.25 (229.7 to 358.8)	P
AT4G38020	1.72	0.0075	253020_at	others	RNA methyl transferase, putative	186.85 (165 to 208.7)	P	141.45 (128.2 to 154.7)	P	147 (130.6 to 163.4)	P	244.075 (213.9 to 265.9)	P
AT3G61870	1.71	0.0065	251243_at	unknown	unknown protein (272aa)	1,700.15 (1,678.7 to 1,721.6)	P	1,685.4 (1,307.9 to 2,062.9)	P	1,855.25 (1,794 to 1,916.5)	P	3,071.5 (2,954.4 to 3,334.7)	P
AT3G62220	1.67	>0.05	251251_at	signaling	RLCKVIII serine threonine protein kinase-like protein	106.75 (99.8 to 113.7)	A	96.15 (51.4 to 140.9)	M,A	115.2 (114 to 116.4)	M,A	190.2 (142.5 to 242.1)	P
AT2G27360	1.67	0.0010	265646_at	metabolism lipid	putative lipase	415.75 (387.9 to 443.6)	P	388.55 (374.7 to 402.4)	P	308.45 (298.1 to 318.8)	P	500.025 (473 to 536.8)	P
AT5G28500	1.66	0.0401	245952_at	unknown	unknown protein	1,799.95 (1,474.4 to 2,125.5)	P	2,141.5 (1,953.7 to 2,329.3)	P	1,454.1 (1,241.8 to 1,666.4)	P	2,323.425 (2,175.9 to 2,637)	P
AT1G50000	1.66	0.0036	256215_at	unknown	unknown protein (175aa)	1,838.95 (1,710.7 to 1,967.2)	P	2,624.4 (2,312.3 to 2,936.5)	P	2,209.25 (1,901.1 to 2,517.4)	P	3,527.375 (3,214.2 to 3,801.8)	P
AT5G09770	1.64	0.0030	250495_at	protein metabolism	similar to ribosomal protein L17, chloroplast	651.6 (613 to 690.2)	P	344.2 (281.9 to 406.5)	P	404.35 (399.7 to 409)	P	644.325 (578.5 to 677)	P
AT5G65760	1.64	0.0021	247156_at	others	lysosomal Pro-X carboxypeptidase	381.35 (377.8 to 384.9)	P	353.65 (306.5 to 400.8)	P	361.2 (348.5 to 373.9)	P	573.9 (539.6 to 628.8)	P
AT2G44920	1.63	0.0010	266813_at	chloroplast	thylakoid lumen peptidyprolyl isomerase repeat family protein	1,004.55 (963.9 to 1,047.2)	P	1,371.05 (1,354.9 to 1,387.2)	P	1,157.4 (1,037.9 to 1,276.9)	P	1,823.275 (1,715.6 to 1,949.6)	P
AT2G18710	1.62	0.0036	266018_at	chloroplast	preprotein translocase SECY protein, putative	1,478.6 (1,459.1 to 1,498.1)	P	1,747.4 (1,743.3 to 1,751.5)	P	1,315.3 (1,163.7 to 1,466.9)	P	2,050.375 (1,865.1 to 2,150.2)	P
AT3G14067	1.61	0.0446	256997_at	signaling	subtilisin-like serine protease, putative	1,992.15 (1,987.1 to 1,997.2)	P	2,331.9 (2,255.7 to 2,408.1)	P	1,643.05 (1,500.2 to 1,785.9)	P	2,589.325 (2,036.6 to 3,333.2)	P
AT4G31820	1.60	0.0014	245493_at	unknown	putative protein NPH3 family and methylase	191.4 (188.1 to 194.7)	A	309.65 (289.8 to 329.5)	P	192 (174.1 to 209.9)	A	297.5 (282.5 to 324.2)	P

AT5G10370	1.60	0.0092	255600_s_at	metabolism RNA	putative protein (similar to ATP dependent RNA helicases)	231.3 (183 to 279.6)	P	255.95 (242 to 269.9)	P	232.45 (224.1 to 240.8)	P	361.15 (342.8 to 377.5)	P
AT4G08280	1.60	0.0031	255131_at	unknown	unknown protein	1,128.4 (947.1 to 1,309.7)	P	941.45 (888.3 to 994.6)	P	1,053.35 (1,028.9 to 1,077.8)	P	1,633.125 (1,545.4 to 1,726.5)	P
AT4G38490	1.59	0.0010	253001_at	unknown	unknown protein	1,016.6 (987.7 to 1,045.5)	P	395.7 (337.6 to 453.8)	P	630.8 (580.4 to 681.2)	P	974.7 (850.4 to 1,050.8)	P
AT1G77060	1.59	0.0086	264954_at	metabolism	carboxyphosphonoenolpyruvate mutase, putative	386.2 (336.4 to 436)	P	332.7 (307.8 to 357.6)	P	307.4 (277.8 to 337)	P	471.65 (458.4 to 481.8)	P
AT4G21860	1.58	0.0019	254388_at	stress	SelR domain Expressed protein	3,060.9 (2,953.2 to 3,168.6)	P	3,388.15 (3,177.6 to 3,598.7)	P	2,967.7 (2,933 to 3,002.4)	P	4,564.75 (4,222.1 to 4,874.9)	P
AT1G78140	1.58	0.0096	260056_at	unknown	unknown protein	680.5 (622.9 to 738.1)	P	411 (379.2 to 442.8)	P	518.45 (458 to 578.9)	P	794.8 (648.9 to 902.4)	P
AT2G29360	1.57	0.0021	266293_at	metabolism	tropinone reductase, putative	654.65 (595.6 to 713.7)	P	311.35 (254.9 to 367.8)	P	482.8 (430.3 to 535.3)	P	733.475 (699.9 to 784.7)	P
AT4G29220	1.57	0.0002	253709_at	metabolism	pyrophosphate-dependent phosphofructokinase-like protein	890.65 (880.1 to 901.2)	P	967.35 (886.5 to 1,048.2)	P	898.85 (894.1 to 903.6)	P	1,369.525 (1,340.2 to 1,394.4)	P
AT2G41120	1.55	0.0002	267063_at	unknown	unknown protein	478.85 (465.8 to 491.9)	P	530.25 (509.6 to 550.9)	P	519.35 (509.2 to 529.5)	P	780.25 (758.9 to 805.3)	P
AT1G24625	1.55	0.0121	265029_at	transcription factor	ZFP7 (zinc finger protein 7)	252.9 (247.7 to 258.1)	P,A	299.55 (288.2 to 310.9)	P	274.35 (222.9 to 325.8)	P	405.6 (367.5 to 441.8)	P
AT1G75100	1.55	0.0075	259927_at	unknown	unknown protein	1,181.7 (1,144.8 to 1,218.6)	P	889.55 (782.1 to 997)	P	904.4 (849.4 to 959.4)	P	1,357.3 (1,209.2 to 1,467.5)	P
AT5G55380	1.54	0.0033	248080_at	metabolism lipid	wax synthase-like protein	217.05 (205.8 to 228.3)	P	391.7 (375.5 to 407.9)	P	291.35 (271.8 to 310.9)	P	436.725 (361.9 to 515.8)	P
AT2G48070	1.54	0.0014	265773_at	unknown	unknown protein	996.85 (986.7 to 1,007)	P	861.85 (849.1 to 874.6)	P	756.45 (703.8 to 809.1)	P	1,125.525 (1,085.2 to 1,194.7)	P
AT1G71480	1.53	0.0089	259943_at	transport nucleus	nuclear transport factor 2 (NTF2) protein family	660.15 (616 to 704.3)	P	888.5 (775.4 to 1,001.6)	P	690.35 (681.2 to 699.5)	P	1,025.675 (960.6 to 1,153)	P
AT1G22430	1.51	0.0025	261931_at	metabolism	alcohol dehydrogenase ADH, putative	461 (396.9 to 525.1)	P	541.3 (517.7 to 564.9)	P	514.25 (500.6 to 527.9)	P	751.1 (718.1 to 792.5)	P

List of genes with increased expression in *ino80* plants (29genes)

AGI number	FC	ANOVA	probe set	funct. cat	description	*ino80* -2 raw	flags	*ino80* -3 raw	flags	*ino80* -1 raw	flags3	wt raw	flags4
AT1G55265	**2.95**	**0.0007**	**259661_at**	**unknown**	**unknown protein (176aa)**	1,794.65 (1,739.1 to 1,850.2)	P	2,136.3 (1,784.4 to 2,488.2)	P	1,627.55 (1,406.8 to 1,848.3)	P	530.15 (486.7 to 554.6)	P
AT3G51330	**2.71**	**0.0133**	**252098_at**	**metabolism protein**	**aspartyl protease, putative (560aa)**	357.3 (280.6 to 434)	P	240.7 (168.8 to 312.6)	P	455.3 (400.4 to 510.2)	P	161.8 (151.7 to 172.8)	P
AT1G07500	**2.35**	**0.0046**	**261065_at**	**unknown**	**unknown protein (75aa)**	225.2 (215.9 to 234.5)	P,A	260 (240.8 to 279.2)	P	305.8 (299.8 to 311.8)	P	127.575 (103.5 to 150.5)	P,A
AT2G43590	**2.21**	**0.0039**	**260560_at**	**others**	**endochitinase, putative**	1,924.6 (1,601.1 to 2,248.1)	P	2,882.6 (2,119.3 to 3,645.9)	P	1,406.7 (1,336.2 to 1,477.2)	P	628.425 (467 to 780.4)	P
AT1G68880	**2.06**	**>0.05**	**260030_at**	**transcription fatcor**	**bZIP transcription factor, putative**	229.15 (193.6 to 264.7)	P	261.7 (191.1 to 332.3)	P	289.6 (253.4 to 325.8)	P	138.7 (91.7 to 167)	P
AT4G23680	1.95	0.0041	254234_at	stress	major latex protein type 1, putative	2,070.75 (1,789.1 to 2,352.4)	P	3,571.75 (3,384.5 to 3,759)	P	2,522.95 (2,099.6 to 2,946.3)	P	1,243.05 (1,047.7 to 1,413.4)	P
AT1G18970	1.91	0.0081	259481_at	others	germin (GLP1), putative	398.9 (392.2 to 405.6)	P	289.6 (279.6 to 299.6)	P	443.25 (357 to 529.5)	P	221.475 (194.4 to 255.8)	P
AT3G53950	1.90	0.0007	251931_at	others	protein glyoxal oxidase (glx2), putative	497.95 (478 to 517.9)	P	410.8 (400.6 to 421)	P	380.15 (363.7 to 396.6)	P	194.3 (174.3 to 214.3)	P
AT1G11100	1.89	0.0097	260468_at	transcription fatcor	transcription factor RUSH-1alpha isolog	177.45 (150.3 to 204.6)	P	161.2 (145.4 to 177)	P	204.6 (186 to 223.2)	P	104.975 (92.7 to 112.4)	P
AT2G37520	1.86	0.0147	267163_at	transcription fatcor	transcription factor, putative (826aa)	334.85 (302.6 to 367.1)	P	271.8 (263.6 to 280)	P	348 (314.5 to 381.5)	P	183.575 (155.8 to 242.6)	P
AT1G51420	1.80	0.0021	260517_at	metabolism	sucrose phosphatase, putative	334.9 (334.5 to 335.3)	P	441.7 (401.6 to 481.8)	P	518.25 (484.9 to 551.6)	P	279.15 (244.4 to 301.9)	P
AT4G25240	1.72	0.0074	254109_at	cell wall	putative pectinesterase (pectin methylesterase)	286 (279.6 to 292.4)	P	292.35 (236.8 to 347.9)	P	243.8 (234.2 to 253.4)	P	138.675 (108.6 to 160.1)	P
AT1G47270	1.72	0.0008	260502_at	metabolism protein	F-box containing tubby family protein	611.2 (591.2 to 631.2)	P	452.85 (404.6 to 501.1)	P	568.4 (546.5 to 590.3)	P	321.2 (309.6 to 331.3)	P
AT2G18980	1.65	0.0136	266941_at	others	peroxidase (ATP22a)	1,112.85 (1,058.9 to 1,166.8)	P	1,089.85 (912.2 to 1,267.5)	P	1,421.9 (1,408.4 to 1,435.4)	P	837.375 (767.8 to 939.8)	P
AT1G14130	1.63	0.0097	262653_at	others	dioxygenase-like protein	842.8 (731.7 to 953.9)	P	669.25 (575.1 to 763.4)	P	593.6 (524.1 to 663.1)	P	354.025 (279.4 to 396.2)	P
AT1G48100	1.63	0.0136	260727_at	others	polygalacturonase PG1, putative	1,253.65 (1,069.7 to 1,437.6)	P	1,046 (859.5 to 1,232.5)	P	1,135.8 (1,099.3 to 1,172.3)	P	676.575 (637.1 to 712.4)	P
AT5G05060	1.62	0.0075	250815_s_at	unknown	unknown protein	1,422.95 (1,321.3 to 1,524.6)	P	946.8 (823 to 1,070.6)	P	1,080.35 (1,053.6 to 1,107.1)	P	649.975 (548.7 to 733.5)	P
AT1G55130	1.61	0.0007	256151_at	unknown	multispanning membrane protein, putative	591.55 (545.3 to 637.8)	P	631.15 (624.9 to 637.4)	P	644.9 (640.6 to 649.2)	P	387.5 (374.1 to 401.3)	P
AT4G19200	1.59	0.0037	254559_at	unknown	glycine/proline-rich protein GPRP family	1,697.3 (1,682.2 to 1,712.4)	P	1,502.4 (1,491 to 1,513.8)	P	1,775.45 (1,602.9 to 1,948)	P	1,078.8 (986.1 to 1,118.3)	P
AT1G45145	1.58	0.0034	260943_at	metabolism	thioredoxin H-type 5 (TRX-H-5) (TOUL) family	2,757.35 (2,647.5 to 2,867.2)	P	2,484.05 (2,458.8 to 2,509.3)	P	2,436.75 (2,110.5 to 2,763)	P	1,482.025 (1,362.8 to 1,649.6)	P
AT3G53980	1.58	0.0046	251928_at	others	protease inhibitor/lipid transfer protein (LTP) family	2,508.6 (2,356.1 to 2,661.1)	P	1,432.75 (1,287.2 to 1,578.3)	P	2,723.2 (2,566.3 to 2,880.1)	P	1,677.55 (1,518.3 to 1,919)	P
AT1G49310	1.57	0.0133	262446_at	unknown	unknown protein	504.1 (442.1 to 566.1)	P	490.05 (455 to 525.1)	P	542.6 (510.4 to 574.8)	P	335.775 (291.7 to 378.3)	P
AT2G40100	1.56	0.0021	265722_at	energy	chlorophyll a/b binding protein, putative	4,290.15 (4,252.9 to 4,327.4)	P	2,911.2 (2,824.8 to 2,997.6)	P	3,374.05 (3,174.6 to 3,573.5)	P	2,099.2 (1,858.5 to 2,311.9)	P
AT5G47540	1.56	0.0106	248751_at	unknown	Mo25 eucaryotic protein family	963.65 (883.4 to 1,043.9)	P	884 (787.3 to 980.7)	P	911.75 (794.8 to 1,028.7)	P	563.85 (528.5 to 607.3)	P
AT3G18280	1.55	0.0084	257066_at	metabolism lipids	lipid transfer protein, putative	3,832 (3,396.6 to 4,267.4)	P	2,789.5 (2,726.3 to 2,852.7)	P	4,166.75 (3,840.4 to 4,493.1)	P	2,596.1 (2,373.8 to 2,748.2)	P
AT1G69830	1.52	0.0009	260412_at	metabolism	putative alpha-amylase	728.3 (705.6 to 751)	P	577.4 (559.8 to 595)	P	742.15 (705.8 to 778.5)	P	471.825 (442.5 to 492.5)	P
AT1G20160	1.51	>0.05	261224_at	metabolism protein	subtilisin-like serine protease	803.15 (724.6 to 881.7)	P	664.35 (555.4 to 773.3)	P	766.5 (654.1 to 878.9)	P	488.525 (404 to 524.6)	P
AT5G17650	1.51	0.0040	246440_at	unknown	glycine/proline-rich protein GPRP family	352.95 (317.7 to 388.2)	P	607.3 (596.9 to 617.7)	P	642.45 (576.8 to 708.1)	P	411.85 (390.7 to 426.6)	P
AT1G10830	1.50	0.0063	262791_at	unknown	unknown protein	1,283.95 (1,056.5 to 1,511.4)	P	1,028 (985.4 to 1,070.6)	P	1,018.55 (1,014.7 to 1,022.4)	P	656.95 (610.3 to 689.5)	P

Acknowledgments

First of all, I would like to thank Barbara Hohn, for giving me the opportunity to do my PhD in her lab and in such a great scientific environment as the FMI. I also want to thank her for her support and patience during all these years as well as the extreme freedom she gave me for the orientation of my research. Thanks to J. Masson and J. Paszkowski for being part of my thesis committee and all their advice and criticisms. Special thank to J. Masson for deep discussion on science as well as orientation. A very special thank to D. Schürmann and J. Molinier for the great atmosphere of our small "recombi-team", for all the shared work, for all the discussion at anytime and anywhere.

Thanks to J. Lucht who initiated this project. Also thanks to Philippe Crouzet, Etienne Bucher, Cyril Zipfel and Estelle Arn for stimulating discussions, ideas and support. Thank to all other members of the B. Hohn's lab as well as many people in the FMI. Special thanks to Veronique Kalk and Cynthia Ramos for their excellent technical assistance as well as Delphine Joly, Sabine Flury and Nicolas Helmstetter.

Further, I would like to thank Giovanna Benvenuto and Chris Bowler for our collaborative effort the interaction of INO80 with the chromatin and Haico van Attikum and Susan Gasser for sharing unpublished results and ideas on INO80.